DETERMINATION OF STRESS DISTRIBUTION IN A TWO-DIMENSIONAL BODY WITH AN ELLIPTICAL INSERT FOR PLANE STRESS CONDITIONS UNDER UNIAXIAL TENSION

By

Krishan Lal Kumra

Submitted to the Faculty of Pure and Applied Science

of the University of Ottawa

in partial fulfillment of the requirements

for the degree of

MASTER OF APPLIED SCIENCE

in Mechanical Engineering

August , 1969

ACKNOWLEDGEMENT

I express my deep sense of gratitude to Dr. Adolph Feingold, and Dr. Bilgin Kaftanoglu, under whose supervision this work was carried out, for their personal interest, valuable suggestions, critical discussions, and illuminating remarks at every stage of the work.

I am grateful to Dr. Feingold for the award of a Teaching Assistantship and especially for the hours he so willingly spent with me. Sincere thanks are also extended to the National Research Council of Canada for the financial support of this project, to the personnel of the Computing Centre and Physics Department Workshop of the University of Ottawa for their co-operation.

The help and encouragement for the completion of the thesis, from my colleagues, Mr. K. G. Gupta in particular, is gratefully acknowledged.

ABSTRACT

The stress distribution around a centrally located eiliptical insert of different material in a plate of finite width subjected to uniform axial loading is investigated in this thesis.

A computer program for the numerical solution of the problem is presented. It was found that a solution can best be arrived at using the finite - difference method. Experimental results were obtained by means of photoelasticity. Stress distributions at the boundaries were found for a wide range of parameters, such as different ratios of the moduli of elasticity, E , of the insert and the parent material; widths of the models; and different shapes of the inserts. Stress concentration factors were computed for the points of maximum tensile stress. The results were compared with those appearing in the existing literature.

NOMENCLATURE

Number 1 refers to the insert and number 2 to the parent material.

A	Width of the specimen
B	Length of the specimen
A_x	Cross-sectional area of the specimen along x-axis
A_y	Cross-sectional area of the specimen along y-axis
2a	Maximum dimension of ellipse
2b	Minimum width of ellipse
f	Material fringe value
δ	Standard horizontal step
$C(\delta)$	Standard vertical step
E_1	Modulus of elasticity of the insert
E_2	Modulus of elasticity of the parent material
G	Modulus of rigidity
h	Thickness of the specimen
$\nu 1$	Poisson's ratio of the insert
$\nu 2$	Poisson's ratio of the parent material
x,y	Rectangular coordinates
ℓ,m	Direction cosines of outward normal
σ_{xx},σ_{yy}	Normal components of stress parallel to x and y axes
τ_{xy}	Shearing stress component in rectangular coordinates
P_1,P_2	Principal stresses
P_x,P_y	Applied loads in x and y directions
T_x,T_y	Applied shearing forces

S	Total stress on a plane
S_n	Normal stress on a plane
S_s	Shear stress on a plane
u,v	Components of displacement
e_{xx}, e_{yy}	Unit elongations in x and y directions
e_{xy}	Shear-strain component in rectangular coordinates

TABLE OF CONTENTS

1. INTRODUCTION

Engineering profession continually strives for improvement of detailed design. The consequences of failure of parts vary from the cost of replacement and loss of productive time to the more serious accidents involving loss of life. Failuresare seldom due to faulty material; experience shows that corrective measures usually involve a design modification.

The elementary formulas used in design are based on members having a constant section or a section with a gradual change of contour. Such conditions, however, are hardly attained in actual machine parts or structural members. The presence of shoulders, holes, grooves,keyways, threads, etc. - or a discontinuity of properties at the surface along which two different materials are bonded - result in a modification of the simple stress distributions. Consequently, localized high stresses are generated at the discontinuities. This localization of high stresses is known as stress concentration.

By studying stress concentration factors and evaluating the influence of various geometrical features much can be learned about the ways to produce designs which will be superior from the standpoint of resistance to repeated loads. An intuitive feeling for the relative severity of stress raisers is helpful to the engineer in making preliminary comparisons of design alternatives and in interpolating or extrapolating from available information in order to foretell the stress concentration in a similar, but somewhat different case.

In this investigation, the influence of the ratios of E and ν and the shape of the insert in a finite body on the stress concentra-

tion at the boundary between the insert and the parent material was studied.

Considering the complexity of the problem, it was decided that numerical analysis technique of finite differences would be best suited for solving the biharmonic equation $\nabla^4\phi = 0$ for the present case, in order to get an overall picture of stress distribution. For experimental analysis, photoelasticity method, which is very useful in determining peak stresses at the points of abrupt changes was adopted. A highly sophisticated photoelastic polariscope was used. The principal stresses were separated by the shear-difference method. The modulus of elasticity of the special plastics used in these experiments varies from E = 1000 psi to E = 340000 psi. The use of metallic inserts extends the range of E to 30,000,000 psi in the case of steel.

One material was embedded in the other and special cement was used in order to obtain a perfect bond. The specimen was then placed in the polariscope. As load was applied to it, the lines of stress between the two materials were projected in vivid colour on a circular screen ten times their actual size. Photographs were also taken of the projected lines for future reference. Readings of isoclinics and isochromatics were taken for the purpose of determining the overall stress distribution and in order to calculate the stress concentration factor.

2. LITERATURE SURVEY

The literature was surveyed completely for the study of stress distribution in a two-dimensional body with a perfectly bonded elliptical insert for plane stress conditions under uniaxial tension. The problem of stresses around holes, keyways, grooves, etc. has been extensively treated in the literature. On the other hand, comparatively little work has been done on the problem of stress distribution around an inclusion in a body under tension which is of considerable importance in many practical cases.

Using photoelastic method Durelli, Parks, and Feng (6)* analyzed the distribution of stresses around a centrally located elliptical hole in a plate of finite width subjected to uniform axial loading. They have given the results for a wide range of parameters such as the widths of the models and the ellipses. Unlike the present investigator, however, they have used no inserts.

In 1938 Thibodeau and Wood (19) analyzed the stress around a rigid circular inclusion in a very soft rubber sheet by photoelastic method. In this report the value of the moduli of elasticity E and Poisson's ratios ν of the insert and of the parent material have not been specified.

Donnell (4) determined the stress distribution for the case of the elliptical inclusion in an infinite plate. He plotted results for ratios E1/E2 smaller than one and for different ratios of minor and major axes of ellipse.

* Number in the parenthesis refers to the number in the reference list.

No published work is available which takes into account the influence of the ratios of E or of ν on the stress concentration at the boundary between the insert and the finite parent material. Also, no attempt was made by any of the previous workers to relate the stress concentration factor to the change of shape of an insert in a finite body.

3. PLAN OF PROJECT

The project consists of the theoretical and experimental study of the problem. A brief outline of these two parts follows :

a) Theoretical Investigation

An attempt was also made to solve the problem theoretically. Due to the complexity of the equations involved in the solution, it becomes essential to resort to numerical methods.Finite difference technique was used for solving this problem. Because of the geometrical and loading symmetry about the coordinate axes, it was sufficient to consider only a quarter part of the specimen for analysis. A computer program was developed to generate and solve the resulting system of finite difference equations.

b) Experimental Investigation

The problem basically is the study of stress distribution around a centrally located elliptical insert of different material in a plate of finite dimensions under uniaxial tension. Photoelastic technique has been used to investigate the problem. Shear difference method was applied to analyse the state of stress completely at any arbitrary point. The influence of the ratios of moduli of elasticity, E , of the insert and of the parent material; and also the variation of the geometrical properties of the shape of the insert and the specimen has been studied.

3.1 Theoretical Investigation

The analytical solution of the problem gives rise to complicated expressions and at a certain point, the use of numerical methods becomes inevitable to reach the final results. Therefore, it was found that

in this case it was better to use an all-numerical method from the very begining. The details of this numerical technique are discussed here in detail.

3.1.1 Derivation of stress function

Usually problems involving theory of elasticity require determination of the state of stress in a body subjected to the action of given forces. for the solution of such problems it is necessary to solve the differential equations of equilibrium along with the compatibilty of deformation and boundary conditions.

Neglecting the body forces, the differential equations of equilibrium for a two-dimensional problem, in Cartesian coordinates are

$$\frac{\partial \sigma_{xx}}{\partial x} + \frac{\partial \tau_{xy}}{\partial y} = 0 \qquad (1)$$

$$\frac{\partial \sigma_{yy}}{\partial y} + \frac{\partial \tau_{xy}}{\partial x} = 0 \qquad (2)$$

These equations must be satisfied at all points of the body. The stress components vary over the entire area of the body in the x and y directions. At the points adjacent to the boundary the stress components must be such as to be in equilibrium with the external forces on the boundary of the body, so that the external forces may be regarded as a continuation of the internal stress distribution.

Equations (1) and (2) contain three unknown stress components $\sigma_{xx}, \sigma_{yy}, \tau_{xy}$. The problem is statically indeterminate and in order to

obtain the solution, the elastic deformation must also be considered. For a two-dimensional plane stress problem the three strain-displacement relations are,

$$e_{xx} = \frac{\partial u}{\partial x} \tag{3}$$

$$e_{yy} = \frac{\partial v}{\partial y} \tag{4}$$

$$e_{xy} = \frac{\partial u}{\partial y} + \frac{\partial v}{\partial x} \tag{5}$$

Where u and v express the displacements in the x and y directions respectively. Since these three strain components are expressed only by two functions u and v , they cannot be taken arbitrarily and there exists a certain relation between the strain components. Differentiating equation (3) twice with respect to y, equation (4) twice with respect to x, equation (5) once with respect to x and once with respect to y, and simplifying these we obtain

$$\frac{\partial^2 e_{xy}}{\partial x \partial y} = \frac{\partial^2 e_{xx}}{\partial y^2} + \frac{\partial^2 e_{yy}}{\partial x^2} \tag{6}$$

This differential equation is called the condition of compatibility.

Using Hooke's law, the stress-strain relations for a two-dimensional stress field are written as follows :

$$e_{xx} = \frac{1}{E}(\sigma_{xx} - \nu \sigma_{yy}) \tag{7}$$

$$e_{yy} = \frac{1}{E}\left(\sigma_{yy} - \nu\,\sigma_{xx}\right) \tag{8}$$

$$e_{xy} = \frac{2(1+\nu)}{E}\,\tau_{xy} = \frac{\tau_{xy}}{G} \tag{9}$$

Substituting equations (7), (8), and (9) into (6) and simplifying, we get the condition of compatibility in terms of components of stresses as

$$\left(\frac{\partial^2}{\partial x^2} + \frac{\partial^2}{\partial y^2}\right)\left(\sigma_{xx} + \sigma_{yy}\right) = 0 \tag{10}$$

Thus the two-dimensional problem of determining the state of stress in a body under external forces reduces to the solution of equations (1) , (2), and (10) with the given boundary conditions.

Let the solution of the above problem be given by a stress function $\phi(x,y)$. The function $\phi(x,y)$ satisfies equations (1) and (2), if

$$\sigma_{xx} = \frac{\partial^2 \phi}{\partial y^2} \tag{11}$$

$$\sigma_{yy} = \frac{\partial^2 \phi}{\partial x^2} \tag{12}$$

$$\tau_{xy} = -\frac{\partial^2 \phi}{\partial x\,\partial y} \tag{13}$$

This gives a variety of solutions of the equations (1) and (2). The true solution $\phi(x,y)$ is that which also satisfies equation (10). In order to simplify the mathematical problem, equations (11), (12), and (13) are combined with equation (10) to yield,

$$\frac{\partial^4 \phi}{\partial x^4} + 2\frac{\partial^4 \phi}{\partial x^2 \partial y^2} + \frac{\partial^4 \phi}{\partial y^4} = 0 \tag{14}$$

Symbolically this equation is written as

$$\nabla^4 \phi = 0$$

Thus the problem has finally reduced to solving equations (14) with the given boundary conditions.

3.1.2 Boundary Conditions

Equation (14) is to be solved for two sets of boundary conditions given below :

External Boundary Conditions - These are obtained from the loading conditions stated in the problem.

Internal Boundary Conditions - The perfect bond between the material and the insert gives rise to these boundary conditions.

3.1.2.1 External Boundary Conditions

The specimen under consideration is loaded with uniform forces P_x , P_y , T_x , and T_y as shown in figure 1.

The values of function ϕ at the boundaries in terms of the known stresses are obtained as follows.

The direct stress σ_{yy} in terms of function ϕ is given by equation (12) on the boundary $y = \pm B/2$ the condition which the stress must satisfy is,

$$\sigma_{yy}\Big|_{\pm \frac{B}{2}} = \frac{P_y}{A_x} = \sigma'_{yy} \qquad (15)$$

By successive integration of equation (15) with respect to x, we get

$$\frac{\partial \phi}{\partial x} = \sigma'_{yy}\, x + C1 \qquad (16)$$

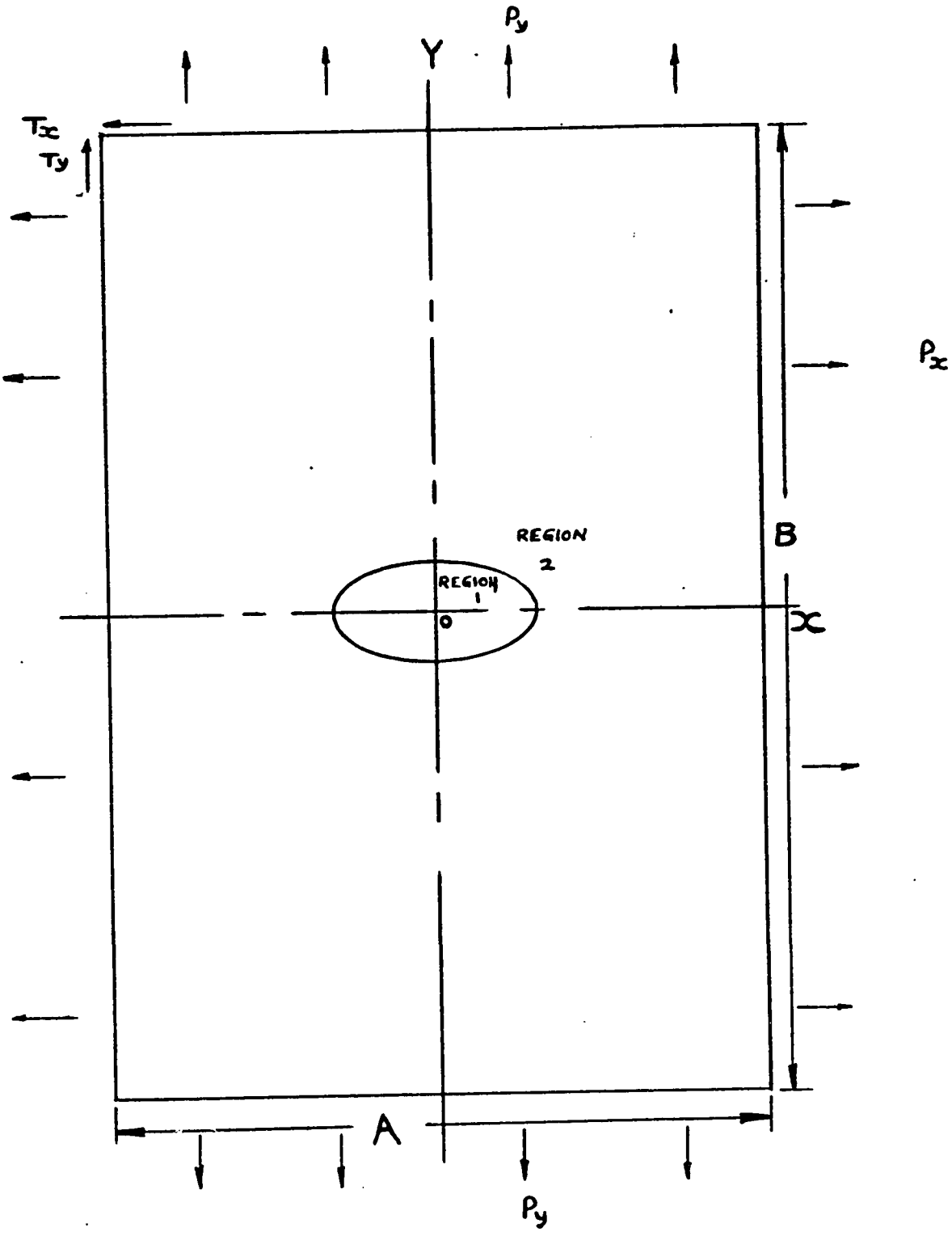

FIGURE 1

$$\phi = \sigma'_{yy} \frac{x^2}{2} + C1\,x + C2 \tag{17}$$

Because of the symmetric nature of the problem C1 and C2 are constants. The shearing stress τ_{xy} in terms of the function ϕ is given by equation (13). The shearing stress on the boundary is designated by τ'_{xy}. Integrating equation (13) with respect to x, we get

$$\frac{\partial \phi}{\partial y} = -\tau'_{xy}\,x + C3 \tag{18}$$

Similarly, using equation (11) and denoting the normal stress on the boundary $x = A/2$ by σ'_{xx}, it follows that

$$\sigma'_{xx} = \frac{P_x}{A_y} = \frac{\partial^2 \phi}{\partial y^2} \tag{19}$$

$$\frac{\partial \phi}{\partial y} = \sigma'_{xx}\,y + C4 \tag{20}$$

$$\phi = \sigma'_{xx} \frac{y^2}{2} + C4\,y + C5 \tag{21}$$

Proceeding in the same manner and specifying the shearing stress on the boundary by τ'_{xy} we get after integrating equation (13) with respect to y,

$$\frac{\partial \phi}{\partial x} = -\tau'_{xy}\,y + C6 \tag{22}$$

Since the stress pattern is symmetrical in all the four quadrants, it is sufficient to find the stresses in only one quadrant. Considering the portion of the specimen bounded between the positive x and y axes, the following relations hold good.

$$(\Phi)_{x=0.5A} = (\Phi)_{y=0.5B} \tag{23}$$

$$\left(\frac{\partial \Phi}{\partial x}\right)_{x=0.5A} = \left(\frac{\partial \Phi}{\partial x}\right)_{y=0.5B} \tag{24}$$

$$\left(\frac{\partial \Phi}{\partial y}\right)_{x=0.5A} = \left(\frac{\partial \Phi}{\partial y}\right)_{y=0.5B} \tag{25}$$

Also because of symmetry, at $x=0$, $\frac{\partial \Phi}{\partial x} = 0$ and at $y=0$, $\frac{\partial \Phi}{\partial y} = 0$. Therefore, from equation (16), $C1 = 0$ and from equation (20), $C4 = 0$. The constants C2, C3, C5, and C6 are obtained from equations (23), (24), and (25).

From equations (16), (22), and (24) we get

$$0.5A\,\sigma'_{yy} = -0.5B\,\tau'_{xy} + C6$$

From the above equation we write

$$C6 = 0.5\left(A\,\sigma'_{yy} + B\,\tau'_{xy}\right) \tag{26}$$

From equations (18), (20), and (25) we get

$$-0.5A\,\tau'_{xy} + C3 = 0.5B\,\sigma'_{xx}$$

From the abcve equation we write

$$C3 = 0.5\left(B\,\sigma'_{xx} + A\,\tau'_{xy}\right) \tag{27}$$

From equations (17), (21), and (23) we get

$$\frac{\sigma'_{yy}}{2}(0.5A)^2 + C2 = \frac{\sigma'_{xx}}{2}(0.5B)^2 + C5$$

The stresses being second derivatives of stress function ϕ, they are unaltered by any arbitrary choice of constants C2 or C5. Hence we set C5 = 0. Therefore, from the above equation

$$C2 = \frac{\sigma'_{xx}}{2} \; 0.25 \; B^2 - \frac{\sigma'_{yy}}{2} \; 0.25 \; A^2$$

Substituting these values of the constants in eqs. (16), (17), (18), (20), (21), and (22), we get

$$\phi = \frac{\sigma'_{yy}}{2} x^2 + \frac{\sigma'_{xx}}{2} \; 0.25 \; B^2 - \frac{\sigma'_{yy}}{2} \; 0.25 \; A^2 \qquad (17a)$$

$$\frac{\partial \phi}{\partial x} = \sigma'_{yy} \; x \qquad (16a)$$

$$\frac{\partial \phi}{\partial y} = - \tau'_{xy} \; x + \sigma'_{xx} \; 0.5 \; B + \tau'_{xy} \; 0.5 \; A \qquad (18a)$$

$$\phi = \frac{\sigma'_{xx}}{2} \; y^2 \qquad (21a)$$

$$\frac{\partial \phi}{\partial x} = - \tau'_{xy} \; y + 0.5 \; B \; \tau'_{xy} + 0.5 \; A \cdot \sigma'_{yy} \qquad (20a)$$

$$\frac{\partial \phi}{\partial y} = \sigma'_{xx} \cdot y \qquad (22a)$$

Thus, the function ϕ is completly defined in terms of known stresses at the external boundaries.

3.1.2.2 Internal Boundary Conditions

In the specimen when it is loaded, the amount of normal stress, shear stress and displacements along x and y axes experienced by the insert and the parent material at any point along the interface is exactly the same. This is due to perfect bond between them at the junction. Denoting the insert by subscript 1 and the parent material by 2, the four internal boundary conditions are written as :

Normal stress : $$(S_n)_1 = (S_n)_2 \quad (28)$$

Shear stress : $$(S_s)_1 = (S_s)_2 \quad (29)$$

Displacement along x-axis : $$(u)_1 = (u)_2 \quad (30)$$

Displacement along y-axis : $$(v)_1 = (v)_2 \quad (31)$$

The expressions for the normal and shear stress at a point on a curvilinear surface which is specified by the direction cosines (l, m) are

$$S_n = \sigma_{xx} l^2 + \sigma_{yy} m^2 + 2 \tau_{xy} l m \quad (32)$$

and

$$S_s = \sigma_{xx} l m - \sigma_{yy} l m - \tau_{xy} (l^2 - m^2) \quad (33)$$

Using relation (32) in equation (28), and (33) in equation (29) we get,

$$(\sigma_{xx})_1 l^2 + (\sigma_{yy})_1 m^2 + 2 (\tau_{xy})_1 l m$$

$$= (\sigma_{xx})_2 l^2 + (\sigma_{yy})_2 m^2 + 2 (\tau_{xy})_2 l m \quad (34)$$

and

$$(\sigma_{xx})_1 \, l\, m - (\sigma_{yy})_1 \, l\, m - (\tau_{xy})_1 (l^2 - m^2)$$

$$= (\sigma_{xx})_2 \, l\, m - (\sigma_{yy})_2 \, l\, m - (\tau_{xy})_2 (l^2 - m^2) \qquad (35)$$

Multiplying equation (34) by $(l^2 - m^2)$ and equation (35) by $2lm$ and adding we get

$$(\sigma_{xx})_1 (l^4 - l^2m^2 + 2l^2m^2) + (\sigma_{yy})_1 (l^2m^2 - m^4 - 2l^2m^2)$$

$$= (\sigma_{xx})_2 (l^4 - l^2m^2 + 2l^2m^2) + (\sigma_{yy})_2 (l^2m^2 - m^4 - 2l^2m^2)$$

Simplifying the above equation, we get

$$(\sigma_{yy})_1 m^2 - (\sigma_{xx})_1 l^2 = (\sigma_{yy})_2 m^2 - (\sigma_{xx})_2 l^2 \qquad (36)$$

Substituting for σ_{xx} and σ_{yy} from equations (11) and (12), we have

$$m^2 \left(\frac{\partial^2\phi}{\partial x^2}\right)_1 - l^2 \left(\frac{\partial^2\phi}{\partial y^2}\right)_1 = m^2 \left(\frac{\partial^2\phi}{\partial x^2}\right)_2 - l^2 \left(\frac{\partial^2\phi}{\partial y^2}\right) \qquad (36a)$$

To express this equation in a finite difference form, we refer to figure 2. This figure is the network of the points used for this conversion. The quantities δ and $C(\delta)$ represent standard horizontal and vertical step length respectively.

Thus equation (36a) is expressed in finite difference form as ,

$$m^2 \left[\frac{1}{m3(\delta^2)} \left[\frac{\phi 1(I-2, J)}{m4} - \phi 1(I-1, J)\left(\frac{1}{m4} + \frac{1}{m3}\right) + \frac{\phi 1(I, J)}{m3} \right] \right]$$

$$- l^2 \left[\frac{1}{m3(\delta^2)} \left[\frac{\phi 1(I, J-2)}{m4} - \phi 1(I, J-1)\left(\frac{1}{m3} + \frac{1}{m4}\right) + \frac{\phi 1(I, J)}{m3} \right] \right]$$

$$= m^2 \left[\frac{1}{m2(\delta^2)} \left[\frac{\Phi 2(I+2,J)}{m1} - \Phi 2(I+1,J)\left(\frac{1}{m1}+\frac{1}{m2}\right) + \frac{\Phi 2(I,J)}{m2} \right] \right]$$

$$- l^2 \left[\frac{1}{m2(\delta^2)} \left[\frac{\Phi 2(I,J+2)}{m1} - \Phi 2(I,J+1)\left(\frac{1}{m2}+\frac{1}{m1}\right) + \frac{\Phi 2(I,J)}{m2} \right] \right]$$

The coefficients m4,m3,m2,m1,n4,n3,n2, and n1 allow for the local variability of steps due to the boundary crossing the standard network. Combining the coefficients of $\phi 2(I,J)$, and rearranging we get

$$\Phi 2(I,J)_{I \text{ at } P2} = \Phi 1(I,J)_{I \text{ at } P2} \frac{m^2(m3)^2 - l^2(m3)^2}{(m3)^2(m3)^2} \frac{(m2)^2(m2)^2}{m^2(m2)^2 - l^2(m2)^2}$$

$$+ \frac{m^2}{(m3)^2} \frac{(m2)^2(m2)^2}{m^2(m2)^2 - l^2(m2)^2} \left(\frac{\Phi 1(I-2,J)}{m4} - \Phi 1(I-1,J)\left(\frac{1}{m4}+\frac{1}{m3}\right) \right)$$

$$- \frac{l^2}{(m3)^2} \frac{(m2)^2(m2)^2}{m^2(m2)^2 - l^2(m2)^2} \left(\frac{\Phi 1(I,J-2)}{m4} - \Phi 1(I,J-1)\left(\frac{1}{m3}+\frac{1}{m4}\right) \right)$$

$$- \frac{m^2}{m2} \frac{(m2)^2(m2)^2}{m^2(m2)^2 - l^2(m2)^2} \left(\frac{\Phi 2(I+2,J)}{m1} - \Phi 2(I+1,J)\left(\frac{1}{m1}+\frac{1}{m2}\right) \right)$$

$$+ \frac{l^2}{m2} \frac{(m2)^2(m2)^2}{m^2(m2)^2 - l^2(m2)^2} \left(\frac{\Phi 2(I,J+2)}{m1} - \Phi 2(I,J+1)\left(\frac{1}{m2}+\frac{1}{m1}\right) \right) \quad (37)$$

So far we have used only the boundary conditions for the stresses at the interface (equations 28 and 29) and arrived at the relation between $\phi 1(I,J)$ and $\phi 2(I,J)$. Now we proceed further to use displacement boundary conditions at the interface (equations 30 and 31) along with

$$= m^2 \left[\frac{1}{m2(\delta^2)} \left[\frac{\phi 2(I+2,J)}{m1} - \phi 2(I+1,J)\left(\frac{1}{m1}+\frac{1}{m2}\right) + \frac{\phi 2(I,J)}{m2} \right] \right]$$

$$- l^2 \left[\frac{1}{m2(\delta^2)} \left[\frac{\phi 2(I,J+2)}{m1} - \phi 2(I,J+1)\left(\frac{1}{m2}+\frac{1}{m1}\right) + \frac{\phi 2(I,J)}{m2} \right] \right]$$

The coefficients m4,m3,m2,m1,n4,n3,n2, and n1 allow for the local variability of steps due to the boundary crossing the standard network. Combining the coefficients of $\phi 2(I,J)$, and rearranging we get

$$\phi 2(I,J)_{I \text{ at } P2} = \phi 1(I,J)_{I \text{ at } P2} \frac{m^2(m3)^2 - l^2(m3)^2}{(m3)^2(m3)^2} \frac{(m2)^2(m2)^2}{m^2(m2)^2 - l^2(m2)^2}$$

$$+ \frac{m^2}{(m3)^2} \frac{(m2)^2(m2)^2}{m^2(m2)^2 - l^2(m2)^2} \left(\frac{\phi 1(I-2,J)}{m4} - \phi 1(I-1,J)\left(\frac{1}{m4}+\frac{1}{m3}\right) \right)$$

$$- \frac{l^2}{(m3)^2} \frac{(m2)^2(m2)^2}{m^2(m2)^2 - l^2(m2)^2} \left(\frac{\phi 1(I,J-2)}{m4} - \phi 1(I,J-1)\left(\frac{1}{m3}+\frac{1}{m4}\right) \right)$$

$$- \frac{m^2}{m2} \frac{(m2)^2(m2)^2}{m^2(m2)^2 - l^2(m2)^2} \left(\frac{\phi 2(I+2,J)}{m1} - \phi 2(I+1,J)\left(\frac{1}{m1}+\frac{1}{m2}\right) \right)$$

$$+ \frac{l^2}{m2} \frac{(m2)^2(m2)^2}{m^2(m2)^2 - l^2(m2)^2} \left(\frac{\phi 2(I,J+2)}{m1} - \phi 2(I,J+1)\left(\frac{1}{m2}+\frac{1}{m1}\right) \right) \quad (37)$$

So far we have used only the boundary conditions for the stresses at the interface (equations 28 and 29) and arrived at the relation between $\phi 1(I,J)$ and $\phi 2(I,J)$. Now we proceed further to use displacement boundary conditions at the interface (equations 30 and 31) along with

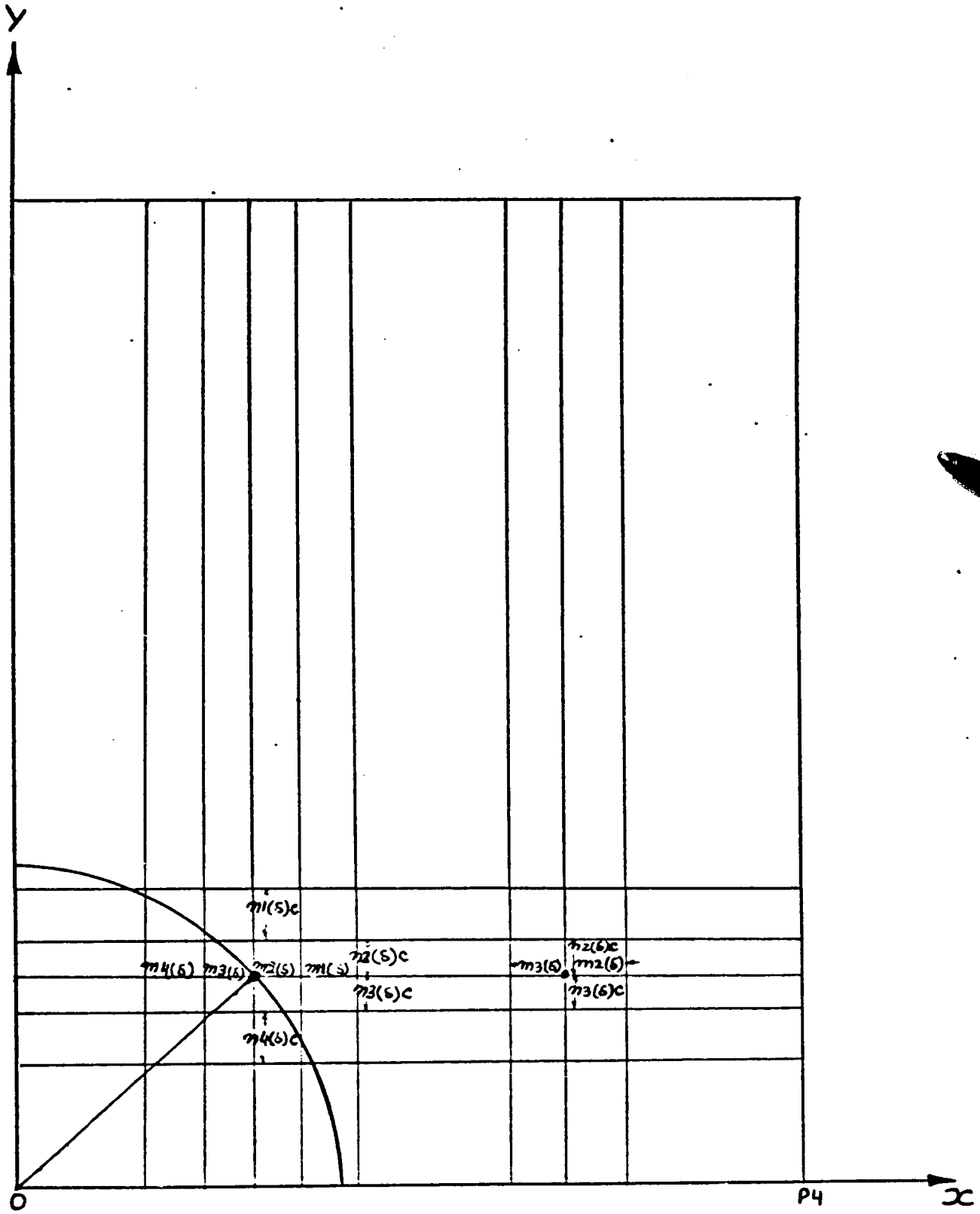

FIGURE 2

the known stresses on the external boundary to obtain the other relation in $\phi 1(I,J)$ and $\phi 2(I,J)$.

If the nodal line parallel to x-axis crosses the boundary, we utilize equation (30) i.e. $(u)_1 = (u)_2$ to obtain the relation between $\phi 1$ and $\phi 2$, and if it is parallel to y-axis, we use equation (31) i.e. $(v)_1 = (v)_2$. This would give us two equations with two unknowns. Solving these two equations we get $\phi 1(I,J)$ and $\phi 2(I,J)$ separately.

First we consider a point at the intersection of the internal boundary and the nodal line parallel to x-axis : Starting from point O in figure 2 where the displacement u is zero due to symmetry. The displacement at different points along x-axis are calculated using stress-strain and strain-displacement relations. Five-point Lagrangian method is used to calculate $\partial u/\partial x$ at the external boundary point P4 and is then equated to $\partial u/\partial x$ obtained from the known external boundary conditions.

From equations (3) and (7), we get

$$e_{xx} = \frac{\partial u}{\partial x} = \frac{1}{E}(\sigma_{xx} - \nu \sigma_{yy})$$

The number of mesh lines between any two consecutive points P_n and P_{n-1} or P_{n+1} is left completely arbitrary at this stage. These will be fixed at the time of numerical computations. As such, figure 3 is only partly representative of the actual grid-work. Making use of the mesh size shown in figure 3 and considering the variation in the deformation function as δu, we write

$$\delta u = \frac{\delta x}{E}(\sigma_{xx} - \nu \sigma_{yy}) \qquad (38)$$

In figure 3 the mesh size is varying from point to point. The point P0 which is also the centre of the specimen is located at the origin of the coordinate system.

Displacements at points P0, P1, and P2 are

$$u_{p0} = 0$$

$$u_{p1} = u_{p0} + \sum_{I=1}^{P1} (\delta u)_I$$

$$u_{p2} = u_{p1} + \sum_{I=P1+1}^{P2-2} (\delta u)_I$$

$$+ \left[\frac{1}{E_1} \left[\frac{1}{m2(\delta)^2} \left[\frac{\phi 1(I, J+1)}{m2} - \phi 1(I,J)\left(\frac{1}{m2} + \frac{1}{m3}\right) + \frac{\phi 1(I,J-1)}{m3} \right] \right. \right.$$

$$\left. \left. - \frac{\nu 1}{E_1} \left[\frac{1}{m2(\delta)^2} \left[\frac{\phi 1(I+1,J)}{m2} - \phi 1(I,J)\left(\frac{1}{m3} + \frac{1}{m2}\right) + \frac{\phi 1(I-1,J)}{m3} \right] \right] \right]_{I \text{ at } P2}$$

The coefficients m3, m2, n2, and n3 as shown in figure 2 take care of the variation of step length in x and y directions.

Rearranging, we get

$$u_{p2} = \sum_{I=1}^{P1} (\delta u)_I + \sum_{I \text{ at } P1}^{P2-2} (\delta u)_I - \left[\frac{\nu 1}{E1(\delta) m2} \phi 1(I+1, J) \right]_{I \text{ at } P2-1}$$

$$+ \frac{m2}{E_1(\delta) m2} \left[\frac{\phi 1(I, J+1)}{m2} - \phi 1(I,J)\left(\frac{1}{m2} + \frac{1}{n3}\right) + \frac{\phi 1(I,J-1)}{n3} \right]_{I \text{ at } P2-1}$$

$$- \frac{\nu 1}{E_1(\delta)} \left[\frac{\phi 1(I-1, J)}{m3} - \phi 1(I, J)\left(\frac{1}{m3} + \frac{1}{m2}\right) \right]_{I \text{ at } P2-1}$$

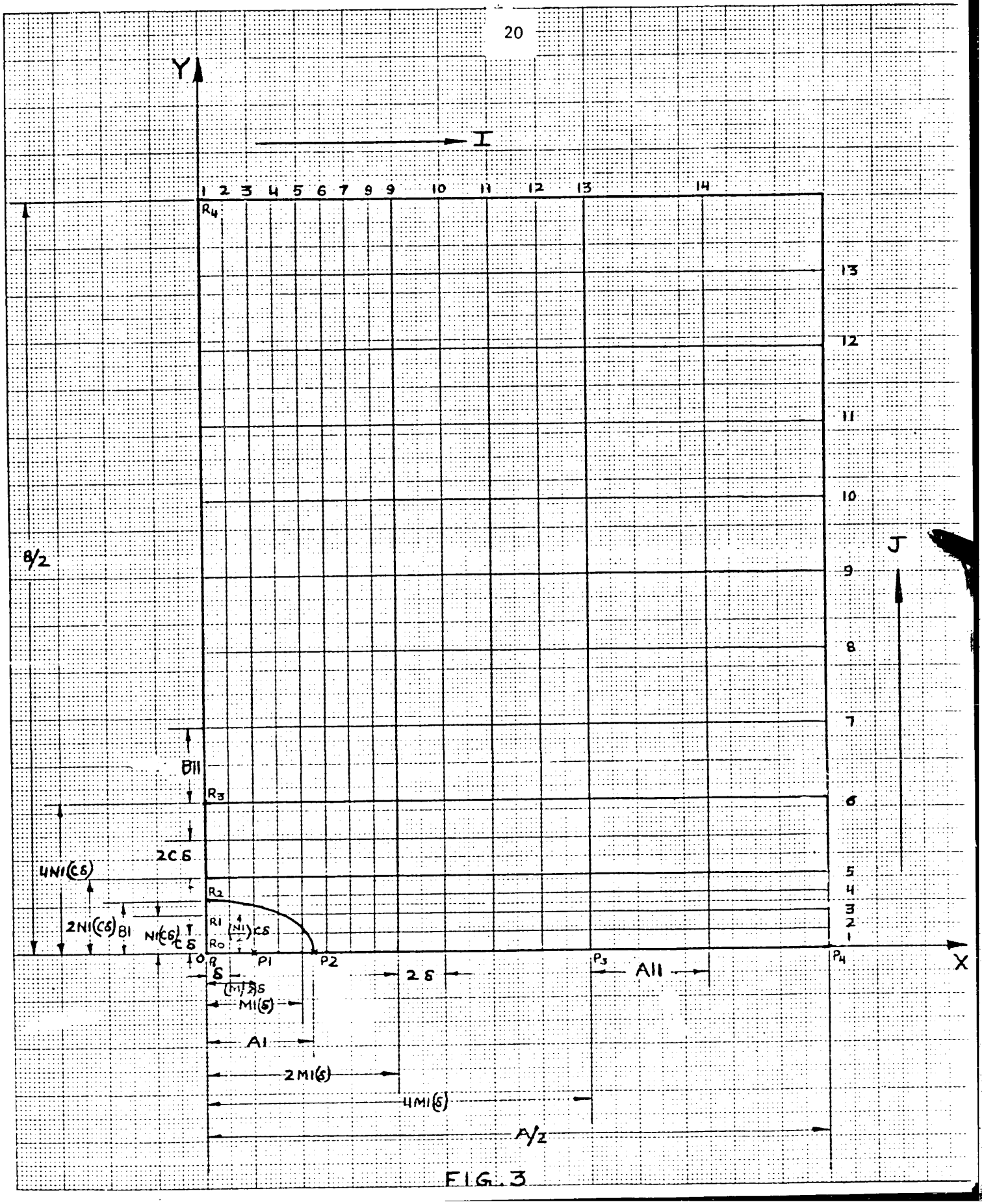
Y
I
J
X
1 2 3 4 5 6 7 8 9 10 11 12 13 14
R4
R3
R2
R1
R0
P1
P2
P3
P4
O
B/2
BII
2CS
4NI(CS)
2NI(CS)
BI
NI(CS)
CS
(NI/2)CS
δ
(MI)δ
MI(δ)
AI
2δ
AII
2MI(δ)
4MI(δ)
A/2

FIG. 3

In order to find the displacement at point P3 which lies in region 2, we use the displacement boundary condition $(u_{P2})_1 = (u_{P2})_2$. Hence, we get

$$u_{P3} = u_{P2} + \sum_{I \text{ at } P2+1}^{P3} (\delta u)_I$$

Substituting for u_{P2} and expressing δu in finite difference form at a point on the boundary i.e. at I= P2, we get

$$u_{P3} = \sum_{I=1}^{P1} (\delta u)_I + \sum_{I \text{ at } P1+1}^{P2-2} (\delta u)_I + \sum_{I \text{ at } (P2+1)}^{P3} (\delta u)_I$$

$$+ \frac{m2}{E_1(s)\, n2} \left[\frac{\phi 1(I, J+1)}{n2} - \phi 1(I,J)\left(\frac{1}{n2}+\frac{1}{n3}\right) + \frac{\phi 1(I,J)}{n3} \right]_{I \text{ at } P2-1}$$

$$- \frac{\nu 1}{E_1(s)} \left[\frac{\phi 1(I-1,J)}{n3} - \phi 1(I,J)\left(\frac{1}{n3}+\frac{1}{n2}\right) \right]_{I \text{ at } P2-1}$$

$$- \frac{\nu 1}{E_1(s)\, n2} \left[\phi 1(I+1, J) \right]_{I \text{ at } P2-1}$$

$$+ \left[\frac{1}{E_2} \left[\frac{1}{n2(s)^2} \left[\frac{\phi 2(I, J+2)}{n1} - \phi 2(I,J+1)\left(\frac{1}{n2}+\frac{1}{n1}\right) + \frac{\phi 2(I,J)}{n2} \right] \right] \right.$$

$$\left. - \frac{\nu 2}{E_2} \left[\frac{1}{n2(s)^2} \left[\frac{\phi 2(I+2,J)}{n1} - \phi 2(I+1,J)\left(\frac{1}{n1}+\frac{1}{n2}\right) + \frac{\phi 2(I,J)}{n2} \right] \right] n2(s) \right]_{I \text{ at } P2}$$

Rearranging, we get

$$u_{p3} = \sum_{I=1}^{p1} (\delta u)_I + \sum_{I \text{ at } p1}^{p2-2} (\delta u)_I + \sum_{I \text{ at } (p2+1)}^{p3} (\delta u)_I$$

$$+ \frac{m2}{E_1(\delta) n2} \left[\frac{\phi 1(I, J+1)}{n2} - \phi 1(I, J)\left(\frac{1}{m2} + \frac{1}{m3}\right) + \frac{\phi 1(I, J)}{m3} \right]_{I \text{ at } p2-1}$$

$$- \frac{\nu 1}{E_1(\delta)} \left[\frac{\phi 1(I-1, J)}{m3} - \phi 1(I, J)\left(\frac{1}{m3} + \frac{1}{m2}\right) \right]_{I \text{ at } p2-1}$$

$$- \frac{\nu 1}{E_1(\delta) m2} \left[\phi 1(I+1, J) \right]_{I \text{ at } p2-1}$$

$$+ \frac{m2}{E_2(\delta) n2} \left[\frac{\phi 2(I, J+2)}{m1} - \phi 2(I, J+1)\left(\frac{1}{m2} + \frac{1}{m1}\right) \right]_{I \text{ at } p2}$$

$$- \frac{\nu 2}{E_2(\delta)} \left[\frac{\phi 2(I+2, J)}{m1} - \phi 2(I+1, J)\left(\frac{1}{m1} + \frac{1}{m2}\right) \right]_{I \text{ at } p2}$$

$$+ \left[\frac{m2}{E_2(\delta) n2} \frac{\phi 2(I, J)}{n2} - \frac{\nu 2}{E_2(\delta)} \frac{\phi 2(I, J)}{m2} \right]_{I \text{ at } p2} \qquad (39)$$

Substituting the value of $\phi 2(I,J)_{I \text{ at } p2}$ from equation (37) into equation (39) and putting $XX = (m2/E_2(\delta)(n2)^2 - \nu 2/E_2 (\delta)\, m2)$, we get

$$U_{p3} = \sum_{I=1}^{p1} (\delta u)_I + \sum_{I \text{ at } p1}^{p2-2} (\delta u)_I + \sum_{I \text{ at } (p2+1)}^{p3} (\delta u)_I$$

$$+ \frac{m_2}{E_1(\delta)\, m_2} \left[\frac{\phi_1(I,J+1)}{m_2} - \phi_1(I,J)\left(\frac{1}{m_2} + \frac{1}{m_3}\right) + \frac{\phi_1(I,J)}{m_3} \right]_{I \text{ at } p2-1}$$

$$- \frac{\nu_1}{E_1(\delta)} \left[\frac{\phi_1(I-1,J)}{m_3} - \phi_1(I,J)\left(\frac{1}{m_2} + \frac{1}{m_3}\right) \right]_{I \text{ at } p2-1}$$

$$- \frac{\nu_1}{E_1(\delta)\, m_2} \left[\phi_1(I+1,J) \right]_{I \text{ at } p2-1}$$

$$+ \frac{m_2}{E_2(\delta)\, m_2} \left[\frac{\phi_2(I,J+2)}{m_1} - \phi_2(I,J+1)\left(\frac{1}{m_1} + \frac{1}{m_2}\right) \right]_{I \text{ at } p2}$$

$$- \frac{\nu_2}{E_2(\delta)} \left[\frac{\phi_2(I+2,J)}{m_1} - \phi_2(I+1,J)\left(\frac{1}{m_1} + \frac{1}{m_2}\right) \right]_{I \text{ at } p2}$$

$$+ XX \frac{m^2 (m_2)^2 (n_2)^2}{(m^2(m_2)^2 - l^2(m_2)^2)\, m_3} \left[\frac{\phi_1(I-2,J)}{m_4} - \phi_1(I-1,J)\left(\frac{1}{m_3} + \frac{1}{m_4}\right) \right]_{I \text{ at } p2}$$

$$- XX \frac{l^2}{m_3} \frac{(m_2)^2 (n_2)^2}{m^2(n_2)^2 - l^2(m_2)^2} \left[\frac{\phi_1(I,J-2)}{m_4} - \phi_1(I,J-1)\left(\frac{1}{m_3} + \frac{1}{m_4}\right) \right]_{I \text{ at } p2}$$

$$- XX \frac{m^2}{m_2} \frac{(m_2)^2 (n_2)^2}{m^2(n_2)^2 - l^2(m_2)^2} \left[\frac{\phi_2(I+2,J)}{m_1} - \phi_2(I+1,J)\left(\frac{1}{m_1} + \frac{1}{m_2}\right) \right]_{I \text{ at } p2}$$

$$+ XX \frac{l^2}{m_2} \frac{(m_2)^2 (n_2)^2}{m^2(n_2)^2 - l^2(m_2)^2} \left[\frac{\phi_2(I,J+2)}{m_1} - \phi_2(I,J+1)\left(\frac{1}{m_1} + \frac{1}{m_2}\right) \right]_{I \text{ at } p2}$$

$$+ XX \left[\frac{m^2 (m_3)^2 - l^2 (m_3)^2}{(m_3)^2 (n_3)^2} \; \frac{(m_2)^2 (n_2)^2}{m^2(n_2)^2 - l^2(m_2)^2} \right] \phi_1(I,J)_{I \text{ at } p2}$$

Displacement at point P4 is

$$u_{P4} = u_{P3} + \sum_{x \text{ at } P_{3+1}}^{P4} (\delta u)_x$$

Since we know $\partial u/\partial x$ at the edge of the specimen i.e. at point P4, we now proceed further to obtain $\partial u/\partial x$ from the previously evaluated displacements u_{P0}, u_{P1}, u_{P2}, u_{P3}, and u_{P4}. Use is made of the five-point Lagrangian method in evaluating these displacements gradients. Denoting the coordinates of points P0, P1, P2, P3, and P4 by x0, x1, x2, x3, and x4 respectively, the value of function u at any x is given as follows.

$$\begin{aligned} u = &\left[\frac{x-x1}{x0-x1} \quad \frac{x-x2}{x0-x2} \quad \frac{x-x3}{x0-x3} \quad \frac{x-x4}{x0-x4}\right] u_{P0} \\ &+ \left[\frac{x-x0}{x1-x0} \quad \frac{x-x2}{x1-x2} \quad \frac{x-x3}{x1-x3} \quad \frac{x-x4}{x1-x4}\right] u_{P1} \\ &+ \left[\frac{x-x0}{x2-x0} \quad \frac{x-x1}{x2-x1} \quad \frac{x-x3}{x2-x3} \quad \frac{x-x4}{x2-x4}\right] u_{P2} \\ &+ \left[\frac{x-x0}{x3-x0} \quad \frac{x-x1}{x3-x1} \quad \frac{x-x2}{x3-x2} \quad \frac{x-x4}{x3-x4}\right] u_{P3} \\ &+ \left[\frac{x-x0}{x4-x0} \quad \frac{x-x1}{x4-x1} \quad \frac{x-x2}{x4-x2} \quad \frac{x-x3}{x4-x3}\right] u_{P4} \end{aligned}$$

Differentiating function u with respect to x, we get

$$\begin{aligned} \left(\frac{\partial u}{\partial x}\right) = &\frac{u_{P0}}{(x0-x1)(x0-x2)(x0-x3)(x0-x4)} \\ &\left[(x-x2)(x-x3)(x-x4) + (x-x1)(x-x3)(x-x4) + (x-x1)(x-x2)(x-x4) \right. \\ &\left. + (x-x1)(x-x2)(x-x3)\right] \\ &+ \frac{u_{P1}}{(x1-x0)(x1-x2)(x1-x3)(x1-x4)} \\ &\left[(x-x2)(x-x3)(x-x4) + (x-x0)(x-x3)(x-x4) + (x-x0)(x-x2)(x-x4) \right. \\ &\left. + (x-x0)(x-x2)(x-x3)\right] \end{aligned}$$

$$+ \frac{u_{p2}}{(x_2-x_0)(x_2-x_1)(x_2-x_3)(x_2-x_4)}$$

$$\left[(x-x_1)(x-x_3)(x-x_4) + (x-x_0)(x-x_3)(x-x_4) + (x-x_0)(x-x_1)(x-x_4) + (x-x_0)(x-x_1)(x-x_3) \right]$$

$$+ \frac{u_{p3}}{(x_3-x_0)(x_3-x_1)(x_3-x_2)(x_3-x_4)}$$

$$\left[(x-x_1)(x-x_2)(x-x_4) + (x-x_0)(x-x_2)(x-x_4) + (x-x_0)(x-x_1)(x-x_4) + (x-x_0)(x-x_1)(x-x_2) \right]$$

$$+ \frac{u_{p4}}{(x_4-x_0)(x_4-x_1)(x_4-x_2)(x_4-x_3)}$$

$$\left[(x-x_1)(x-x_2)(x-x_3) + (x-x_0)(x-x_2)(x-x_3) + (x-x_0)(x-x_1)(x-x_3) + (x-x_0)(x-x_1)(x-x_2) \right]$$

The slope $\frac{\partial u}{\partial x}$, at P4 is

$$\left(\frac{\partial u}{\partial x}\right)_{x=x_4} = \frac{(x_4-x_1)(x_4-x_2)(x_4-x_3)}{(x_0-x_1)(x_0-x_2)(x_0-x_3)(x_0-x_4)} u_{p0}$$

$$+ \frac{(x_4-x_0)(x_4-x_2)(x_4-x_3)}{(x_1-x_0)(x_1-x_2)(x_1-x_3)(x_1-x_4)} u_{p1}$$

$$+ \frac{(x_4-x_0)(x_4-x_1)(x_4-x_3)}{(x_2-x_0)(x_2-x_1)(x_2-x_3)(x_2-x_4)} u_{p2}$$

$$+ \frac{(x_4-x_0)(x_4-x_1)(x_4-x_2)}{(x_3-x_0)(x_3-x_1)(x_3-x_2)(x_3-x_4)} u_{p3}$$

$$+\left[\frac{1}{x_4-x_0}+\frac{1}{x_4-x_1}+\frac{1}{x_4-x_2}+\frac{1}{x_4-x_3}\right] u_{p4} \quad (40)$$

For simplicity let us put

$$L0 = \frac{(x_4-x_1)(x_4-x_2)(x_4-x_3)}{(x_0-x_1)(x_0-x_2)(x_0-x_3)(x_0-x_4)}$$

$$L1 = \frac{(x_4-x_0)(x_4-x_2)(x_4-x_3)}{(x_1-x_0)(x_1-x_2)(x_1-x_3)(x_1-x_4)}$$

$$L2 = \frac{(x_4-x_0)(x_4-x_1)(x_4-x_3)}{(x_2-x_0)(x_2-x_1)(x_2-x_3)(x_2-x_4)}$$

$$L3 = \frac{(x_4-x_0)(x_4-x_1)(x_4-x_2)}{(x_3-x_0)(x_3-x_1)(x_3-x_2)(x_3-x_4)}$$

$$L4 = \frac{1}{x_4-x_0}+\frac{1}{x_4-x_1}+\frac{1}{x_4-x_2}+\frac{1}{x_4-x_3}$$

Substituting u_{P0}, u_{P1}, u_{P2}, u_{P3}, and u_{P4} into equation (40), we get

$$\left(\frac{\partial u}{\partial x}\right)_{x=x_4} = L0(x_0) + L1 \sum_{I=1}^{P1} (\delta u)_I + \left[L2 \sum_{I=1}^{P1} (\delta u)_I + L2 \sum_{I \text{ at } P1+1}^{P2-2} (\delta u)_I - \frac{\nu_1}{E1(\delta) m_2} L2 \; \phi 1(I+1, J)_{I \text{ at } (P2-1)} + L2 \frac{m_2}{m_1(\delta) E_1} \left[\frac{\phi 1(I, J+1)}{m_2} - \phi 1(I, J)\left(\frac{1}{m_2}+\frac{1}{m_3}\right) + \frac{\phi 1(I, J-1)}{m_3} \right]_{I \text{ at } P2} - L2 \frac{\nu_1}{E_1(\delta)} \left[\phi 1(I-1, J) - \phi 1(I, J)\left(\frac{1}{m_3}+\frac{1}{m_2}\right) \right]_{I \text{ at } P2-1} \right]$$

$$+\left[L3 \sum_{I=1}^{P1} (\delta u)_I + L3 \sum_{I \text{ at } (P1+1)}^{P2-2} (\delta u)_I - L3 \frac{\nu_1}{m2(\delta) E_1} \phi 1(I+1, J) \right]_{I \text{ at } P2-1}$$

$$+ L3 \frac{m2}{m2(\delta) E_1} \left[\frac{\phi 1(I, J+1)}{m2} - \phi 1(I, J)\left(\frac{1}{m2} + \frac{1}{m3}\right) + \frac{\phi 1(I, J-1)}{m3} \right]_{I \text{ at } P2-1}$$

$$- L3 \frac{\nu_1}{E_1(\delta)} \left[\frac{\phi 1(I-1, J)}{m3} - \phi 1(I, J)\left(\frac{1}{m2} + \frac{1}{m3}\right) \right]_{I \text{ at } P2-1}$$

$$+ L3 \frac{m2}{m2(\delta) E_2} \left[\frac{\phi 2(I, J+2)}{m1} - \phi 2(I, J+1)\left(\frac{1}{m1} + \frac{1}{m2}\right) \right]_{I \text{ at } P2}$$

$$- L3 \frac{\nu_2}{E_2(\delta)} \left[\frac{\phi 2(I+2, J)}{m1} - \phi 2(I+1, J)\left(\frac{1}{m1} + \frac{1}{m2}\right) \right]_{I \text{ at } P2}$$

$$+ L3 \sum_{I \text{ at } P2+1}^{P3} (\delta u)_I + L3 \, XX \, \phi 1(I, J)_{I \text{ at } P2} \frac{m^2 (m3)^2 - l^2 (m3)^2}{(m3)^2 (m3)^2} \frac{(m2)^2 (n2)^2}{m^2 (n2)^2 - l^2 (m2)^2}$$

$$+ L3 (XX) \frac{m^2}{m3} \frac{(m2)^2 (n2)^2}{m^2 (n2)^2 - l^2 (m2)^2} \left[\frac{\phi 1(I-2, J)}{m4} - \phi 1(I-1, J)\left(\frac{1}{m3} + \frac{1}{m4}\right) \right]$$

$$- L3 (XX) \frac{l^2}{m3} \frac{(m2)^2 (n2)^2}{m^2 (n2)^2 - l^2 (m2)^2} \left[\frac{\phi 1(I, J-2)}{m4} - \phi 1(I, J-1)\left(\frac{1}{m3} + \frac{1}{m4}\right) \right]_{I \text{ at } P2}$$

$$- L3 (XX) \frac{m^2}{m2} \frac{(m2)^2 (n2)^2}{m^2 (n2)^2 - l^2 (m2)^2} \left[\frac{\phi 2(I+2, J)}{m1} - \phi 2(I+1, J)\left(\frac{1}{m1} + \frac{1}{m2}\right) \right]_{I \text{ at } P2}$$

$$+ L3 (XX) \frac{l^2}{n2} \frac{(m2)^2 (n2)^2}{m^2 (n2)^2 - l^2 (m2)^2} \left[\frac{\phi 2(I, J+2)}{m1} - \phi 2(I, J+1)\left(\frac{1}{m1} + \frac{1}{m2}\right) \right]_{I \text{ at } P2}$$

$$+ \left[L4 \sum_{I \text{ at } (P3+1)}^{P4} (\delta u)_I + L4 \sum_{I=1}^{P1} (\delta u)_I + L4 \sum_{I \text{ at } (P1+1)}^{P2-2} (\delta u)_I \right.$$

$$+ L4\,\frac{m2}{E_1(\delta)\,m2}\left[\frac{\phi1(I,J+1)}{m2} - \phi1(I,J)\left(\frac{1}{m2}+\frac{1}{m3}\right) + \frac{\phi1(I,J-1)}{m3}\right]_{I \text{ at } P2-1}$$

$$- L4\,\frac{\mu_1}{E_1(\delta)}\left[\frac{\phi1(I-1,J)}{m3} - \phi1(I,J)\left(\frac{1}{m2}+\frac{1}{m3}\right)\right]_{I \text{ at } P2-1}$$

$$- L4\,\frac{\mu_1}{E_1(\delta)\,m2}\;\phi1(I+1,J)_{I \text{ at } P2-1}$$

$$+ L4\,\frac{m2}{E_2(\delta)\,m2}\left[\frac{\phi2(I,J+2)}{m1} - \phi2(I,J+1)\left(\frac{1}{m1}+\frac{1}{m2}\right)\right]_{I \text{ at } P2}$$

$$- L4\,\frac{\mu_2}{E_2(\delta)}\left[\frac{\phi2(I+2,J)}{m1} - \phi2(I+1,J)\left(\frac{1}{m1}+\frac{1}{m2}\right)\right]_{I \text{ at } P2}$$

$$+ L4\sum_{I \text{ at } P2+1}^{P3}(\delta4)_I + L4(XX)\left[\frac{m^2(m3)^2 - l^2(m3)^2}{(m3)^2(m3)^2}\,\frac{(m2)^2(m2)^2}{m^2(m2)^2 - l^2(m2)^2}\right]\phi1(I,J)_{I \text{ at } P2}$$

$$+ L4(XX)\,\frac{m^2}{m3}\,\frac{(m2)^2(m2)^2}{m^2(m2)^2 - l^2(m2)^2}\left[\frac{\phi1(I-2,J)}{m4} - \phi1(I-1,J)\left(\frac{1}{m3}+\frac{1}{m4}\right)\right]_{I \text{ at } P2}$$

$$- L4(XX)\,\frac{l^2}{m3}\,\frac{(m2)^2(m2)^2}{m^2(m2)^2 - l^2(m2)^2}\left[\frac{\phi1(I,J-2)}{m4} - \phi1(I,J-1)\left(\frac{1}{m3}+\frac{1}{m4}\right)\right]_{I \text{ at } P2}$$

$$- L4(XX)\,\frac{m^2}{m2}\,\frac{(m2)^2(m2)^2}{m^2(m2)^2 - l^2(m2)^2}\left[\frac{\phi2(I+2,J)}{m1} - \phi2(I+1,J)\left(\frac{1}{m1}+\frac{1}{m2}\right)\right]_{I \text{ at } P2}$$

$$+ L4(XX)\,\frac{m^2}{m2}\,\frac{(m2)^2(m2)^2}{m^2(m2)^2 - l^2(m2)^2}\left[\frac{\phi2(I,J+2)}{m1} - \phi2(I,J+1)\left(\frac{1}{m1}+\frac{1}{m2}\right)\right]_{I \text{ at } P2}$$

From equations (3) and (7) the slope at P4 is

$$\left(\frac{\partial u}{\partial x}\right)_{x=x4} = \frac{1}{E_2}\left(\sigma_{xx} - \nu_2\,\sigma_{yy}\right)$$

In this equation σ_{xx} is known directly from the boundary conditions and we express σ_{yy} in terms of stress function ϕ to obtain,

$$\left(\frac{\partial u}{\partial x}\right)_{x=x4} = \frac{1}{E_2}\,\sigma'_{xx} - \frac{\nu_2}{E_2}\left(\frac{\partial^2 \phi}{\partial x^2}\right)_{x=x4}$$

This appears in finite difference form as

$$\left(\frac{\partial u}{\partial x}\right)_{x=x4} = \frac{1}{E_2}\,\sigma'_{xx} - \frac{\nu_2}{E_2}\left[\frac{\phi 2(I-2,J) - 2\,\phi 2(I-1,J) + \phi 2(I,J)}{(\Delta 11)^2}\right]_{I \text{ at } P4} \quad (42)$$

The coefficient, say AX, of $\phi 1(I,J)_{I \text{ at } P2}$ in equation (41) is

$$AX = \frac{\nu_1}{E_1(\delta)\,m2}\left(L2+L3+L4\right) - (L3+L4)(XX)\,\frac{m^2(m3)^2 - l^2(m3)^2}{(m3)^2(m3)^2}\,\frac{(m2)^2\,(m2)^2}{m^2(m2)^2 - l^2(m2)^2}$$

Comparing equations (41) and (42), we get the value of the function ϕ for the region 1 at the boundary of the insert and the parent material as

$$\phi 1\,(I,J)_{I \text{ at } P2} = \frac{1}{AX}\Bigg[(\delta u)_I\,(L1+L2+L3+L4) + \sum_{I \text{ at } P1+1}^{P2-2}(\delta u)_I\,(L2+L3+L4) + \sum_{I \text{ at } (P2+1)}^{P3}(\delta u)_I\,(L3+L4) + L4\sum_{I \text{ at } (P3+1)}^{P4}(\delta u)_I - (L2+L3+L4)\,\frac{\nu_1}{E_1(\delta)}\left[\frac{\phi 1(I-1,J)}{m3} - \phi 1(I,J)\left(\frac{1}{m_2}+\frac{1}{m3}\right)\right]_{I \text{ at } P2-1}$$

$$+(L2+L3+L4)\frac{m2}{E_1(\delta)\,n2}\left[\frac{\phi1(I,J+1)}{n2}-\phi1(I,J)\left(\frac{1}{n2}+\frac{1}{n3}\right)+\frac{\phi1(I,J-1)}{n3}\right]$$

$$+(L3+L4)\frac{m2}{E_2(\delta)\,n2}\left[\frac{\phi2(I,J+2)}{n1}-\phi2(I,J+1)\left(\frac{1}{n1}+\frac{1}{n2}\right)\right]_{I\text{ at }P2-1}^{I\text{ at }P2}$$

$$-(L3+L4)\frac{\mu_2}{E_2(\delta)}\left[\frac{\phi2(I+2,J)}{n1}-\phi2(I+1,J)\left(\frac{1}{n1}+\frac{1}{n2}\right)\right]_{I\text{ at }P2}$$

$$+(L3+L4)(XX)\frac{m^2}{n3}\frac{(n2)^2(n2)^2}{m^2(n2)^2-l^2(n2)^2}\left[\frac{\phi1(I-2,J)}{n4}-\phi1(I-1,J)\left(\frac{1}{n3}+\frac{1}{n4}\right)\right]_{I\text{ at }P2}$$

$$-(L3+L4)(XX)\frac{l^2}{n3}\frac{(n2)^2(n2)^2}{m^2(n2)^2-l^2(n2)^2}\left[\frac{\phi1(I,J-2)}{n4}-\phi1(I,J-1)\left(\frac{1}{n3}+\frac{1}{n4}\right)\right]_{I\text{ at }P2}$$

$$-(L3+L4)(XX)\frac{m^2}{n2}\frac{(n2)^2(n2)^2}{m^2(n2)^2-l^2(n2)^2}\left[\frac{\phi2(I+2,J)}{n1}-\phi2(I+1,J)\left(\frac{1}{n1}+\frac{1}{n2}\right)\right]_{I\text{ at }P2}$$

$$+(L3+L4)(XX)\frac{l^2}{n2}\frac{(n2)^2(n2)^2}{m^2(n2)^2-l^2(n2)^2}\left[\frac{\phi2(I,J+2)}{n1}-\phi2(I,J+1)\left(\frac{1}{n1}+\frac{1}{n2}\right)\right]_{I\text{ at }P2}$$

$$-\frac{1}{E_2}\sigma'_{xx}+\frac{\mu_2}{E_2}\left[\frac{\phi2(I-2,J)-2\phi2(I-1,J)+\phi2(I,J)}{(A11)^2}\right]_{I\text{ at }P4}\qquad(43)$$

Once $\phi1(I,J)_{I\text{ at }P2}$ is found, then $\phi2(I,J)_{I\text{ at }P2}$ is calculated with the help of equation (37).

Proceeding as before an equation similar to equation (43) can be obtained for a point at the intersection of the boundary and a nodal line parallel to y-axis. This yields the following equation.

$$\phi 1(I,J)_{J \text{ at } R2} = \frac{1}{BB}\Bigg[\sum_{J=1}^{R1} (\delta v)_I \,(M1+M2+M3+M4)$$

$$+ \sum_{J \text{ at } R1+1}^{R2-2} (\delta u)_J \,(M2+M3+M4) + \sum_{J \text{ at } R2+1}^{R3} (\delta u)_J \,(M3+M4)$$

$$+ M4 \sum_{J \text{ at } R3+1}^{R4} (\delta u)_J$$

$$+(M2+M3+M4)\frac{m2}{E_1(\delta)\,m2}\left[\frac{\phi 1(I+1,J)}{m2} - \phi 1(I,J)\left(\frac{1}{m2}+\frac{1}{m3}\right) + \frac{\phi 1(I-1,J)}{m3}\right]_{J \text{ at } R2-1}$$

$$-(M2+M3+M4)\frac{\nu_1}{E_1(\delta)}\left[\frac{\phi 1(I,J-1)}{m3} - \phi 1(I,J)\left(\frac{1}{m2}+\frac{1}{m3}\right)\right]_{J \text{ at } R2-1}$$

$$+ (M3+M4)\frac{m2}{E_2(\delta)\,m2}\left[\frac{\phi 2(I+2,J)}{m1} - \phi 2(I+1,J)\left(\frac{1}{m1}+\frac{1}{m2}\right)\right]_{J \text{ at } R2}$$

$$- (M3+M4)\frac{\nu_2}{E_2(\delta)}\left[\frac{\phi 2(I,J+2)}{m1} - \phi 2(I,J+1)\left(\frac{1}{m1}+\frac{1}{m2}\right)\right]_{J \text{ at } R2}$$

$$+ (M3+M4)(yy)\frac{m^2}{m3}\,\frac{(m2)^2(m2)^2}{m^2(m2)^2 - l^2(m2)^2}\left[\frac{\phi 1(I-2,J)}{m4} - \phi 1(I-1,J)\left(\frac{1}{m3}+\frac{1}{m4}\right)\right]_{J \text{ at } R2}$$

$$-(M3+M4)(YY)\frac{l^2}{m3}\frac{(m2)^2(n2)^2}{m^2(n2)^2-l^2(m2)^2}\left[\frac{\phi 1(I,J-2)}{n4}-\phi 1(I,J-1)\left(\frac{1}{n3}+\frac{1}{n4}\right)\right]_{J\text{ at }R2}$$

$$-(M3+M4)(YY)\frac{m^2}{m2}\frac{(m2)^2(n2)^2}{m^2(n2)^2-l^2(m2)^2}\left[\frac{\phi 2(I+2,J)}{n1}-\phi 2(I+1,J)\left(\frac{1}{m1}+\frac{1}{m2}\right)\right]_{J\text{ at }R2}$$

$$+(M3+M4)(YY)\frac{l^2}{m2}\frac{(m2)^2(n2)^2}{m^2(n2)^2-l^2(m2)^2}\left[\frac{\phi 2(I,J+2)}{n1}-\phi 2(I,J+1)\left(\frac{1}{m1}+\frac{1}{n2}\right)\right]_{J\text{ at }R2}$$

$$-\frac{1}{E_2}\sigma'_{yy}+\frac{\nu_2}{E_2}\left[\frac{\phi 2(I,J-2)-2\phi 2(I,J-1)+\phi 2(I,J)}{(B11)^2}\right]_{J\text{ at }R4} \qquad (44)$$

Where

$$YY=\frac{n2}{E_2(6)(m2)^2}-\frac{\nu_2}{E_2(6)\,n2}$$

$$BB=\frac{\nu_1}{E_1(6)\,n2}(M2+M3+M4)-(M3+M4)\,YY\;\frac{m^2(n3)^2-l^2(m3)^2}{(m3)^2(n3)^2}\;\frac{(m2)^2(n2)^2}{m^2(n2)^2-l^2(m2)^2}$$

The values of M0, M1, M2, M3, and M4 are the same as those of L0, L1, L2, L3, and L4 except change x to y.

3.1.3 Numerical Procedure

A finite difference method for solving the Biharmonic equation $\nabla^4\phi = 0$ was adopted in order to get an overall picture of stress distribution in a specimen. To provide a mathematical tool of fairly wide scope, a computer program of sufficient flexibility was written to permit the study of any insert possessing two axes of symmetry without being restricted specifically to ellipses. This flexibility causes the program to be very complicated and that is why seven versions of the Biharmonic equation $\nabla^4\phi = 0$ had to be derived in finite difference form. When this equation is written at the nodal points, there will be cases when some points lie outside the region bounded by the internal boundary as shown in figure 4. Because of this we have three versions of equation (43) and similar three of equation (44). Due to symmetry, only one quarter of the specimen was taken and was divided into a number of steps along x and y axes. The steps are of variable length, being the smallest near the boundary of the insert and the parent material and getting larger as they fall away from the boundary. This was made so because the variation of stress is large near this boundary. The variation of step length was decided from experimental data.

The derivation of equation $\nabla^4\phi = 0$ in a central difference form is presented here and only the final equations of other six versions of this equation are given as these follow the same procedure for their derivation.

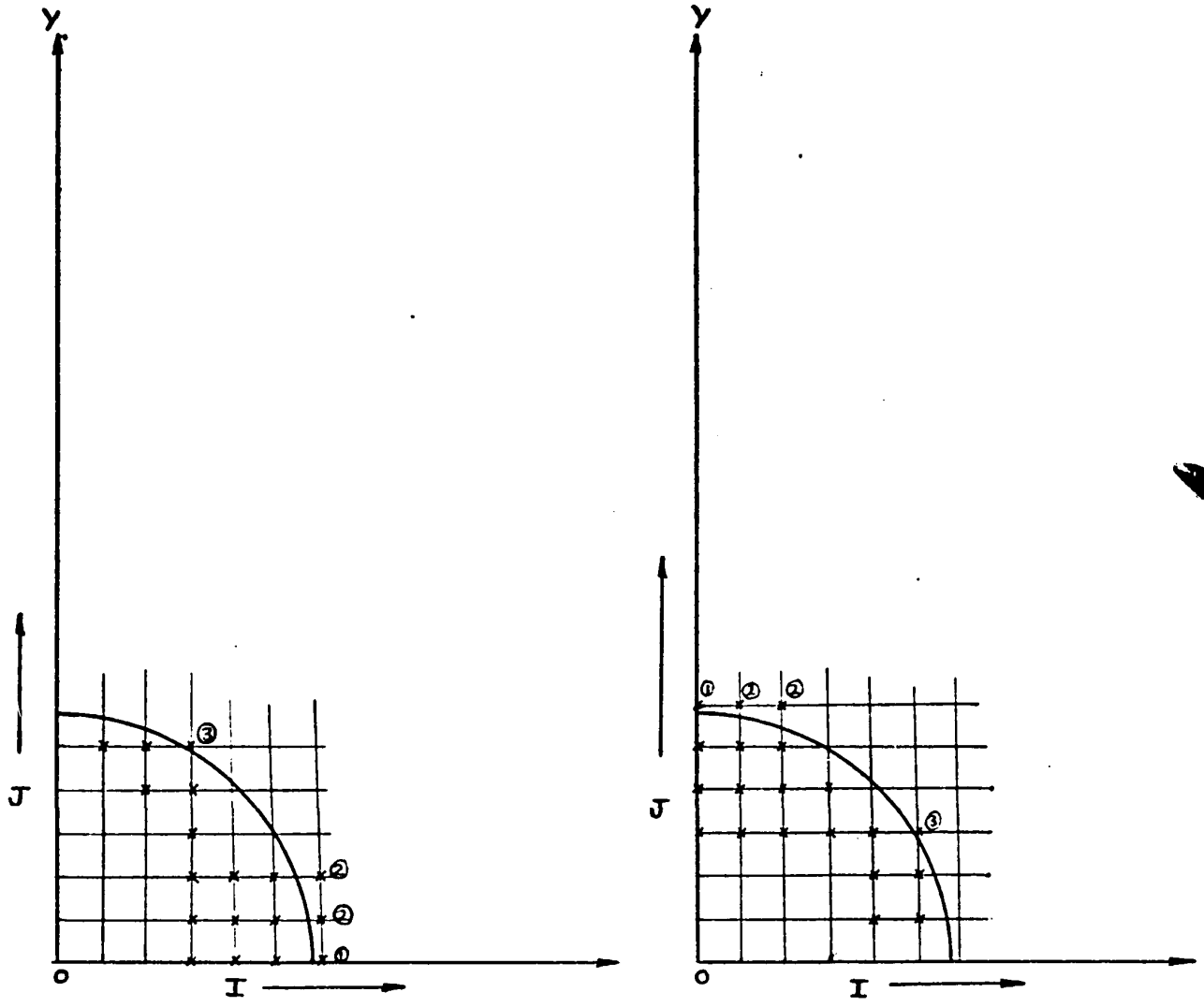

FIGURE 4

3.1.3.1 Finite Difference Versions of The Biharmonic Equation

Derivation of the Biharmonic equation in central difference form:

The Biharmonic equation as mentioned earlier is

$$\frac{\partial^4 \phi}{\partial x^4} + 2 \frac{\partial^4 \phi}{\partial x^2 \partial y^2} + \frac{\partial^4 \phi}{\partial y^4} = 0 \qquad (14)$$

Figure 5 shows the network of points used for conversion of the above differential equation into central difference form. Similar figures (figure 6 to figure 11) are drawn subsequently for the points near a boundary, where either the backward or the forward finite difference formulae had to be used. In all these figures δ represents the standard horizontal step and c(δ) represents the standard vertical step. In addition, the coefficients m1, m2, m3, m4, n1, n2, n3, and n4 allow for the local variability of step due to the boundary crossing the standard network.

The approximate values of the partial derivatives of Φ with respect to x at a point 0 are

$$\left(\frac{\partial \phi}{\partial x}\right)_0 \approx \frac{\phi 1 - \phi 0}{\delta (m_2)}$$

$$\left(\frac{\partial^2 \phi}{\partial x^2}\right)_0 \approx \frac{1}{\delta(m_2)} \left[\left(\frac{\partial \phi}{\partial x}\right)_1 - \left(\frac{\partial \phi}{\partial x}\right)_0 \right]$$

$$\approx \frac{1}{\delta^2(m_2)} \left[\frac{\phi 1 - \phi 0}{m_2} - \frac{\phi_0 - \phi_3}{m_3} \right] \qquad (45)$$

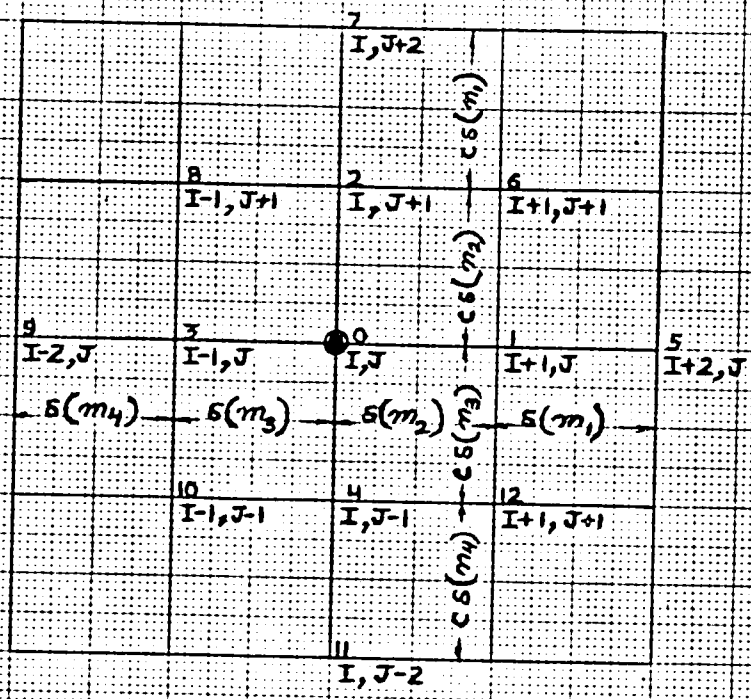
7
I, J+2
8
I-1, J+1
2
I, J+1
6
I+1, J+1
9
I-2, J
3
I-1, J
0
I, J
1
I+1, J
5
I+2, J
10
I-1, J-1
4
I, J-1
12
I+1, J+1
11
I, J-2
δ(m4)
δ(m3)
δ(m2)
δ(m1)
cδ(m1)
cδ(m2)
cδ(m3)
cδ(m4)

FIG. 5

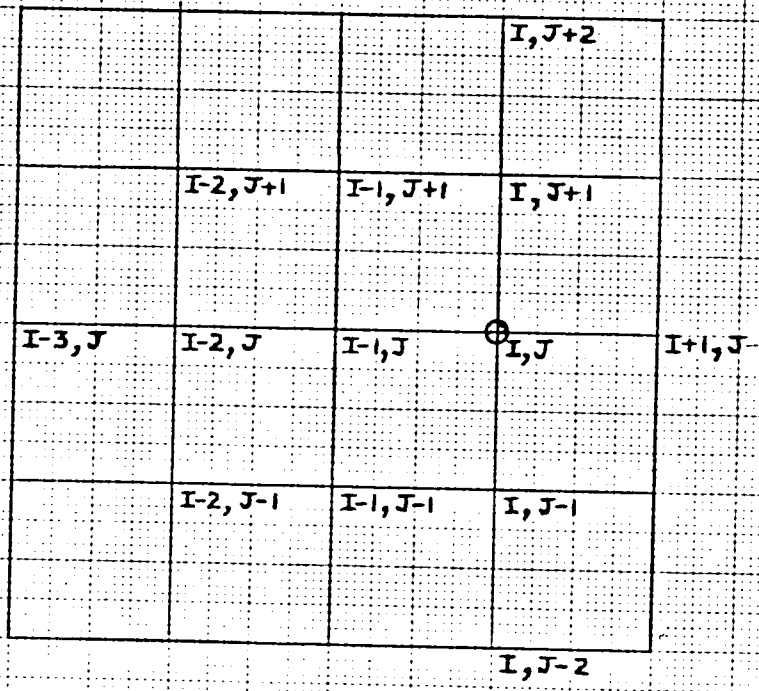
I, J+2
I-2, J+1
I-1, J+1
I, J+1
I-3, J
I-2, J
I-1, J
I, J
I+1, J
I-2, J-1
I-1, J-1
I, J-1
I, J-2

FIG. 6

Similarly for point 1 and 3

$$\left(\frac{\partial^2\phi}{\partial x^2}\right)_1 \approx \frac{1}{\delta^2(m1)}\left[\frac{\phi_5-\phi_1}{m1} - \frac{\phi_1-\phi_0}{m2}\right] \quad (46)$$

$$\left(\frac{\partial^2\phi}{\partial x^2}\right)_3 \approx \frac{1}{\delta^2(m3)}\left[\frac{\phi_0-\phi_3}{m3} - \frac{\phi_3-\phi_9}{m4}\right] \quad (47)$$

Considering the fourth derivative of ϕ with respect to x we note that,

$$\left(\frac{\partial^4\phi}{\partial x^4}\right)_0 = \frac{\partial^2}{\partial x^2}\left(\frac{\partial^2\phi}{\partial x^2}\right)_0$$

Using equation (45), we get

$$\left(\frac{\partial^4\phi}{\partial x^4}\right)_0 \approx \frac{\partial^2}{\partial x^2}\left[\frac{1}{\delta^2(m2)}\left[\frac{\phi1-\phi_0}{m2} - \frac{\phi_0-\phi_3}{m3}\right]\right]$$

$$\approx \frac{1}{\delta^2(m2)}\left[\frac{\left(\frac{\partial^2\phi}{\partial x^2}\right)_1-\left(\frac{\partial^2\phi}{\partial x^2}\right)_0}{m2} - \frac{\left(\frac{\partial^2\phi}{\partial x^2}\right)_0-\left(\frac{\partial^2\phi}{\partial x^2}\right)_3}{m3}\right]$$

Again from equations (45), (46), and (47), we get

$$\left(\frac{\partial^4\phi}{\partial x^4}\right)_0 \approx \frac{1}{\delta^2(m2)}\left[\frac{1}{(\delta^2)m1}\left(\frac{\phi_5-\phi_1}{m1} - \frac{\phi_1-\phi_0}{m2}\right) - \frac{1}{\delta^2(m3)}\left(\frac{\phi1-\phi_0}{m2} - \frac{\phi_0-\phi_3}{m3}\right)\right.$$

$$\left. - \frac{1}{\delta^2(m2)}\left(\frac{\phi1-\phi_0}{m2} - \frac{\phi_0-\phi_3}{m3}\right) + \frac{1}{\delta^2(m3)}\left(\frac{\phi_0-\phi_3}{m3} - \frac{\phi_3-\phi_9}{m4}\right)\right]$$

Rearranging, we get

$$\left(\frac{\partial^4\phi}{\partial x^4}\right)_0 \approx \frac{1}{\delta^4(m2)}\left[\frac{\phi_5}{(m1)^2 m2} - \frac{\phi_1}{(m1)^2 m2} - \frac{\phi_1}{m1(m2)^2}\right.$$

$$+ \frac{\phi_0}{(m1)(m2)^2} - \frac{\phi_1}{(m2)^3} + \frac{\phi_0}{(m2)^3} + \frac{\phi_0}{(m2)^2 m3}$$

$$- \frac{\phi_3}{(m2)^2 m3} - \frac{\phi_1}{(m2)^2 m3} + \frac{\phi_0}{(m2)^2 m3} + \frac{\phi_0}{m2(m3)^2}$$

$$- \frac{\phi_3}{m2(m3)^2} + \frac{\phi_0}{(m3)^3} - \frac{\phi_3}{(m3)^3} - \frac{\phi_3}{(m3)^2 m4}$$

$$\left. + \frac{\phi_9}{(m3)^2 m4}\right] \qquad (48)$$

Now $\partial^4\phi/\partial^4 y$ in finite difference form at point 0 (figure 5) , is obtained as,

$$\left(\frac{\partial\phi}{\partial y}\right)_0 \approx \frac{\phi_2 - \phi_0}{c(\delta)\, m2}$$

$$\left(\frac{\partial^2\phi}{\partial y^2}\right)_0 \approx \frac{1}{c(\delta)\, m2}\left(\left(\frac{\partial\phi}{\partial y}\right)_2 - \left(\frac{\partial\phi}{\partial y}\right)_0\right)$$

$$\approx \frac{1}{c^2(\delta)^2 m2}\left[\frac{\phi_2 - \phi_0}{m2} - \frac{\phi_0 - \phi_4}{m3}\right] \qquad (49)$$

Similarly for point 2 and 4

$$\left(\frac{\partial^2\phi}{\partial y^2}\right)_2 \approx \frac{1}{c^2(\delta)^2 m1}\left[\frac{\phi_7 - \phi_2}{m1} - \frac{\phi_2 - \phi_0}{m2}\right] \qquad (50)$$

$$\left(\frac{\partial^2\phi}{\partial y^2}\right)_4 \approx \frac{1}{c^2(\delta)^2 m3}\left[\frac{\phi_0 - \phi_4}{m3} - \frac{\phi_4 - \phi_{11}}{m4}\right] \qquad (51)$$

$$\left(\frac{\partial^4\phi}{\partial y^4}\right)_o = \frac{\partial^2}{\partial y^2}\left(\frac{\partial^2\phi}{\partial y^2}\right)_o$$

Using equation (49), we get

$$\left(\frac{\partial^4\phi}{\partial y^4}\right)_o \approx \frac{\partial^2}{\partial y^2}\left[\frac{1}{c^2(\delta)^2 m_2}\left(\frac{\phi_2-\phi_o}{m_2} - \frac{\phi_o-\phi_4}{m_3}\right)\right]$$

$$\approx \frac{1}{c^2(\delta)^2 m_2}\left[\frac{\left(\frac{\partial^2\phi}{\partial y^2}\right)_2 - \left(\frac{\partial^2\phi}{\partial y^2}\right)_o}{m_2} - \frac{\left(\frac{\partial^2\phi}{\partial y^2}\right)_o - \left(\frac{\partial^2\phi}{\partial y^2}\right)_4}{m_3}\right]$$

Using equations (49), (50), and (51) and rearranging, we get

$$\left(\frac{\partial^4\phi}{\partial y^4}\right)_o \approx \frac{1}{c^4(\delta)^4 m_2}\left[\frac{\phi_7}{(m_1)^2 m_2} - \frac{\phi_2}{(m_1)^2 m_2} - \frac{\phi_2}{m_1(m_2)^2}\right.$$

$$+ \frac{\phi_o}{m_1(m_2)^2} - \frac{\phi_2}{(m_2)^3} + \frac{\phi_o}{(m_2)^3} + \frac{\phi_o}{(m_2)^2 m_3}$$

$$- \frac{\phi_4}{(m_2)^2 m_3} - \frac{\phi_2}{(m_2)^2 m_3} + \frac{\phi_o}{(m_2)^2 m_3} + \frac{\phi_o}{m_2(m_3)^2} - \frac{\phi_4}{m_2(m_3)^2}$$

$$\left. + \frac{\phi_o}{(m_3)^3} - \frac{\phi_4}{(m_3)^3} - \frac{\phi_4}{(m_3)^2 m_4} + \frac{\phi_{11}}{(m_3)^2 m_4}\right] \quad (52)$$

For the mixed derivative in equation 14, we obtain the central difference formula as,

$$\left(\frac{\partial^4\phi}{\partial x^2\,\partial y^2}\right)_o = \frac{\partial^2}{\partial x^2}\left(\frac{\partial^2\phi}{\partial y^2}\right)_o$$

Using equation (49), we get

$$\left(\frac{\partial^4\phi}{\partial x^2\partial y^2}\right)_0 \approx \frac{\partial^2}{\partial x^2}\left[\frac{1}{c^2(s)^2 m2}\left[\frac{\phi_2-\phi_0}{m2} - \frac{\phi_0-\phi_4}{m3}\right]\right]$$

$$\approx \frac{1}{c^2(s)^2 m2}\left[\frac{\left(\frac{\partial^2\phi}{\partial x^2}\right)_2 - \left(\frac{\partial^2\phi}{\partial x^2}\right)_0}{m2} - \frac{\left(\frac{\partial^2\phi}{\partial x^2}\right)_0 - \left(\frac{\partial^2\phi}{\partial x^2}\right)_4}{m3}\right]$$

Using equations (45) and rearranging, we obtain

$$\left(\frac{\partial^4\phi}{\partial x^2\partial y^2}\right)_0 \approx \frac{1}{c^2(s)^4(m2)\,m2}\left[\frac{\phi_6}{m2(m2)} - \frac{\phi_2}{m2(m2)} - \frac{\phi_2}{m2(m3)}\right.$$

$$+ \frac{\phi_8}{m2(m3)} - \frac{\phi_1}{m2(m2)} + \frac{\phi_0}{m2(m2)} + \frac{\phi_0}{m2(m3)} - \frac{\phi_3}{m2(m3)}$$

$$- \frac{\phi_1}{m3(m2)} + \frac{\phi_0}{m3(m2)} + \frac{\phi_0}{m3(m3)} - \frac{\phi_3}{m3(m3)} + \frac{\phi_{12}}{m3(m2)}$$

$$\left. - \frac{\phi_4}{m3(m2)} - \frac{\phi_4}{m3(m3)} + \frac{\phi_{10}}{m3(m3)}\right] \qquad (53)$$

Substituting equations (48), (52), and (53) into equation (14) and rearranging the terms, we get

$$\phi_0\left[\frac{1}{(m1)(m2)^3} + \frac{1}{(m2)^4} + \frac{2}{m3(m2)^3} + \frac{1}{(m2)^2(m3)^2} + \frac{1}{(m2)(m3)^3}\right.$$

$$\left. + \frac{1}{c^4\,m1(m2)^3} + \frac{1}{c^4(m2)^4} + \frac{2}{c^4\,m3(m2)^3} + \frac{1}{c^4(m2)^2(m3)^2} + \frac{1}{c^4(m3)^3 m2}\right.$$

$$+\frac{2}{c^2(m2)^2(m2)^2}+\frac{2}{c^2(m2)^2(m2)m3}+\frac{2}{c^2m2(m2)^2m3}+\frac{2}{c^2m2(m2)m3(m3)}\Bigg]$$

$$-\Phi_1\Bigg[\frac{1}{(m1)^2(m2)^2}+\frac{1}{m1(m2)^3}+\frac{1}{(m2)^4}+\frac{1}{m3(m2)^3}$$

$$+\frac{2}{c^2(m2)^2(m2)^2}+\frac{2}{c^2m2(m2)^2m3}\Bigg]$$

$$-\Phi_2\Bigg[\frac{1}{c^4(m1)^2(m2)^2}+\frac{1}{c^4m1(m2)^3}+\frac{1}{c^4(m2)^4}$$

$$+\frac{1}{c^4m3(m2)^3}+\frac{2}{c^2(m2)^2(m2)^2}+\frac{2}{c^2m2(m2)^2m3}\Bigg]$$

$$-\Phi_3\Bigg[\frac{1}{m3(m2)^3}+\frac{1}{(m2)^2(m3)^2}+\frac{1}{m2(m3)^3}+\frac{1}{m2(m3)^2m4}$$

$$+\frac{2}{c^2m2(m2)^2m3}+\frac{2}{c^2m2(m2)(m3)m3}\Bigg]$$

$$-\Phi_4\Bigg[\frac{1}{c^4m3(m2)^3}+\frac{1}{c^4(m2)^2(m3)^2}+\frac{1}{c^4m2(m3)^3}$$

$$+\frac{1}{c^4m2(m3)^2m4}+\frac{2}{c^2m2(m2)^2m3}+\frac{2}{c^2m2(m2)(m3)m3}\Bigg]$$

$$+2\Bigg[\frac{\Phi_6}{c^2(m2)^2(m2)^2}+\frac{\Phi_8}{c^2m2(m2)^2m3}+\frac{\Phi_{10}}{c^2m2(m2)(m3)m3}+\frac{\Phi_{12}}{c^2m2(m2)^2m3}\Bigg]$$

$$+\frac{\Phi_5}{(m1)^2(m2)^2}+\frac{\Phi_7}{c^4(m1)^2(m2)^2}+\frac{\Phi_9}{m2(m3)^2m4}+\frac{\Phi_{11}}{c^4m2(m3)^2m4}=0 \quad (54)$$

Figures 6, 7, and 8 show the network of points in region 1 used for the derivation of second, third, and fourth versions respectively of the Biharmonic equation $\nabla^4\phi = 0$. These forms are arrived at by the backward difference method.

Second version of $\nabla^4\phi = 0$ is :

$$\frac{\Phi(I+1,J)}{(m1)^2(m2)^2} - \Phi(I,J)\left[\frac{1}{m1(m2)^3} + \frac{1}{(m1)^2(m2)^2} + \frac{1}{(m2)^4} + \frac{1}{m3(m2)^3} - \frac{1}{c\,(m2)^4} - \frac{1}{c^4\,m1(m2)^3} - \frac{1}{c4\,m3(m2)^3} - \frac{1}{c^4(m2)^2(m3)^2} - \frac{1}{c^4\,m3(m2)^3} - \frac{1}{c^4\,m2(m3)^3} + \frac{2}{c^2(m2)^2(m2)^2} + \frac{2}{c^2(m2)^2\,m2(m3)}\right]$$

$$+ \Phi(I-1,J)\left[\frac{1}{m1(m2)^3} + \frac{1}{(m2)^4} + \frac{2}{m3(m2)^3} + \frac{1}{(m2)^2(m3)^2} + \frac{1}{m2(m3)^3} + \frac{2}{c^2(m2)^2(m2)^2} + \frac{2}{c^2\,m2(m2)^2\,m3} + \frac{2}{c^2\,m2(m2)^2\,m3} + \frac{2}{c^2\,m2(m3)(m2)\,m3}\right]$$

$$- \Phi(I-2,J)\left[\frac{1}{m3(m2)^3} + \frac{1}{(m2)^2(m3)^2} + \frac{1}{m2(m3)^3} + \frac{1}{m2(m3)^2\,m4} + \frac{2}{c^2\,m2(m2)^2\,m3} + \frac{2}{c^2\,m2(m3)(m2)\,m3}\right]$$

$$+ \frac{\phi(I-3,J)}{m2(m3)^2 m4} + \frac{\phi(I,J+2)}{c^4 (m1)^2 (m2)^4}$$

$$- \phi(I,J+1)\left[\frac{1}{c^4(m1)^2(m2)^2} + \frac{1}{c^4 m1(m2)^3} + \frac{1}{c^4 m3(m2)^3} + \frac{1}{c^4(m2)^4} + \frac{2}{c^2(m2)^2(m2)^2}\right]$$

$$- \phi(I,J-1)\left[\frac{1}{c^4 m3(m2)^3} + \frac{1}{c^4(m2)^2(m3)^2} + \frac{1}{c^4 m2(m3)^3}\right.$$

$$\left. + \frac{1}{c^4 m2(m3)^2 m4} - \frac{2}{c^2 m2(m2)^2 m3}\right]$$

$$+ \frac{\phi(I,J-2)}{c^4 m2(m3)^2 m4} + \frac{2\phi(I-2,J+1)}{c^2 m2(m2)^2 m3} + \frac{2\phi(I-2,J-1)}{c^2 m2(m3)(m2)m3}$$

$$- \phi(I-1,J+1)\left[\frac{2}{c^2(m2)^2(m2)^2} + \frac{2}{c^2 m2(m2)^2 m3}\right]$$

$$- 2\phi(I-1,J-1)\left[\frac{1}{c^2 m2(m3)(m2)m3} + \frac{1}{c^2 m2(m2)^2 m3}\right]$$

$$= 0 \qquad (55)$$

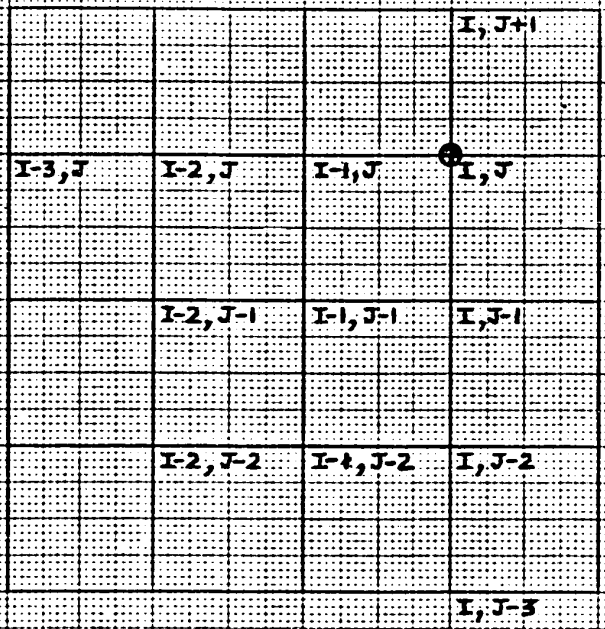
I, J+1
I-3, J
I-2, J
I-1, J
I, J
I+1, J
I-2, J-1
I-1, J-1
I, J-1
I-2, J-2
I-1, J-2
I, J-2
I, J-3

FIG. 7

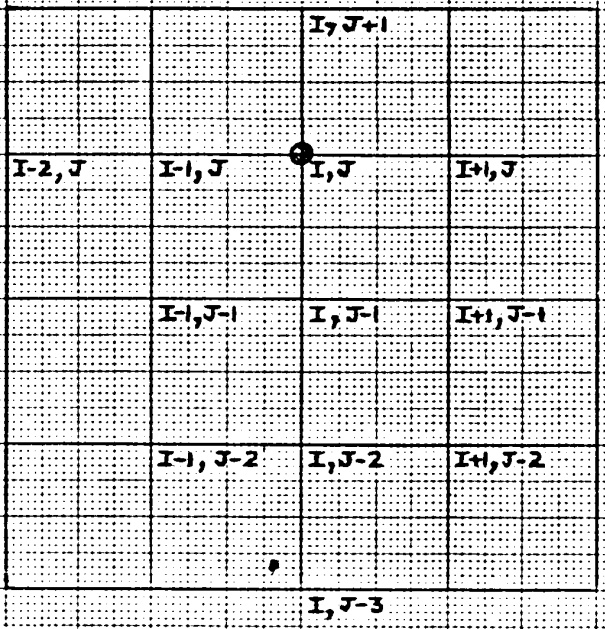
I, J+1
I-2, J
I-1, J
I, J
I+1, J
I+2, J
I-1, J-1
I, J-1
I+1, J-1
I-1, J-2
I, J-2
I+1, J-2
I, J-3

FIG. 8

Third version of $\nabla^4\phi = 0$ is :

$$\frac{\phi(I+1,J)}{(m1)^2(m2)^2} - \phi(I,J)\left[\frac{1}{(m1)^2(m2)^2} + \frac{1}{(m1)(m2)^3} + \frac{1}{(m2)^4}\right.$$

$$+ \frac{1}{m3(m2)^3} + \frac{1}{c^4(m1)^3 m2} + \frac{1}{c^4 m1(m2)^3} + \frac{1}{c^4(m2)^4}$$

$$\left. + \frac{2}{c^2(m1)^2(m2)^2} + \frac{2}{c^2 m1(m2)^2 m2}\right]$$

$$+ \phi(I-1,J)\left[\frac{1}{m1(m2)^3} + \frac{1}{(m2)^4} + \frac{2}{m3(m2)^3} + \frac{1}{(m3)^2(m2)^2}\right.$$

$$+ \frac{1}{m2(m3)^3} + \frac{2}{c^2(m1)^2(m2)^2} + \frac{2}{c^2 m1(m2)^2 m2} + \frac{2}{c^2 m2(m1)^2 m3}$$

$$\left. + \frac{2}{c^2(m1)m2(m2)m3} + \left[\frac{m1+m2+m3}{m2+m3}\ \frac{m1+m2}{m2}\right]\left[\frac{2}{c^2(m1)^2(m2)^2} + \frac{2}{c^2 m2(m1)^2 m3}\right]\right]$$

$$- \phi(I-2,J)\left[\frac{1}{m2(m3)^3} + \frac{1}{m2(m3)^2 m4} + \frac{1}{(m2)^2(m3)^2}\right.$$

$$+ \frac{1}{m3(m2)^3} + \frac{2}{c^2 m2(m1)^2 m3} + \frac{2}{c^2 m1(m2)m2(m3)}$$

$$\left. - \left[\frac{m1+m2+m3}{m2+m3}\ \frac{m1+m2}{m2}\right]\left[\frac{2}{c^2 m2(m1)^2 m3}\right]\right]$$

$$+ \frac{\phi(I-3,J)}{m2(m3)^2 m4} + \frac{\phi(I,J-3)}{c^4 m3(m2)^2 m4}$$

$$+ \phi(I,J+1)\left[\frac{1}{c^4 m2(m1)^3} + \frac{2}{c^2(m2)^2(m1)^2}\right]$$

$$+\Phi(I,J-1)\left[\frac{1}{c^4(m1)^2(m2)^2}+\frac{1}{c^4\,m1(m2)^3}+\frac{1}{c^4\,m1(m2)^2m3}\right.$$

$$\left.+\frac{1}{c^4\,m3(m2)^3}+\frac{1}{c^4(m2)^2(m3)^2}+\frac{1}{c^4(m2)^4}+\frac{2}{c^2m1(m2)^2m2}\right]$$

$$-\Phi(I,J-2)\left[\frac{1}{c^4m1(m2)^2m3}+\frac{1}{c^4m3(m2)^2m4}+\frac{1}{c^4m3(m2)^3}+\frac{1}{c^4(m2)^2(m3)^2}\right]$$

$$+\Phi(I-2,J-2)\left[\frac{2}{c^2m2(m1)^2m3}\quad\frac{m1+m2}{m3}\quad\frac{m1}{m2+m3}\right]$$

$$-\Phi(I-1,J-1)\left[\frac{2}{c^2\,m1(m2)^2m2}+\frac{2}{c^2\,m1(m2)\,m2(m3)}\right.$$

$$\left.+\left[\frac{m1+m2+m3}{m3}\quad\frac{m1}{m2}\right]\left[\frac{2}{c^2(m1)^2(m2)^2}+\frac{2}{c^2m2(m1)^2m3}\right]\right]$$

$$+\Phi(I-2,J-1)\left[\frac{2}{c^2m2(m1)\,m3\,(m2)}-\left[\frac{m1+m2+m3}{m3}\quad\frac{m1}{m2}\right]\left[\frac{2}{c^2m2(m1)^2m3}\right]\right]$$

$$+\Phi(I-1,J-2)\left[\left(\frac{m1+m2}{m3}\quad\frac{m1}{m2+m3}\right)\left(\frac{2}{c^2(m1)^2(m2)^2}+\frac{2}{c^2m2(m1)^2m3}\right)\right]$$

$$=\quad 0 \qquad (56)$$

Fourth version of $\nabla^4\phi = 0$ is :

$$\frac{\phi(I+2,J)}{(m1)^2(m2)^2} - \phi(I+1,J)\left[\frac{1}{(m1)^2(m2)^2} + \frac{1}{(m1)(m2)^3}\right.$$

$$+\frac{2}{c^2(m1)^2(m2)^2} + \frac{2}{c^2\, m1(m2)^2 m2} + \frac{1}{(m3)(m2)^3} + \frac{1}{(m2)^4}$$

$$\left.+\left[\frac{m1+m2+m3}{m2+m3}\quad\frac{m1+m2}{m2}\quad\frac{2}{c^2(m1)^2(m2)^2}\right]\right]$$

$$+\phi(I,J)\left[\frac{1}{(m1)(m2)^2} + \frac{1}{(m2)^4} + \frac{2}{m3(m2)^3} + \frac{1}{(m2)^2(m3)^2}\right.$$

$$+\frac{1}{m2(m3)^3} - \frac{1}{c^4\, m2(m1)^3} - \frac{1}{c^4(m1)^2(m2)^2} - \frac{1}{c^4\, m1(m2)^3}$$

$$-\frac{1}{c^4(m2)^4} + \frac{2}{c^2(m1)^2(m2)^2} + \frac{2}{c^2\, m1(m2)^2 m2}$$

$$\left.+\frac{2}{c^2\, m2(m1)^2 m3} + \frac{2}{c^2\, m1(m2)\, m2(m3)}\right]$$

$$-\phi(I-1,J)\left[\frac{1}{m3(m2)^3} + \frac{1}{(m2)^2(m3)^2} + \frac{1}{m2(m3)^3}\right.$$

$$+\frac{1}{m2(m3)^2 m4} + \frac{2}{c^2 m2(m1)^2 m3} + \frac{2}{c^2\, m1(m2)\, m2(m3)}$$

$$\left.-\frac{m1+m2+m3}{m2+m3}\quad\frac{m1+m2}{m2}\quad\frac{2}{c^2\, m2(m1)^2 m3}\right]$$

$$+\frac{\phi(I-2,J)}{m2(m3)^2 m4} + \frac{\phi(I,J-3)}{c^4\, m3(m2)^2 m4}$$

$$+\phi(I,J-1)\left[\frac{1}{c^4(m1)^2(m2)^2}+\frac{1}{c^4 m1(m2)^3}+\frac{1}{c^4 m1(m2)^2 m3}\right.$$

$$\left.+\frac{1}{c^4(m2)^4}+\frac{1}{c^4 m3(m2)^3}+\frac{1}{c^4(m2)^2(m3)^2}\right.$$

$$\left.-\frac{2}{c^2 m1(m2)^2 m2}-\frac{2}{c^2 m1(m2)\,m2(m3)}\right]$$

$$-\phi(I,J-2)\left[\frac{1}{c^4 m1(m2)^2 m3}+\frac{1}{c^4 m3(m2)^3}+\frac{1}{c^4(m2)^2(m3)^2}+\frac{1}{c^4 m3(m2)^2 m4}\right]$$

$$+\phi(I+1,J-1)\left[\frac{2}{c^2 m1(m2)^2 m2}-\frac{m1+m2+m3}{m3}\;\frac{m1}{m2}\;\frac{2}{c^2(m1)^2(m2)^2}\right]$$

$$-\phi(I,J+1)\left[\frac{2}{c^2(m1)^2(m2)^2}+\frac{2}{c^2 m2(m1)^2 m3}-\frac{1}{c^4 m2(m1)^3}\right]$$

$$+\phi(I-1,J-1)\left[\frac{2}{c^2 m1(m2)\,m2(m3)}-\frac{m1+m2+m3}{m3}\;\frac{m1}{m2}\;\frac{2}{c^2 m2(m1)^2 m3}\right]$$

$$+\phi(I-1,J-2)\left[\frac{m1+m2}{m3}\;\frac{m1}{m2+m3}\;\frac{2}{c^2 m2(m1)^2 m3}\right]$$

$$+\phi(I+1,J-2)\left[\frac{m1+m2}{m3}\;\frac{m1}{m2+m3}\;\frac{2}{c^2(m1)^2(m2)^2}\right]$$

$$= 0 \qquad (57)$$

Figures 9, 10, and 11 show the network of points in region 2 used for the derivation of fifth, sixth, and seventh versions respectively of the Biharmonic equation $\nabla^4\phi = 0$. These forms are arrived at by the forward difference method.

Fifth version of $\nabla^4\phi = 0$ is :

$$\frac{\phi(I+3,J)}{m1(m2)^2 m3} - \phi(I+2,J)\left[\frac{1}{m1(m2)^2 m3} + \frac{1}{m3(m2)^3}\right.$$

$$+ \frac{1}{(m2)^2(m3)^2} + \frac{1}{m2(m3)^3} + \frac{2}{c^2\, m2(m3)^2 m3} + \frac{2}{c^2 m2(m3)m3(m4)}$$

$$\left. - \frac{m3+m4}{m3}\quad\frac{m2+m3+m4}{m2+m3}\quad\frac{2}{c^2 m2(m3)\,m3(m4)}\right]$$

$$+ \phi(I+1,J)\left[\frac{1}{m3(m2)^3} + \frac{1}{(m2)^2(m3)^2} + \frac{2}{m2(m3)^3} + \frac{1}{(m3)^4}\right.$$

$$+ \frac{1}{m4(m3)^3} + \frac{2}{c^2 m2(m3)^2 m3} + \frac{2}{c^2 m2(m3)m3(m4)} + \frac{2}{c^2(m3)^2(m3)^2}$$

$$\left. + \frac{2}{c^2 m3(m3)^2 m4} - \left[\frac{m3+m4}{m3}\quad\frac{m2+m3+m4}{m2+m3}\right]\left[\frac{2}{c^2 m2(m3)m3(m4)} + \frac{2}{c^2 m3(m3)^2 m4}\right]\right.$$

$$- \phi(I,J)\left[\frac{1}{m2(m3)^3} + \frac{1}{(m3)^4} + \frac{1}{m4(m3)^3} + \frac{1}{(m3)^2(m4)^2}\right.$$

$$+ \frac{1}{c^4(m2)^2(m3)^2} + \frac{1}{c^4 m2(m3)^3} + \frac{1}{c^4(m3)^4} + \frac{1}{c^4 m4(m3)^3}$$

$$\left. + \frac{2}{c^2(m3)^2(m3)^2} + \frac{2}{c^2 m3(m3)^2 m4}\right] + \frac{\phi(I-1,J)}{(m3)^2(m4)^2}$$

$$+\ \phi(I,J-1)\left[\frac{2}{c^2 m3 (m3)^2 m4}+\frac{1}{c^4 m4 (m3)^3}\right]$$

$$+\ \frac{\phi(I,J+3)}{c^4 m2 (m1)^2 m3}+\phi(I,J+1)\left[\frac{1}{c^4 m1 (m2)^2 m3}+\frac{1}{c^4 m3 (m2)^3}\right.$$

$$\left.+\frac{2}{c^4 (m2)^2 (m3)^2}+\frac{1}{c^4 (m2)(m3)^3}+\frac{1}{c^4 (m3)^4}+\frac{2}{c^2 (m3)^2 (m3)^2}\right]$$

$$-\ \phi(I,J+2)\left[\frac{1}{c^4 m2 (m1)^2 m3}+\frac{1}{c^4 m1 (m2)^2 m3}+\frac{1}{c^4 m3 (m2)^3}+\frac{1}{c^4 (m2)^2 (m3)^2}\right]$$

$$+\ \phi(I+2,J+1)\left[\frac{2}{c^2 m2 (m3)^2 m3}-\frac{m4}{m3}\ \frac{m2+m3+m4}{m2}\ \frac{2}{c^2 m2 (m3)\, m3 (m4)}\right]$$

$$+\ \phi(I+2,J+2)\left[\frac{m4}{m2+m3}\ \frac{m3+m4}{m2}\ \frac{2}{c^2 m2 (m3)\, m3 (m4)}\right]$$

$$-\ \phi(I+1,J+1)\left[\frac{2}{c^2 m2 (m3)(m3)^2}+\frac{2}{c^2 (m3)^2 (m3)^2}\right.$$

$$\left.+\ \frac{m4}{m3}\ \frac{m2+m3+m4}{m2}\ \frac{2}{c^2 m2 (m3)\, m3 (m4)}\right]$$

$$-\ \phi(I+1,J+2)\left[\frac{m4}{m2+m3}\ \frac{m3+m4}{m2}\left(\frac{2}{c^2 m2 (m3)\, m3 (m4)}+\frac{2}{c^2 (m3)^2 m3 (m4)}\right)\right]$$

$$=\ 0 \qquad (58)$$

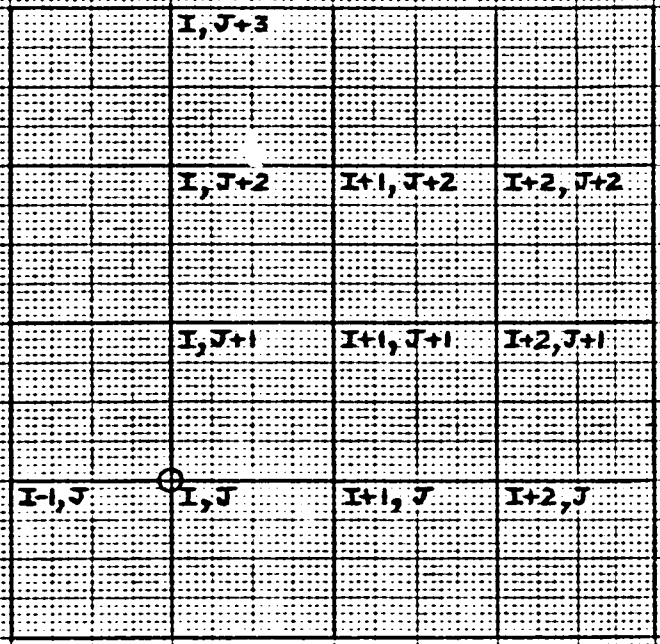
I, J+3
I, J+2
I+1, J+2
I+2, J+2
I, J+1
I+1, J+1
I+2, J+1
I-1, J
I, J
I+1, J
I+2, J
I+3, J
I, J-1

FIG. 9

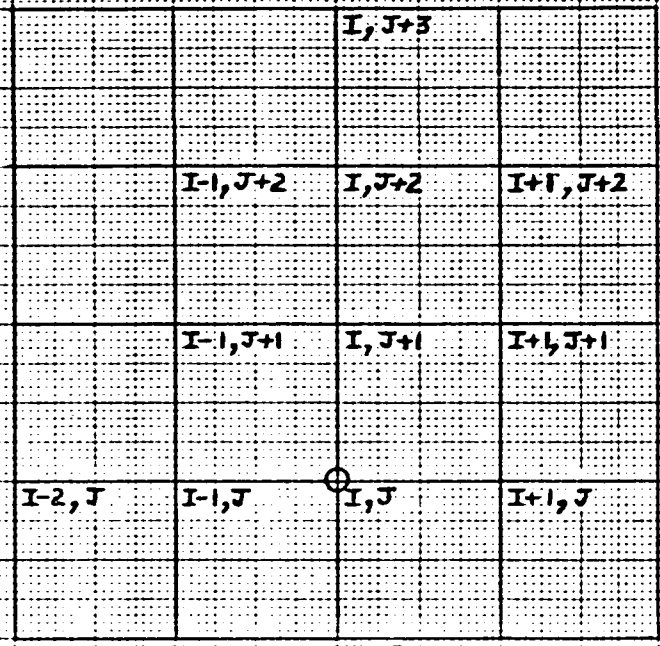
I, J+3
I-1, J+2
I, J+2
I+1, J+2
I-1, J+1
I, J+1
I+1, J+1
I-2, J
I-1, J
I, J
I+1, J
I+2, J
I, J-1

FIG. 10

Sixth version of $\nabla^4\phi = 0$ is :

$$\frac{\Phi(I+2,J)}{(m1)^2(m2)^2} - \Phi(I+1,J)\left[\frac{1}{(m1)^2(m2)^2} + \frac{1}{m1(m2)^3} + \frac{1}{(m2)^4}\right.$$

$$+ \frac{1}{m3(m2)^3} + \frac{2}{c^2(m2)^2(m3)^2} + \frac{2}{c^2 m3(m2)^2 m4}$$

$$\left. - \frac{m3+m4}{m3}\ \frac{m2+m3+m4}{m2+m3}\ \frac{2}{c^2 m3(m2)^2 m4}\right]$$

$$+ \Phi(I,J)\left[\frac{1}{m1(m2)^3} + \frac{1}{(m2)^4} + \frac{2}{m3(m2)^3} + \frac{1}{(m2)^2(m3)^2}\right.$$

$$+ \frac{1}{m2(m3)^3} - \frac{1}{c^4(m2)^2(m3)^2} - \frac{1}{c^4 m2(m3)^3} - \frac{1}{c^4(m3)^4}$$

$$- \frac{1}{c^4 m4(m3)^3} + \frac{2}{c^2(m2)^2(m3)^2} + \frac{2}{c^2 m3(m2)^2 m4}$$

$$\left. + \frac{2}{c^2 m2(m3)^2 m3} + \frac{2}{c^2 m2(m3)m3(m4)}\right] - \Phi(I-1,J)\left[\frac{1}{m3(m2)^3}\right.$$

$$+ \frac{1}{(m2)^2(m3)^2} + \frac{1}{m2(m3)^3} + \frac{1}{m2(m3)^2 m4} + \frac{2}{c^2 m2(m3)^2 m3}$$

$$\left. + \frac{2}{c^2 m2(m3)m3(m4)} - \frac{m3+m4}{m3}\ \frac{m2+m3+m4}{m2+m3}\ \frac{2}{c^2 m2(m3)m3(m4)}\right]$$

$$+ \frac{\Phi(I-2,J)}{m2(m3)^2 m4} + \frac{\Phi(I,J+3)}{c^4 m2(m1)^2 m3} - \Phi(I,J+2)\left[\frac{1}{c^4 m2(m1)^2 m3}\right.$$

$$\left. + \frac{1}{c^4 m1(m2)^2 m3} + \frac{1}{c^4 m3(m2)^3} + \frac{1}{c^4(m2)^2(m3)^2}\right]$$

$$+\phi(I,J+1)\left[\frac{1}{c^4 m1(m2)^2 m3}+\frac{1}{c^4(m2)^2(m3)^2}+\frac{1}{c^4 m3(m2)^3}+\frac{1}{c^4(m2)^3(m3)^2}\right.$$

$$\left.+\frac{1}{c^4 m2(m3)^3}+\frac{1}{c^4(m3)^4}-\frac{2}{c^2(m2)^2(m3)^2}-\frac{2}{c^2 m2(m3)^2 m3}\right]$$

$$+\phi(I,J-1)\left[\frac{1}{c^4 m4(m3)^3}-\frac{2}{c^2 m3(m2)^2 m4}-\frac{2}{c^2 m2(m3)\,m3(m4)}\right]$$

$$+\phi(I+1,J+1)\left[\frac{2}{c^2(m2)^2(m3)^2}-\frac{m4}{m3}\,\frac{m2+m3+m4}{m2}\,\frac{2}{c^2 m3(m2)^2 m4}\right]$$

$$+\phi(I-1,J+1)\left[\frac{2}{c^2 m2(m3)^2 m3}-\frac{m4}{m3}\,\frac{m2+m3+m4}{m2}\,\frac{2}{c^2 m2(m3)\,m3(m4)}\right]$$

$$+\phi(I-1,J+2)\;\frac{m4}{m2+m3}\;\frac{m3+m4}{m2}\;\frac{2}{c^2 m2(m3)\,m3(m4)}$$

$$+\phi(I+1,J+2)\left[\frac{m4}{m2+m3}\;\frac{m3+m4}{m2}\;\frac{2}{c^2 m3(m2)^2 m4}\right]$$

$$=\quad 0 \qquad (59)$$

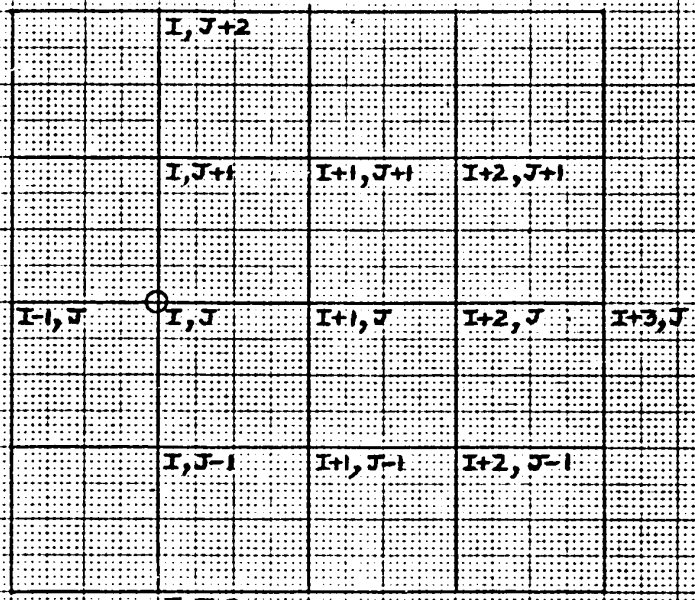

FIG. 11

Seventh version of $\nabla^4\phi = 0$ is:

$$\frac{\phi(I+3,J)}{m1(m2)^2 m3} - \phi(I+2;J)\left[\frac{1}{m1(m2)^2 m3} + \frac{1}{(m2)^3 m3}\right.$$

$$\left. + \frac{1}{(m2)^2(m3)^2} + \frac{1}{m2(m3)^3} + \frac{2}{c^2 m2(m2)^2 m3} + \frac{2}{c^2 m2(m3)(m2)m3}\right]$$

$$+ \phi(I+1,J)\left[\frac{1}{m3(m2)^3} + \frac{1}{(m2)^2(m3)^2} + \frac{2}{m2(m3)^2} + \frac{1}{(m3)^4}\right.$$

$$+ \frac{1}{m4(m3)^3} + \frac{2}{c^2 m2(m2)^2 m3} + \frac{2}{c^2 m2(m2)(m3)m3} + \frac{2}{c^2(m2)^2(m3)^2}$$

$$\left. + \frac{2}{c^2 m2(m3)^2}\right] - \phi(I,J)\left[\frac{1}{m2(m3)^3} + \frac{1}{(m3)^4}\right.$$

$$+ \frac{1}{m4(m3)^3} + \frac{1}{(m3)^2(m4)^2} - \frac{1}{c^4 m1(m2)^3} + \frac{2}{c^2(m2)^2(m3)^2} - \frac{1}{c^4(m2)^4}$$

$$\left. + \frac{2}{c^2 m2(m3)^2 m3} - \frac{1}{c^4 m3(m2)^3} - \frac{1}{c^4 m1(m2)^3} - \frac{1}{c^4(m2)^2(m3)^2} - \frac{1}{c^4 m2(m3)^3}\right]$$

$$+ \frac{\phi(I-1,J)}{(m3)^2(m4)^2} + \frac{\phi(I,J+2)}{c^4(m1)^2(m2)^2} + \frac{\phi(I,J-2)}{c^4 m2(m3)^2 m4} + \frac{2\phi(I+2,J-1)}{c^2 m2(m2)(m3)m3}$$

$$- 2\phi(I+1,J+1)\left[\frac{1}{c^2(m2)^2 m2(m3)} + \frac{1}{c^2(m2)^2(m3)^2}\right]$$

$$- \phi(I,J+1)\left[\frac{1}{c^4(m1)^2(m2)^2} + \frac{2}{c^4 m1(m2)^3} + \frac{1}{c^4(m2)^4} - \frac{2}{c^2(m2)^2(m3)^2}\right]$$

$$- 2\phi(I+1,J-1)\left[\frac{1}{c^2 m2(m2)m3(m3)} + \frac{1}{c^2 m2(m3)^2 m3}\right]$$

$$- \phi(I, J-1) \left[\frac{1}{c^4 m3 (m2)^3} + \frac{1}{c^4 (m2)^2 (m3)^2} + \frac{1}{c^4 m2 (m3)^3} \right.$$

$$\left. + \frac{1}{c^4 m2 (m3)^2 m4} - \frac{2}{c^2 m2 (m2)\, m3 (m3)} \right]$$

$$+ \frac{2 \quad \phi(I+2, J+1)}{c^2 m2 (m2)^2 m3} \quad = \quad 0 \qquad (60)$$

3.1.4 Computer Analysis Procedure

The stress pattern developed in the specimen would be symmetrical about x and y axes because of symmetrical loading. Hence considering a quadrant of the specimen and dividing it into a number of divisions along the two axes, a grid system was developed as shown in figure 3. The intersections of the dividing lines are called nodal points. The Biharmonic equation $\nabla^4\phi = 0$, expressed in finite difference form, is satisfied at every nodal point. This gives rise to a set of nonhomogeneous equations. Iterative techniques are employed to solve these equations, giving values of function ϕ at all the nodal points. From these the values of stresses and strains are evaluated at the nodal points.

The steps in the grid system are of variable length. They are smaller near the interface of region 1 and region 2. This has been done because the variation in stress pattern is large in this portion. The size of the step depends upon the degree of accuracy required, and is limited by the storage capacity of the computer.

The computer program for generating a system of non-homogenous linear equations for all the nodal points consists of a main program and seventeen subroutines. The main program, to start with, determines the number of nodal points and scans them as to their location with respect to the internal and external boundaries. Depending upon the location of each nodal point, the main program calls the different subroutines which represent the seven versions of the Biharmonic equation in finite difference form.

The Biharmonic equation in finite difference form at any nodal point consists of functions at twelve other points in addition to the one at which the equation is being written. If all these thirteen points lie completely in either region 1 or in region 2, subroutine one is used. However, if the point under consideration is in region 1, but not all the other twelve points lie in the same region, then one of the subroutines # 1, # 2, # 3, or # 4 is used. These are supplemented by the subroutines u and v which designate the internal boundary conditions. For the case when the point lies in region 2 and not all the other twelve points lie in the same region, then one of the subroutines # 1, # 5, # 6 or # 7 is used. These are again supplemented by subroutines u and v designating internal boundary conditions. If the point is close to the external boundary we utilise subroutine # 1 and subroutines # 10 to # 13 which designate the external boundary conditions.

The flow charts for the main program and the subroutines are given on pages 59 to 83. Also a flow chart for the computation of the stresses and the strains at the nodal points is given toward the end of the list for subroutines.

MAIN PROGRAM FLOW CHART

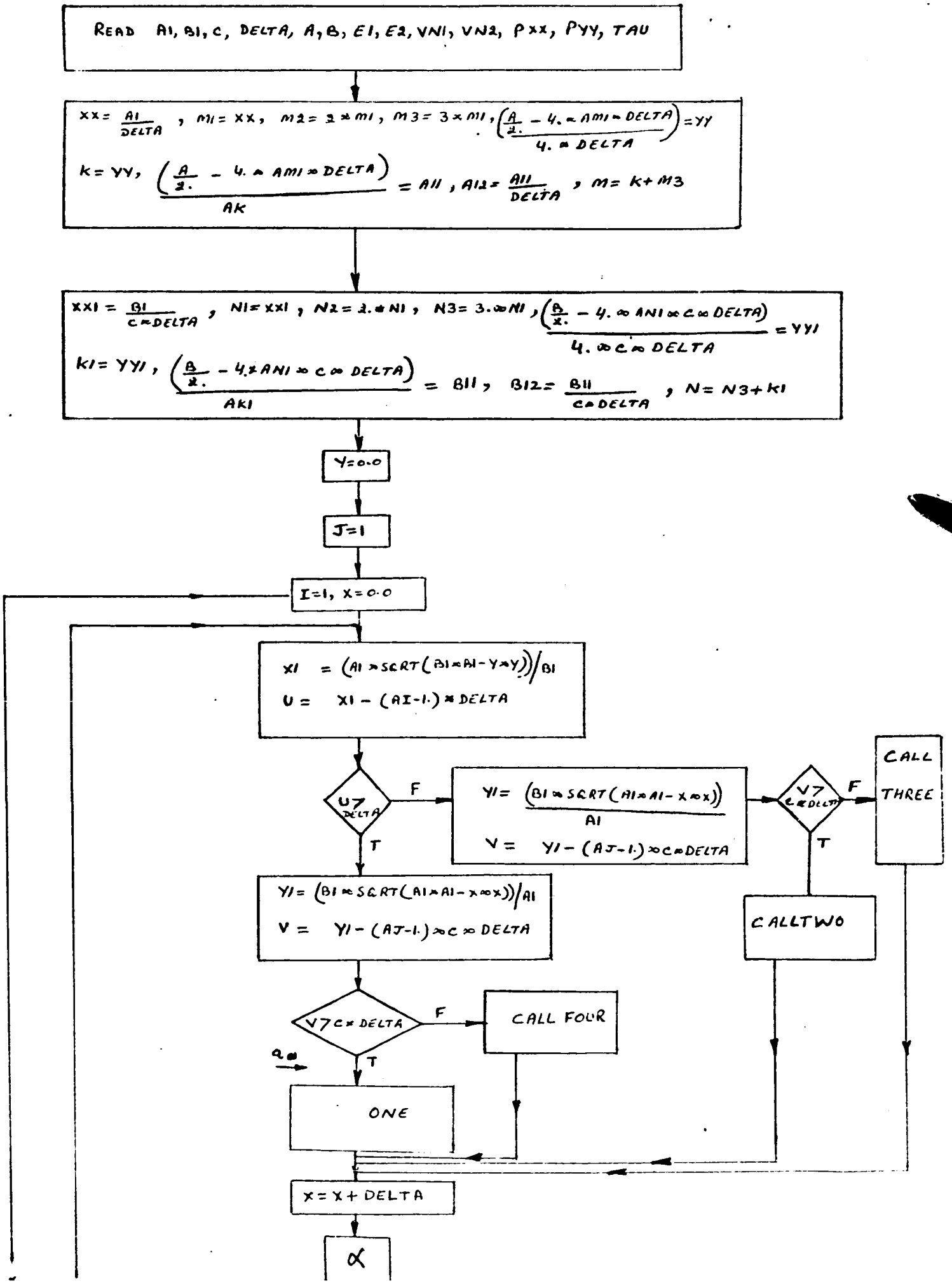

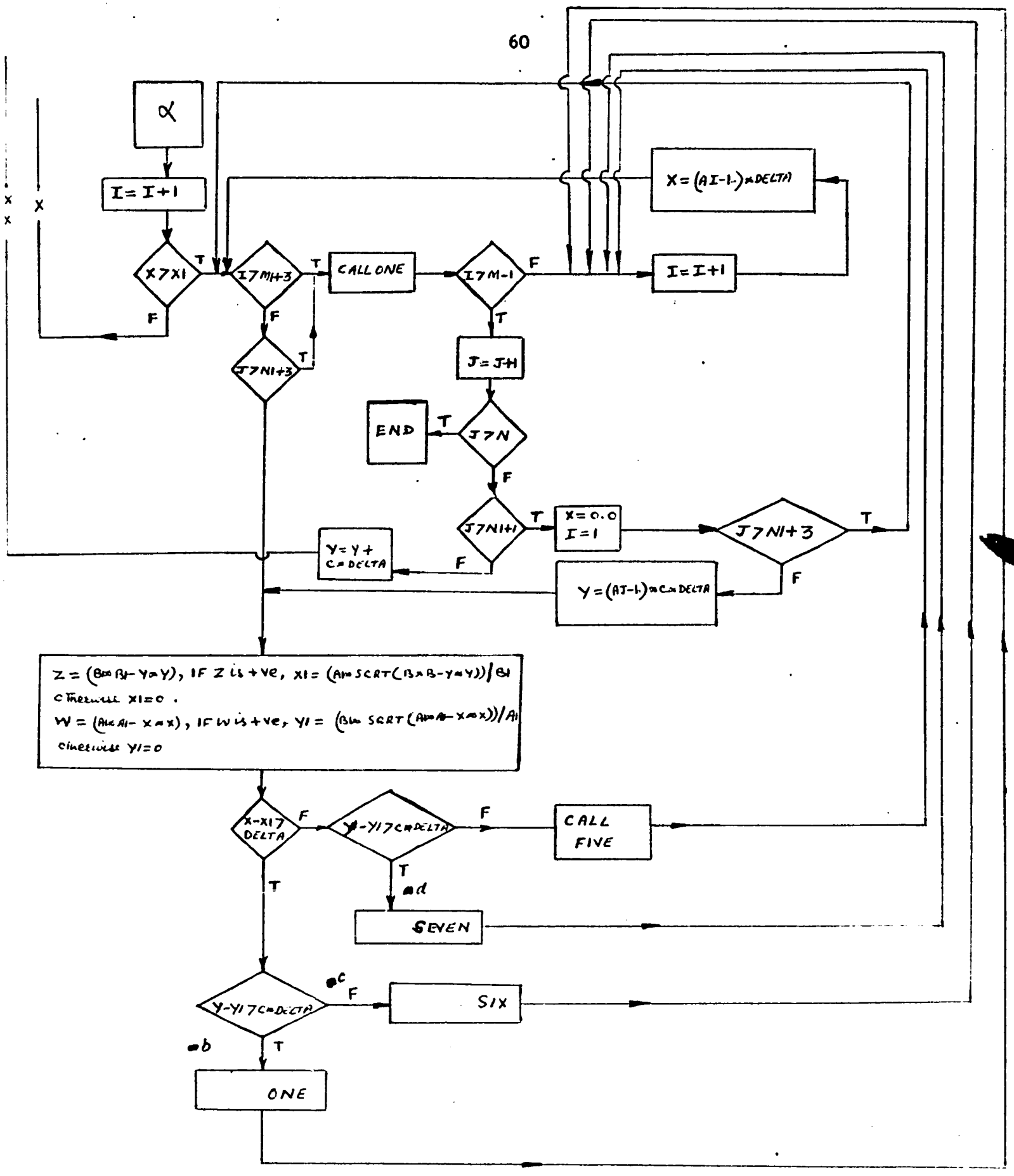
α
I = I+1
X
X7X1
T
F
I7M+3
T
F
CALL ONE
I7M-1
F
T
I = I+1
X = (AI-1-) * DELTA
J7N1+3
T
F
J = J+1
J7N
T
END
F
J7N1+1
T
X = 0.0
I = 1
J7N1+3
T
F
Y = Y + C * DELTA
F
Y = (AI-1) * C * DELTA
Z = (B * B - Y * Y), IF Z is +ve, X1 = (A * SQRT(B * B - Y * Y)) / B
Otherwise X1 = 0 .
W = (A * A1 - X * X), IF W is +ve, Y1 = (B * SQRT(A * A - X * X)) / A
otherwise Y1 = 0
X-X1 7 DELTA
F
Y-Y1 7 C * DELTA
F
CALL FIVE
T
d
SEVEN
Y-Y1 7 C * DELTA
c
F
SIX
b
T
ONE

*a

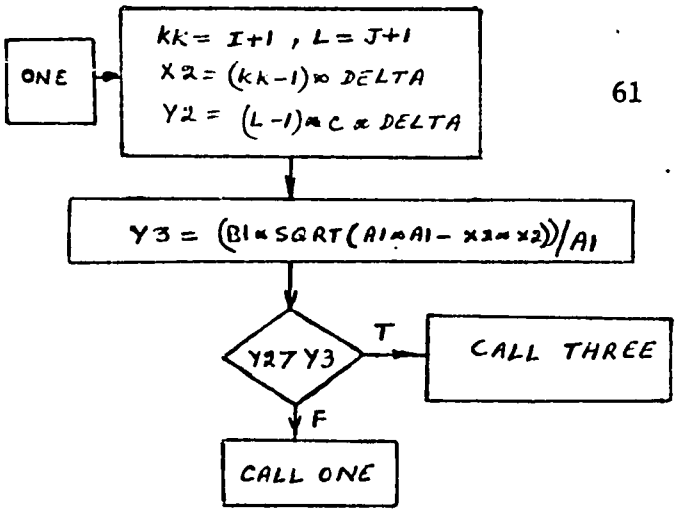
ONE
KK= I+1 , L= J+1
X2= (KK-1)* DELTA
Y2 = (L-1)*C* DELTA
Y3 = (B1*SQRT(A1*A1- X2*X2))/A1
Y2? Y3
T
CALL THREE
F
CALL ONE

*b

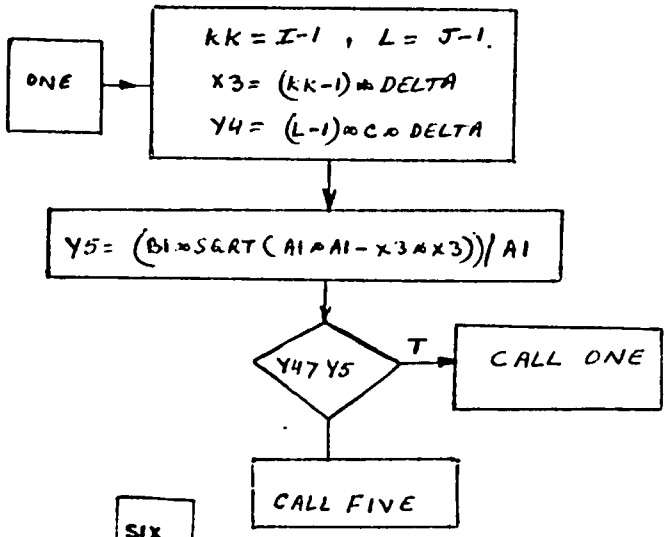
ONE
KK= I-1 , L= J-1.
X3= (KK-1)* DELTA
Y4= (L-1)*C* DELTA
Y5= (B1*SQRT(A1*A1- X3*X3))/A1
Y4? Y5
T
CALL ONE
CALL FIVE

*c

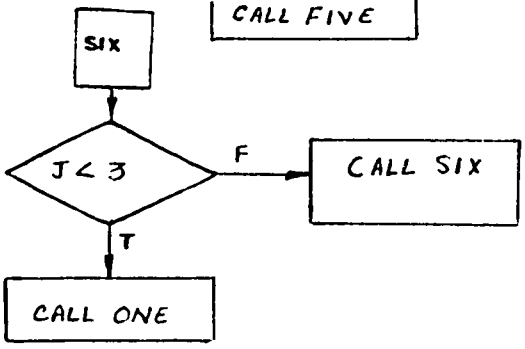
SIX
J< 3
F
CALL SIX
T
CALL ONE

*d

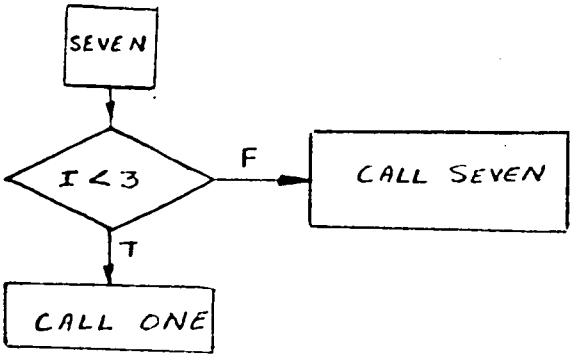
SEVEN
I< 3
F
CALL SEVEN
T
CALL ONE

SUBROUTINE ONE FLOW CHART

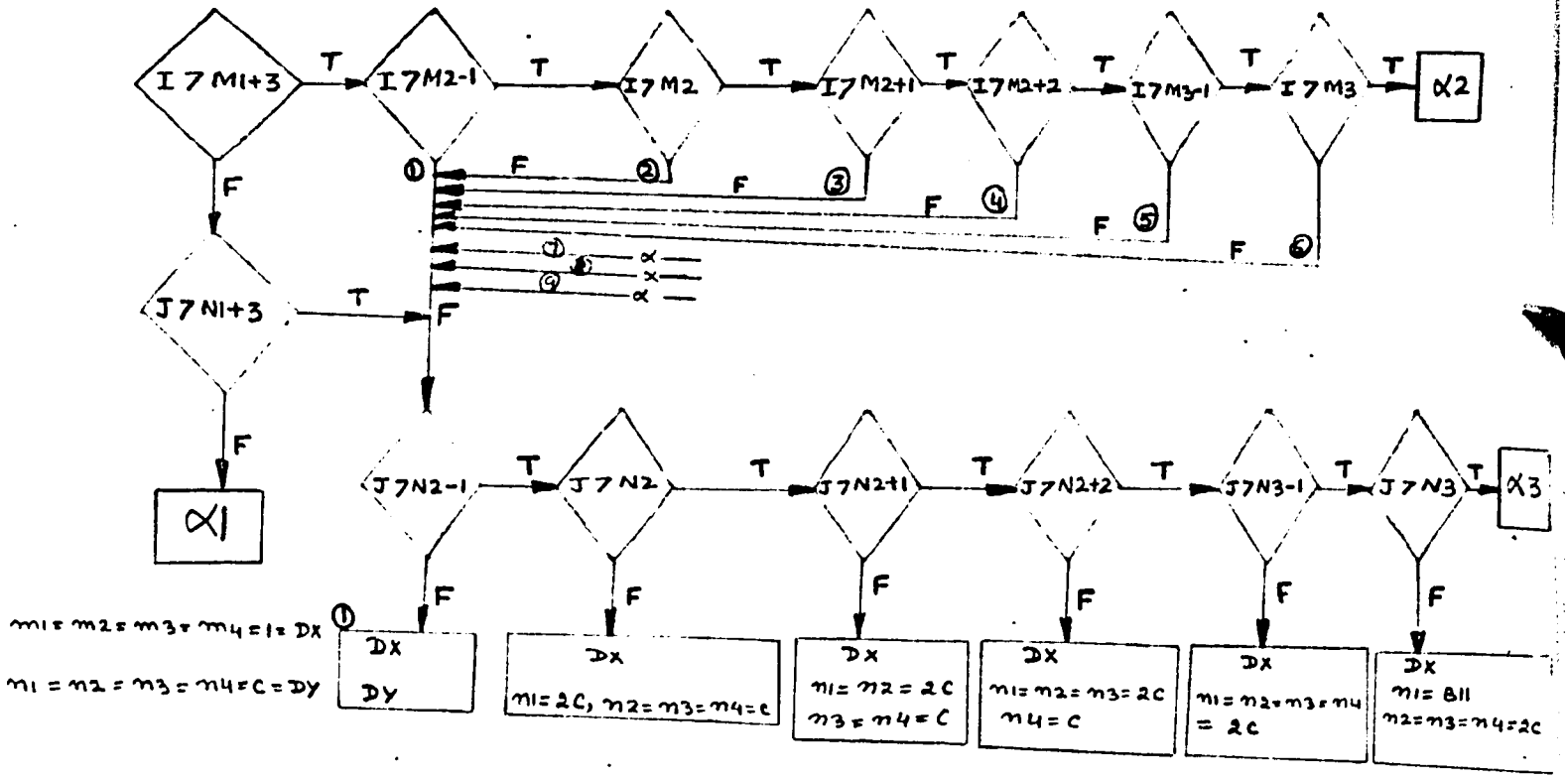

② $m_1 = 2, \quad m_2 = m_3 = m_4 = 1$

③ $m_1 = m_2 = 2, \quad m_3 = m_4 = 1$

④ $m_1 = m_2 = m_3 = 2, \quad m_4 = 1$

⑤ $m_1 = m_2 = m_3 = m_4 = 2$

⑥ $m_1 = All, \quad m_2 = m_3 = m_4 = 2$

⑦ $m_1 = m_2 = All, \quad m_3 = m_4 = 2$

⑧ $m_1 = m_2 = m_3 = All, \quad m_4 = 2$

⑨ $m_1 = m_2 = m_3 = m_4 = All$

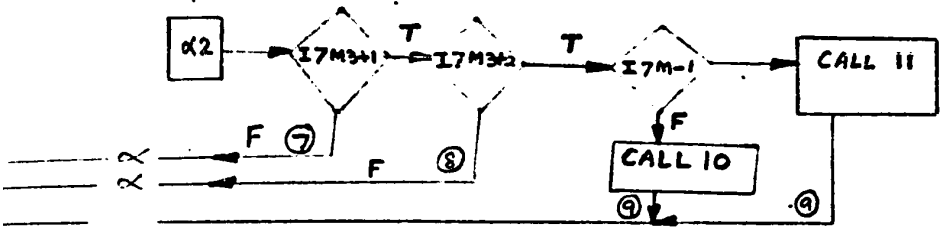
α2
I7M3+1
T
I7M3+2
T
I7M-1
CALL 11
F
F
CALL 10

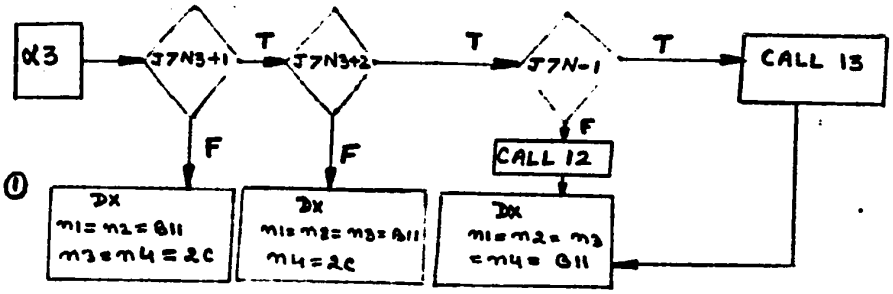
α3
J7N3+1
T
J7N3+2
T
J7N-1
T
CALL 13
F
F
F
CALL 12
DX
m1=m2=B11
m3=m4=2C
DX
m1=m2=m3=B11
m4=2C
DX
m1=m2=m3
=m4=B11

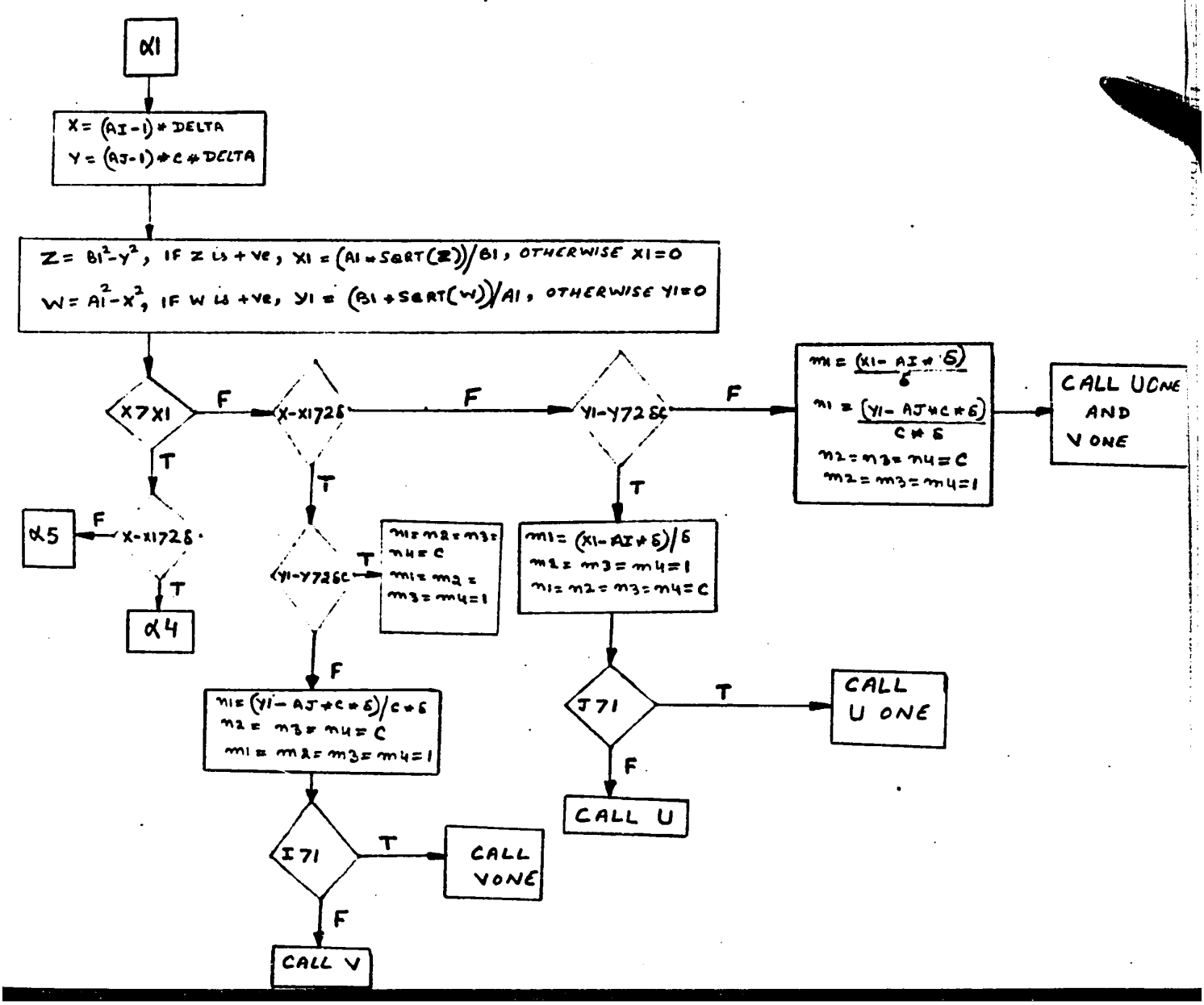
α1
X=(AI-1)*DELTA
Y=(AJ-1)*C*DELTA
Z=B1²-Y², IF Z is +ve, X1=(A1+SQRT(Z))/B1, OTHERWISE X1=0
W=A1²-X², IF W is +ve, Y1=(B1+SQRT(W))/A1, OTHERWISE Y1=0
X?X1
F
X-X1?2δ
F
Y1-Y?2δC
F
m1=(X1-AI*δ)/δ
m1=(Y1-AJ*C*δ)/Cδ
m2=m3=m4=C
m2=m3=m4=1
CALL UONE AND V ONE
T
T
T
α5
F
X-X1?2δ
T
α4
Y1-Y?2δC
T
m1=m2=m3=m4=C
m1=m2=m3=m4=1
m1=(X1-AI*δ)/δ
m2=m3=m4=1
m1=m2=m3=m4=C
F
m1=(Y1-AJ*C*δ)/Cδ
m2=m3=m4=C
m1=m2=m3=m4=1
J?1
T
CALL U ONE
F
CALL U
I?1
T
CALL V ONE
F
CALL V

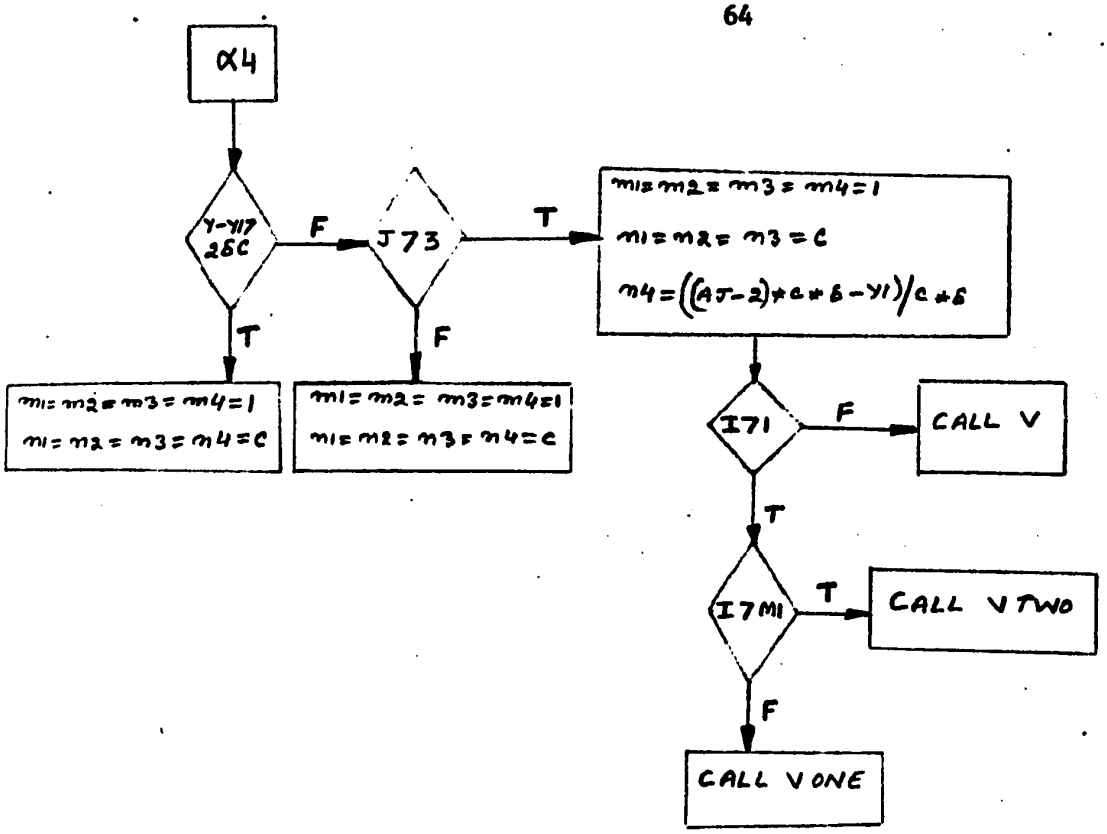
α4
Y-Y17 ≥ 6C
F
J ? 3
T
m1=m2=m3=m4=1
m1=m2=m3=C
m4=((AJ-2)*C*6-Y1)/C*6
T
F
m1=m2=m3=m4=1
m1=m2=m3=m4=C
m1=m2=m3=m4=1
m1=m2=m3=m4=C
I ? 1
F
CALL V
T
I ? M1
T
CALL V TWO
F
CALL V ONE

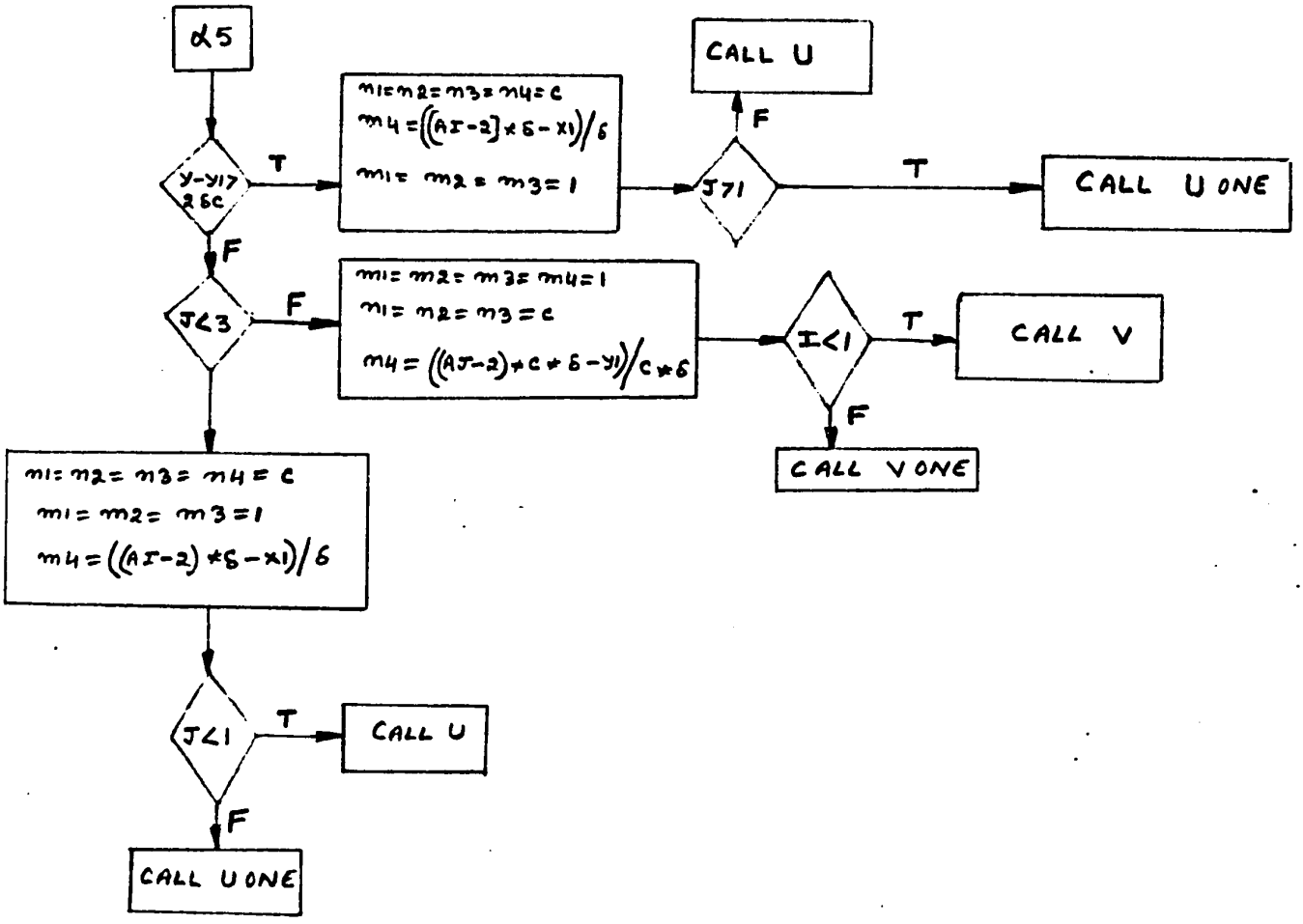
α5
Y-Y17 ≥ 6C
T
m1=m2=m3=m4=C
m4=((AI-2]*6-X1)/6
m1=m2=m3=1
J ? 1
F
CALL U
T
CALL U ONE
F
J < 3
F
m1=m2=m3=m4=1
m1=m2=m3=C
m4=((AJ-2)*C*6-Y1)/C*6
I < 1
T
CALL V
F
CALL V ONE
m1=m2=m3=m4=C
m1=m2=m3=1
m4=((AI-2)*6-X1)/6
J < 1
T
CALL U
F
CALL U ONE

SUBROUTINE TWO FLOW CHART

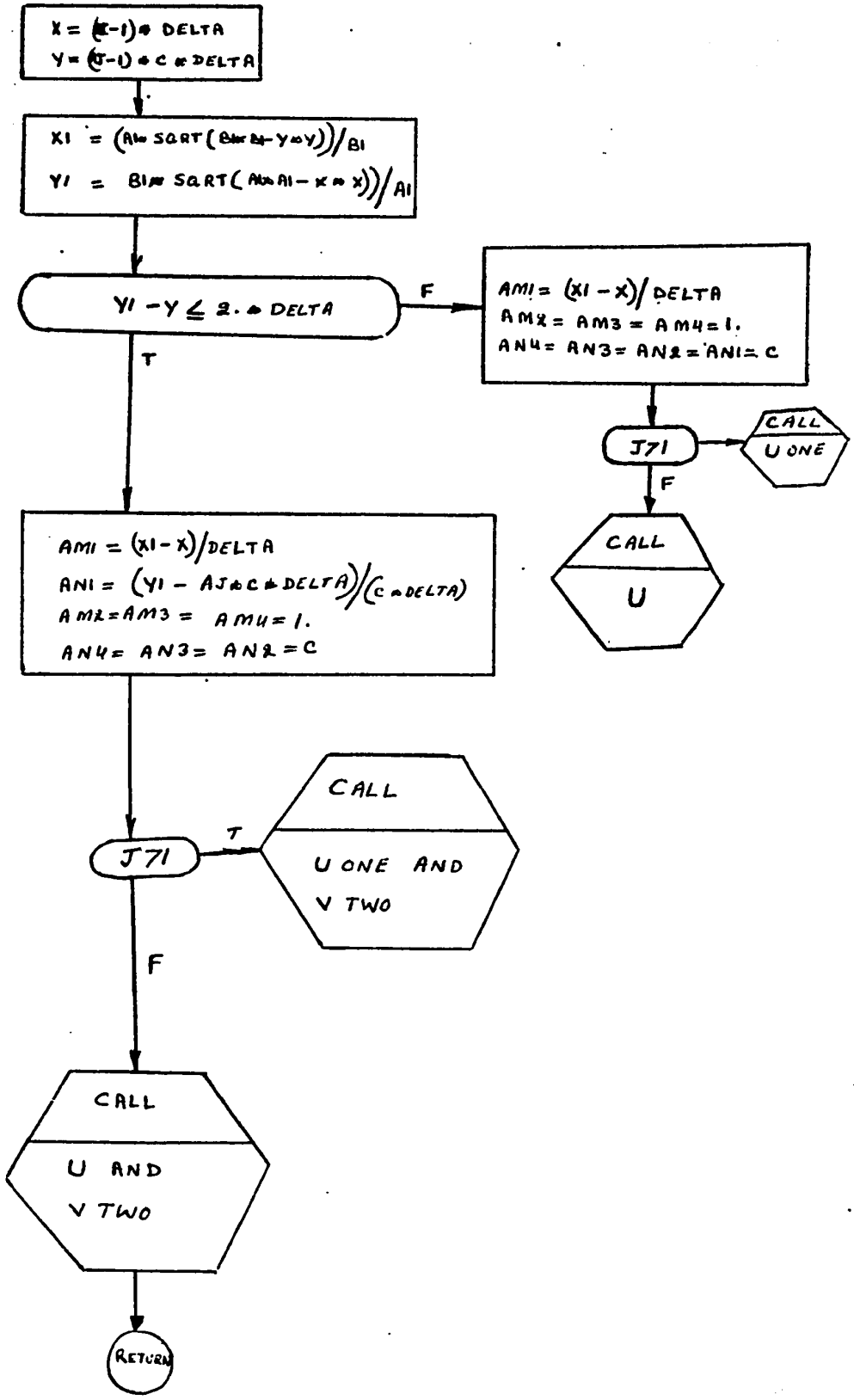

SUBROUTINE THREE FLOW CHART

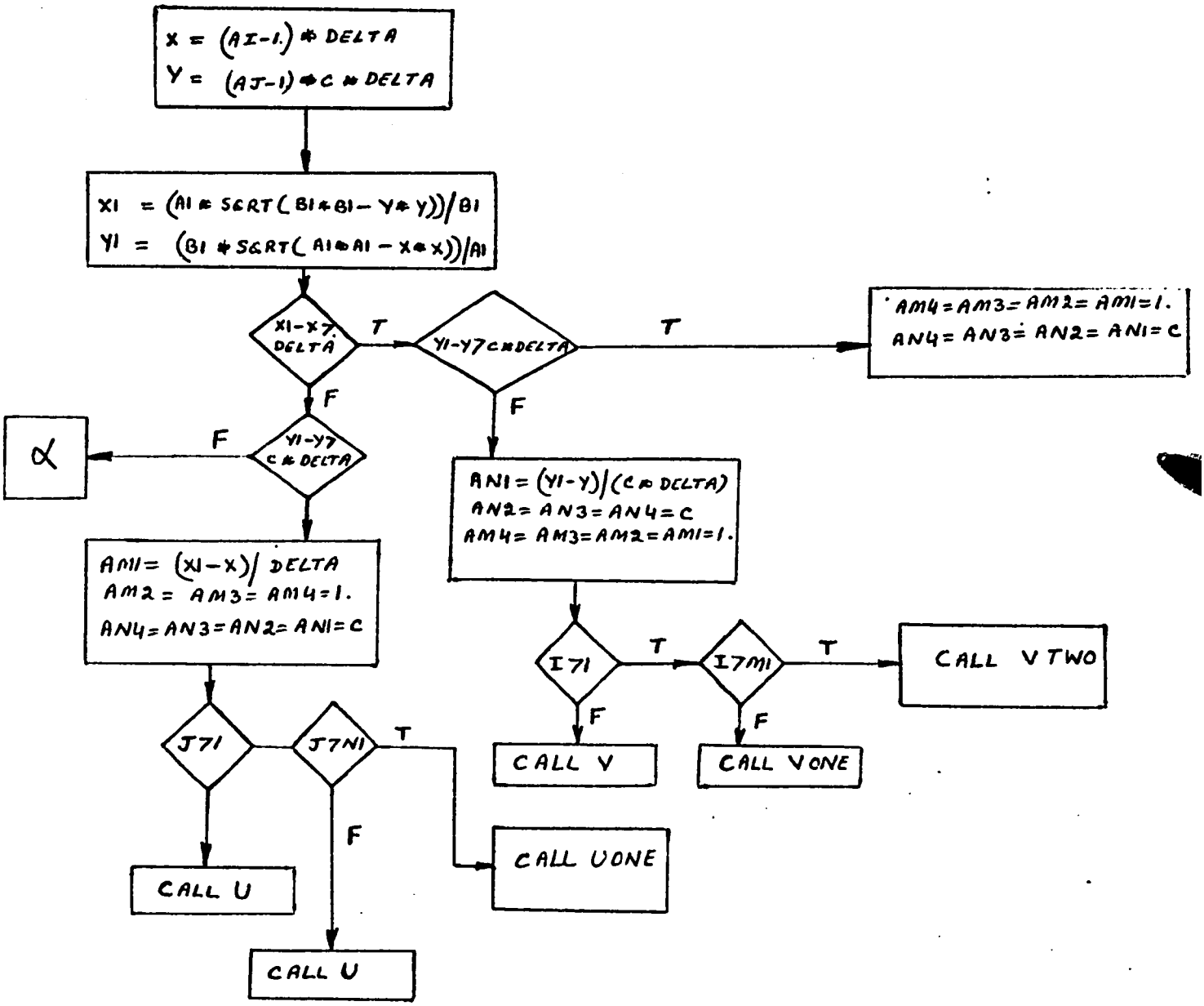

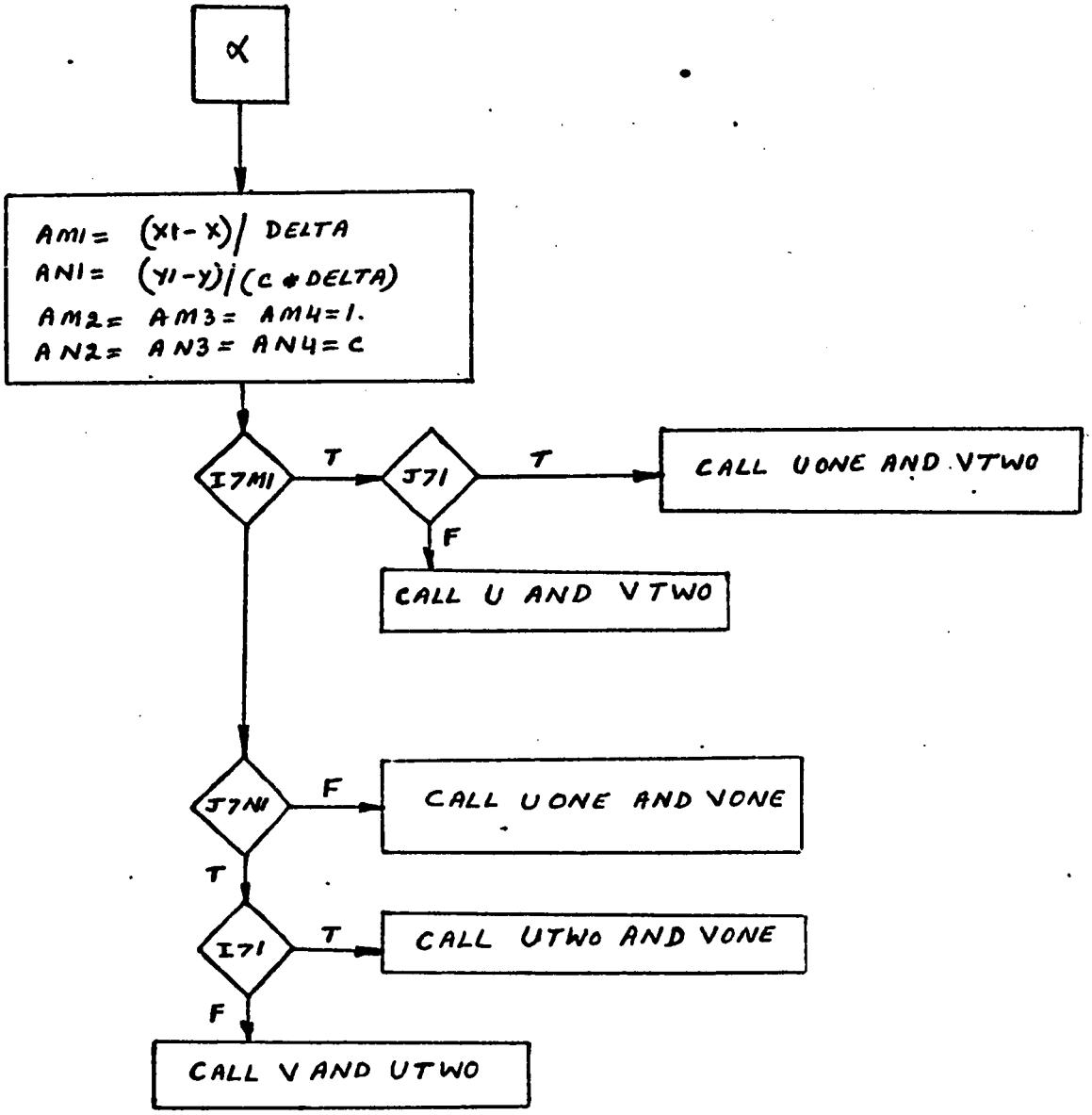
X
AM1 = (X1 - X) / DELTA
AN1 = (Y1 - Y) / (C * DELTA)
AM2 = AM3 = AM4 = 1.
AN2 = AN3 = AN4 = C
I7M1
T
J71
T
CALL UONE AND VTWO
F
CALL U AND VTWO
J7N1
F
CALL UONE AND VONE
T
I71
T
CALL UTWO AND VONE
F
CALL V AND UTWO

SUBROUTINE FOUR FLOW CHART

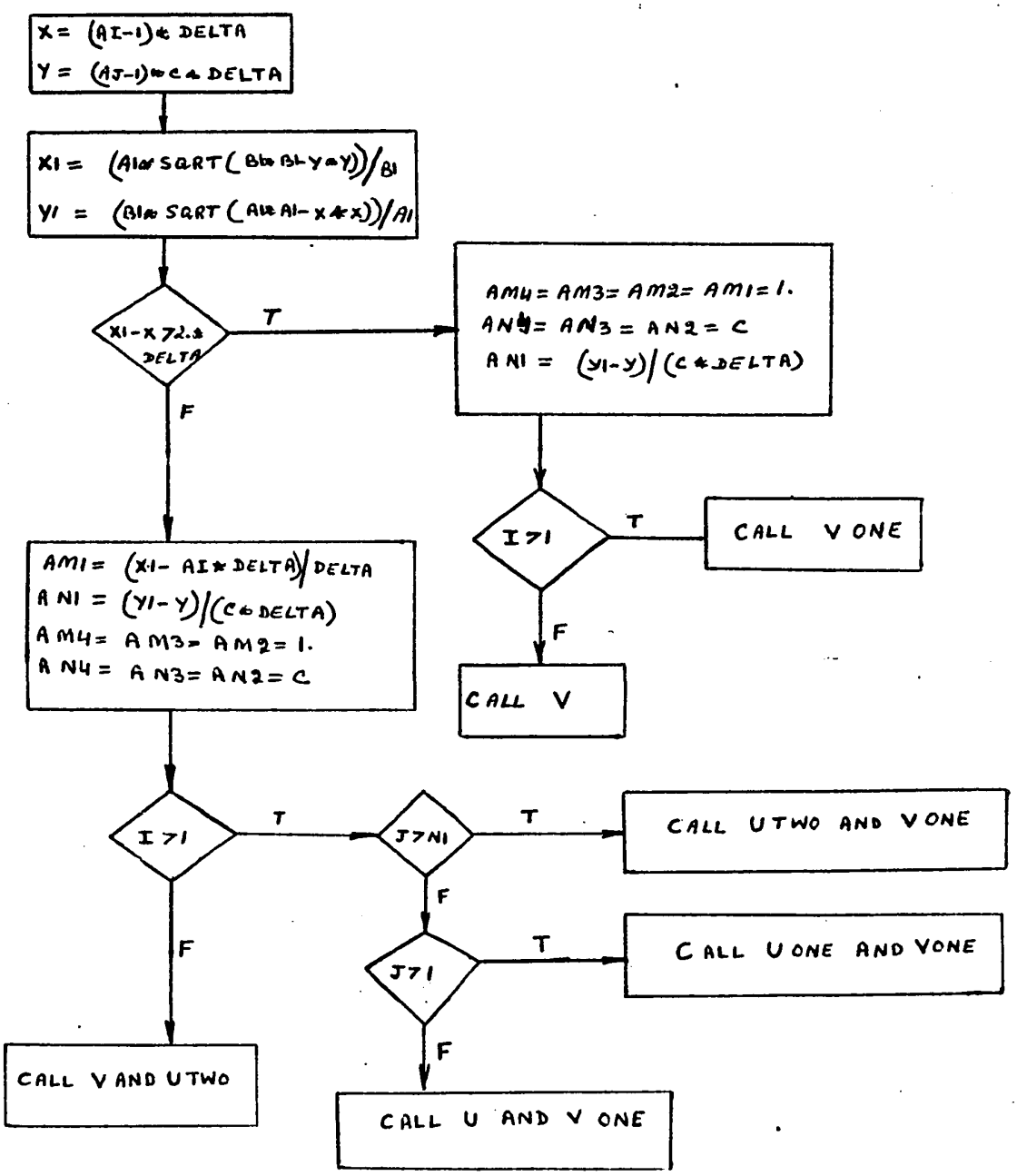

SUBROUTINE FIVE FLOW CHART

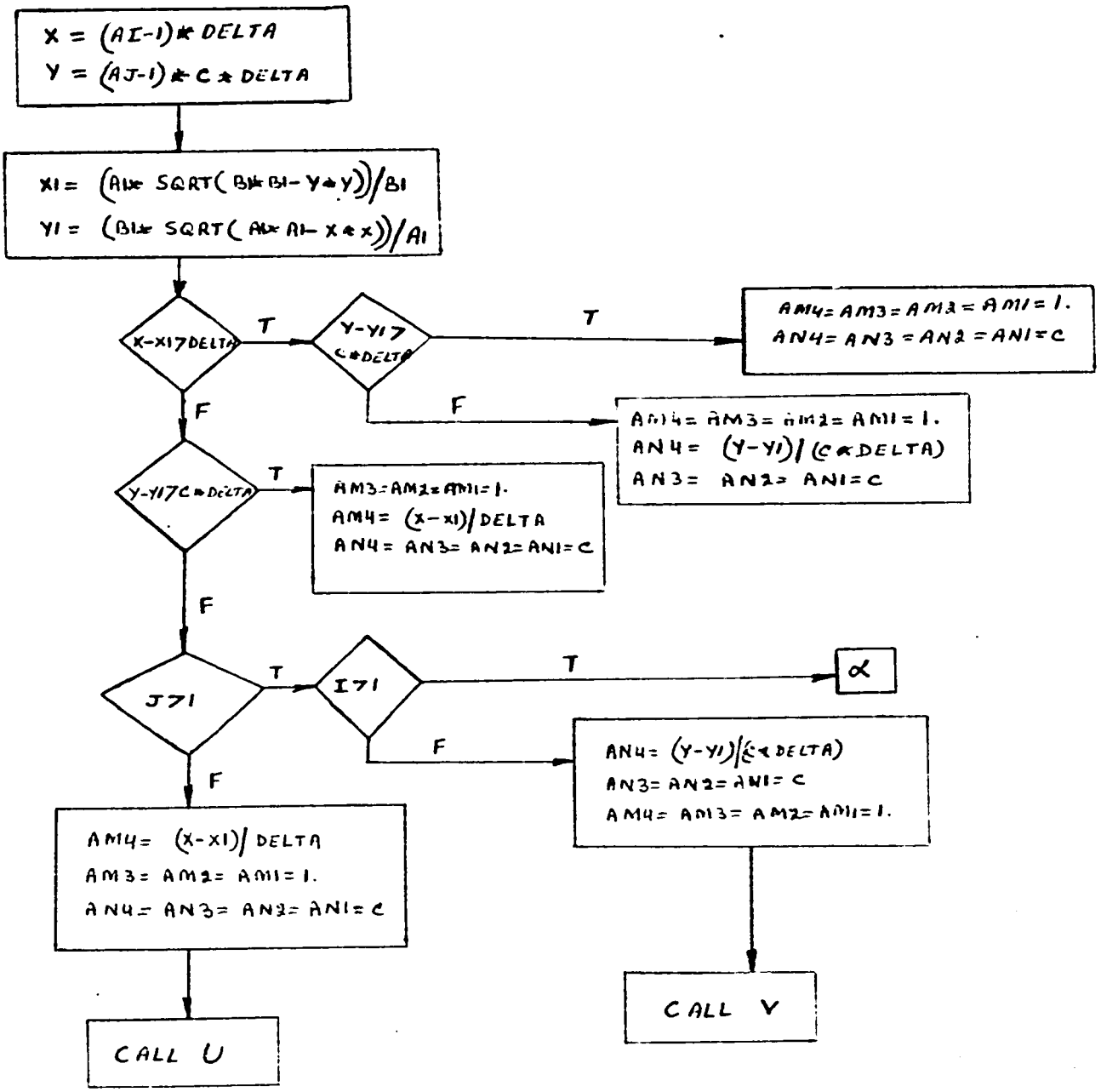

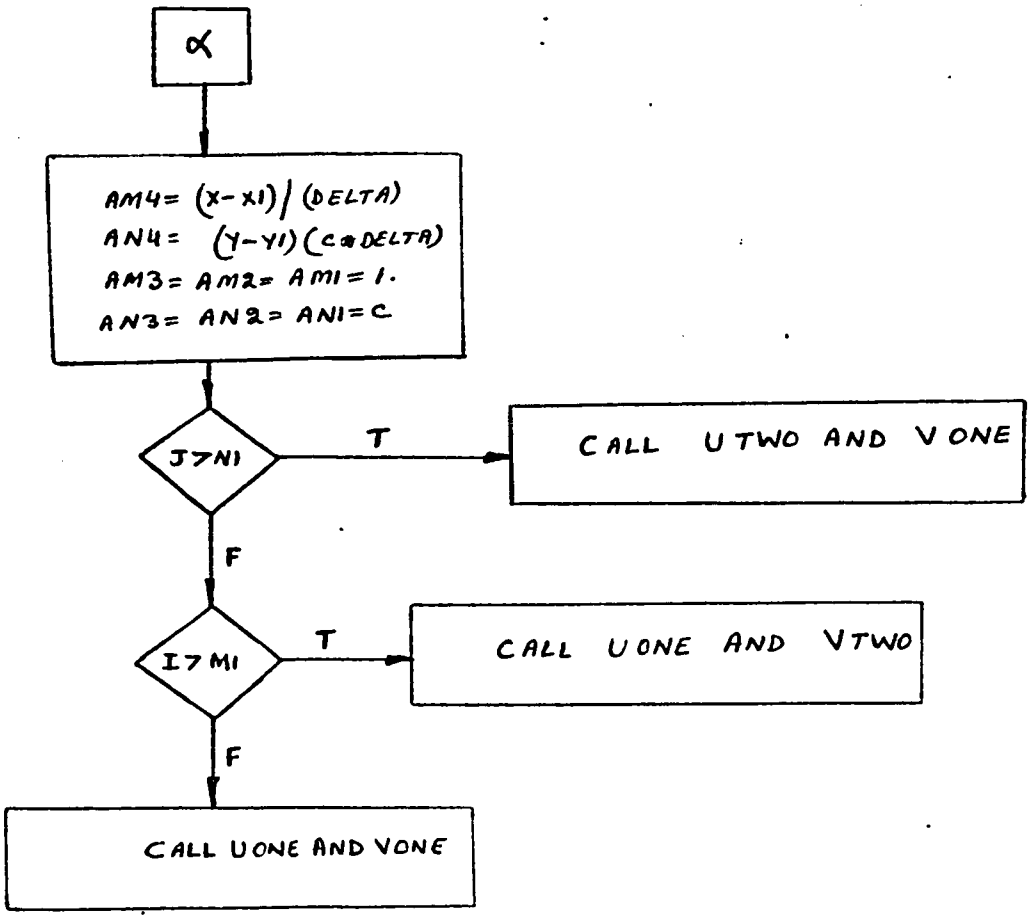
∝
AM4= (X-X1)/(DELTA)
AN4= (Y-Y1)(C*DELTA)
AM3= AM2= AM1= 1.
AN3= AN2= AN1= C
J>N1
T
CALL UTWO AND V ONE
F
I>M1
T
CALL UONE AND VTWO
F
CALL UONE AND VONE

SUBROUTINE SIX FLOW CHART

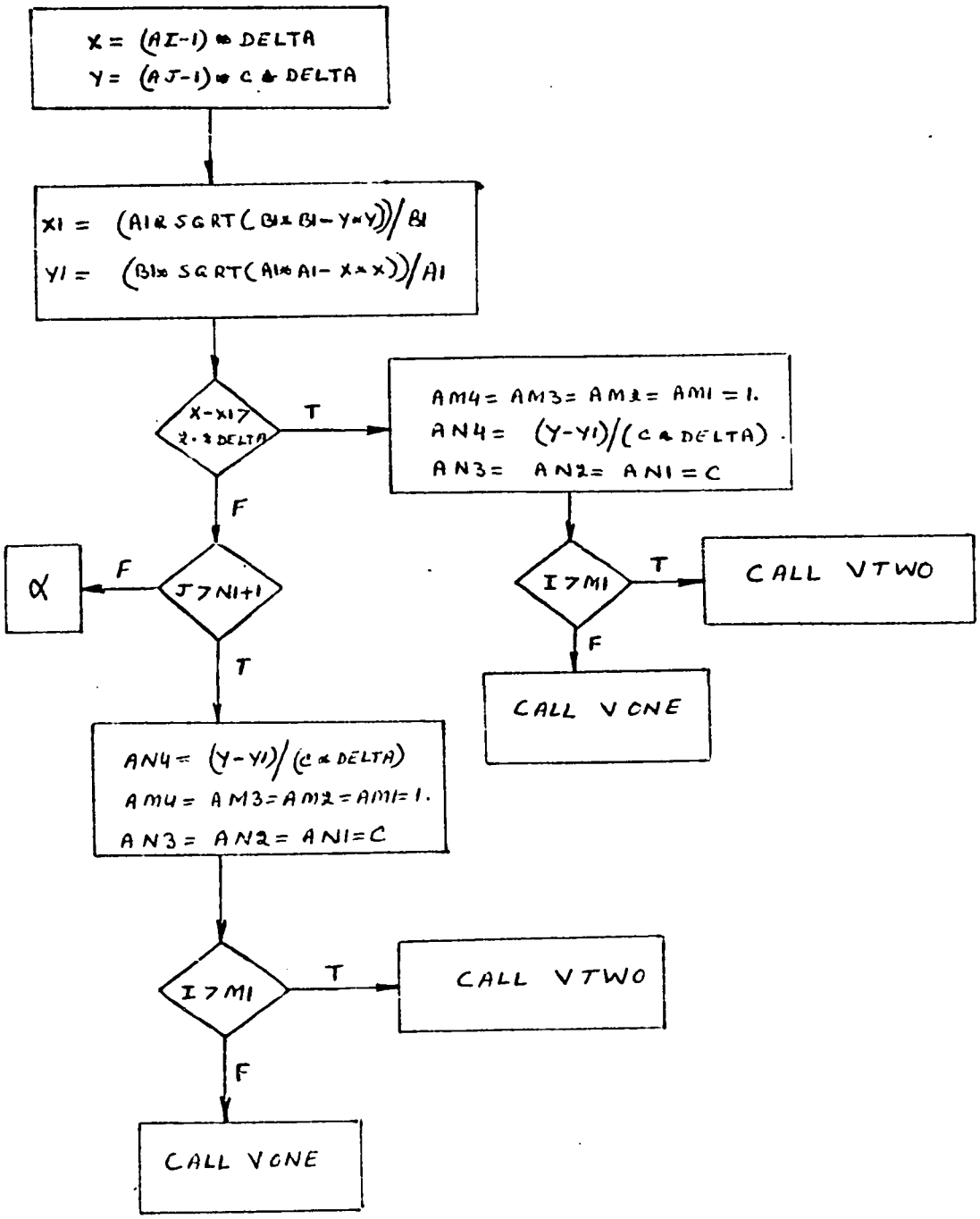

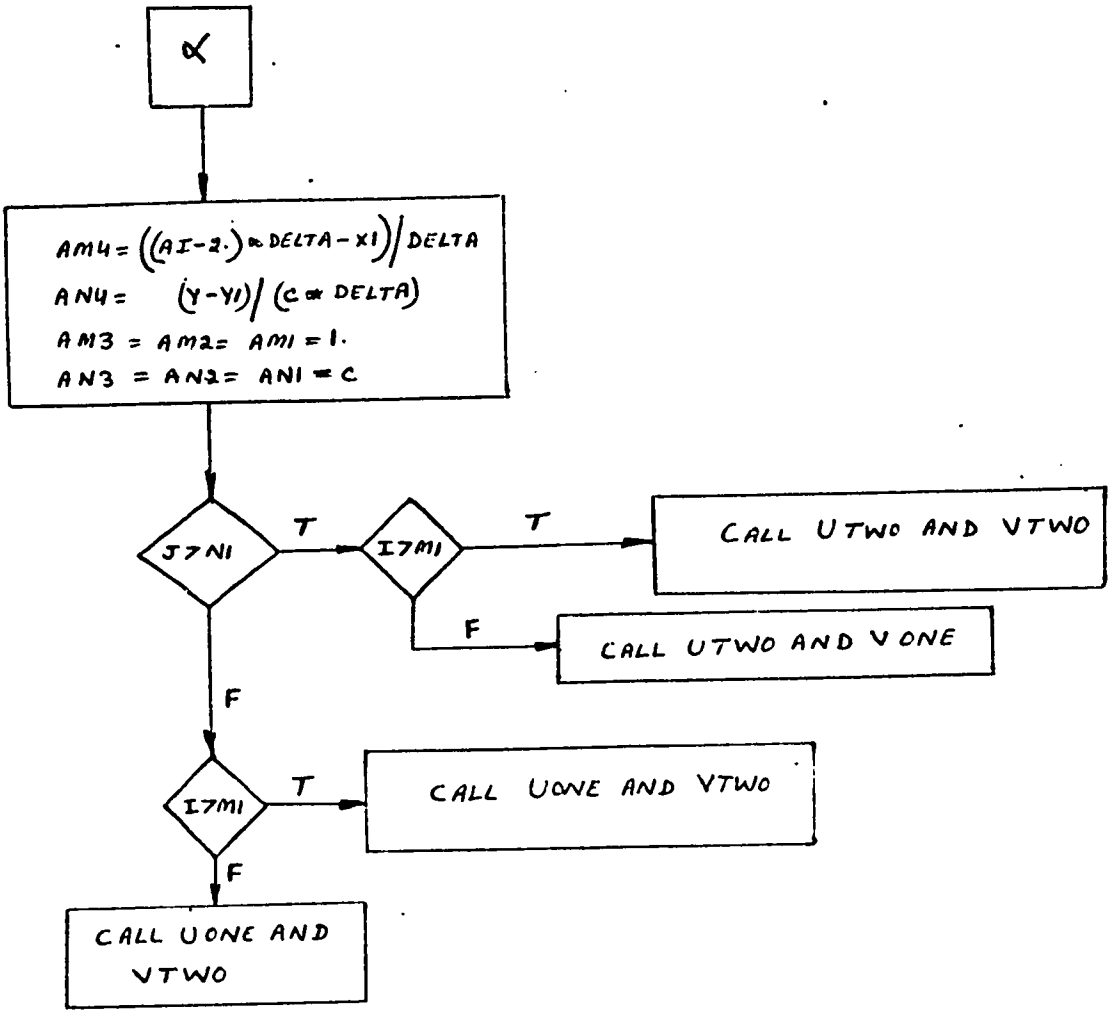
α
AM4 = ((AI-2.) * DELTA - X1) / DELTA
AN4 = (Y-Y1) / (C * DELTA)
AM3 = AM2 = AM1 = 1.
AN3 = AN2 = AN1 = C
J > N1
T
I > M1
T
CALL UTWO AND VTWO
F
CALL UTWO AND V ONE
F
I > M1
T
CALL UONE AND VTWO
F
CALL UONE AND VTWO

SUBROUTINE SEVEN FLOW CHART

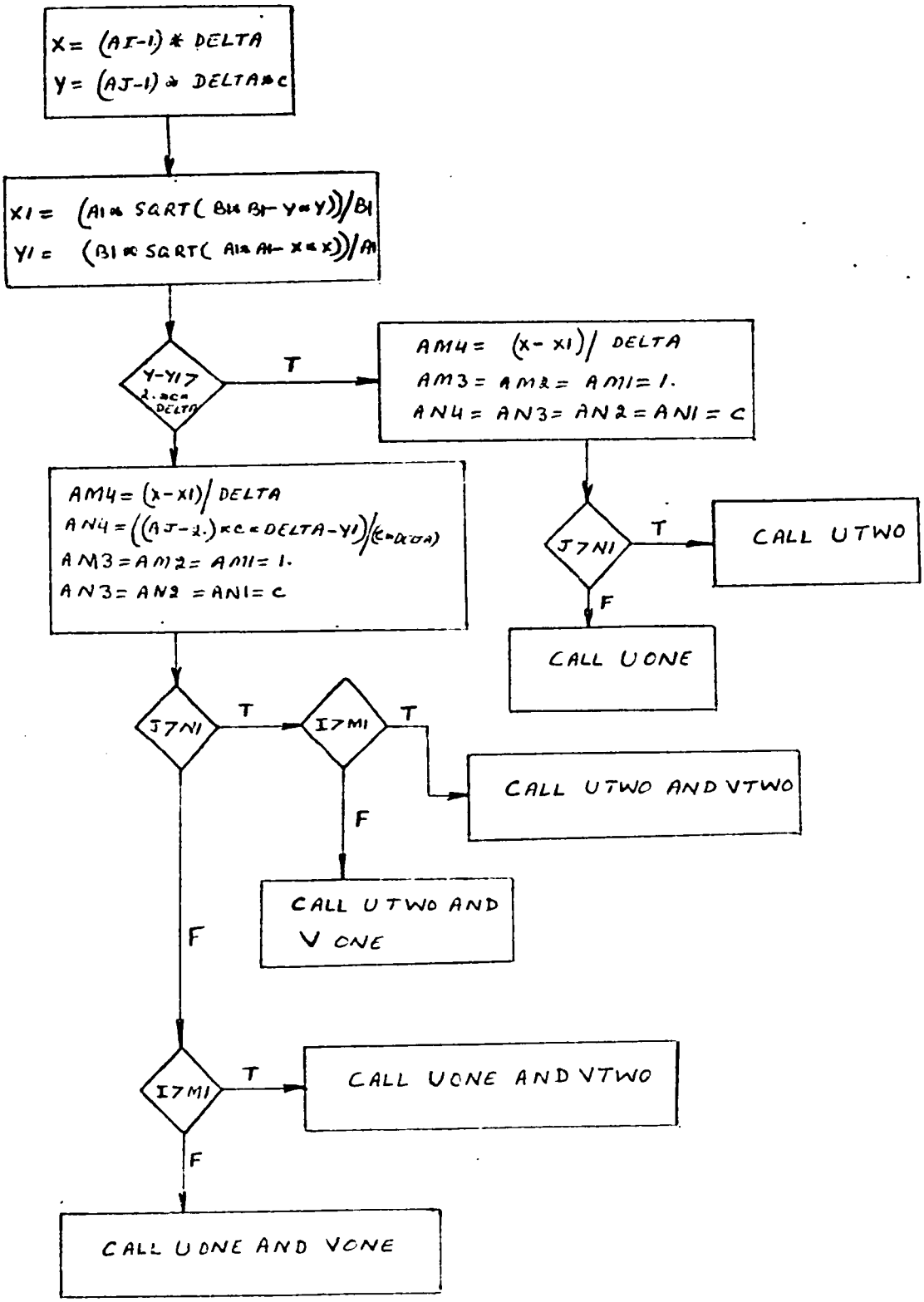

SUBROUTINE TEN FLOW CHART

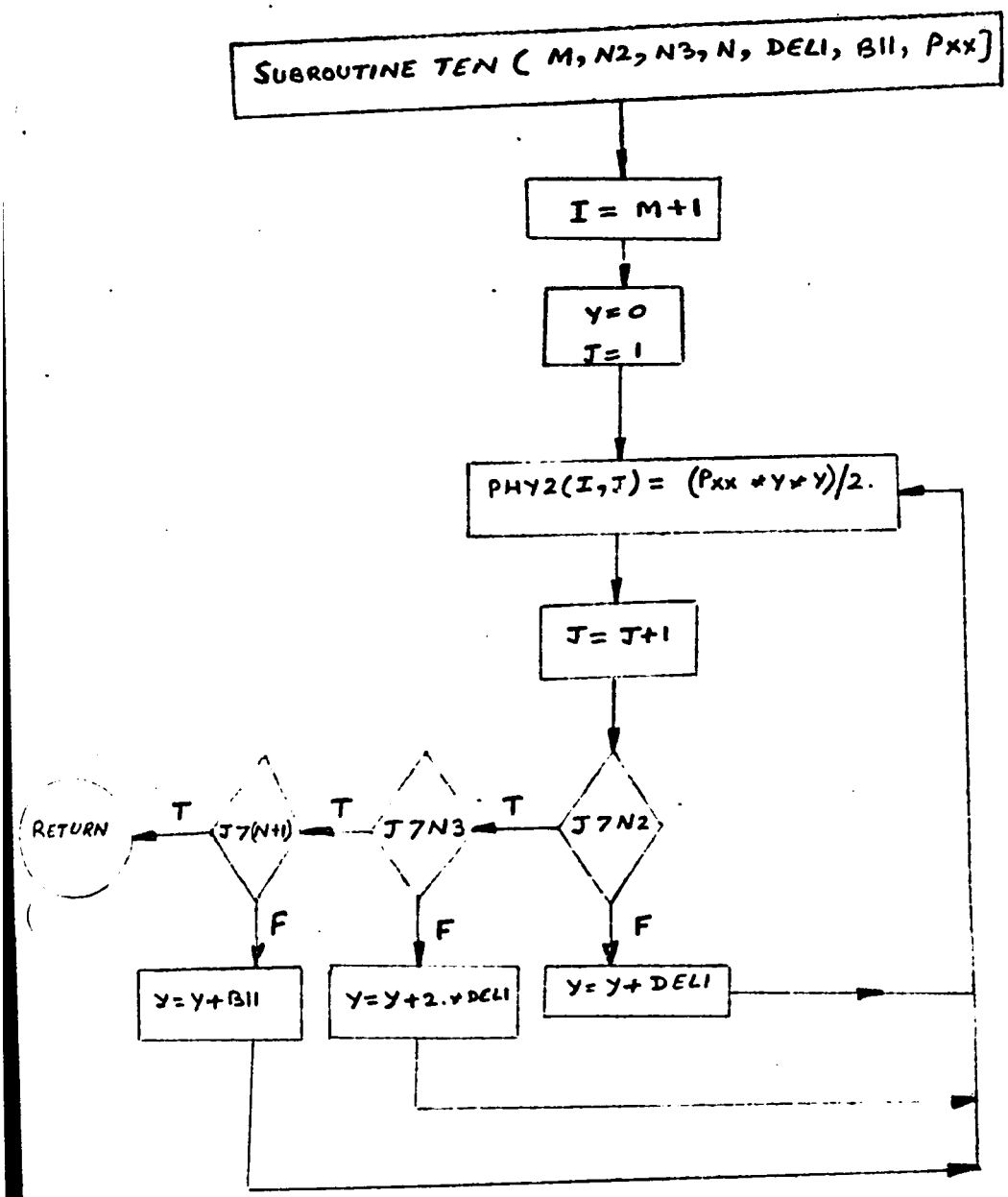

SUBROUTINE ELEVEN FLOW CHART

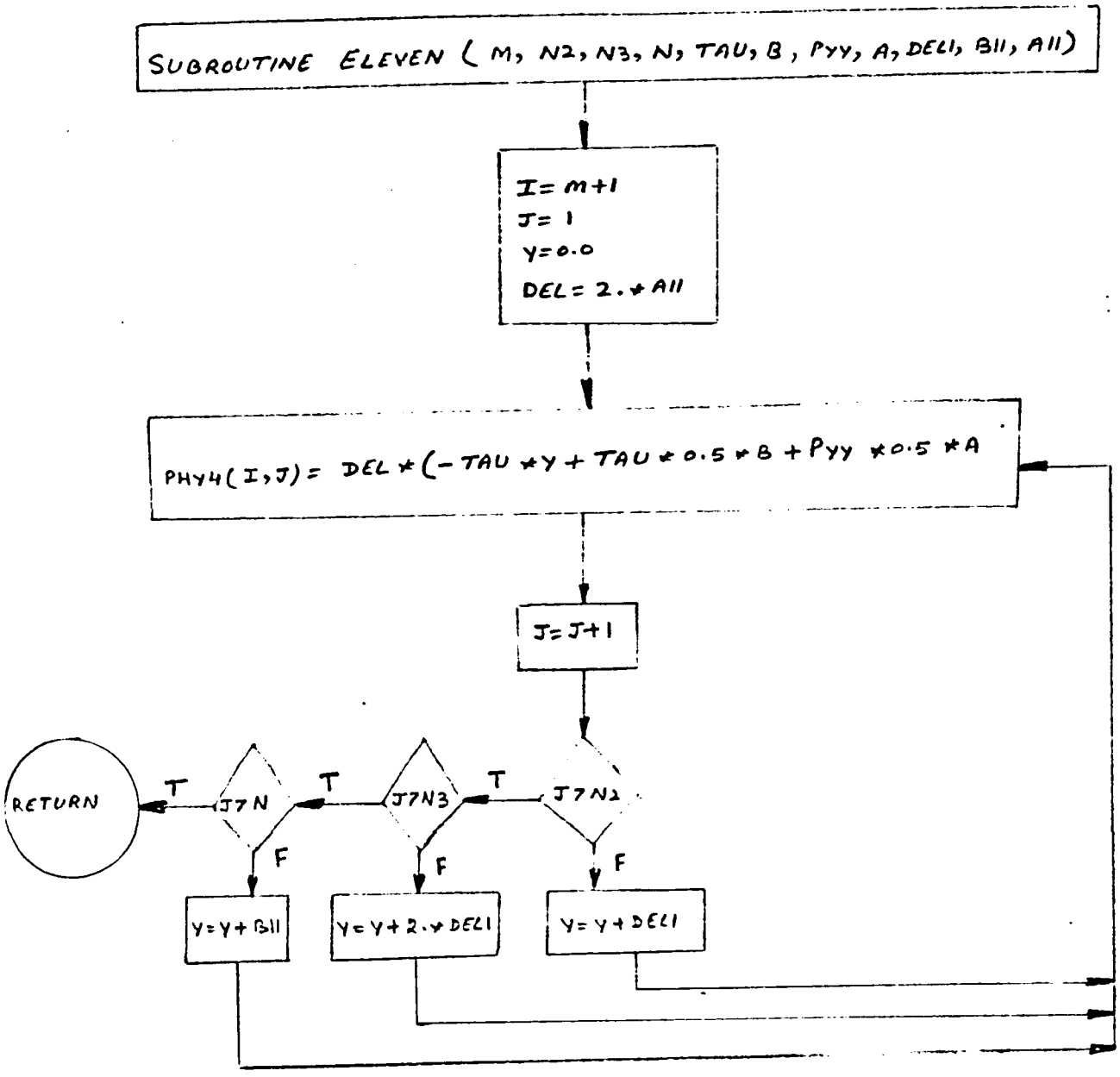

SUBROUTINE TWELVE FLOW CHART

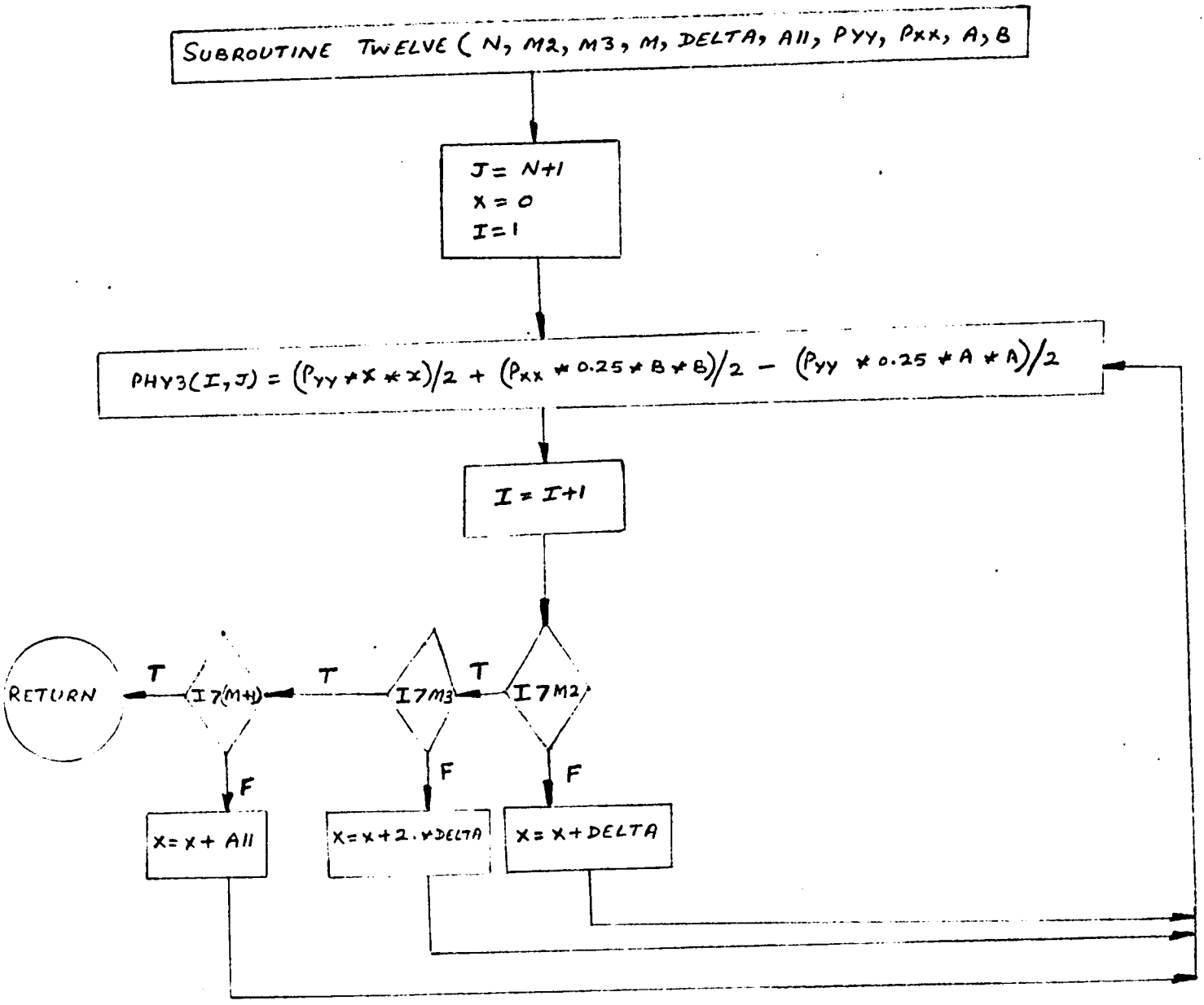

SUBROUTINE THTEEN FLOW CHART

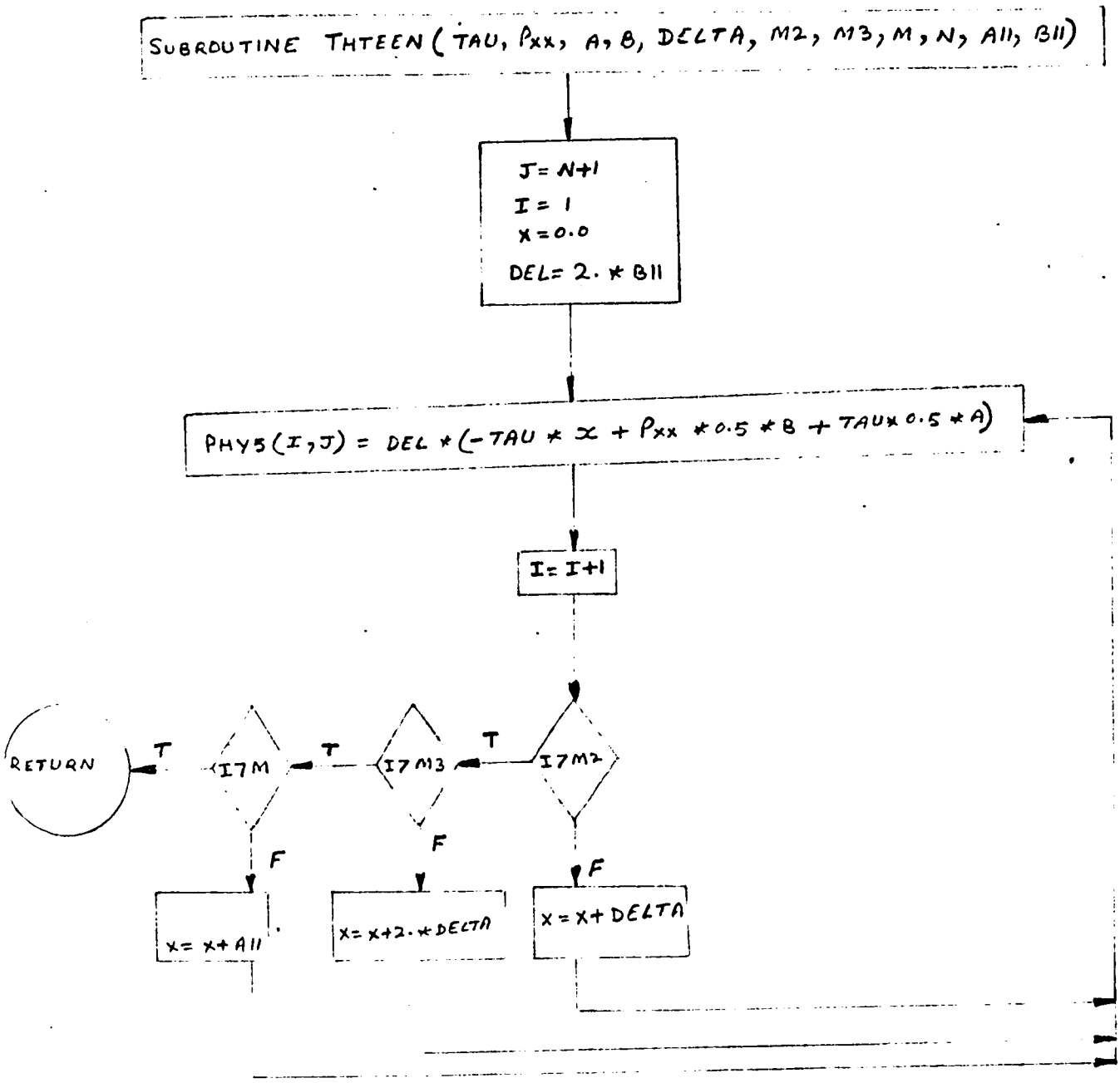

SUBROUTINE U FLOW CHART

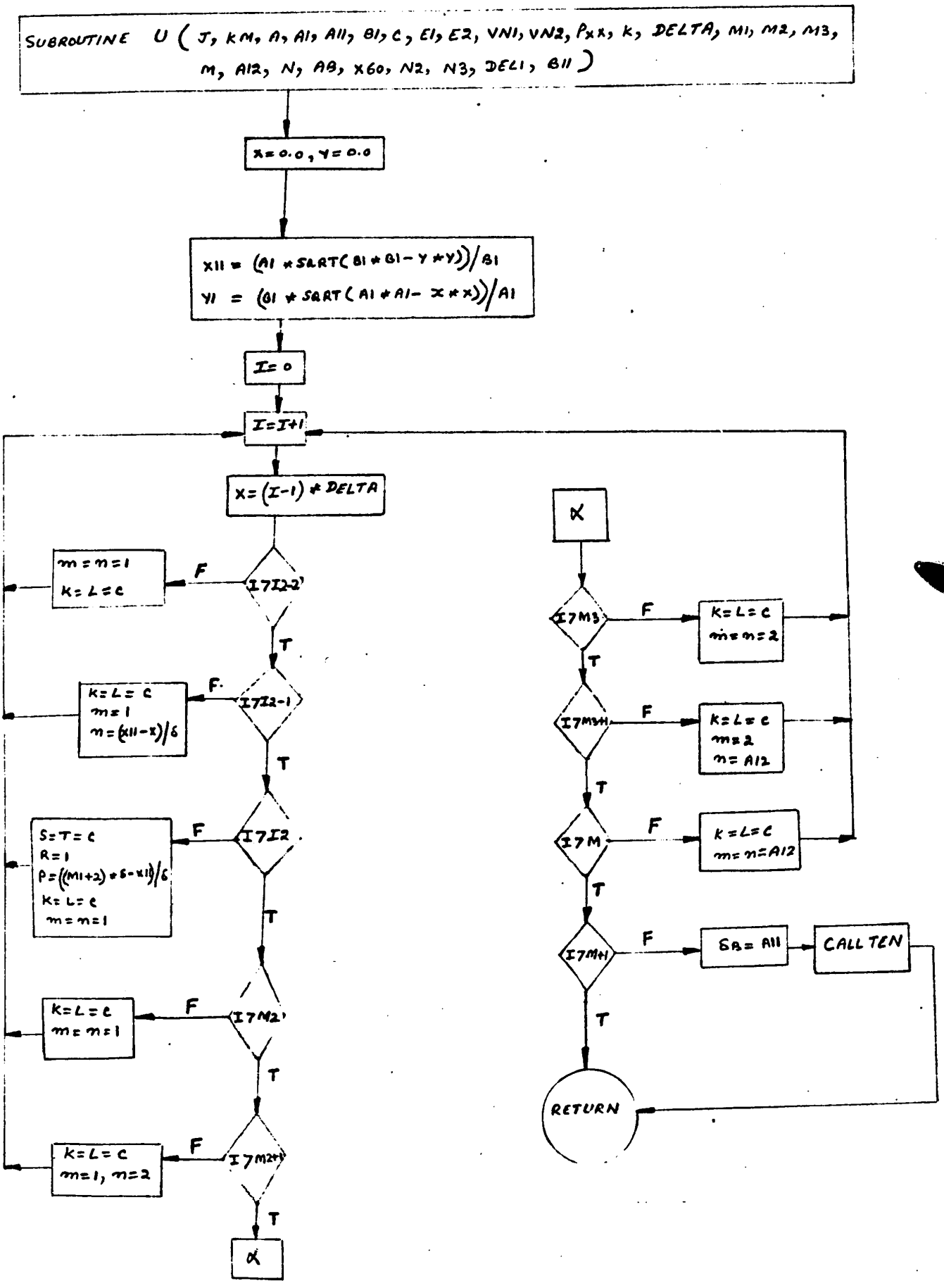

SUBROUTINE U ONE FLOW CHART

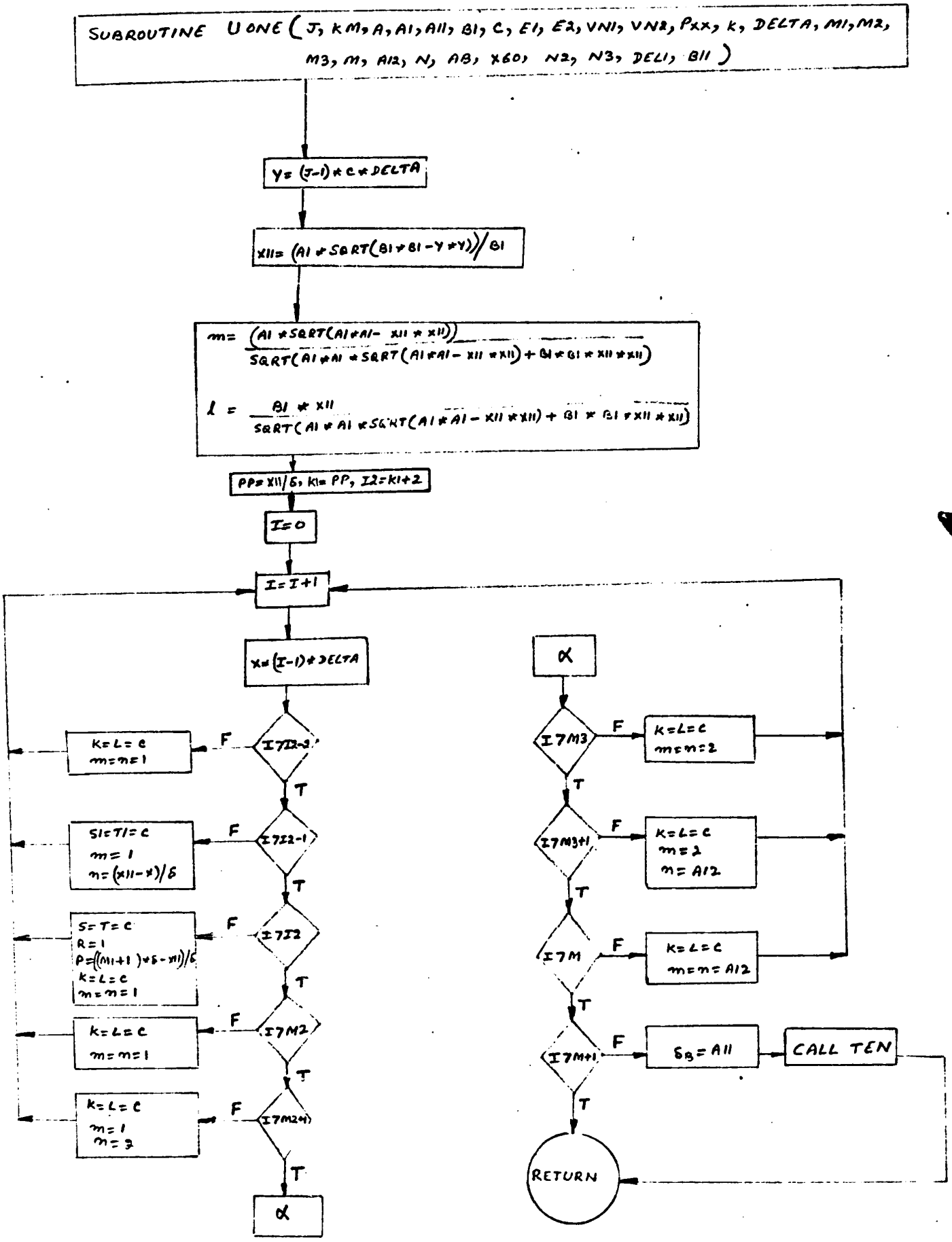

SUBROUTINE U TWO FLOW CHART

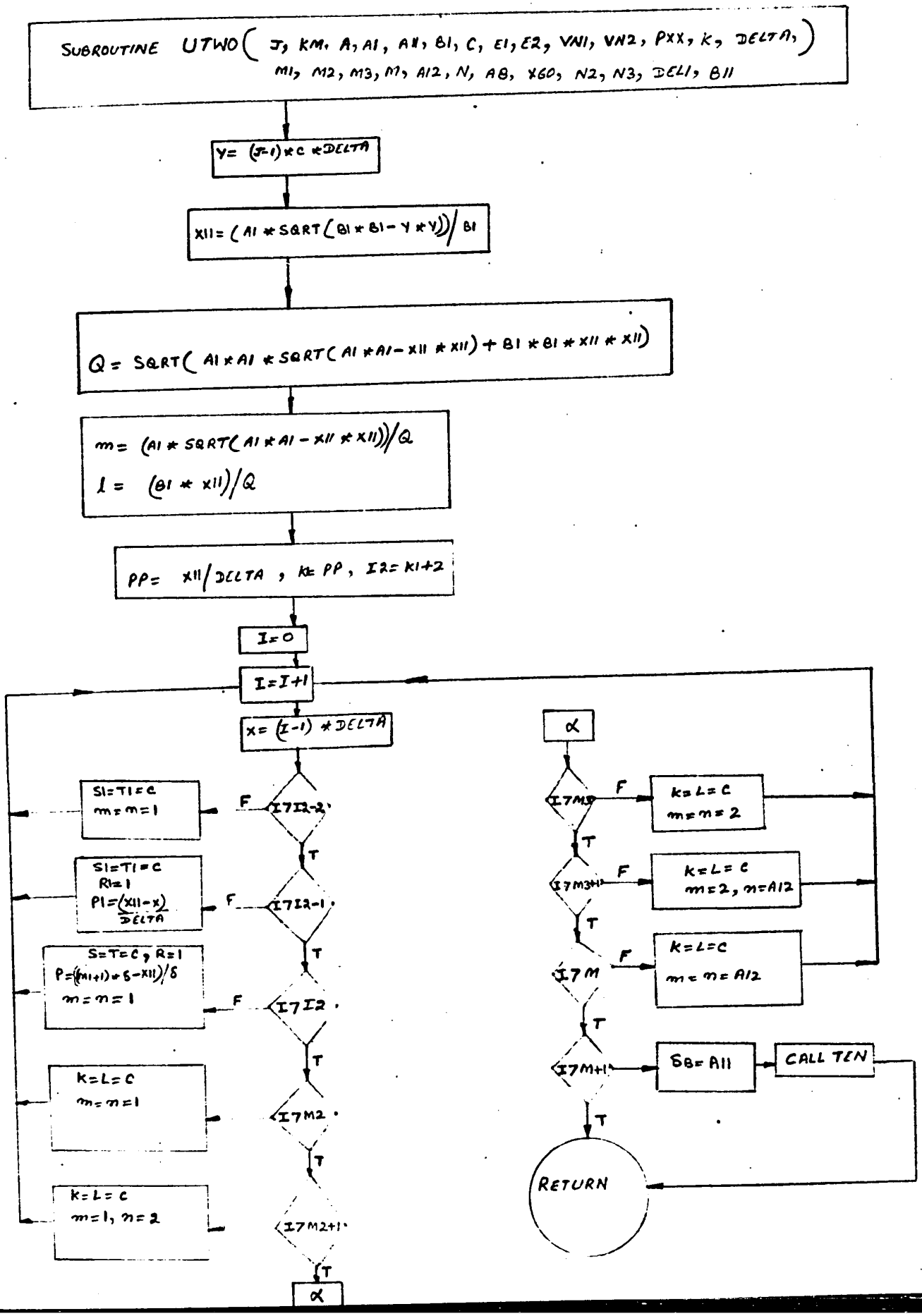

SUBROUTINE V FLOW CHART

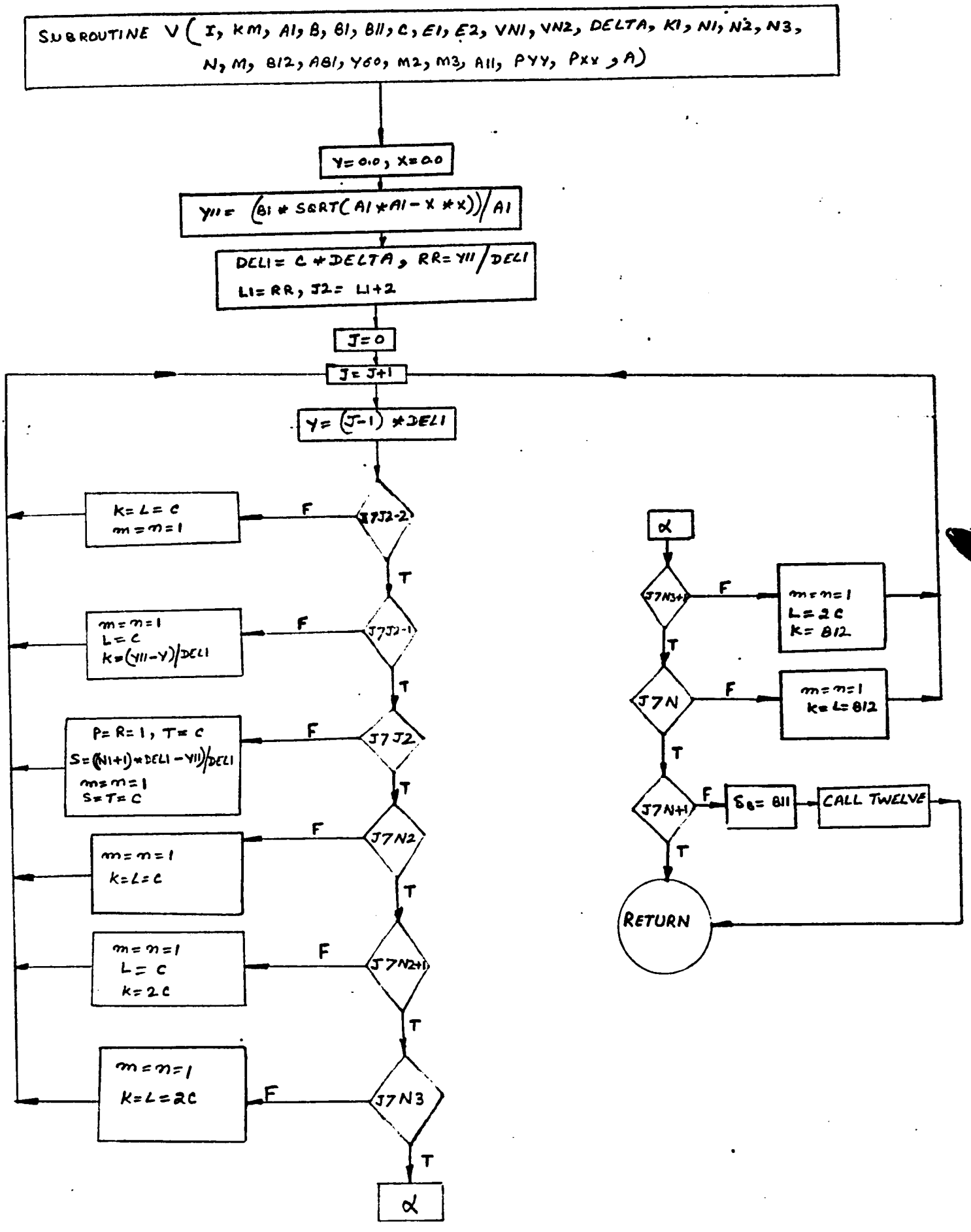

SUBROUTINE VONE FLOW CHART

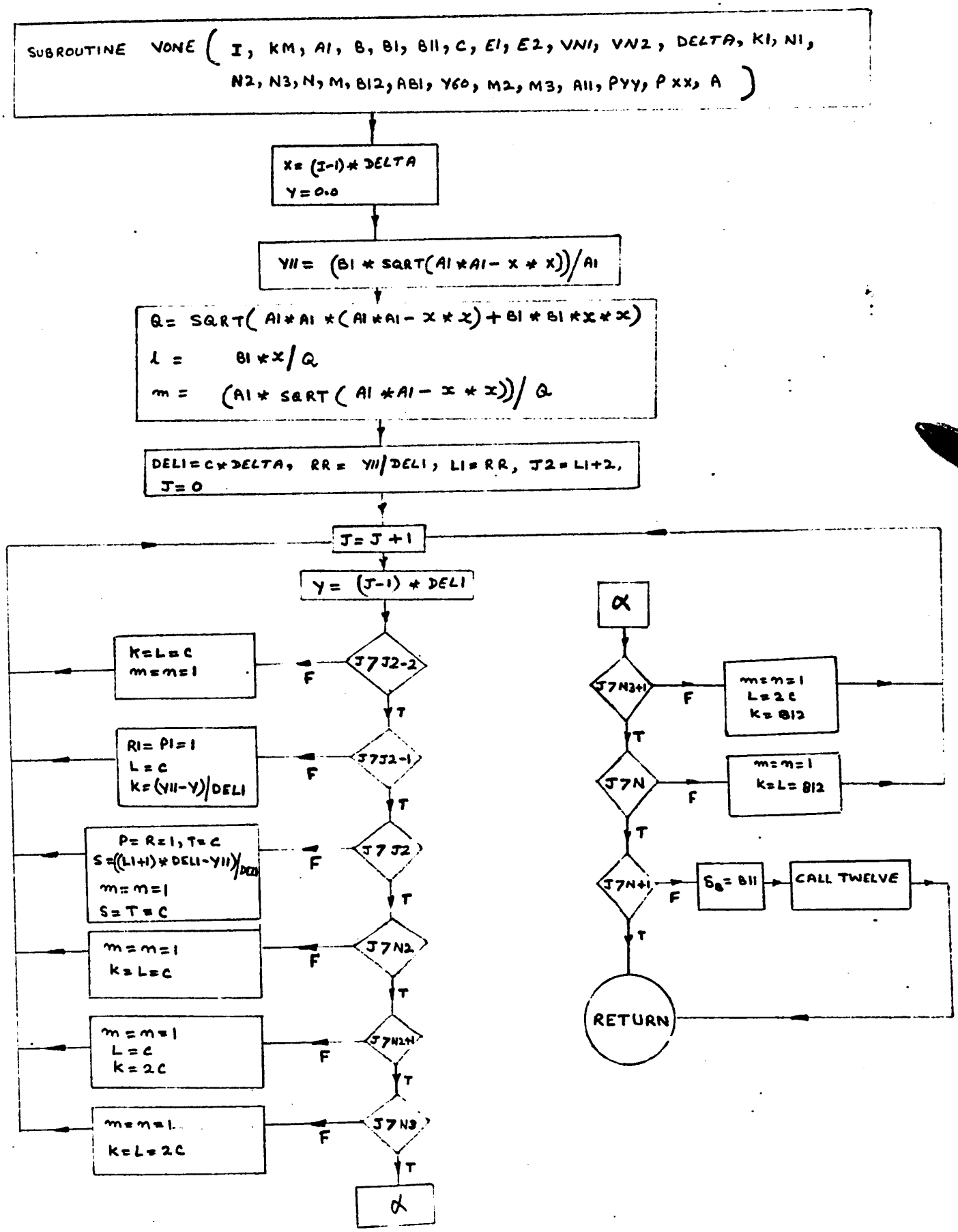

SUBROUTINE VTWO FLOW CHART

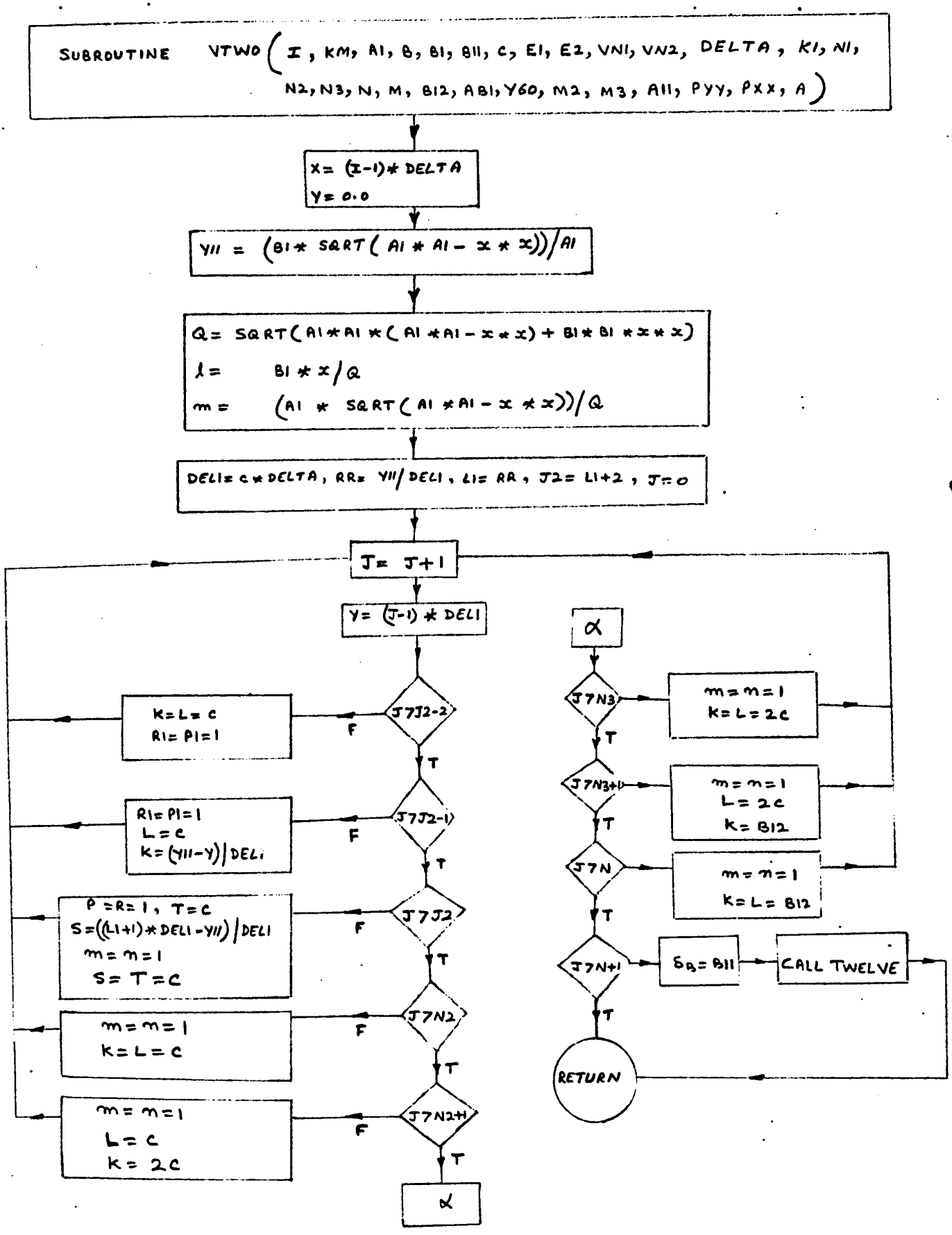

PROGRAM FOR $P_{xx}, P_{yy}, T_{xy}, E_{xx}, E_{yy}, E_{xy}$

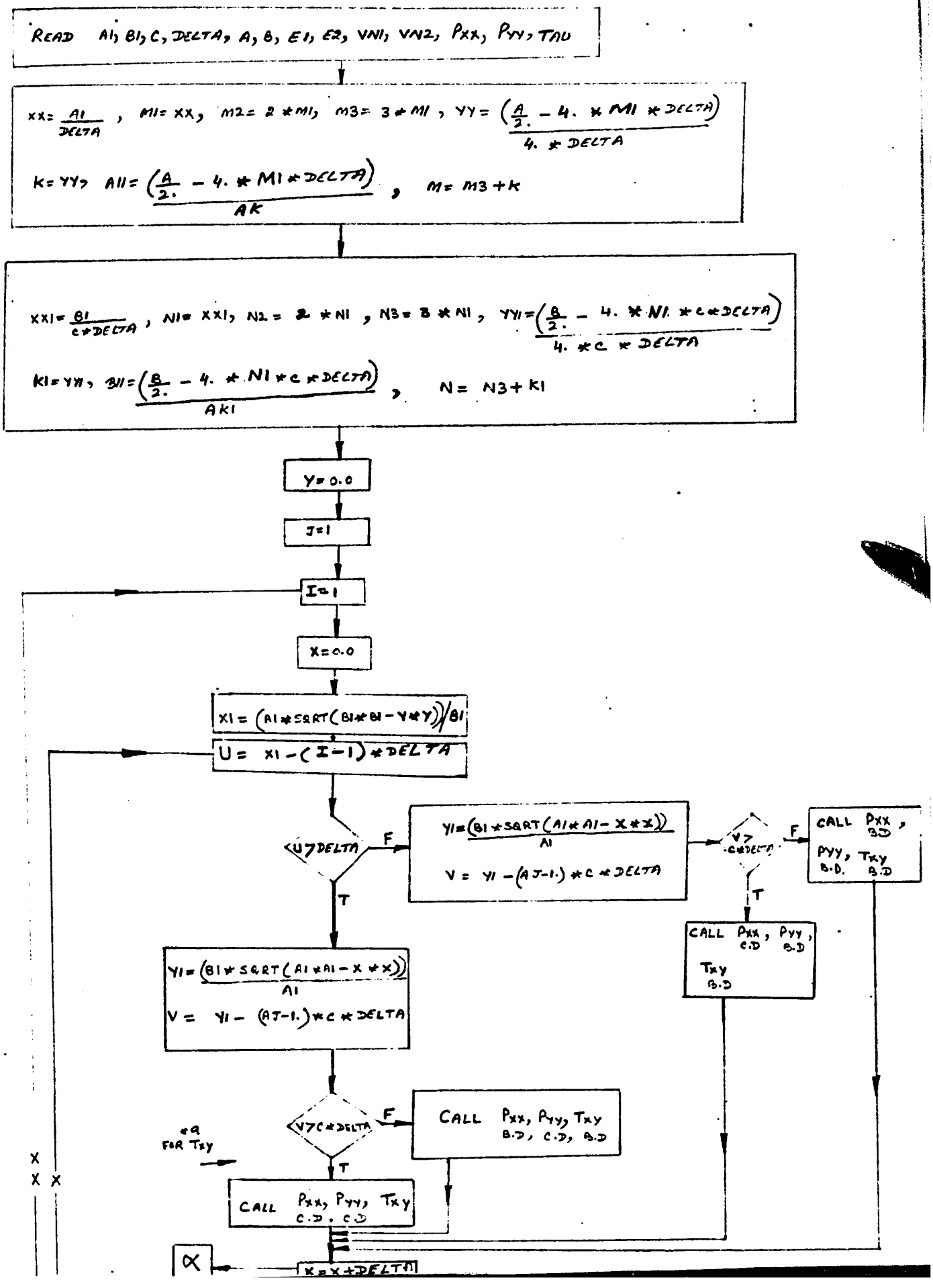

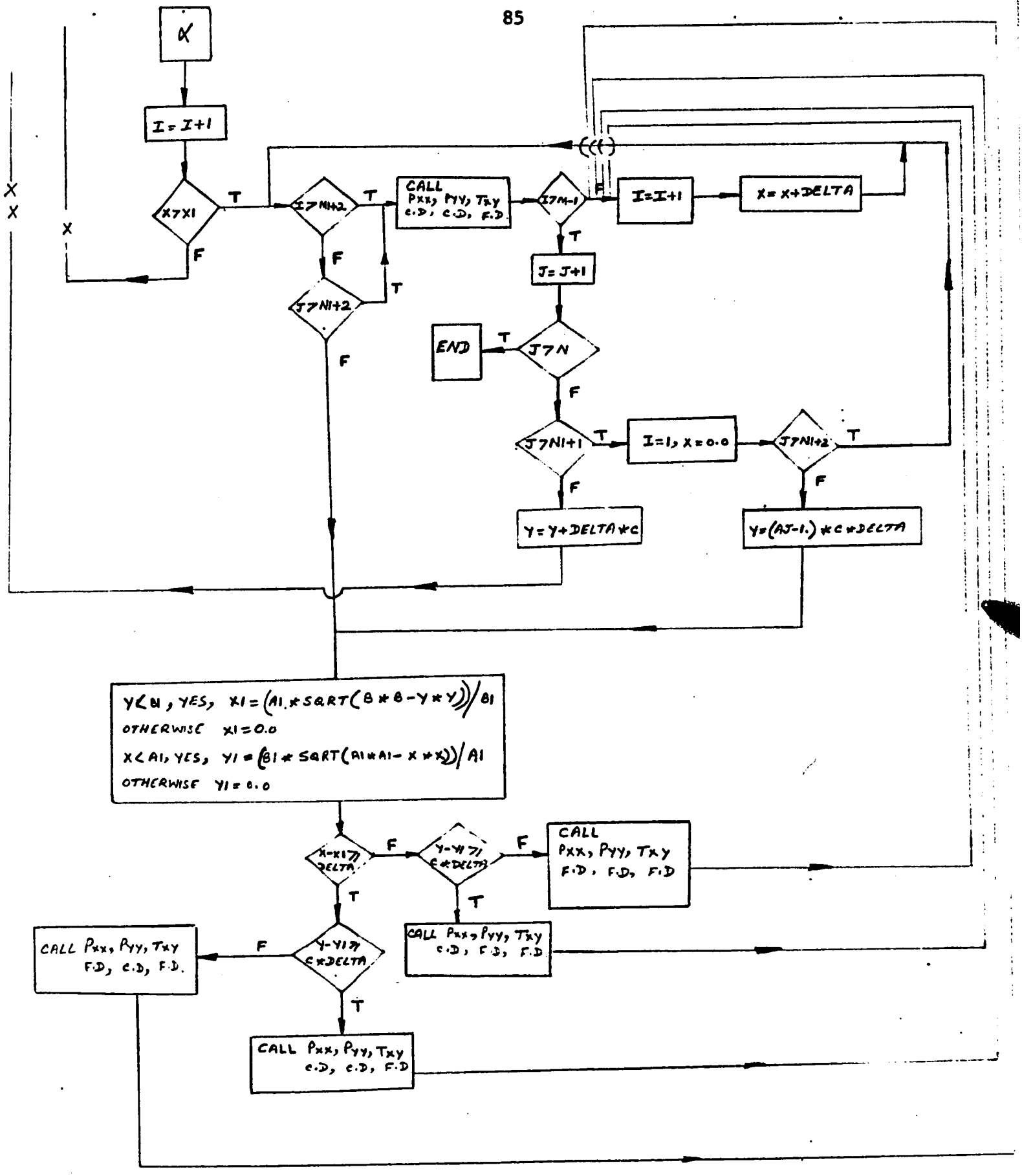
A
I = I+1
X>X1
T
F
I>N1+2
T
F
CALL
Pxx, Pyy, Txy
e.D, e.D, F.D
I>M-1
F
I=I+1
X = X+DELTA
T
J = J+1
J>N1+2
T
F
END
T
J>N
F
J>N1+1
T
I=1, X = 0.0
J>N1+2
T
F
Y = Y+DELTA*C
Y=(AJ-1.)*C*DELTA
Y<B1, YES, X1 = (A1.*SQRT(B*B-Y*Y))/B1
OTHERWISE X1=0.0
X<A1, YES, Y1 = (B1*SQRT(A1*A1-X*X))/A1
OTHERWISE Y1 = 0.0
X-X1?
DELTA
F
Y-Y1?
E*DELTA
F
CALL
Pxx, Pyy, Txy
F.D, F.D, F.D
T
T
CALL Pxx, Pyy, Txy
F.D, e.D, F.D.
F
Y-Y1?
E*DELTA
CALL Pxx, Pyy, Txy
e.D, F.D, F.D
T
CALL Pxx, Pyy, Txy
e.D, e.D, F.D

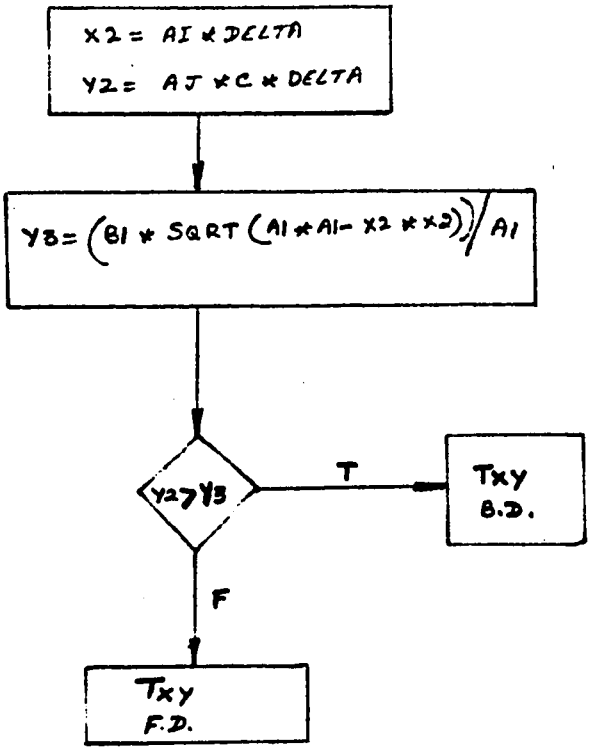
X2 = AI * DELTA
Y2 = AJ * C * DELTA
Y3 = (B1 * SQRT (A1 * A1 - X2 * X2)) / A1
Y2 > Y3
T
Txy
B.D.
F
Txy
F.D.

SUBROUTINE PYYCD FLOW CHART

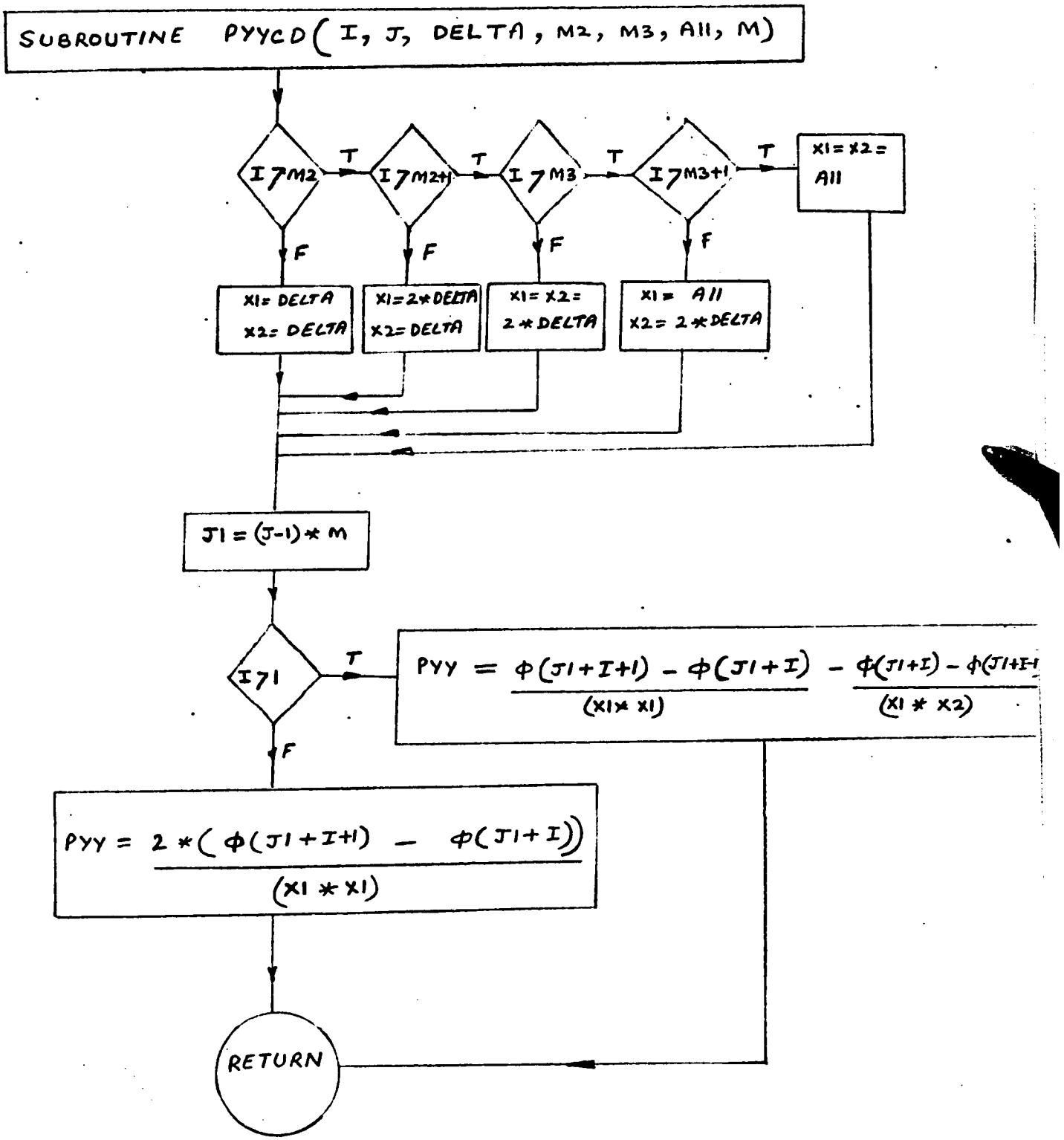

SUBROUTINE PYYBD FLOW CHART

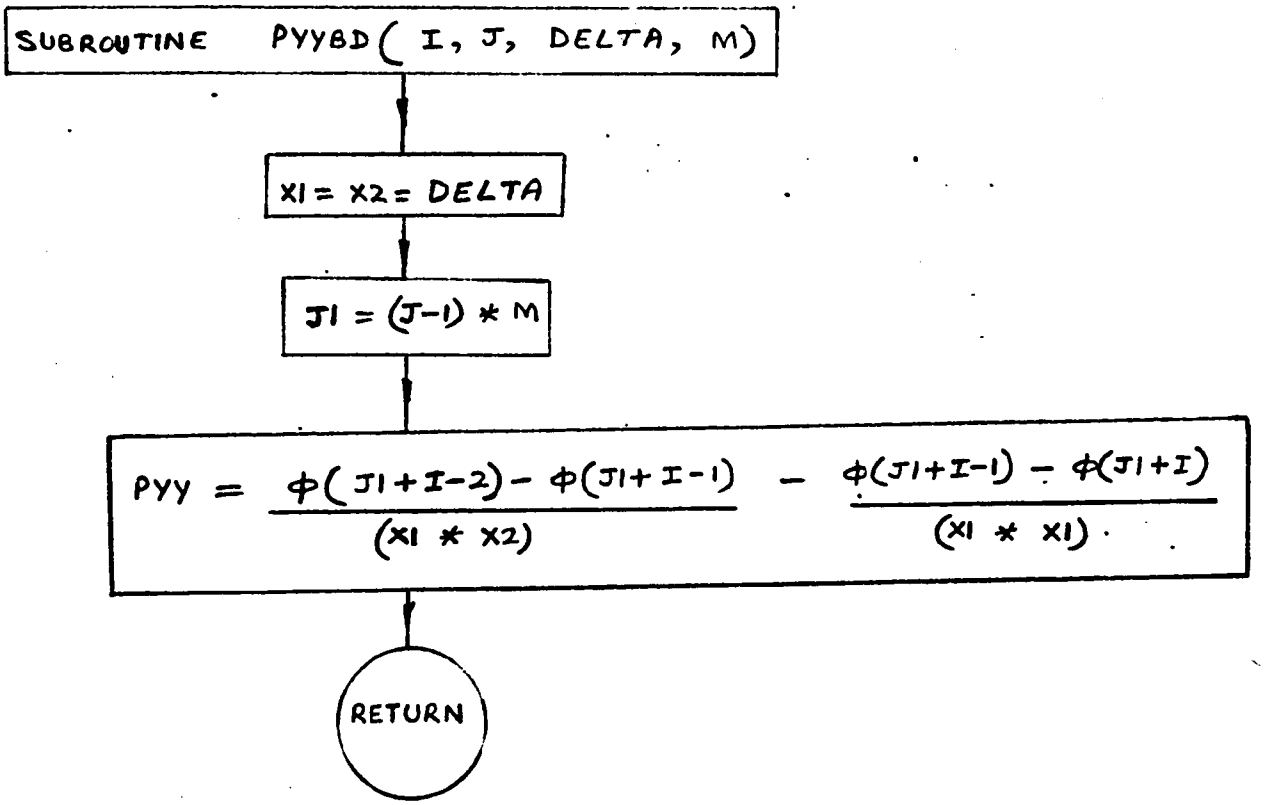

SUBROUTINE PYYFD FLOW CHART

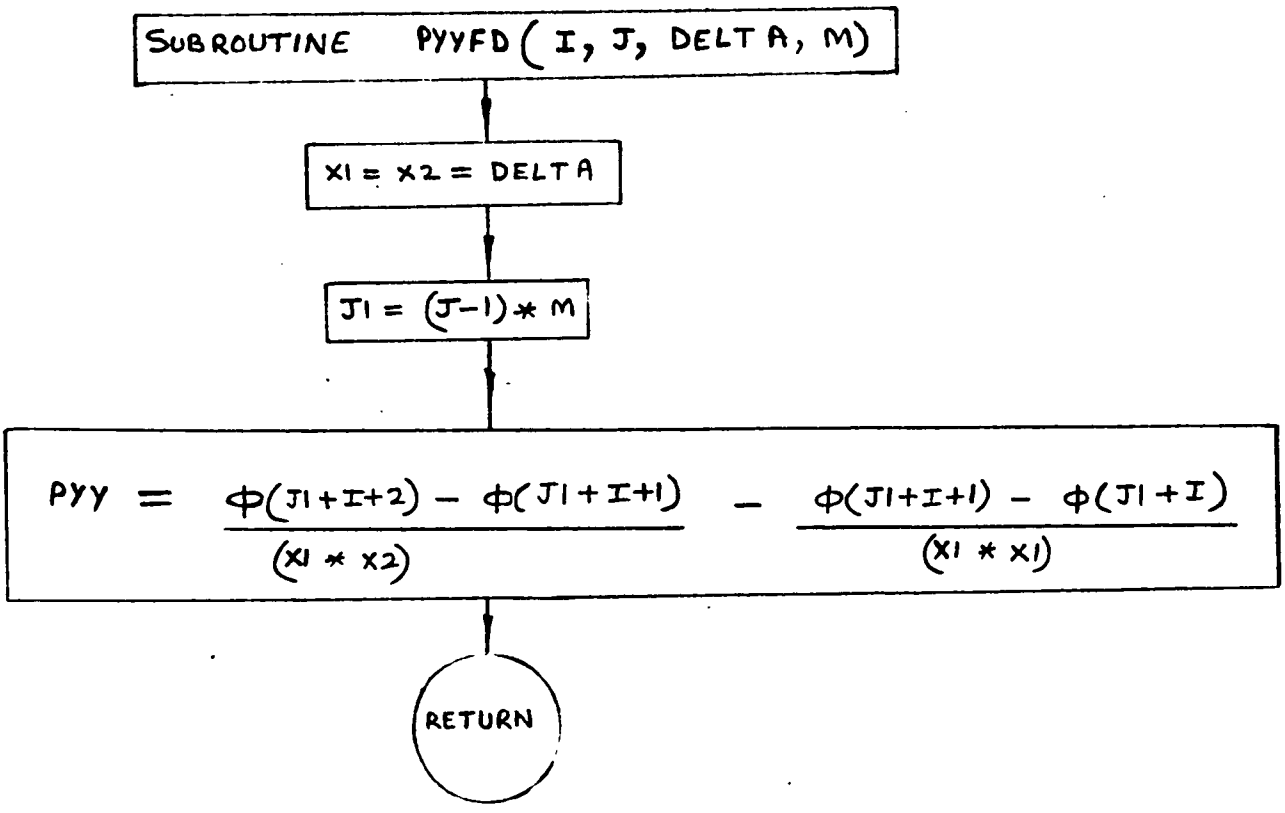

SUBROUTINE PXX CD FLOW CHART

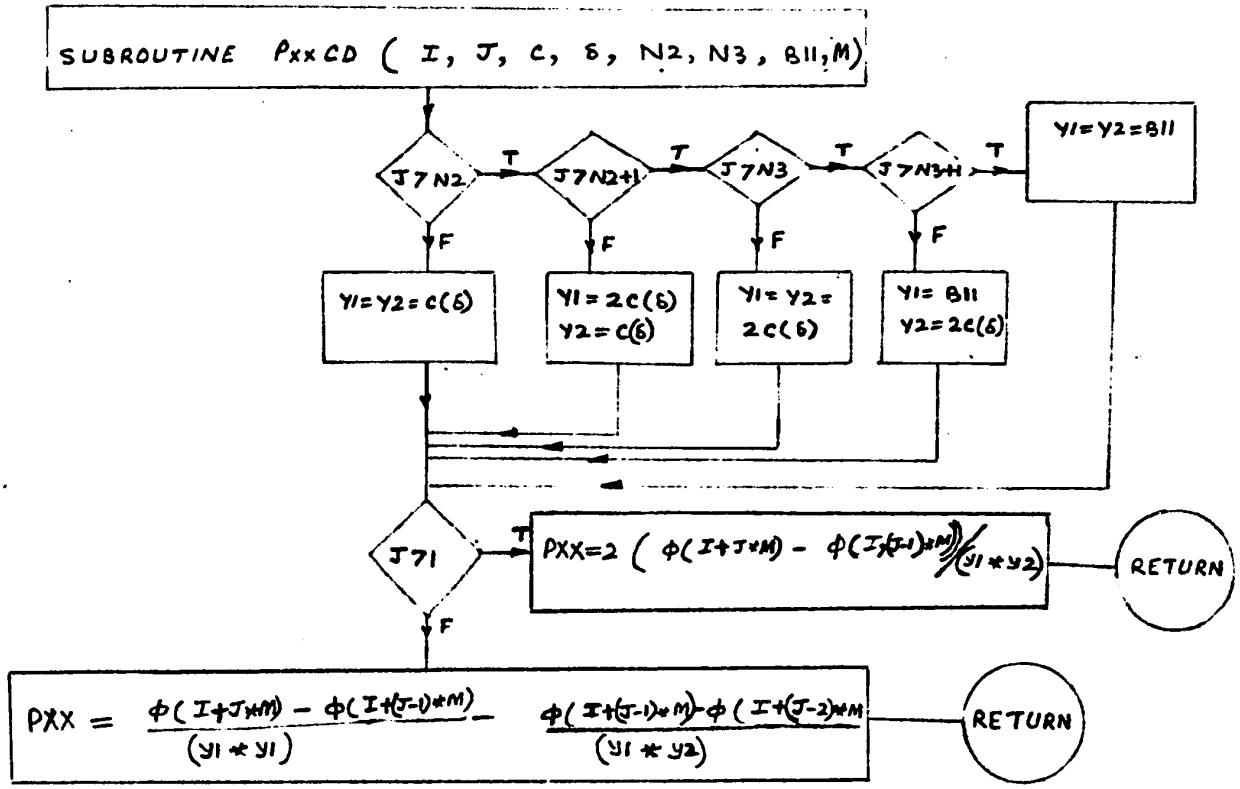

SUBROUTINE PXX FD FLOW CHART

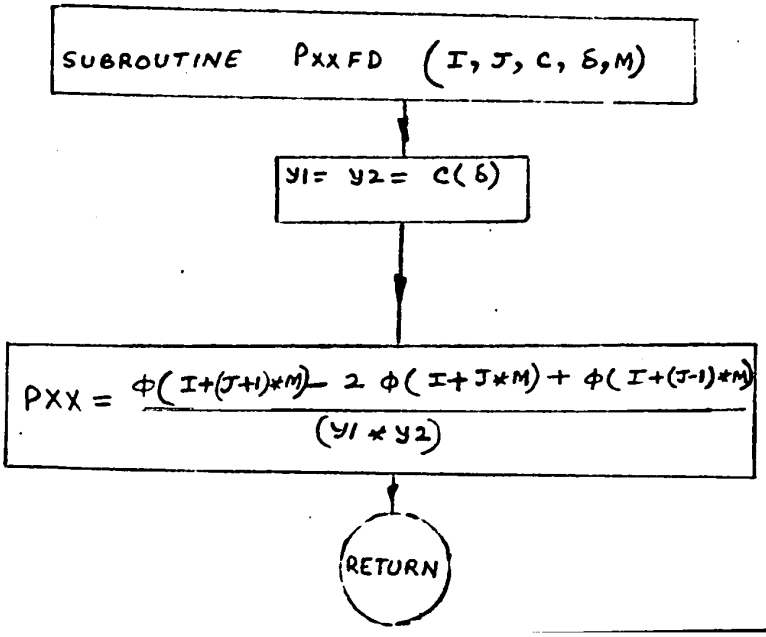

SUBROUTINE PXXBD FLOW CHART

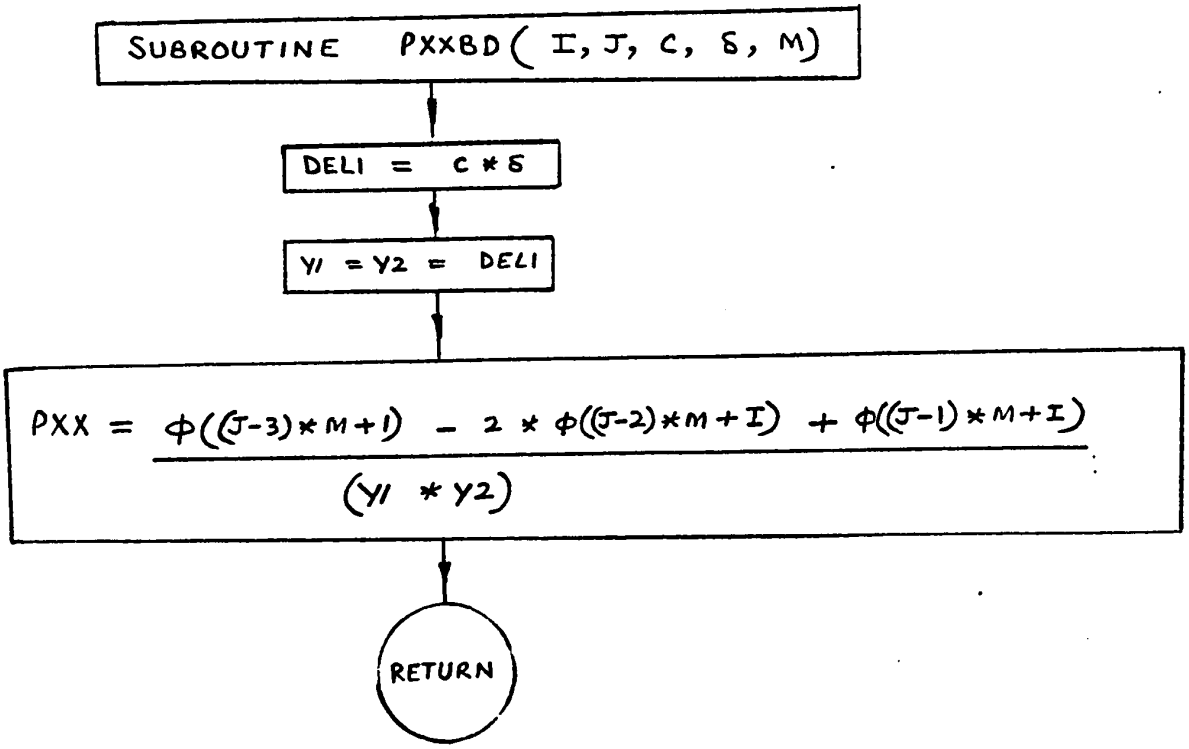

SUBROUTINE TXYFD FLOW CHART

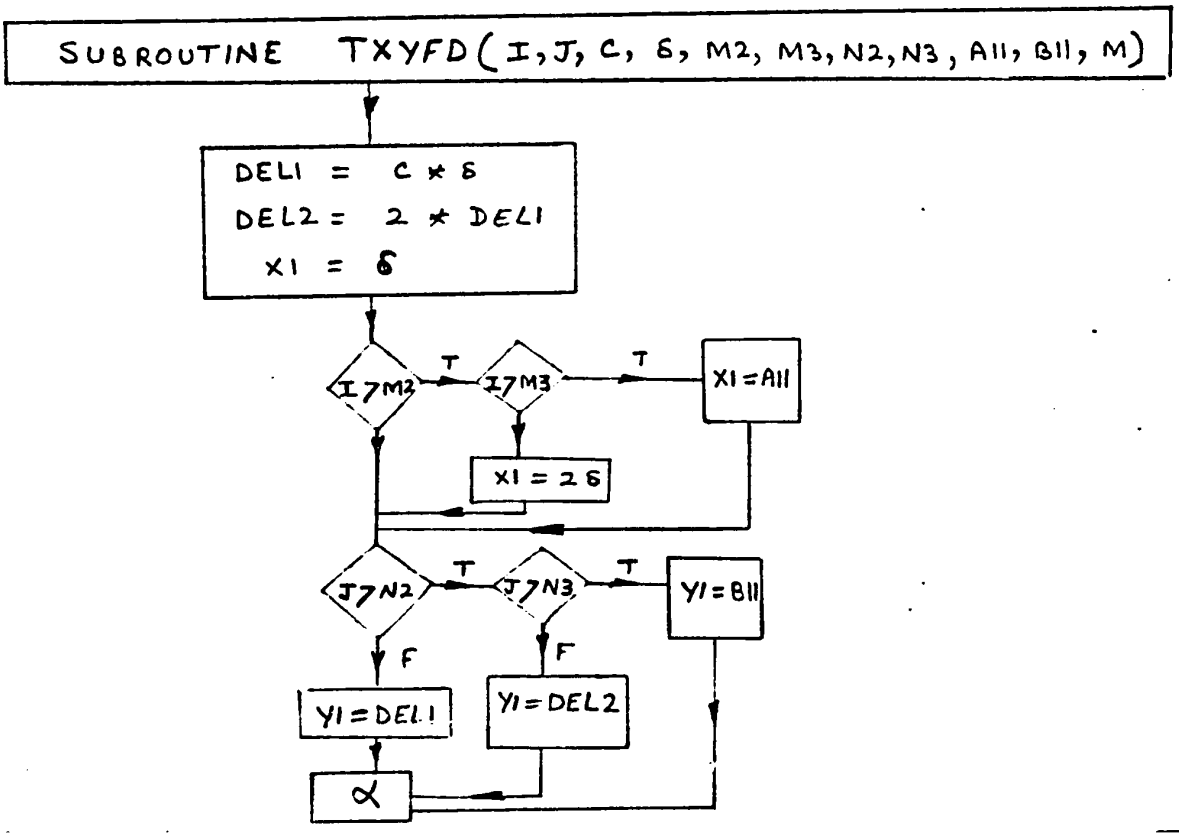

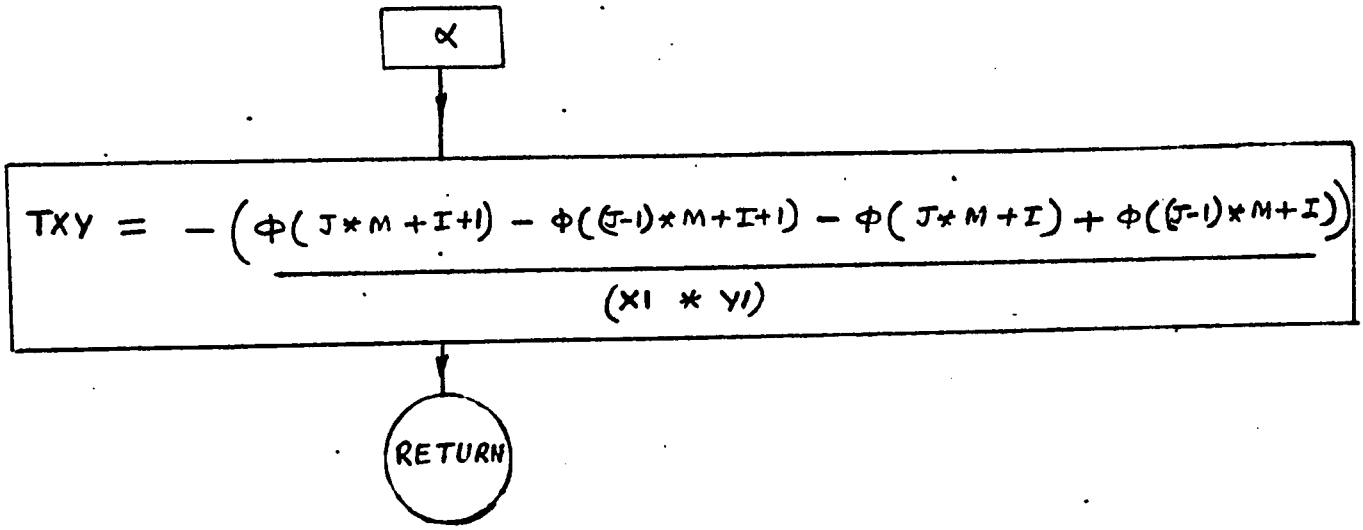

SUBROUTINE TXYBD FLOW CHART

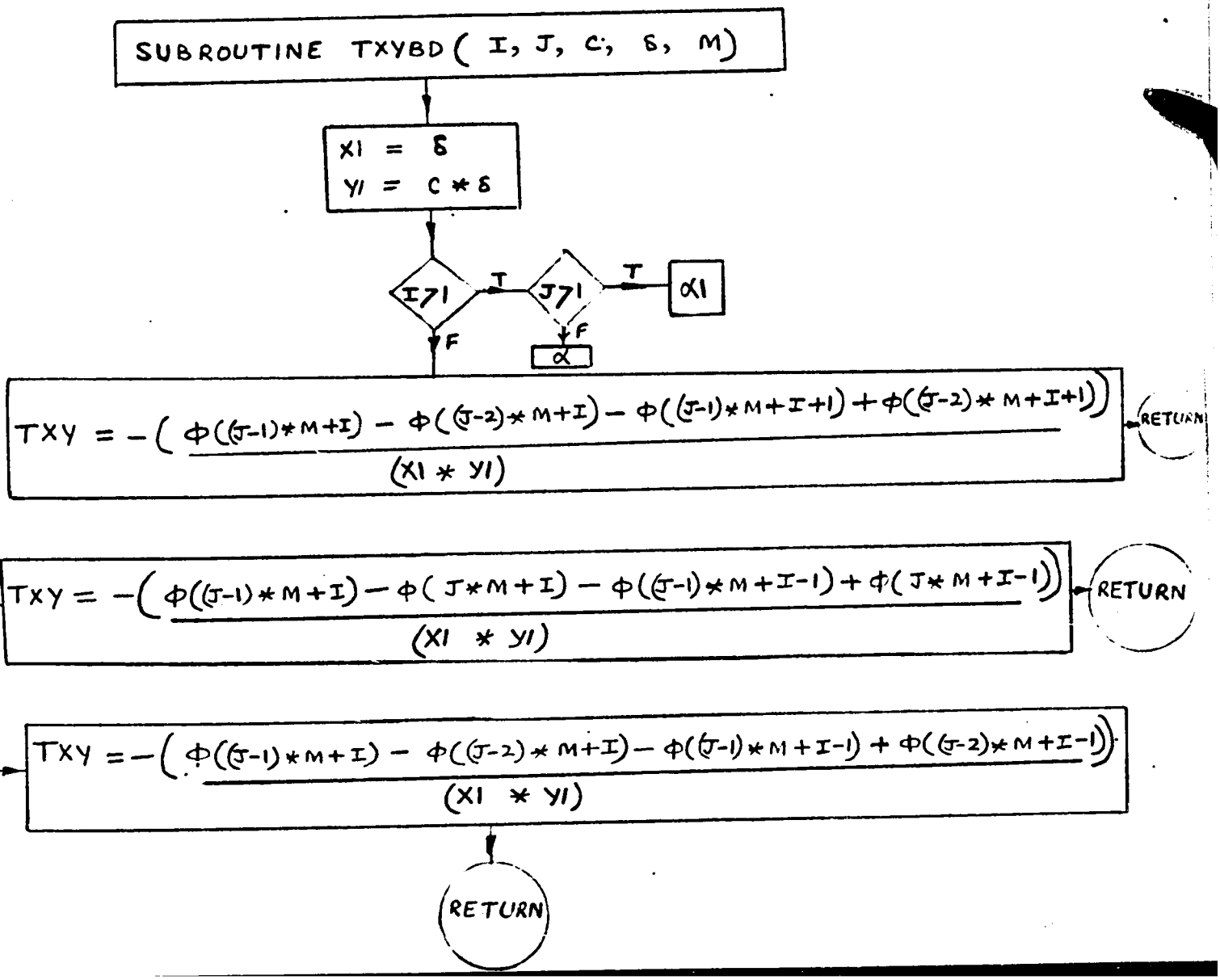

3.2 Experimental Investigation

In order to visualize the stress pattern in the specimen under the specified loading conditions, the experimental investigation was carried out. Photoelastic method was chosen, because it has the advantage of providing a clear overall picture of the stress pattern in the specimen, as well as enabling us to evaluate the magnitude and the location of peak stresses. Fringe patterns was photographed for future reference. A highly sophisticated photoelastic polariscope, along with other attachments for precision measurements was used. The maker of this transmission polariscope, model 050, is Photolastic Inc. The details of this assembly are discussed below.

3.2.1 Description of apparatus

a) Optical Table

This is the stem of the apparatus providing a collimated vertical light path. The basic parts of this system are :

i) A point-like source cooled by a fan

ii) Collimating lens system

iii) Observation screen with hood

iv) Objective lens with magnification of 10:1

v) A system for controlling intensity of light

vi) Additional light source for reflection accessory

b) Precision Table

This supports two-dimensional models exaclty perpendicular to the light pathand provides vertical adjustment for accurate focusing. This is a

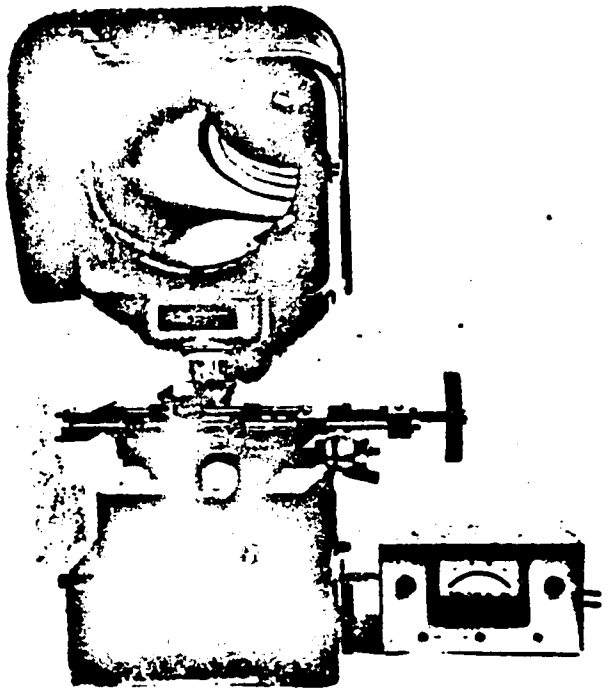

PHOTOELASTIC APPARATUS

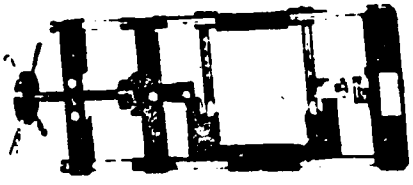

STRAINING FRAME

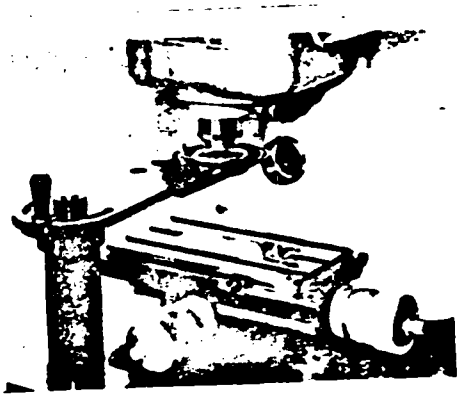

POLARISCOPE ASSEMBLY

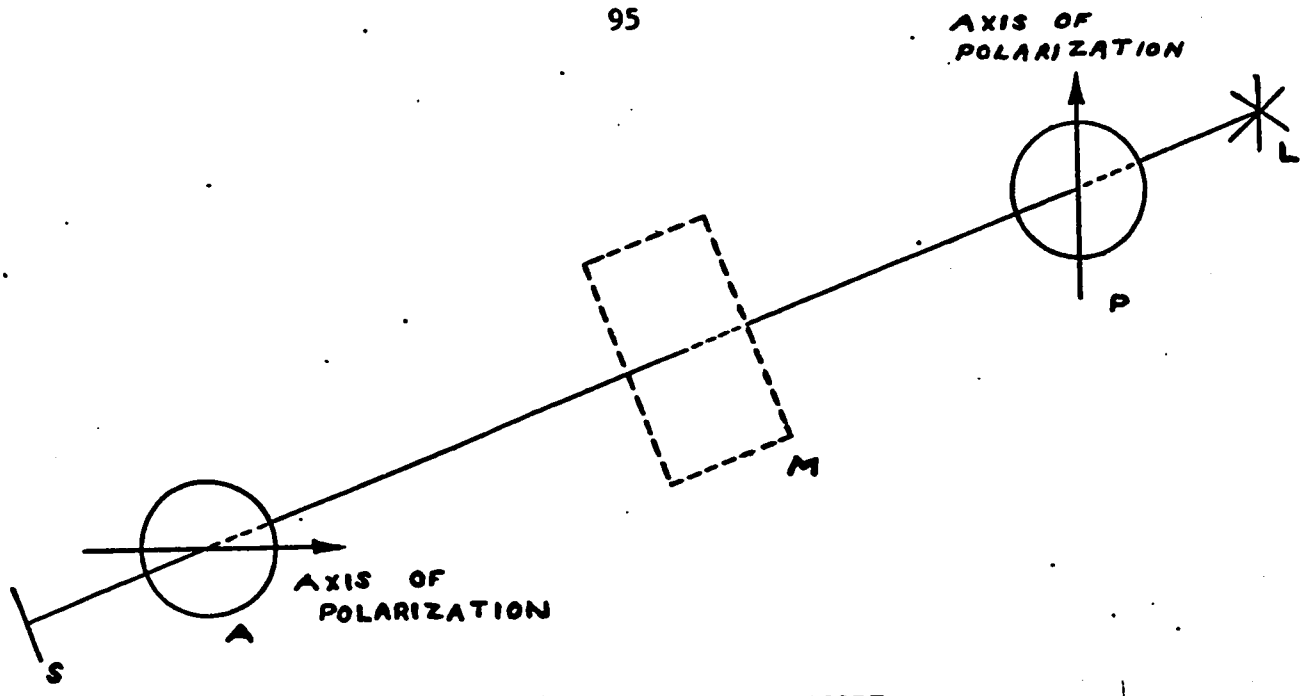

(a) PLANE POLARISCOPE

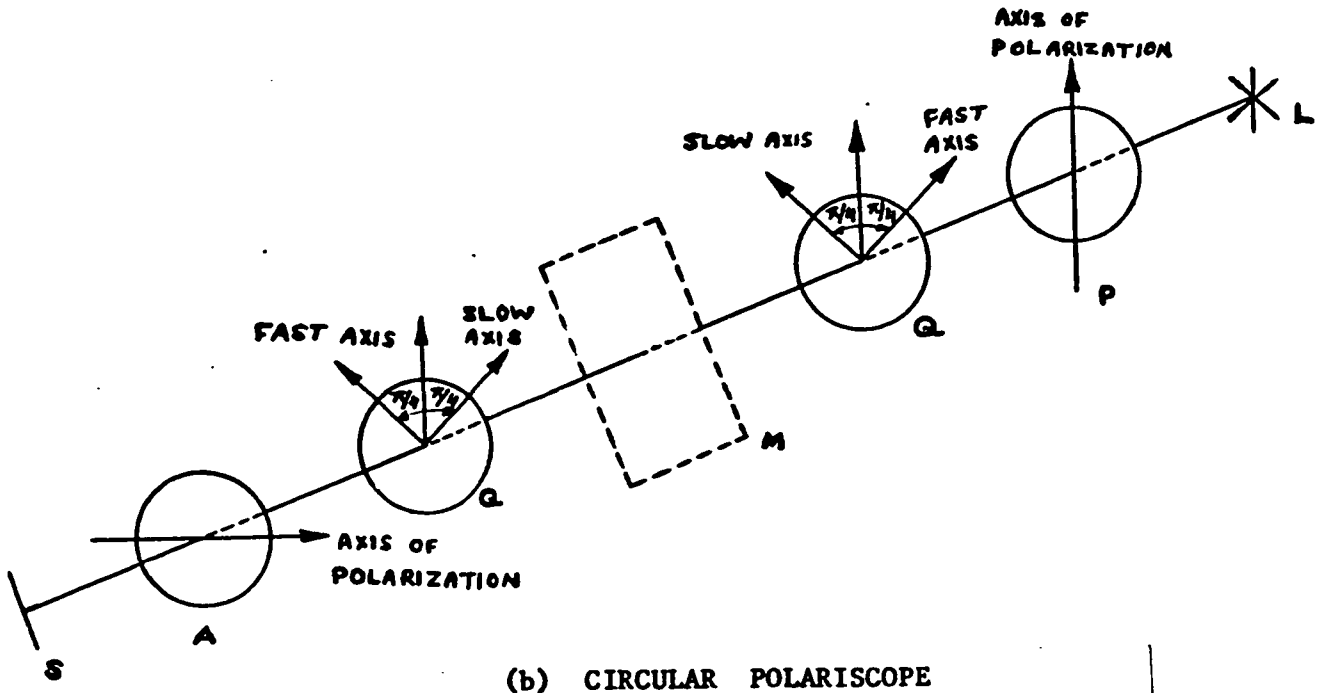

(b) CIRCULAR POLARISCOPE

L = LIGHT SOURCE

P = POLARIZER

M = MODEL

Q = QUARTER-WAVE PLATE

S = SCREEN

A = ANALYZER

FIGURE 12

and works as a bearing for ease of sample positioning. A sliding x-y motion of the frame makes it possible to explore large models with the benefit of high magnification.

e) Load Cell Readout

Load cell readout system which is used with the straining frame consists of a compact universal semi-conductor strain-gage transducer coupled to an indicator to provide a highly accurate load indication. The indicator is equipped with internal calibration, wide-span zero control range, and a tension or compression selector switch. Terminals are also provided on the indicator for recording the load output. The system can be used with either a 500-lb or 1000-lb load cell.

f) Photographic Accessory

A 4 in. x 5 in. photographic attachment can easily replace the ground glass viewing screen. Focussing is the same as for screen observations, and the film is exposed directly to the image for sharp pictures. A double 4 in. x 5 in. back for color or black-and-white polaroid packets. A shutter with cable release is attached to the lens. It has speeds from 1 sec. to 1/250 sec.

g) Monochromator

A narrow-band interferential filter with a wavelength matching the tint of passage observed in white light, constitutes a monochromator. Due to the presence of monochromatic light black fringes instead of coloured fringes are produced.

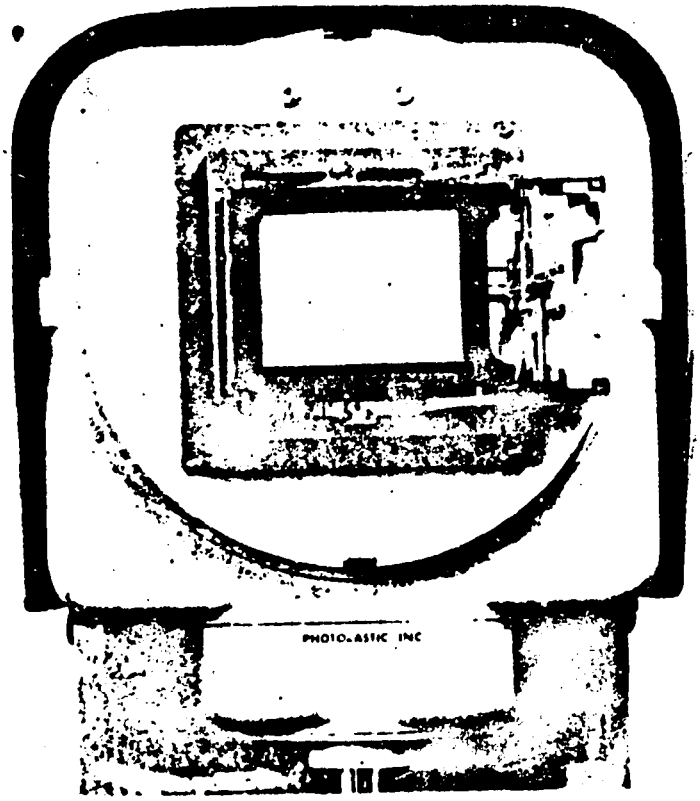

PHOTOGRAPHIC ACCESSORY

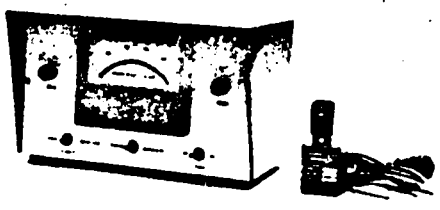

LOAD CELL READOUT

h) Uniform Field Compensator

A calibrated scale identifies fringe orders and also provides for the measurement of fractional orders. This is especially important in cases where the integral fringe order is difficult to determine.

i) Oblique-Incidence Attachment

It consists of prism attachments through which the polarized light beam is deflected to pass through the model obliquely to provide for the separation of the principal stresses. The arrangement permits observation in oblique incidence by directing the light path in a plane containing the principal stresses without the rotation of the model.

3.2.2 Photoelastic materials and cements

Materials:

The experimental program involves materials ranging from E = 1,000 psi to E = 30,000,000 psi. The plastics having trade names PSM1 and PSM4 used for the above purpose were purchased from Photolastic Inc.

i) PSM1

This is a clear polyester sheet, free of creep and edge effects, and with very high photoelastic sensitvity. The properties of this plastic of nominal thickness 0.250 in. are :

modulus of elasticity — E = 340,000 psi

Posisson's ratio — $\nu = 0.38$

stress optical constant — f = 40 psi per fringe per inch.

ii) This is a polyurethane sheet, exhibiting low modulus that requires very low forces for straining. The plastic having nominal thickness

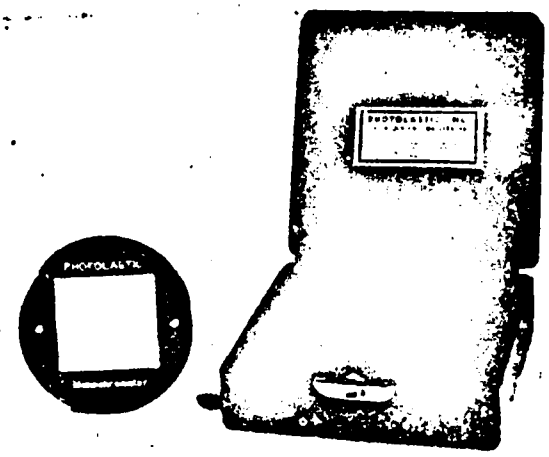

MONOCHROMATOR

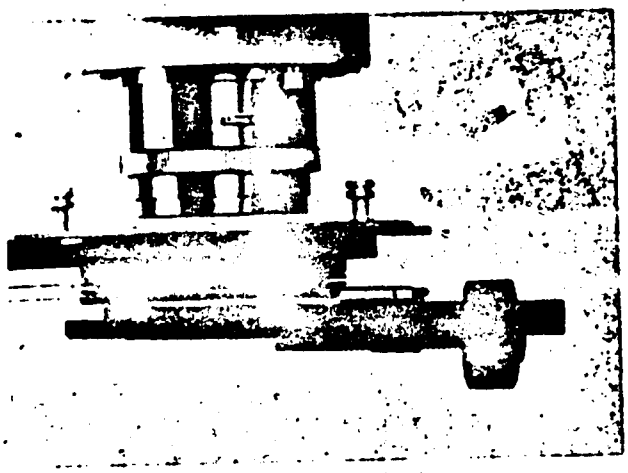

UNIFORM FIELD COMPENSATOR

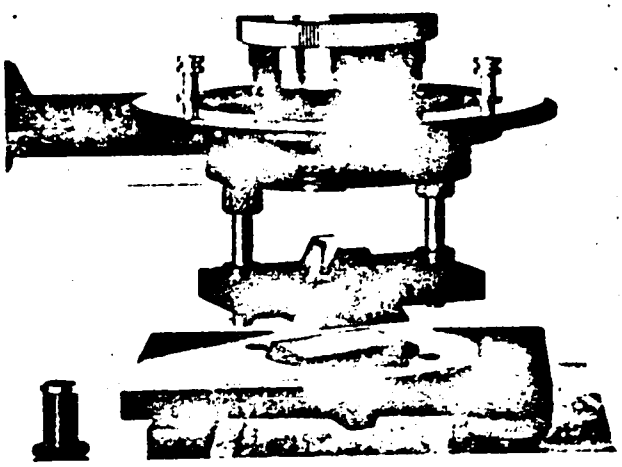

OBLIQUE INCIDENCE ATTACHMENT

of 0.250 in. has modulus of elasticity — E = 1,000 psi

Cements :

Two types of cements, depending upon the parent material, are used in order to get a perfect bond between the insert and the parent material. The Photolastic Inc. trade name of cements and their properties are given below.

i) Resin: PC-1, Hardener: PCH-1

This cement has excellent bond strength, no creep, and low viscosity, and is relatively fast curing i.e. it takes about 12 hours at room temperature. It has modulus of elasticity — E = 450,000 psi and elongation of 3-5 % .

ii) Resin : PC-6, Hardener : PCH-6

This cement has a low modulus of elasticity i.e. E = 30,000 psi and elongation of 50 % . It takes 24 hours for curing at room temperature.

3.2.3 Procedure for preparation and handling of specimens

Much care was taken in the preparation and handling of photoelastic models. All machining operations were carried out with very sharp tools. The templates, eight times the required dimensions of hole and insert, were made. On the pantograph engraving machine, these templates were used to get perfect elliptical hole and insert. The cutting was kept moderate with slow, steady feed, and continuous so as not to produce local rubbing and consequent heat generation. When approaching the finished boundary of the model, the size of the finishing cut was held to a maximum depth of 0.005 in. Holes were drilled undersize

and then bored to the final dimensions. Care was taken to use only the recommended solvents for cleaning the models.

3.2.4 Experimental Procedure

The material fringe value changes with time and temperature. Therefore, it is necessary to find this value before performing any experiment. A separate sample must be made for the calibration.

After calibrating the material the actual specimen is subjected to the required loading conditions on the machine and the readings of isoclinics and isochromatic are taken. The principal stresses are calculated from these readings using shear difference method on a digital computer. Care was taken to maintain the same room temperature during calibration and testing.

3.2.4.1 Calibration of Specimens

The accurate determination of the stress distribution requires a careful calibration of the material fringe value, f . A simple tensile test specimen, shown in figure 13 was employed for the calibration. This specimen was loaded in increments, and the fringe order and the loads were noted. The axial stress, P_1, induced in the necked region of the tensile specimen by the load P is expressed as

$$P_1 = \frac{P}{W\,h}$$

Where W is the width and h is the thickness of the specimen, and the normal stress P_2 is zero. Using the stress optic law for two dimensional case we arrive at the following basic relation.

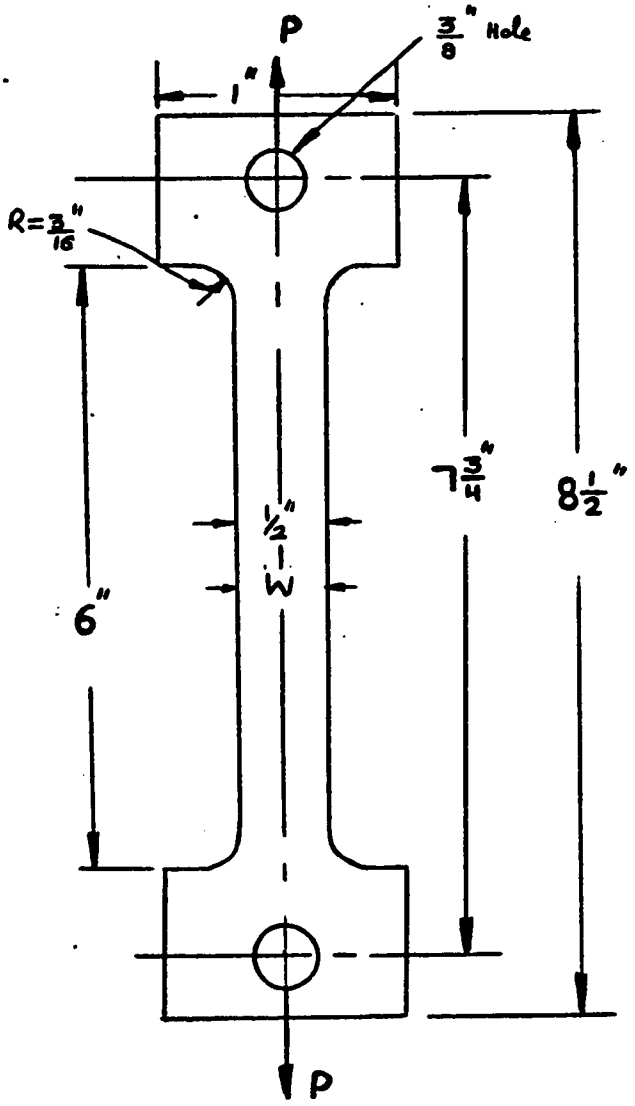

FIGURE 13

$$P_1 - P_2 = \frac{N f}{h} \qquad (A)$$

Substituting for P_1 and P_2 and simplifying we get,

$$f = \frac{P}{W N} \quad \text{psi per fringe per inch} \qquad (61)$$

This shows that the material fringe value is independent of the thickness h of the specimen. In order to average out small errors in the readings of P and N, a graph is plotted between P and N for a fixed value of W . The slope of the straight line drawn through these points is used for evaluating f in equation (61).

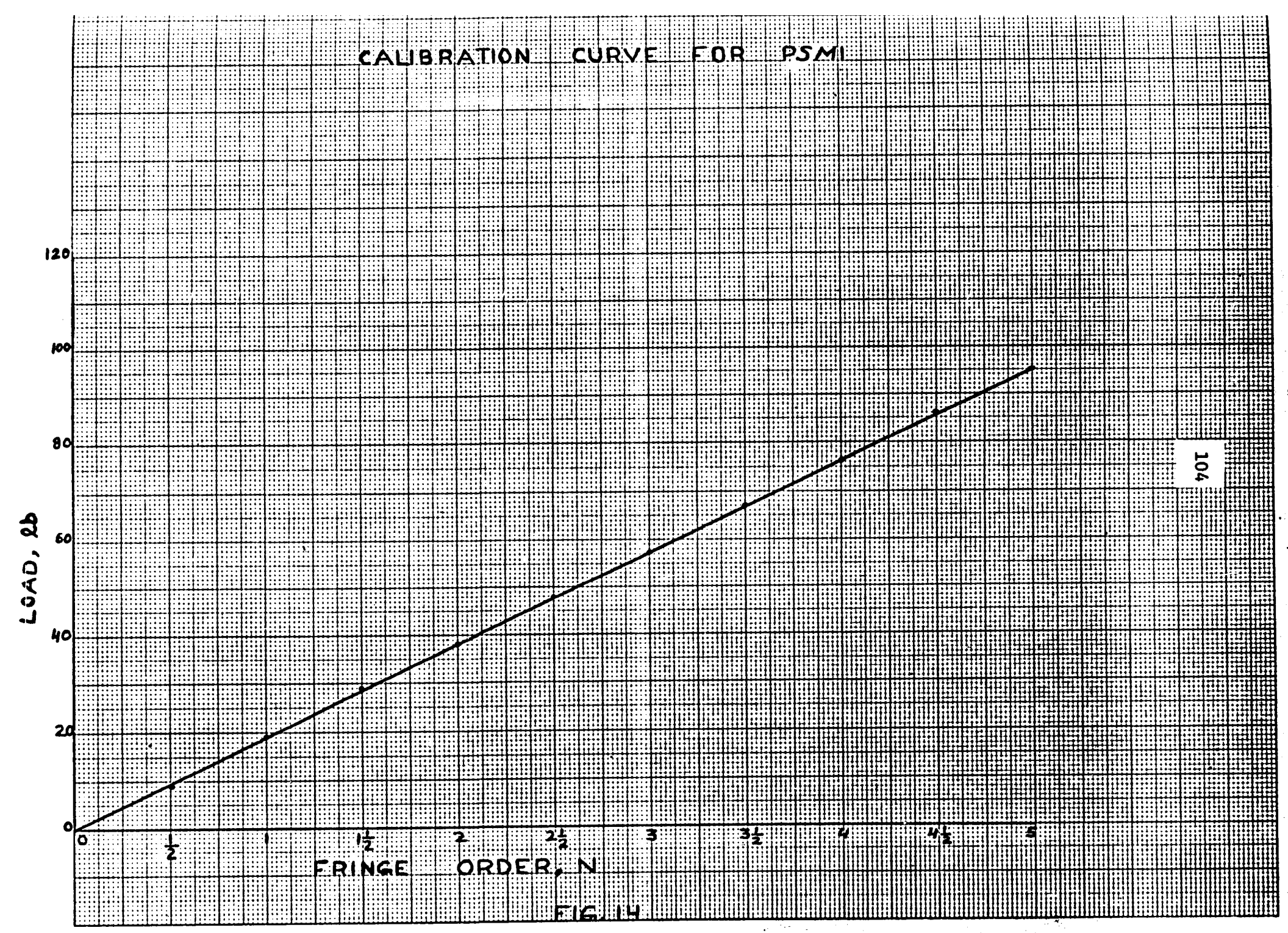
CALIBRATION CURVE FOR PSM1
LOAD, lb
120
100
80
60
40
20
0
0
½
1
1½
2
2½
3
3½
4
4½
5
FRINGE ORDER, N
104

FIG. 14

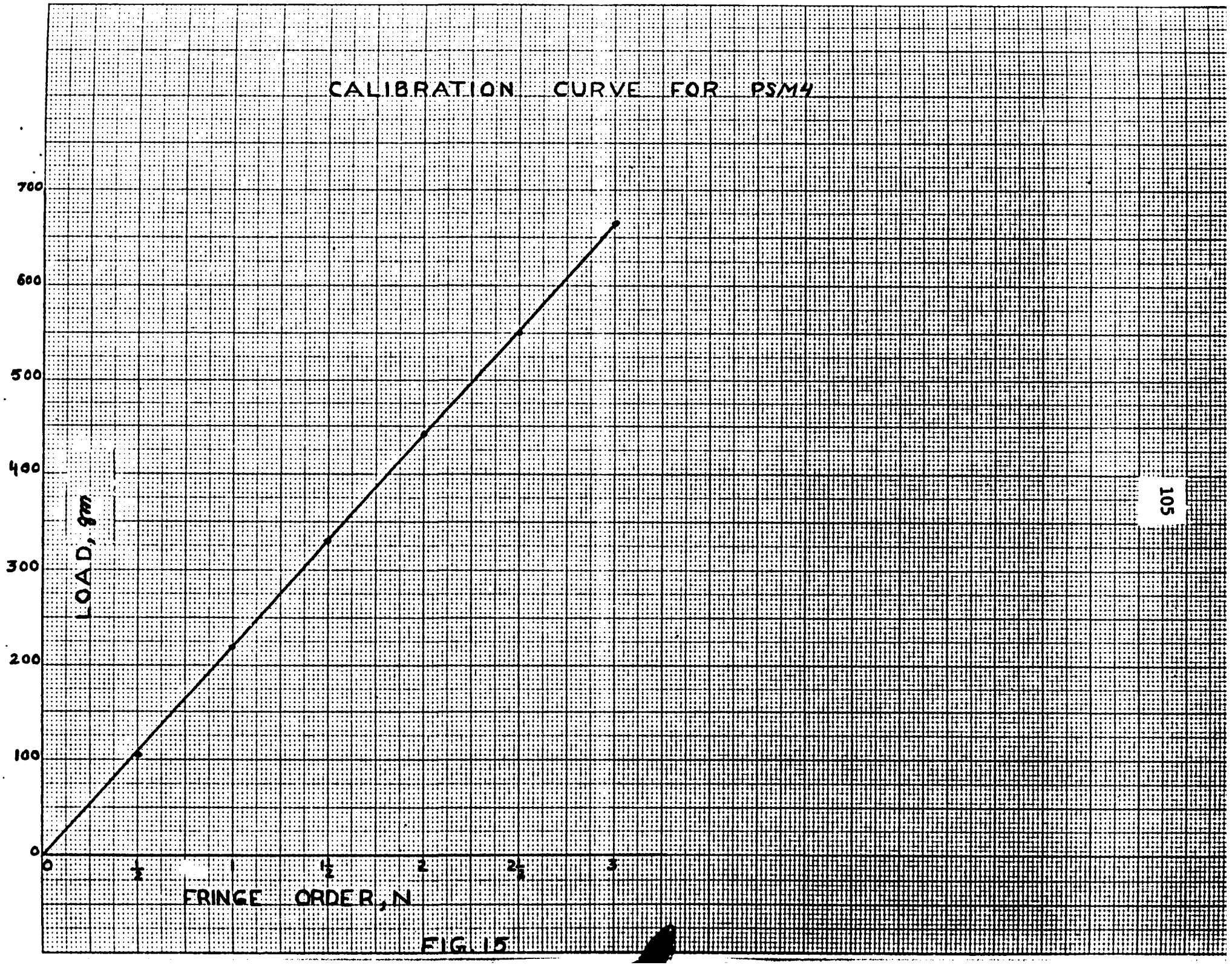
CALIBRATION CURVE FOR PSM4
LOAD, gm
700
600
500
400
300
200
100
0
0
1/4
1
1 1/2
2
2 1/2
3
FRINGE ORDER, N

FIG. 15

3.2.4.2 Testing of Specimens

The specimen was cut from a 10 in. x 10 in. plastic sheet and finished to the required outside dimensions. Two holes, as shown in figure 16, were drilled for holding the specimen on the straining frame. A hole for the insert was made in the centre of the specimen. An insert of the required dimensions was made of a different material. The dimensions of the insert were less than the dimensions of the insert-hole by sixteen thousands of an inch, so as to allow these to be glued to the insert-hole using cement, prepared by the process discussed in section 3.2.2. The specimen was kept for 24 hours for this joint to dry up.

The load cell readout was switched on for 15 minutes for warming up. The straining frame was fixed on the precision table of the machine and then the specimen was fixed on the frame. The load was gradually applied to the specimen and was kept constant after observing at least three fringes. The stress pattern, magnified ten times, was seen on the screen. By moving the table up or down, the picture was brought to proper focus and the photograph was taken after mounting photographic accessories.

The readings of isoclinics and isochromatic were taken at different points starting from the boundary and proceding towards the centre in gradually decreasing steps. The polariscope was arranged to give a plane polarized light field incident on the specimen. This gives both isoclinice (black lines), and isochromatics (colored lines)

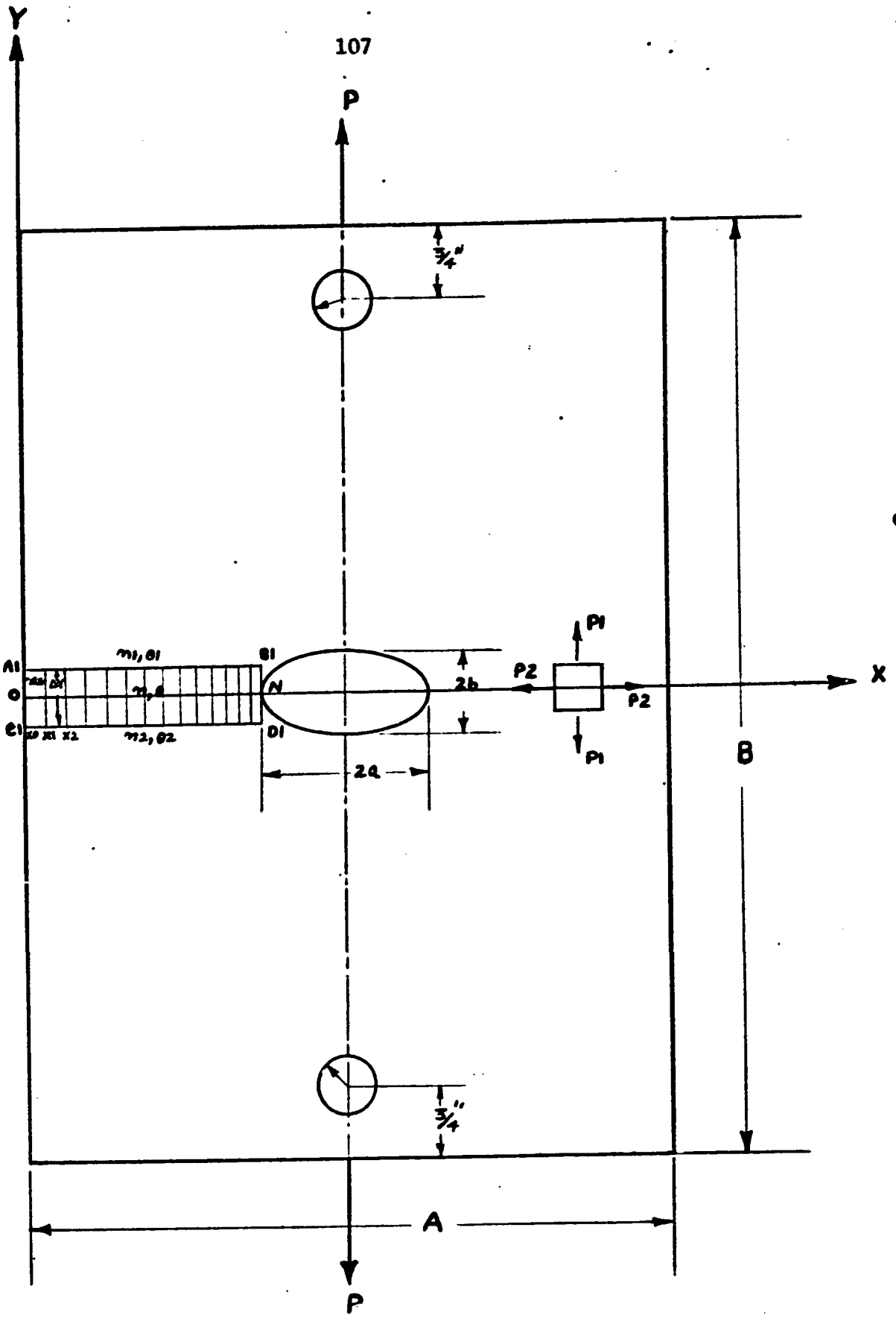

GRID SYSTEM EMPLOYED IN THE SHEAR DIFFERENCE METHOD

FIGURE 16

on the screen. Readings for isoclinices were taken in this position. For isochromatics, the polariscope was set to give circularly polarized light incident on the specimen, in which case isoclinics are eliminated.

The readings were taken for different configurations of the insert as shown below and drawn in figure 17.

	Insert material/ Parent material	E_1/E_2	2a/2b		
			Case 1	case 2	Case 3
a.	PSM4/PSM1	1/340	.5	1	2
b.	PSM1/PSM4	340	.5	1	2
c.	Steel/PSM4	30,000	.5	1	2

The above series of experiments were repeated for three different values of A. Applying shear-difference method to equation (1) a relation between principal stresses P_1 and P_2 was obtained. In order to evaluate P_1 and P_2 separately, another relation between them was obtained from the isochromatic readings. This procedure is explained below by an example.

Suppose the normal and tangential stresses are to be calculated along the line ON, shown in figure 16. First of all equation (1) is integrated with respect to x and then converted to a finite difference form.

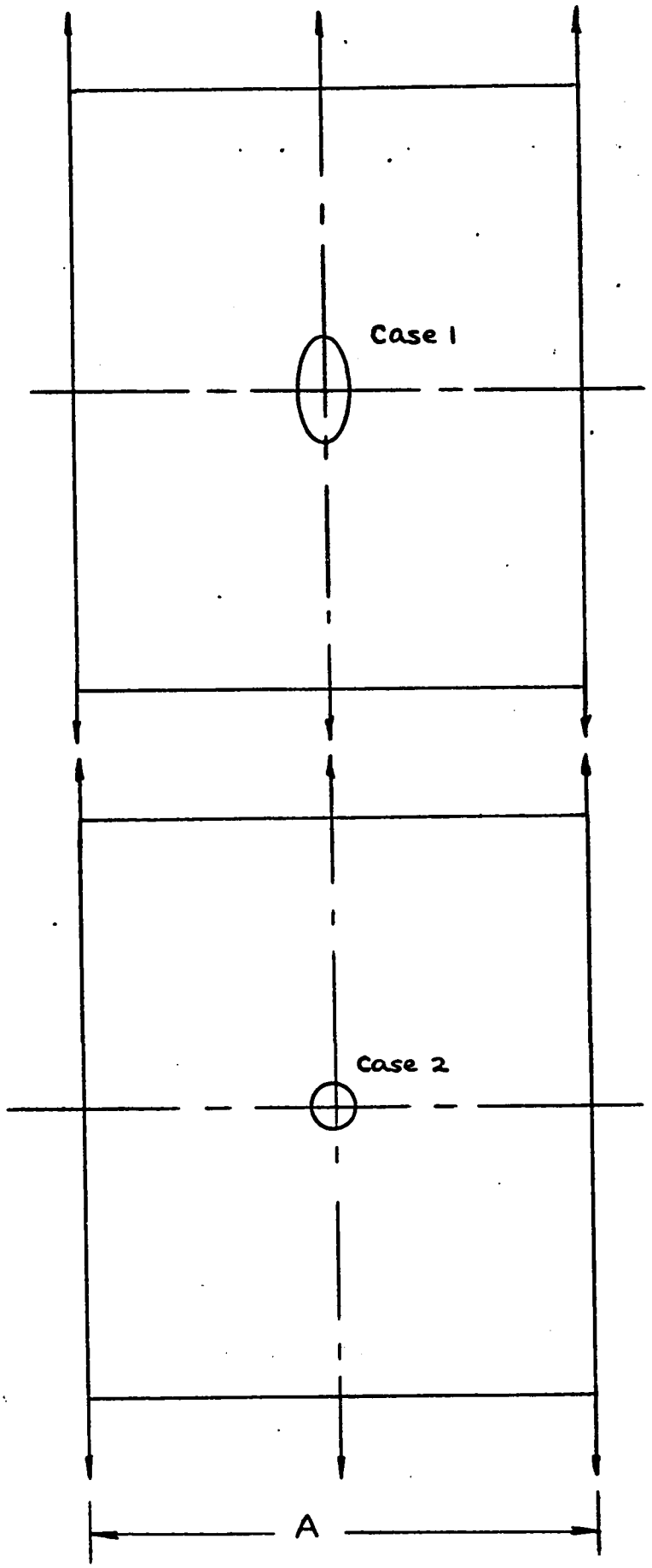

FIGURE 17

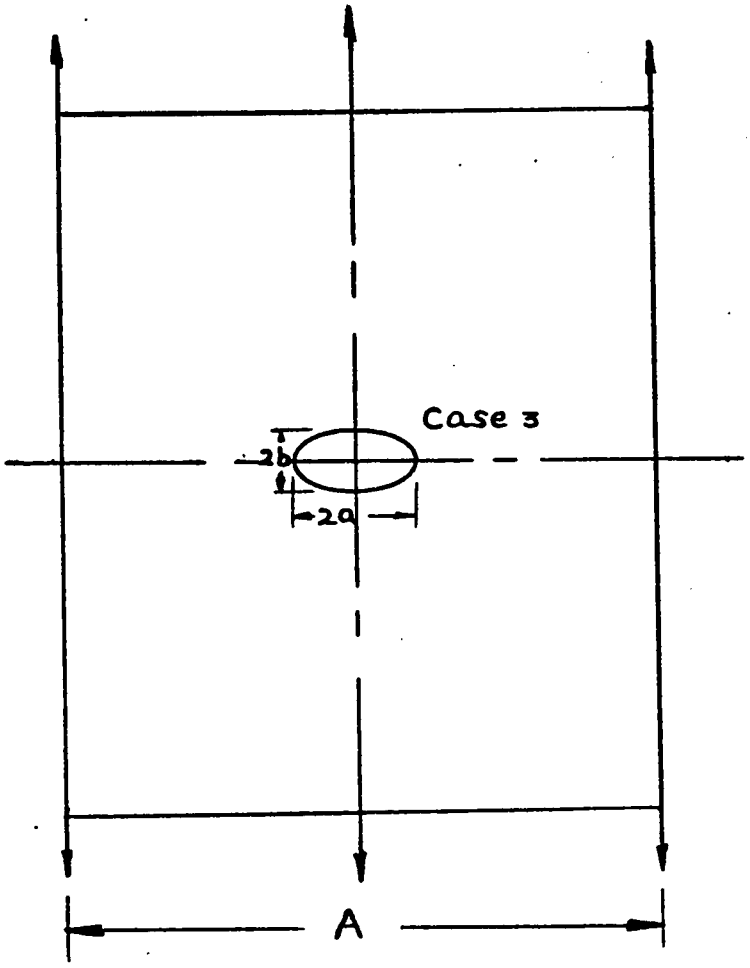

FIGURE 17

$$\int_{x0}^{xn} \frac{\partial \sigma_{xx}}{\partial x}\, \partial x = \int_{x0}^{x1} \frac{\partial \sigma_{xx}}{\partial x}\, \partial x + \int_{x1}^{x2} \frac{\partial \sigma_{xx}}{\partial x}\, \partial x + \cdots\cdots + \int_{x(n-1)}^{xn} \frac{\partial \sigma_{xx}}{\partial x}\, \partial x \qquad (62)$$

Considering only the first integral on the right hand side and substituting for $\frac{\partial \sigma xx}{\partial x}$ from equation (1), we have

$$\int_{x0}^{x1} \frac{\partial \sigma_{xx}}{\partial x}\, \partial x = -\int_{x0}^{x1} \frac{\partial \tau_{xy}}{\partial y}\, \partial x$$

Converting this into a finite difference form, we get

$$\sigma_{xx}\Big|_{x1} - \sigma_{xx}\Big|_{x0} = -\frac{\Delta \tau_{xy}}{\Delta y}\Big|_{\left(\frac{x0+x1}{2}\right)} \Delta x .$$

From this we obtain

$$\sigma_{xx}\Big|_{x1} = \sigma_{xx}\Big|_{x0} - \frac{\Delta \tau_{xy}}{\Delta y}\Big|_{\left(\frac{x0+x1}{2}\right)} \Delta x \qquad (63)$$

Similarly, other integrals on the right hand side of equation (62) give

$$\sigma_{xx}\Big|_{x2} = \sigma_{xx}\Big|_{x1} - \frac{\Delta \tau_{xy}}{\Delta y}\Big|_{\left(\frac{x1+x2}{2}\right)} \Delta x$$

$$\vdots \qquad (63)$$

$$\sigma_{xx}\Big|_{xn} = \sigma_{xx}\Big|_{x(n-1)} - \frac{\Delta \tau_{xy}}{\Delta y}\Big|_{\left(\frac{xn+x(n-1)}{2}\right)} \Delta x$$

The value of $\sigma_{xx}\big|_{X0}$ is obtained directly from isochromatic data, since the point O is on a free boundary (i.e. at X0 = 0). For evaluating $\Delta\tau_{xy}$ at positions $\frac{X0 + X1}{2}$, $\frac{X1 + X2}{2}$, ------ $\frac{X(n-1) + Xn}{2}$, the shear stresses τ_{xy} at above positions along the lines $\overline{A1\ B1}$ and $\overline{C1\ D1}$ are calculated from the isochromatics and isoclinics readings.

$$\Delta\tau_{xy} = \tau_{xy}\Big|_{+\frac{\Delta y}{2}} - \tau_{xy}\Big|_{-\frac{\Delta y}{2}}$$

The values of σ_{xx} at X1, X2, -------- Xn are obtained from equations (63).

Thus having obtained σ_{xx} along ON, we proceed further to evaluate σ_{yy} using Mohr's circle ,as follows

$$\sigma_{yy} = \sigma_{xx} - (P_1 - P_2)\cos 2\theta \qquad (64)$$

in which θ and $(P_1 - P_2)$ along line ON are obtained from isoclinic and isochromatic readings, respectively.

Substituting for $(P_1 - P_2)$ from equation (A) into equation (64), we get

$$\sigma_{yy} = \sigma_{xx} - \frac{N f}{h}\cos 2\theta$$

From the first invariant of stress, we have

$$\sigma_{xx} + \sigma_{yy} = P_1 + P_2 \qquad (65)$$

Solving equation (65) and (A), we get principal stresses P_1 and P_2 along ON as

$$P_1 = \frac{1}{2}\left(\sigma_{xx} + \sigma_{yy} + \frac{N \quad f}{h}\right)$$

$$P_2 = \frac{1}{2}\left(\sigma_{xx} + \sigma_{yy} - \frac{N \quad f}{h}\right)$$

In all experiments, the value of Δy was kept constant at 0.05 in.. The minimum value of Δx near the insert was as low as 0.01 in. and was increased in steps to 0.01, 0.025, 0.05, 0.10, and 0.20 in. as the point of exploration approached the external boundary.

After this, the stress concentration factor is calculated as follows:

$$\text{CONFAI} = \frac{P_1}{\text{PNET1}}$$

Where PNET1 —— average stress computed over the width A

$$= \frac{P_y}{A\,h}$$

A flow chart of the computer program giving the stress distribution and the concentration factor is shown on page 117.

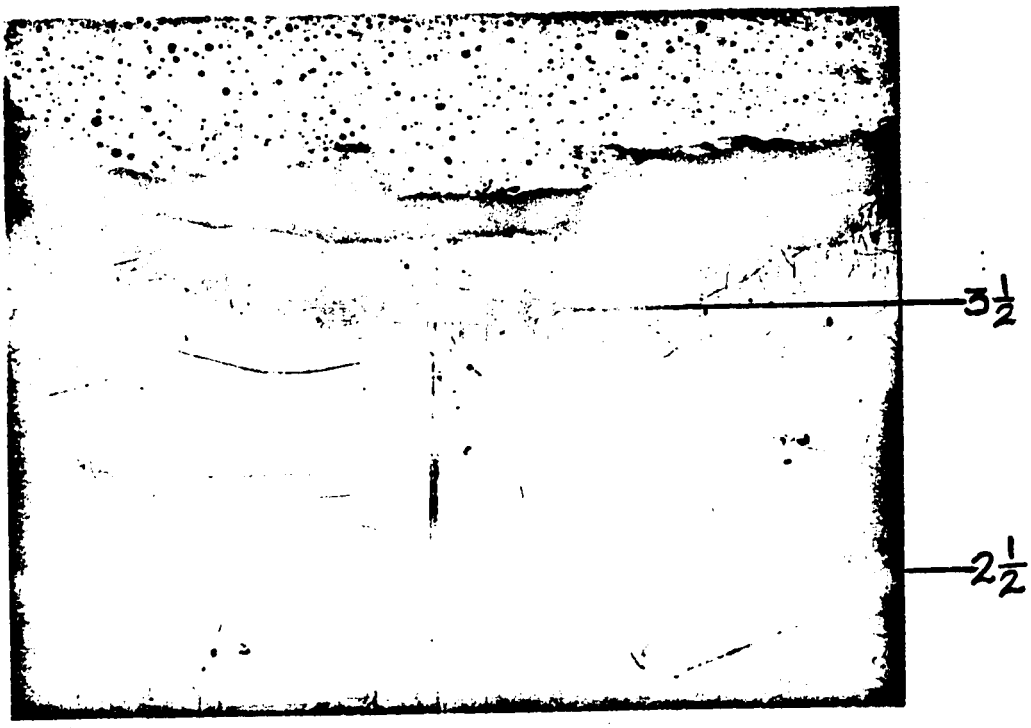

Fig. 18 Stress Pattern of a Specimen with a Central Elliptical Insert Subjected to an Axial Tension.

Parent material — PSM1 ; Insert material — PSM4 ; dimensions of the insert — 2a = 0.50 in, 2b = 1.0 in. ; width of the specimen = 2.50 in. ; thickness = 0.254 in. ; axial load = 200 lb.

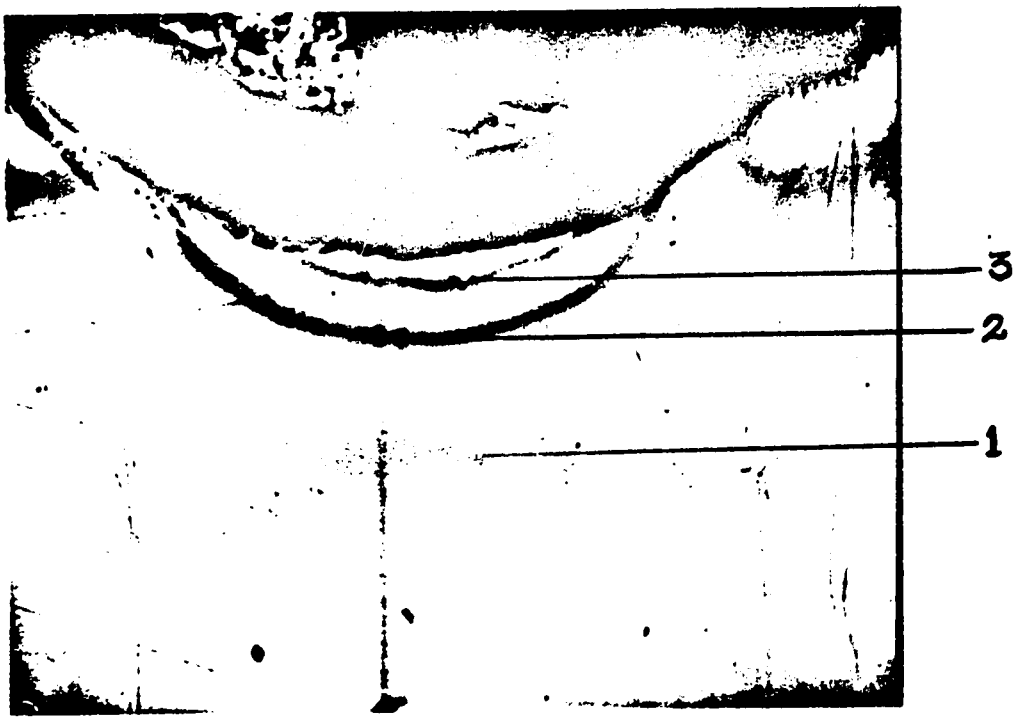

Fig. 19 Stress Pattern of a Specimen with a Central Circular Insert Subjected to an Axial Tension.

Parent material — PSM1 ; Insert material — PSM4 ; dimensions of the insert — 2a = 0.50 in, 2b = 0.50 in.; width of the specimen = 2.50 in.; thickness = 0.254 in.; axial load = 150 lb.

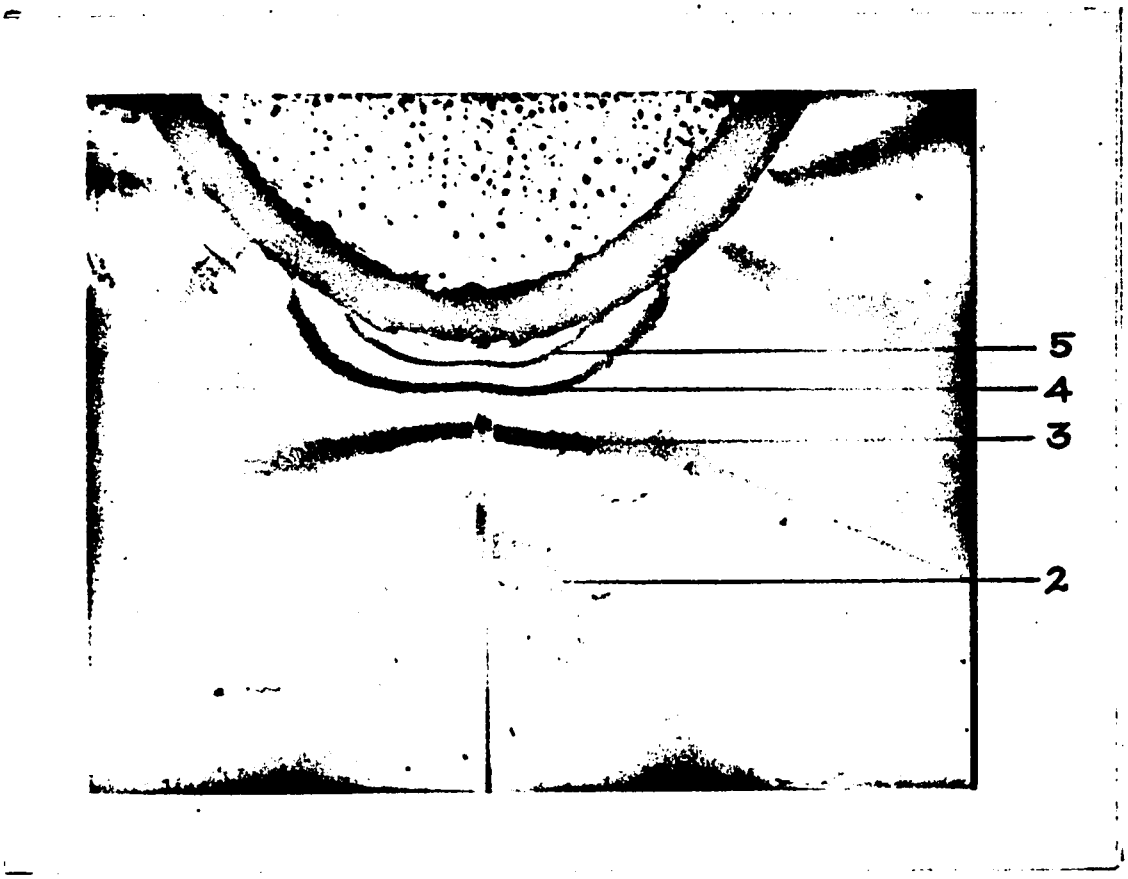

Fig. 20 Stress Pattern of a Specimen with a Central Elliptical Insert Subjected to an Axial Tension.

Parent material -- PSM1; Insert material -- PSM4 ; dimensions of the insert -- 2a = 1.0 in., 2b = 0.50 in.; width of the specimen = 2.50 in.; thickness = 0.254 in.; axial load = 150 lb.

FLOW CHART FOR FINDING PRINCIPAL STRESSES P_1 AND P_2 AND CONCENTRATION FACTORS BY SHEAR DIFFERENCE METHOD.

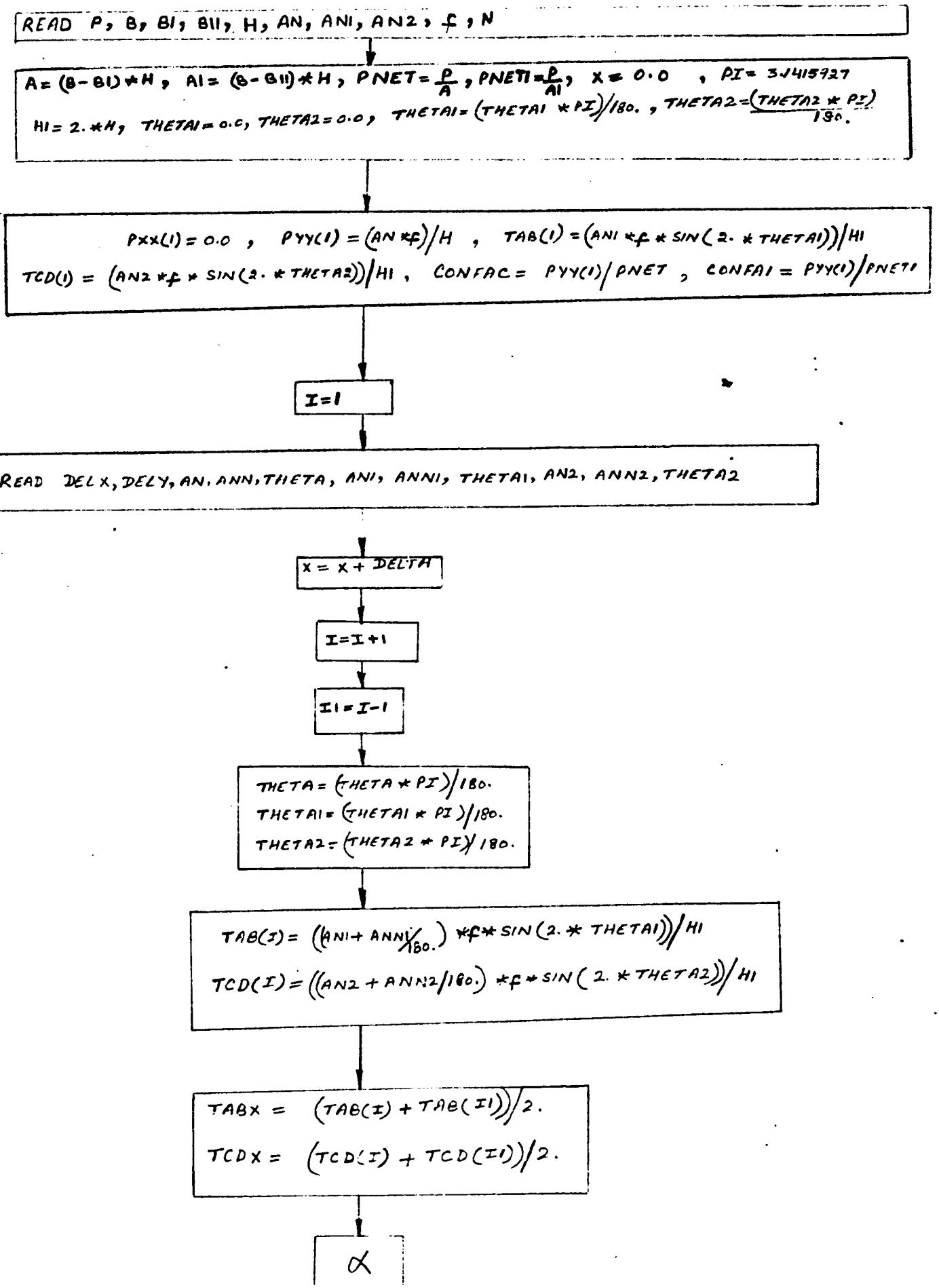

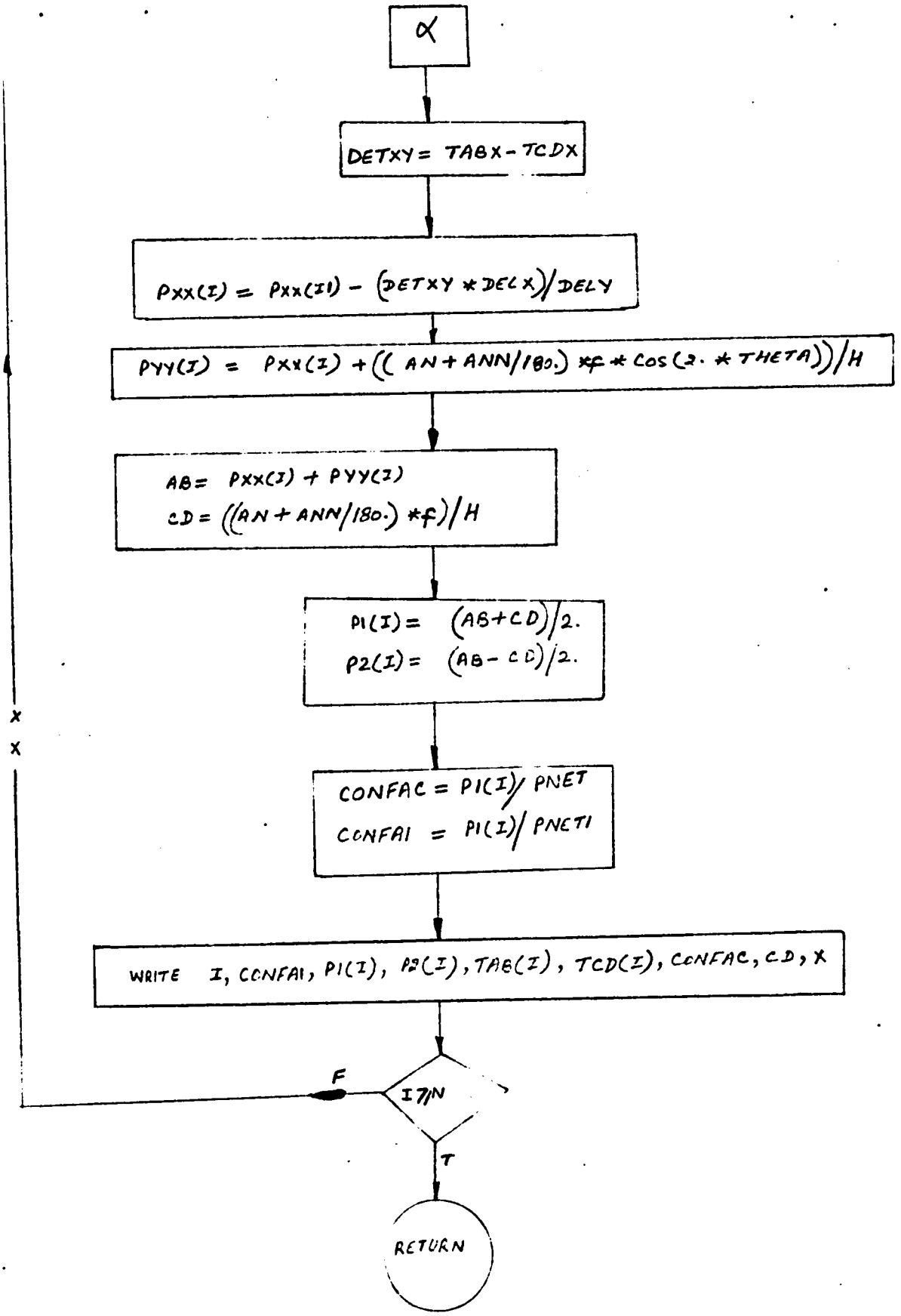
X
X
DETXY = TABX - TCDX
PXX(I) = PXX(I1) - (DETXY * DELX)/DELY
PYY(I) = PXX(I) + ((AN + ANN/180.) * f * COS(2. * THETA))/H
AB = PXX(I) + PYY(I)
CD = ((AN + ANN/180.) * f)/H
P1(I) = (AB+CD)/2.
P2(I) = (AB - CD)/2.
CONFAC = P1(I)/ PNET
CONFAI = P1(I)/ PNETI
WRITE I, CONFAI, P1(I), P2(I), TAB(I), TCD(I), CONFAC, CD, X
F
I ?/N
T
RETURN

4. DISCUSSION OF THE RESULTS AND CONCLUSIONS

The experiments reported in this thesis deal with twenty seven specimens. Each specimen is a rectangular plate having a centrally located insert and is subjected to a tensile load P. The experimentally obtained stress concentration factors are given in table 1. The variables used in this table and in figures 21 to 52 are explained below.

A -- width of the specimen

2a -- transverse axis of the ellipse

2b -- longitudinal axis of the ellipse

$\lambda = 2a/A$

$\mu = b/a$

P_1 -- maximum principal stress

P_2 -- minimum principal stress

PNET1 — average stress computed over the width A

CONFA1— stress concentration factor (K_T)

$K_T = P_1/PNET1$

Figures 21 through 47, show the variation of maximum principal stress P_1 and the stress concentration factor K_T along the x-axis. The curves are plotted starting from the point 0 on the external boundary and ending at the interface. The graphs show the

influence of different shapes and the configurations of the plate and insert material and also that of various (E_1/E_2) ratios on the stress concentration factor.

In figures 21 to 29, the parent material is of hard plastic PSM1 and the insert is of soft plastic PSM4. Three cases for each configuration of the insert are shown in the graphs.

The maximum principal stress P_1 has its highest value at the interface of the two materials on the x-axis, and is lowest at the external boundary. Since the stress concentration factor is proportional to P_1, it also has the highest value at the interface. Experiments on specimens with centrally located holes have exhibited a pronounced rise in stresses at the boundary of the discontinuity. Obviously, this discontinuity in the material acts as a stress riser and has given rise to a high value of stress concentration factor. In our case, instead of a hole we have a very soft insert material at the centre. This is again equivalent to a discontinuity in the parent material. However, the insert shares part of the applied load, and therefore the highest value of the maximum principal stress P_1, and hence of the stress concentration factor are less than those obtained with a central hole. In the case of the elliptical insert, two configurations were studied -- ellipse with its major axis along the longitudinal axis of the plate, and across it. In either case the highest value of P_1 was found to be less than those obtained by Durelli, Parks, and Feng (6) for a finite width plate with a centrally located elliptical hole.

The stress concentration factor at the interface is found to decrease when the overall width is decreased. This is partly due to an increase in the value of PNET1, brought about by a decrease in the area of cross section.

Donnell's (4) work shows the variation of stress concentration factor in the case of an elliptical inclusion in an infinite plate. A linear interpolation, the validity of which is doubtful, is used for obtaining Donnell's results for the ratio (E_1/E_2) = 1/340 so that a comparison can be made.

Reference (17), page 72, Donnell's results are obtained as shown below.

μ	K_T(Kumra)	K_T(Donnell)
0.50	4.0265	4.97
1.0	2.8646	2.989
2.0	1.9849	1.9959

Figures 30 to 38 represent the results obtained using specimens with hard plastic (PSM1) as insert and soft plastic (PSM4) as parent material. The graps show the influence of different shapes and configurations of the plate and insert material and also that of various E_1/E_2 ratios on the stress concentration factors.

This combination of hard insert in a soft body exhibits an interesting phenomenon. The maximum value of stress concentration factor does not occure at the interface of the two materials, but is shifted towards the external boundary as seen in these figures. This shift is found to be more when the width of the specimen is reduced. This phenomenon can be explained as follows. Since the insert is a hard material, displacement in the neighbour of the interface is small. However, farther away from the interface the influence of the hard insert on the displacement of the soft parent material reduces. Again very near the external boundary, the soft plastic is free to undergo a displacement on its own, when stressed. The maximum displacement therefore occures immediately following the region of influence of the hard material. In other words, the material is stressed to a maximum in this region, and hence the stress concentration factor shows a steep rise here.

There are no results available for the purpose of comparison in this high range of moduli ratio.

Figures 39 to 47 show the results obtained with a very hard insert (Steel) on a very soft parent material. The moduli ratio, in this case, is 30,000. As in the previous case, there is a shift of maximum stress concentration factor towards the free boundary. For a given specimen width this shift is found to be more than that of the previous case, which can be attributed to the high modulus of steel as compared to PSM1.

Figures 48 to 52 are the cross plots of the results shown in

figures 21 to 47. These plots are made for a set of dimensionless quantities μ,λ, and K_T. The ratio of longitudinal to transverse axis of the elliptical insert μ is chosen as the parameter and K_T are plotted against λ. With these figures, a knowledge of λ and μ will enable us to obtain the stress concentration factor.

As for the theoretical side of the problem, an attempt was made to solve a system of 165 linear nonhomogeneous equations, to determine the stress distribution at these 165 nodal points. However, satisfactory results could not be obtained with this mesh size, which was dictated by the computer capacity. In order to reduce the mesh size an efficient method of storing the coefficient matrix, involving much further work, has to be developed. Presently this work is in progress. When the theoretical solution is successfully completed, the program can be used to find the stress distribution in specimens with a wide range of centrally located inserts possessing two axes of symmetry.

TABLE 1

Parent material	Insert material	E_1/E_2	$\mu = b/a$	a inches	b inches	A	$\lambda = 2a/A$	Maximum value K_T'	Value at the interface K_T
PSM1	PSM4	1/340	0.50	0.50	0.25	4.385	0.2280	5.2160	5.2160
PSM1	PSM4	1/340	0.50	0.50	0.25	3.50	0.2857	4.099	4.0999
PSM1	PSM4	1/340	0.50	0.50	0.25	2.50	0.40	4.0564	4.0564
PSM1	PSM4	1/340	1.00	0.25	0.25	4.435	0.1127	3.2311	3.2311
PSM1	PSM4	1/340	1.00	0.25	0.25	3.359	0.1488	2.7553	2.7553
PSM1	PSM4	1/340	1.00	0.25	0.25	2.503	0.1997	2.3303	2.3303
PSM1	PSM4	1/340	2.00	0.25	0.50	4.386	0.1139	2.2403	2.2403
PSM1	PSM4	1/340	2.00	0.25	0.50	3.293	0.1518	2.0994	2.0994
PSM1	PSM4	1/340	2.00	0.25	0.50	2.50	0.200	1.9028	1.9028
PSM4	PSM1	340	0.50	0.50	0.25	4.315	0.2317	1.0884	0.9397
PSM4	PSM1	340	0.50	0.50	0.25	3.50	0.2857	0.8812	0.7198
PSM4	PSM1	340	0.50	0.50	0.25	2.49	0.4016	0.8227	0.3452
PSM4	PSM1	340	1.00	0.25	0.25	4.50	0.1111	1.3821	0.8832
PSM4	PSM1	340	1.00	0.25	0.25	3.51	0.1424	1.0516	0.7425

TABLE 1 (Contd.)

Parent material	Insert material	E_1/E_2	$\mu = b/a$	a inches	b inches	A	$\lambda = 2a/A$	Maximum value K_T'	Value at the interface K_T
PSM4	PSM1	340	1.00	0.25	0.25	2.50	0.20	0.5605	0.8499
PSM4	PSM1	340	2.00	0.25	0.50	4.325	0.1156	0.6946	1.0866
PSM4	PSM1	340	2.00	0.25	0.50	3.345	0.1443	0.4889	0.9568
PSM4	PSM1	340	2.00	0.25	0.50	2.50	0.20	0.2516	0.8410
PSM4	STEEL	30,000	0.50	0.50	0.25	4.340	0.2304	0.3048	1.3245
PSM4	STEEL	30,000	0.50	0.50	0.25	3.450	0.2898	0.3225	1.0265
PSM4	STEEL	30,000	0.50	0.50	0.25	2.50	0.40	0.5365	0.9885
PSM4	STEEL	30,000	1.00	0.25	0.25	4.34	0.1152	0.0018	1.0453
PSM4	STEEL	30,000	1.00	0.25	0.25	3.51	0.1424	0.0408	0.9073
PSM4	STEEL	30,000	1.00	0.25	0.25	2.50	0.20	0.1477	0.8015
PSM4	STEEL	30,000	2.00	0.25	0.50	4.335	0.1153	0.0970	1.0016
PSM4	STEEL	30,000	2.00	0.25	0.50	3.465	0.1443	0.1274	0.9873
PSM4	STEEL	30,000	2.00	0.25	0.50	2.50	0.20	0.1437	0.7584

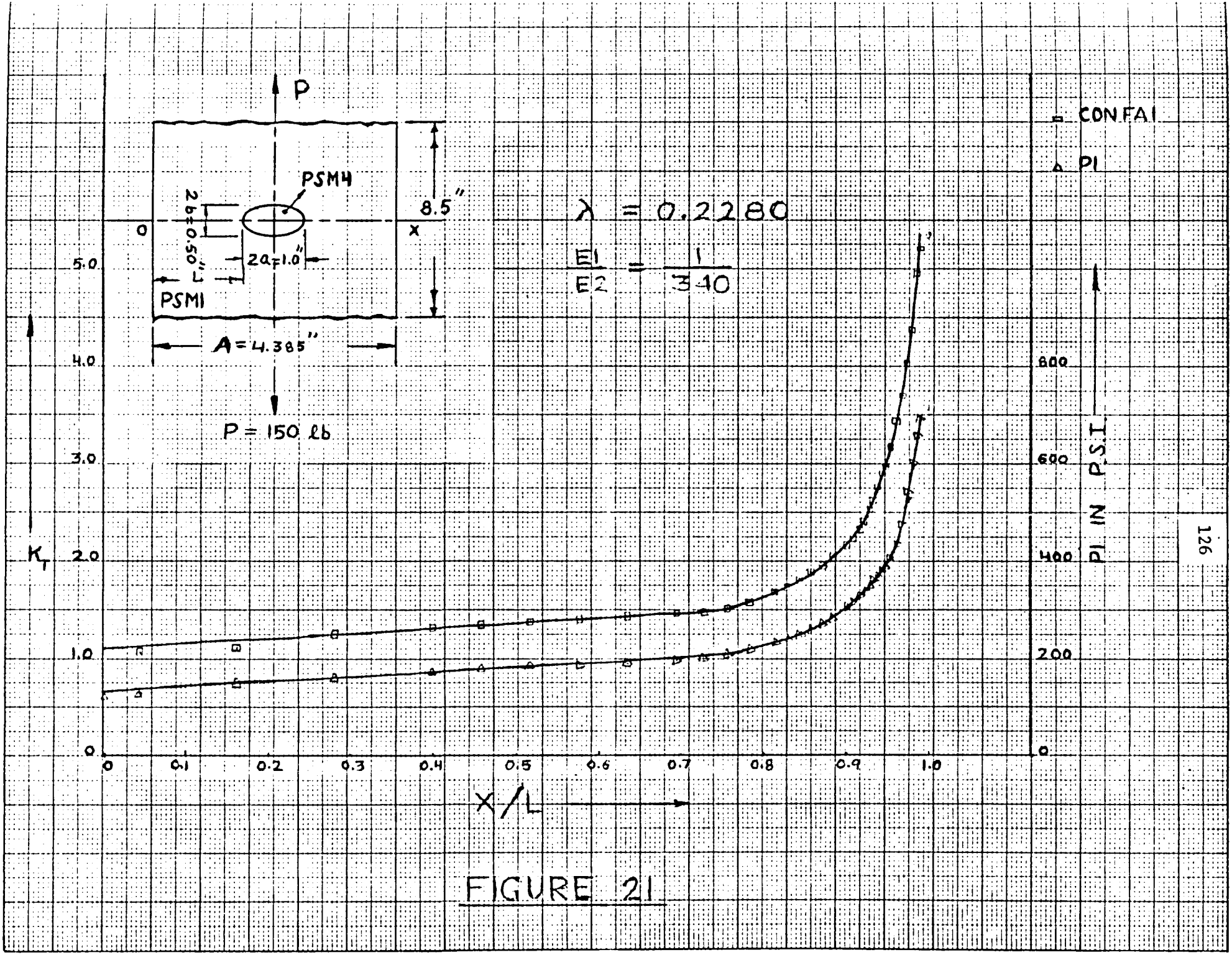
P
PSM4
PSM1
2a=0.50"
2a_F1.0"
8.5"
A=4.385"
P = 150 lb
λ = 0.2280
E1/E2 = 1/3.40
CONFAI
PI
PI IN PSI
K_T
X/L
5.0
4.0
3.0
2.0
1.0
0
800
600
400
200
0
0.1
0.2
0.3
0.4
0.5
0.6
0.7
0.8
0.9
1.0

FIGURE 21

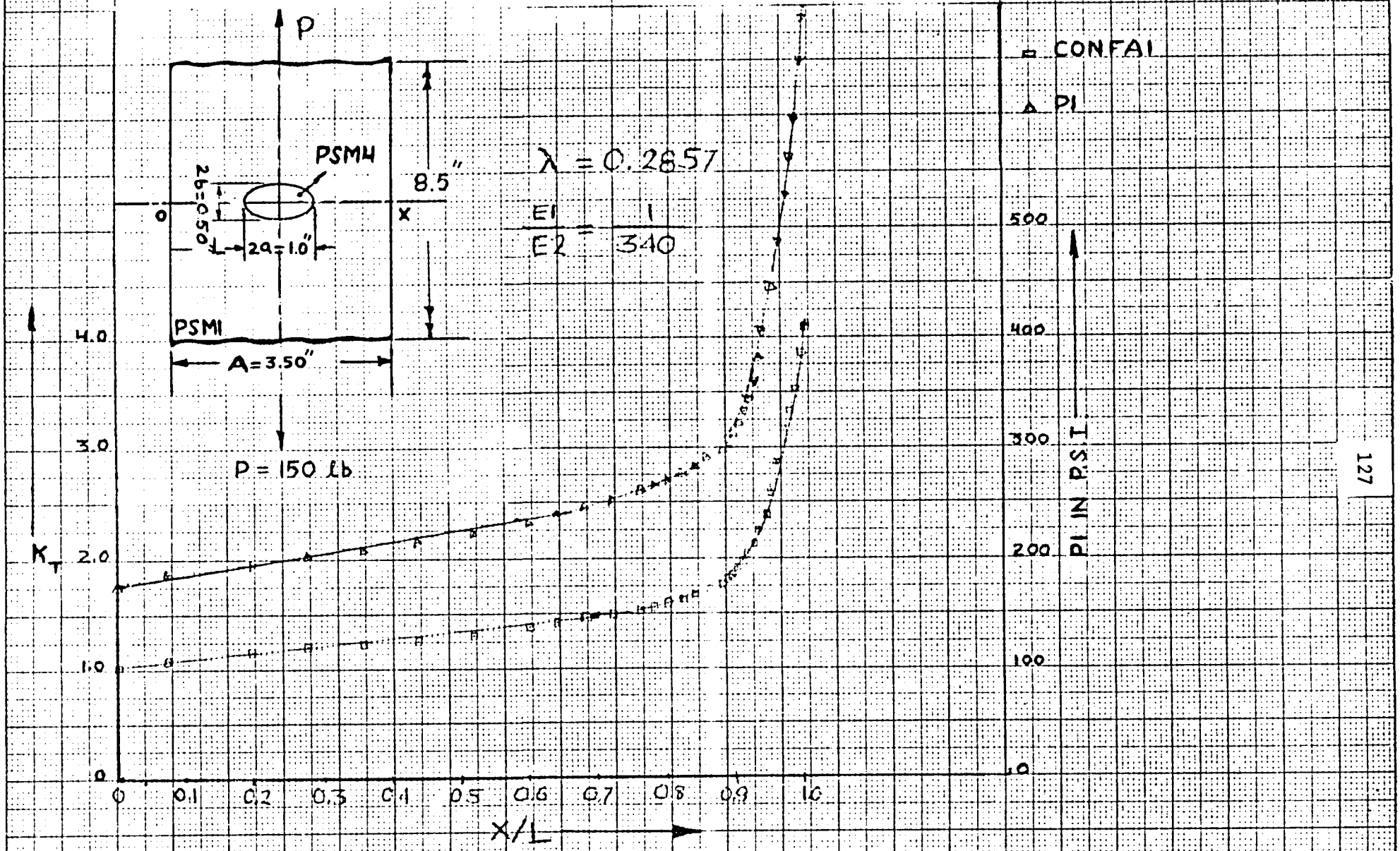
P
PSM4
PSM1
2b=0.50"
2a=1.0"
8.5"
A=3.50"
P = 150 lb
λ = 0.2857
E1 = 1
E2 = 340
0
x
CONFAI
PI
K_T
4.0
3.0
2.0
1.0
0
500
400
300
200
100
0
PI IN PSI
0
0.1
0.2
0.3
0.4
0.5
0.6
0.7
0.8
0.9
1.0
X/L

FIGURE 22

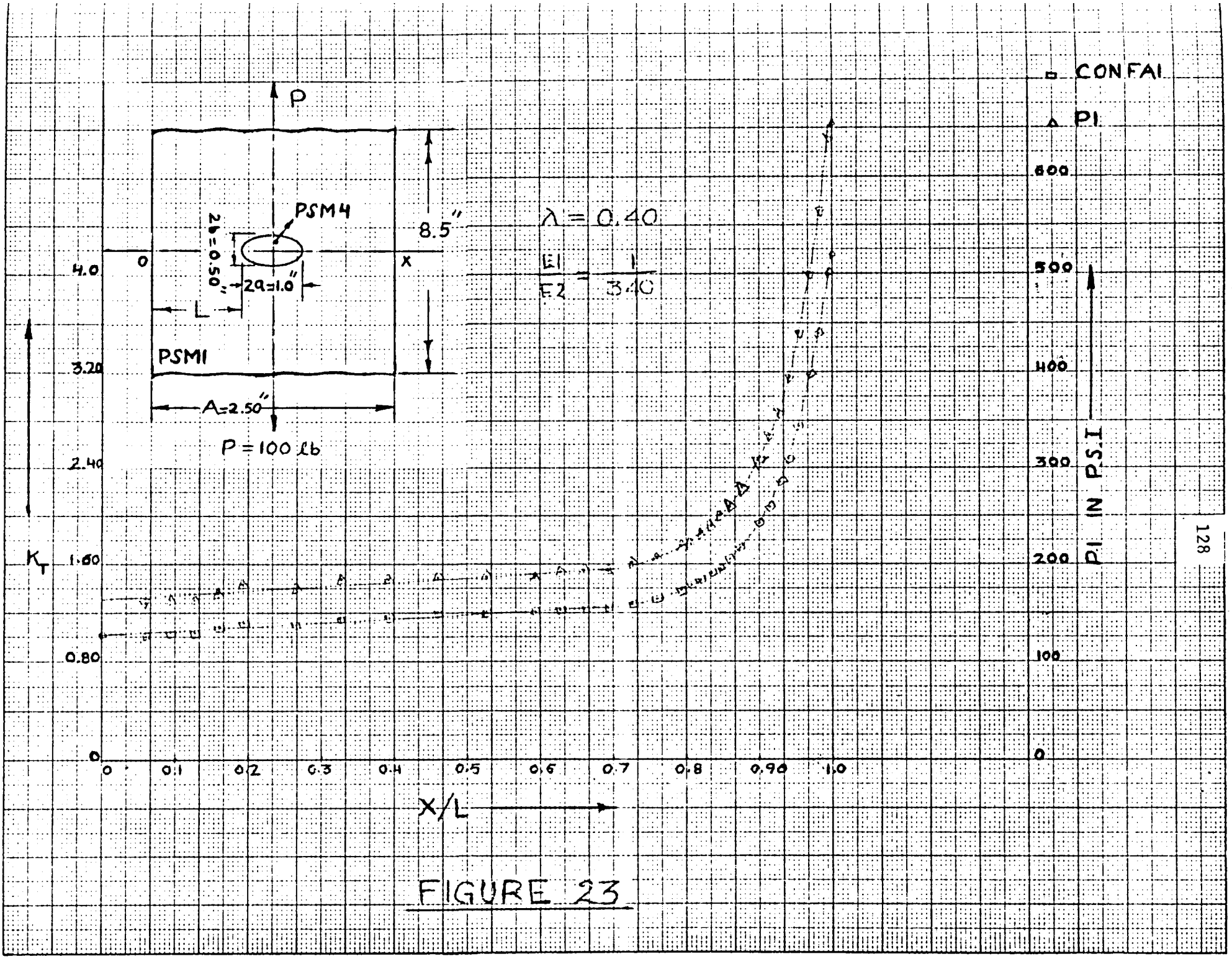
P
PSM4
2b=0.50"
2a=1.0"
8.5"
PSM1
A=2.50"
P=100 lb
0
X
λ = 0.40
E1/E2 = 1/3.40
CONFAI
PI
800
500
400
300
200
100
0
PSI IN PI
K_T
4.0
3.20
2.40
1.60
0.80
0
0
0.1
0.2
0.3
0.4
0.5
0.6
0.7
0.8
0.90
1.0
X/L

FIGURE 23

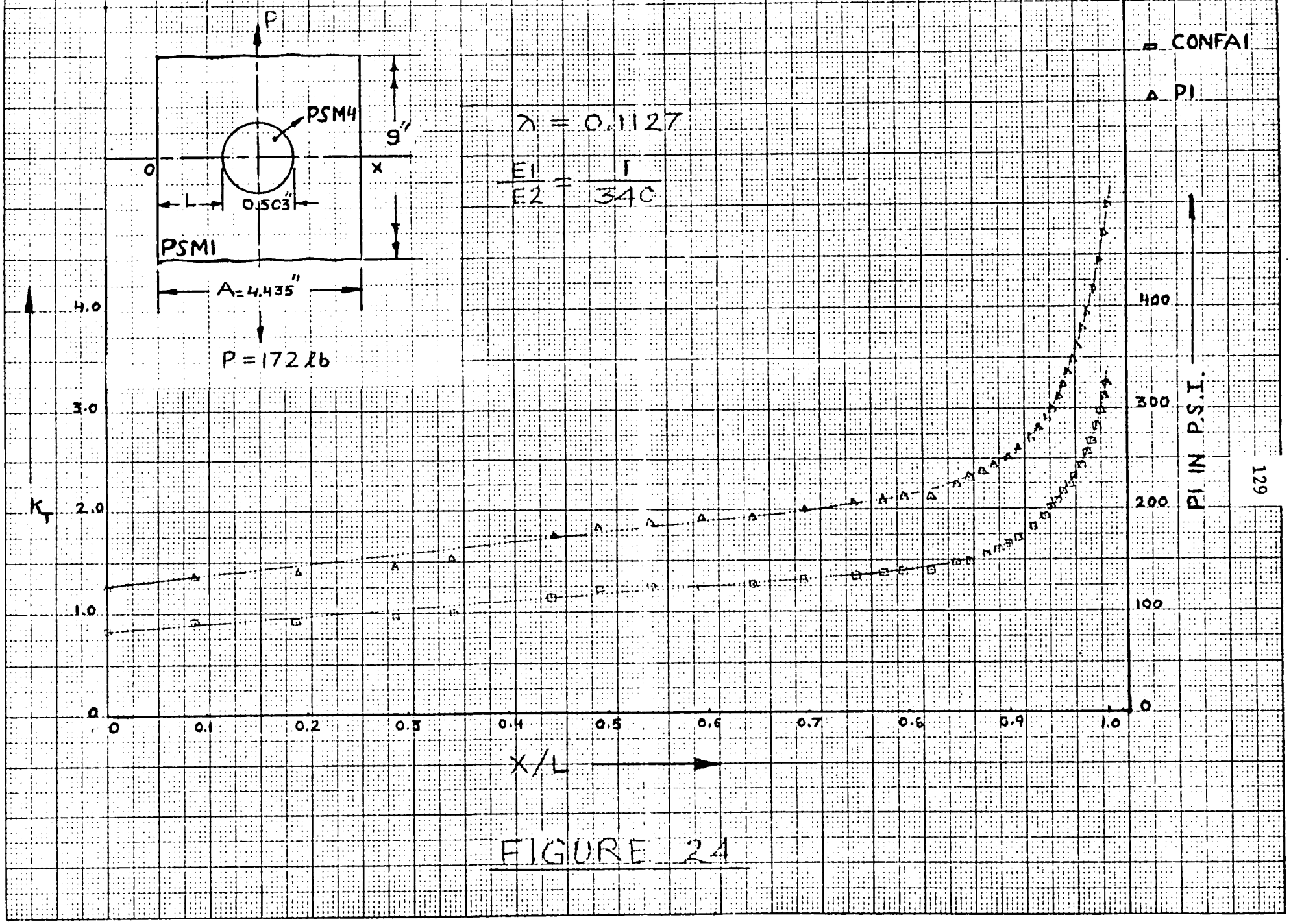
P
PSM4
9"
0
X
L
0.503"
PSM1
A=4.435"
P=172 lb
λ = 0.1127
E1/E2 = T/34C
CONFAI
PI
PI IN P.S.I.
400
300
200
100
0
4.0
3.0
2.0
1.0
0
K_T
0
0.1
0.2
0.3
0.4
0.5
0.6
0.7
0.8
0.9
1.0
X/L

FIGURE 24

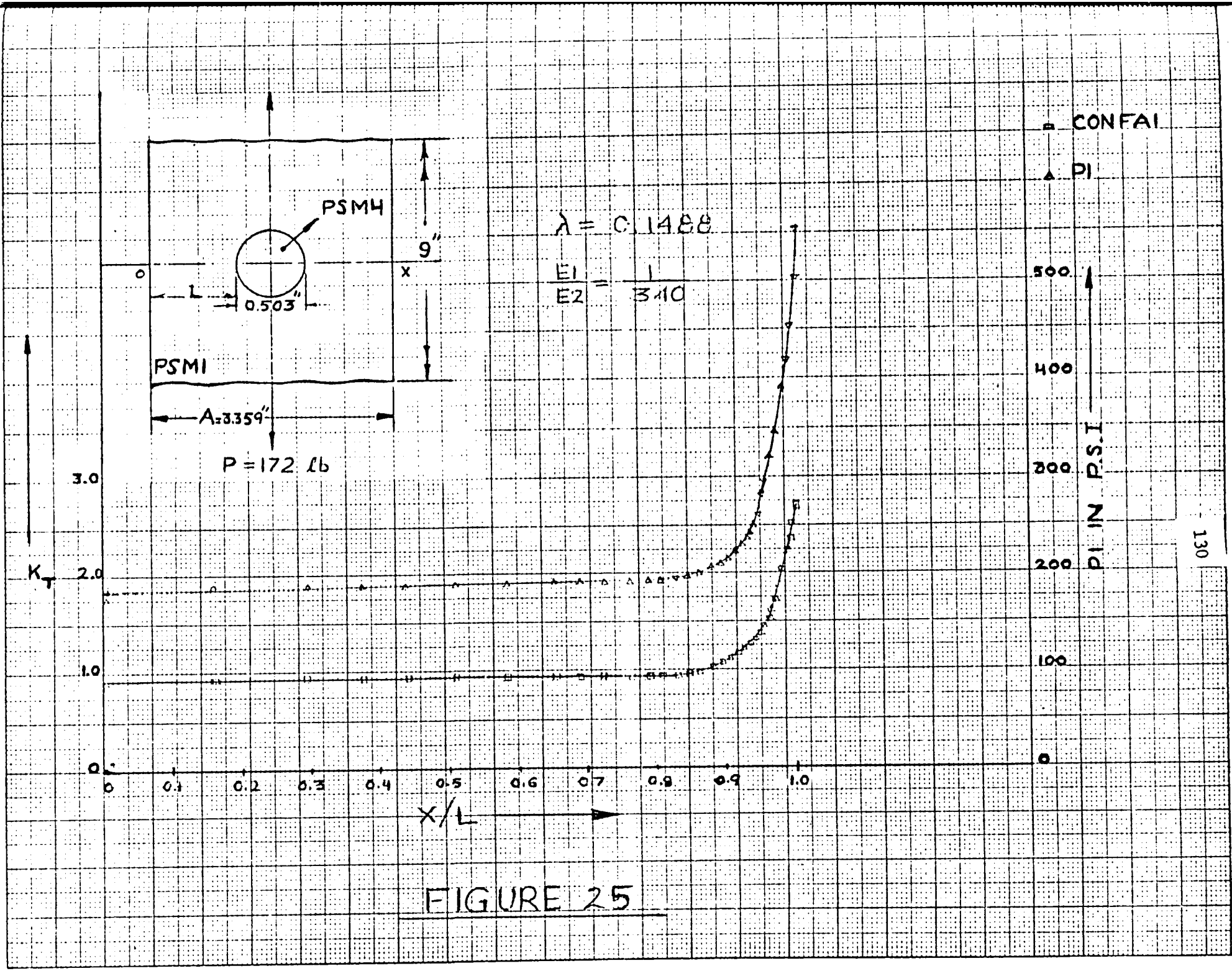
PSM4
9"
0
x
L
0.503"
PSM1
A=3.359"
P=172 lb
λ = 0.1488
E1/E2 = 1/3.10
CONFAI
PI
500
400
300
200
100
0
PSI
3.0
2.0
1.0
0
K_T
0
0.1
0.2
0.3
0.4
0.5
0.6
0.7
0.8
0.9
1.0
X/L

FIGURE 25

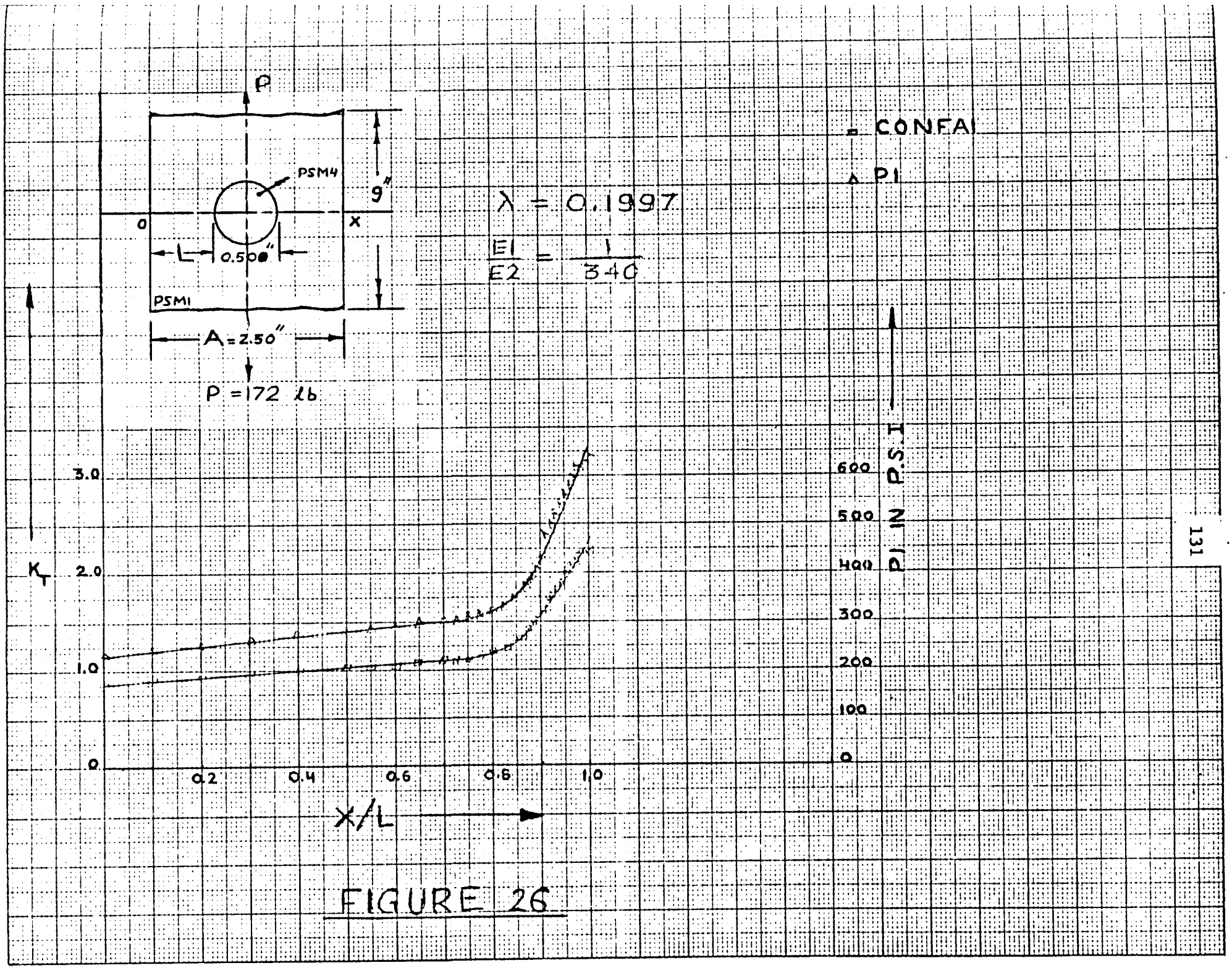
P
PSM4
9"
0
X
L
0.500"
PSM1
A = 2.50"
P = 172 lb
λ = 0.1997
E1/E2 = 1/340
CONFAI
PI
PI IN P.S.I.
600
500
400
300
200
100
0
K_T
3.0
2.0
1.0
0
0.2
0.4
0.6
0.8
1.0
X/L

FIGURE 26

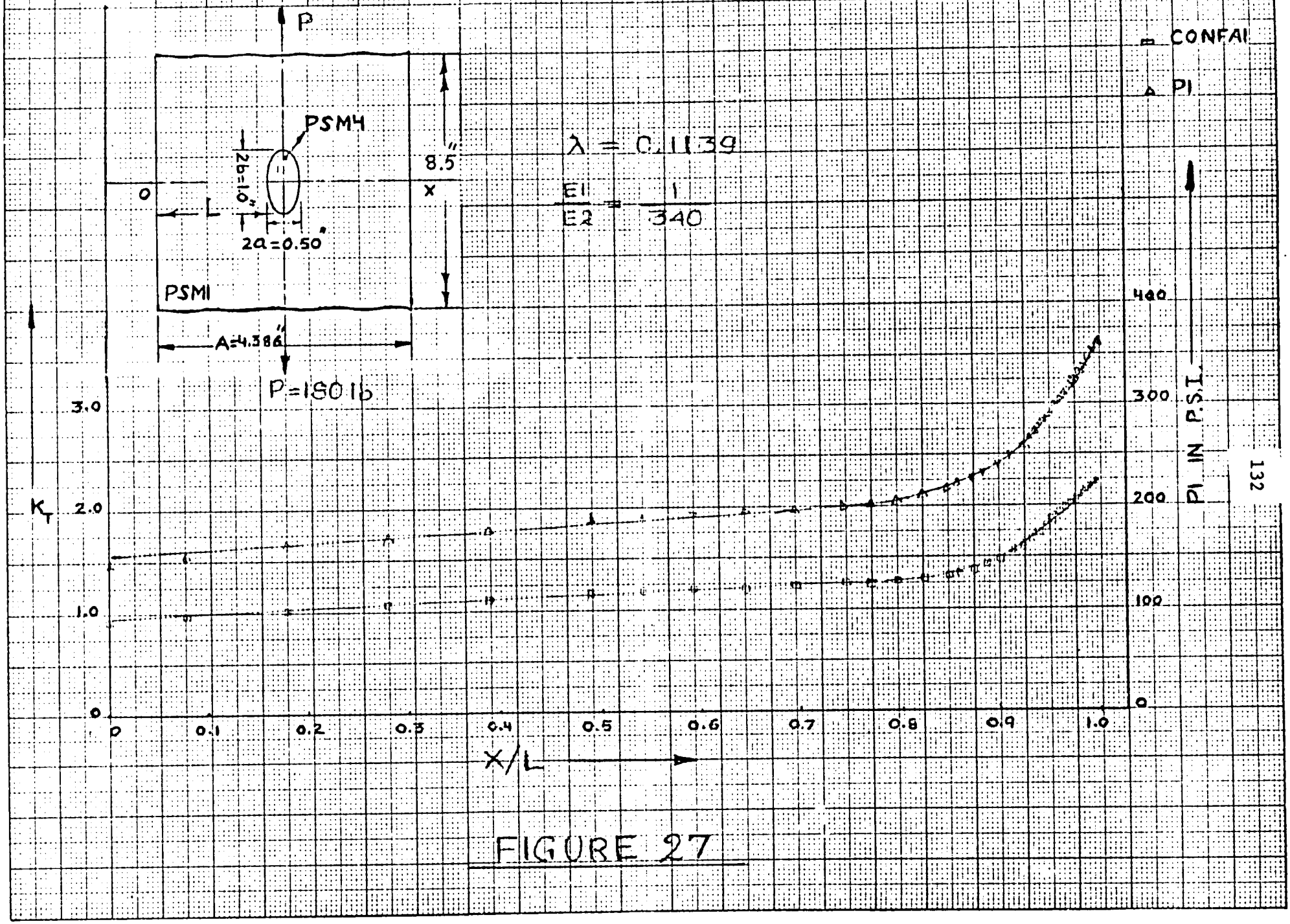
P
PSM4
2b=1.0"
2a=0.50"
8.5"
x
0
L
PSM1
A=4.386"
P=1801b
λ = C.1139
E1/E2 = 1/340
CONFAI
PI
PSI IN PI
400
300
200
100
0
3.0
2.0
1.0
0
K_T
0
0.1
0.2
0.3
0.4
0.5
0.6
0.7
0.8
0.9
1.0
X/L

FIGURE 27

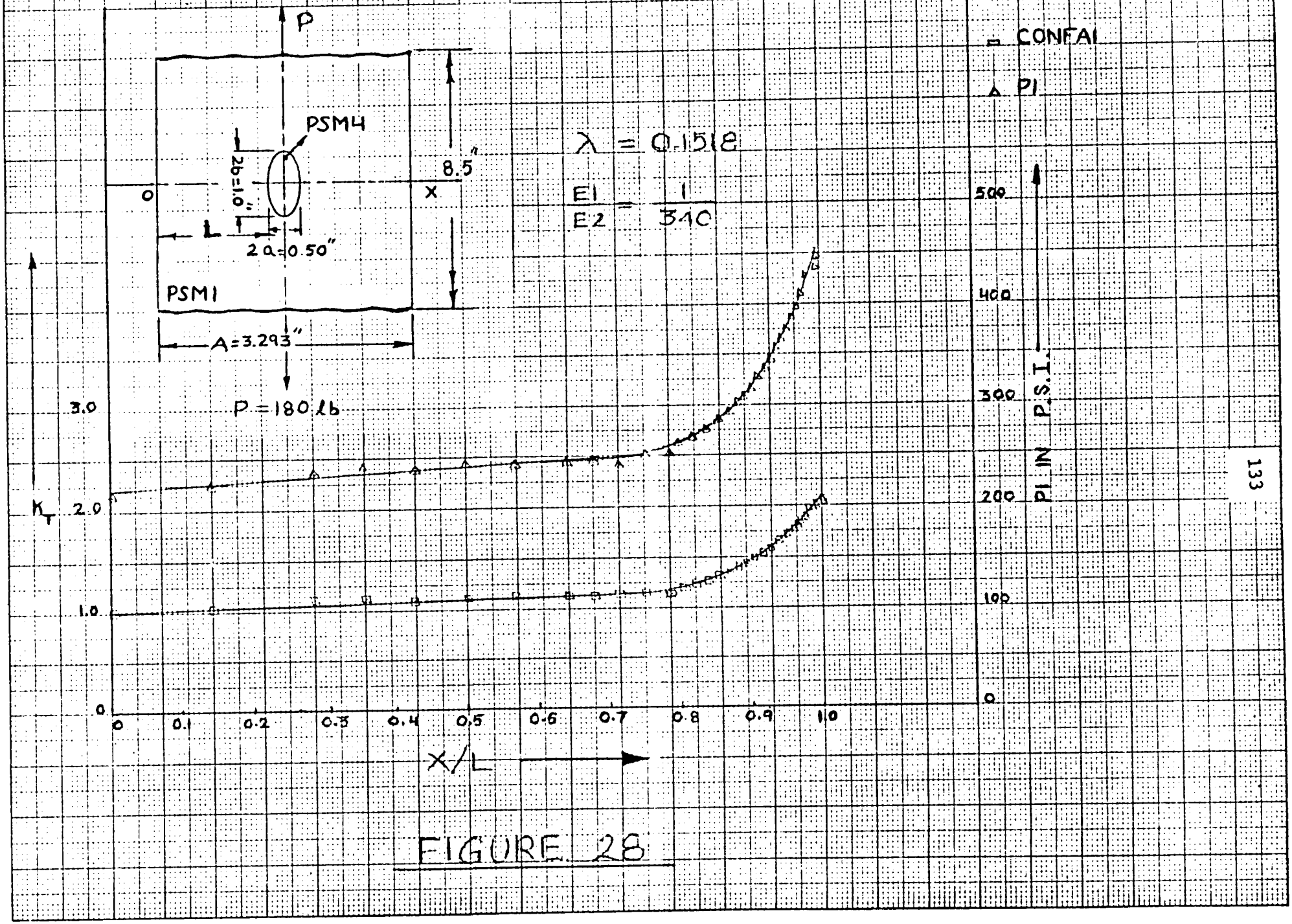
P
PSM4
2b=1.0"
L
2a=0.50"
PSM1
8.5"
x
0
A=3.293"
P=180 lb
λ = 0.158
E1/E2 = 1/340
CONFAI
PI
PI IN P.S.I.
500
400
300
200
100
0
3.0
2.0
1.0
0
K_T
0
0.1
0.2
0.3
0.4
0.5
0.6
0.7
0.8
0.9
1.0
X/L

FIGURE 28

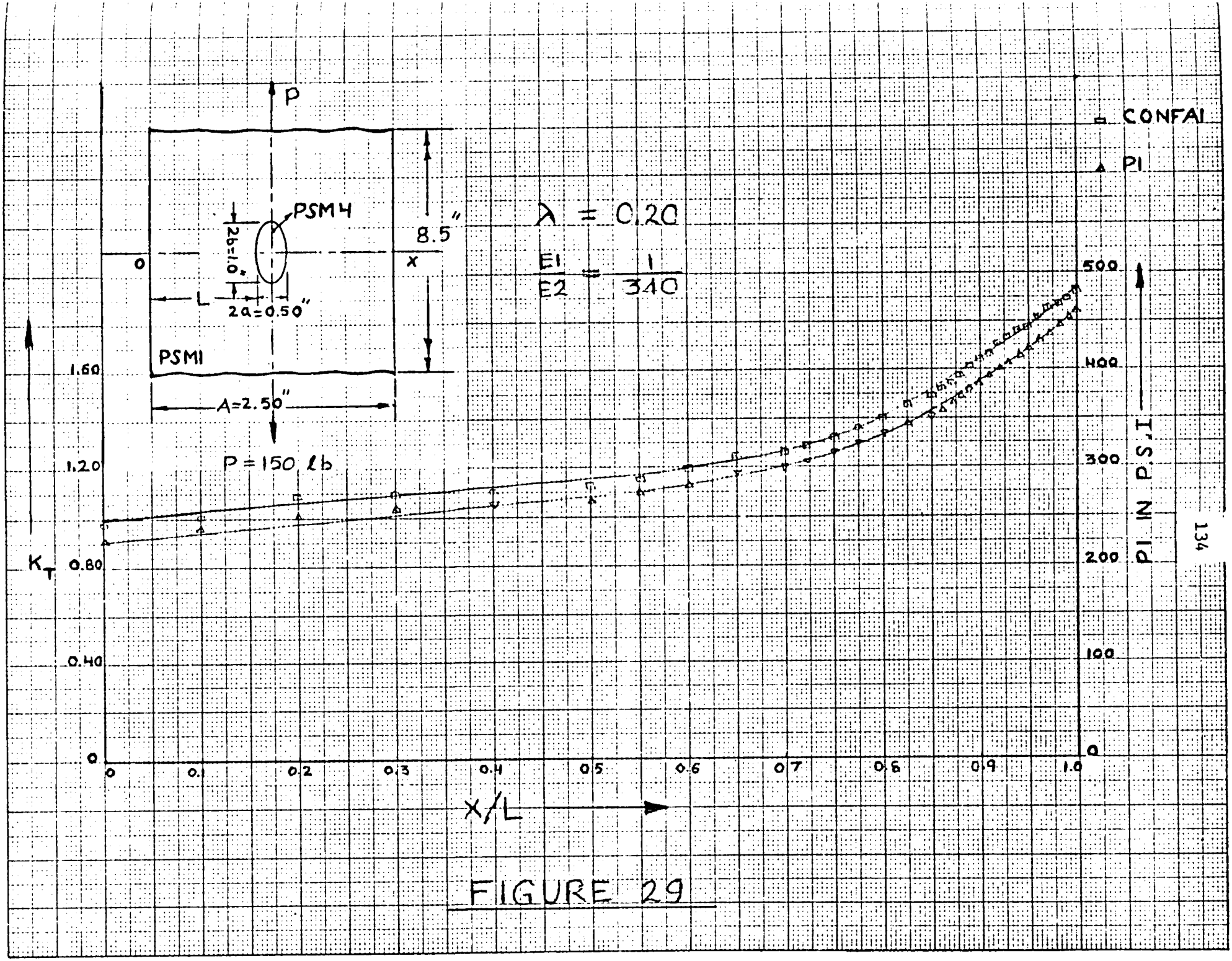
P
PSM4
2b=1.0"
8.5"
x
0
L
2a=0.50"
PSM1
A=2.56"
P = 150 lb
λ = 0.20
E1/E2 = 1/340
CONFAI
PI
PI IN P.S.I.
500
400
300
200
100
0
1.60
1.20
0.80
0.40
0
K_T
0
0.1
0.2
0.3
0.4
0.5
0.6
0.7
0.8
0.9
1.0
X/L

FIGURE 29

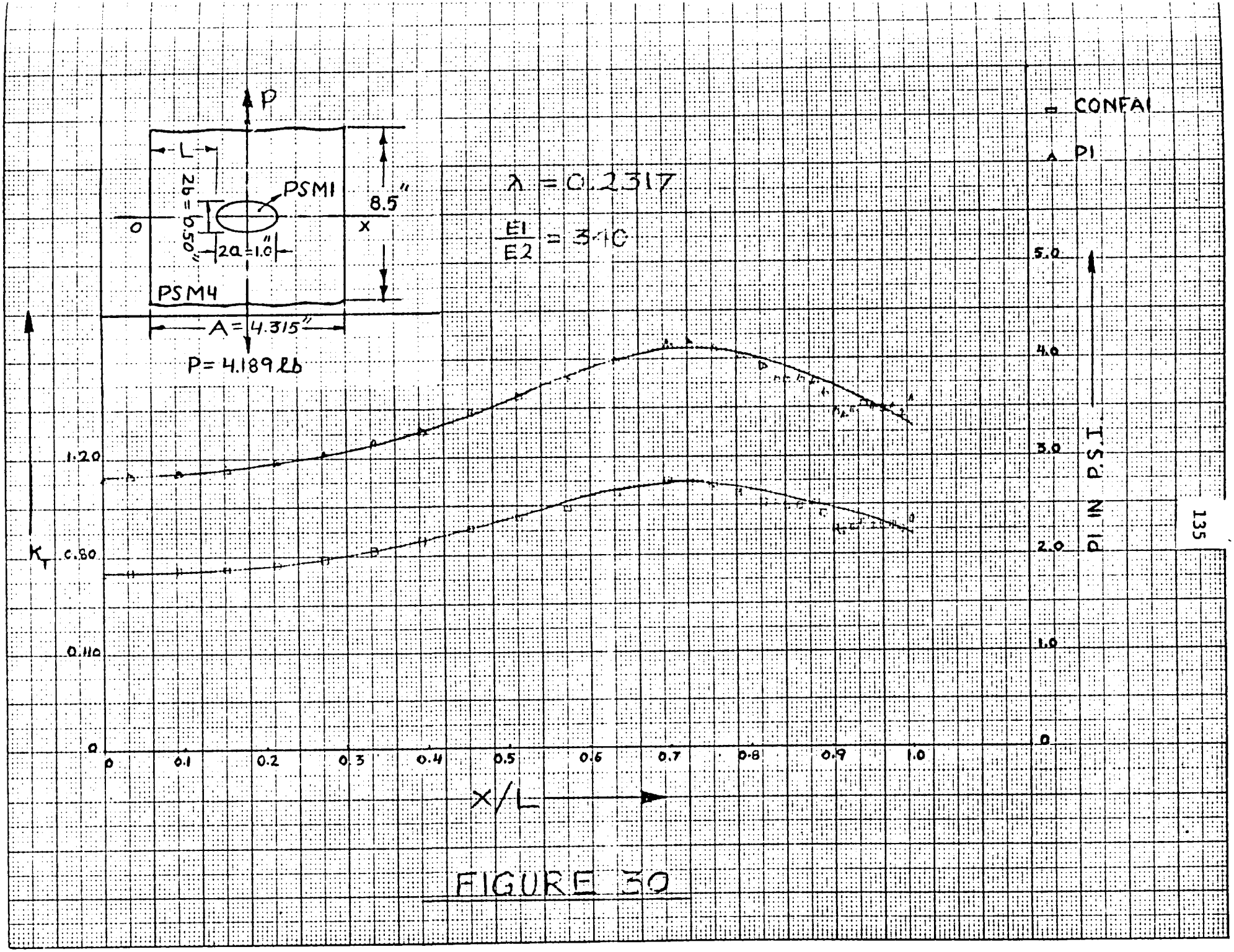
P
L
2b = 0.50"
PSM1
8.5"
0
x
2a = 1.0"
PSM4
A = 4.315"
P = 4.189 Lb
λ = 0.2317
E1/E2 = 3.40
□ CONFAI
△ P1
5.0
4.0
3.0
2.0
1.0
0
P.S.I. IN P1
1.20
K_T
0.80
0.110
0
0
0.1
0.2
0.3
0.4
0.5
0.6
0.7
0.8
0.9
1.0
X/L

FIGURE 30

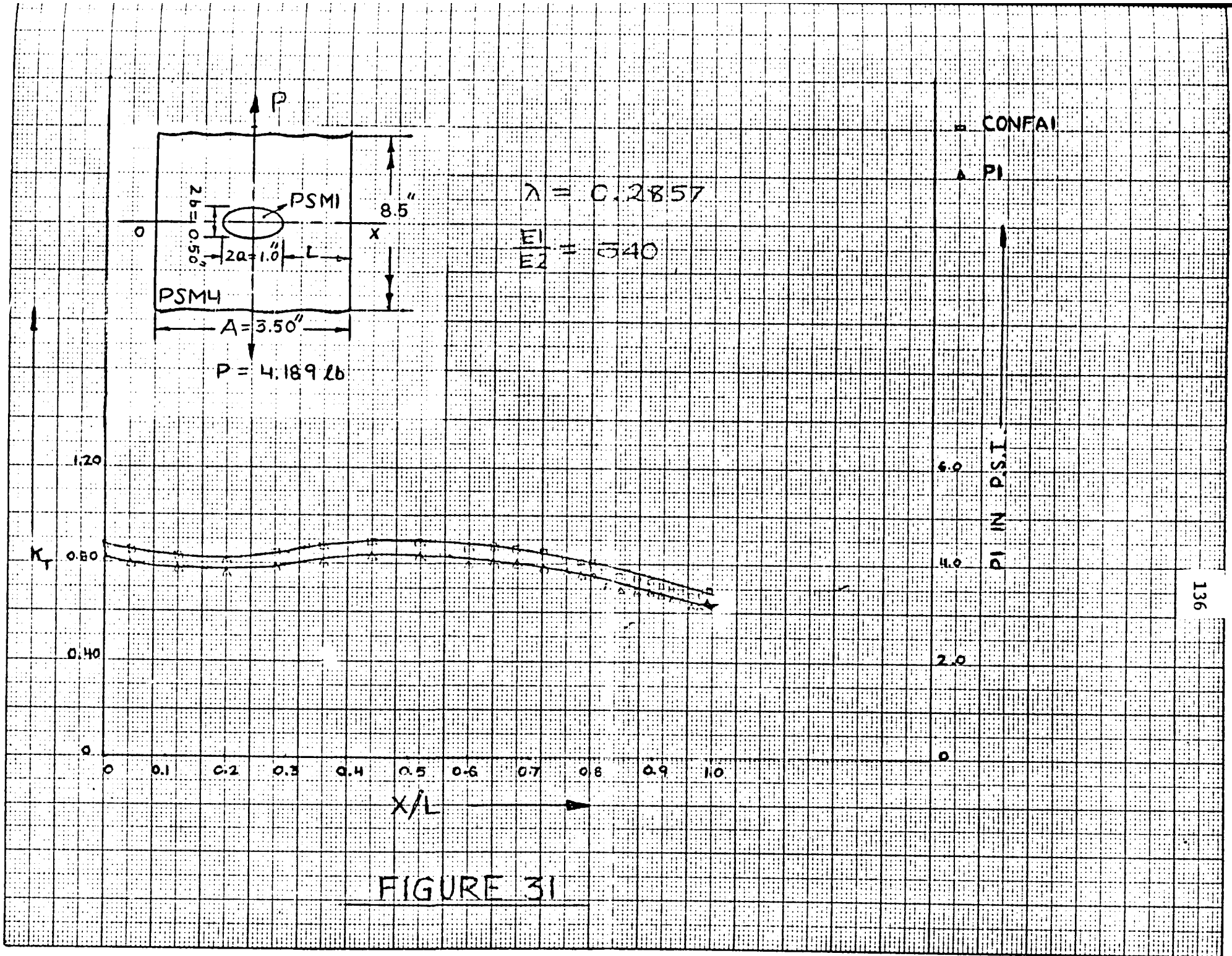
P
PSM1
2b=0.50"
8.5"
0
x
2a=1.0"
L
PSM4
A=3.50"
P = 4.189 lb
λ = 0.2857
EI/E2 = 5.40
CONFAI
PI
PI IN P.S.I.
6.0
4.0
2.0
0
1.20
0.80
0.40
0
K_T
0
0.1
0.2
0.3
0.4
0.5
0.6
0.7
0.8
0.9
1.0
X/L

FIGURE 31

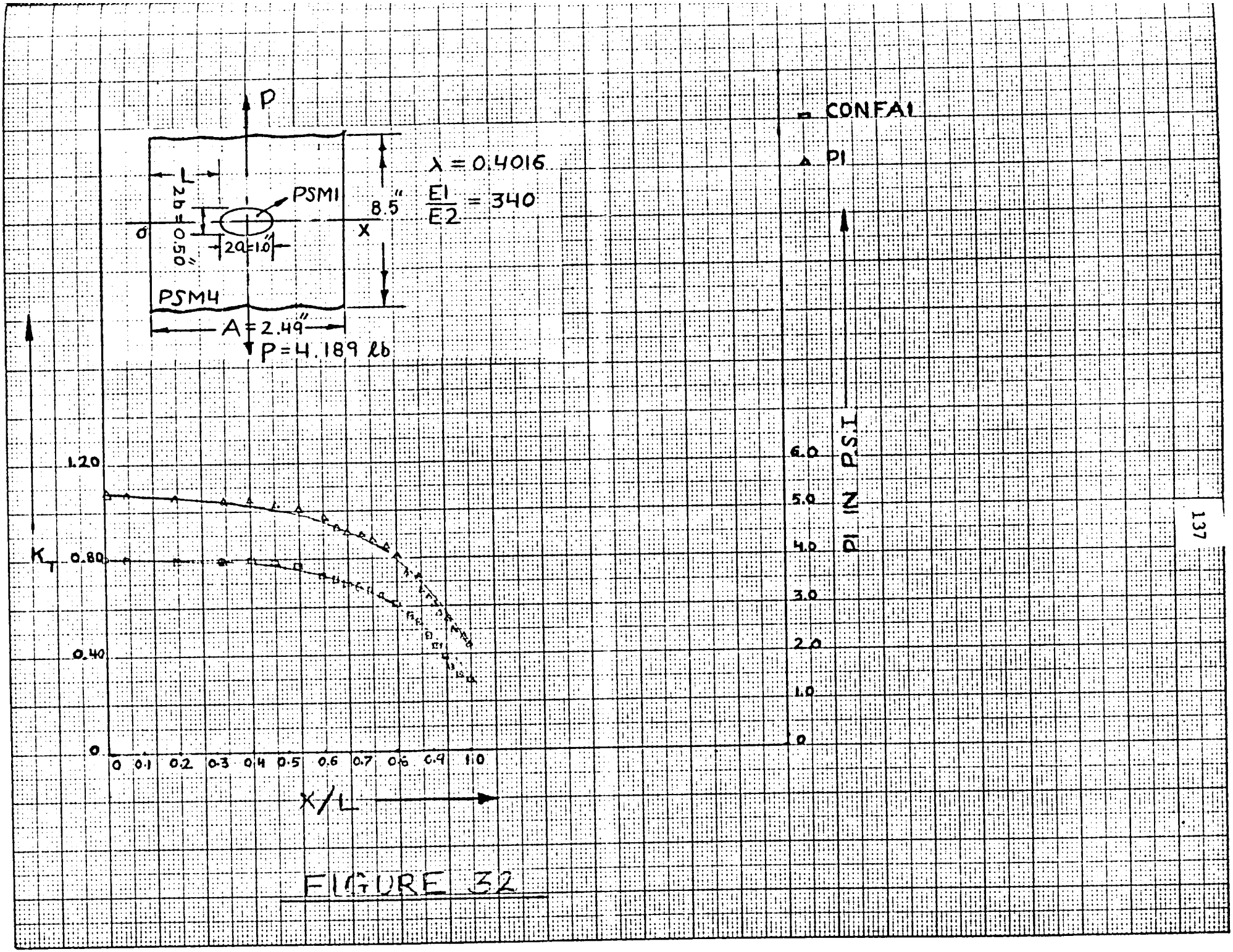
P
L
2a = 0.50"
PSM1
8.5"
X
2a = 1.0"
PSM4
A = 2.49"
P = 4.189 lb
λ = 0.4016
EI/E2 = 340
CONFAI
PI
PI IN P.S.I.
6.0
5.0
4.0
3.0
2.0
1.0
0
K_T
1.20
0.80
0.40
0
0 0.1 0.2 0.3 0.4 0.5 0.6 0.7 0.8 0.9 1.0
X/L

FIGURE 32

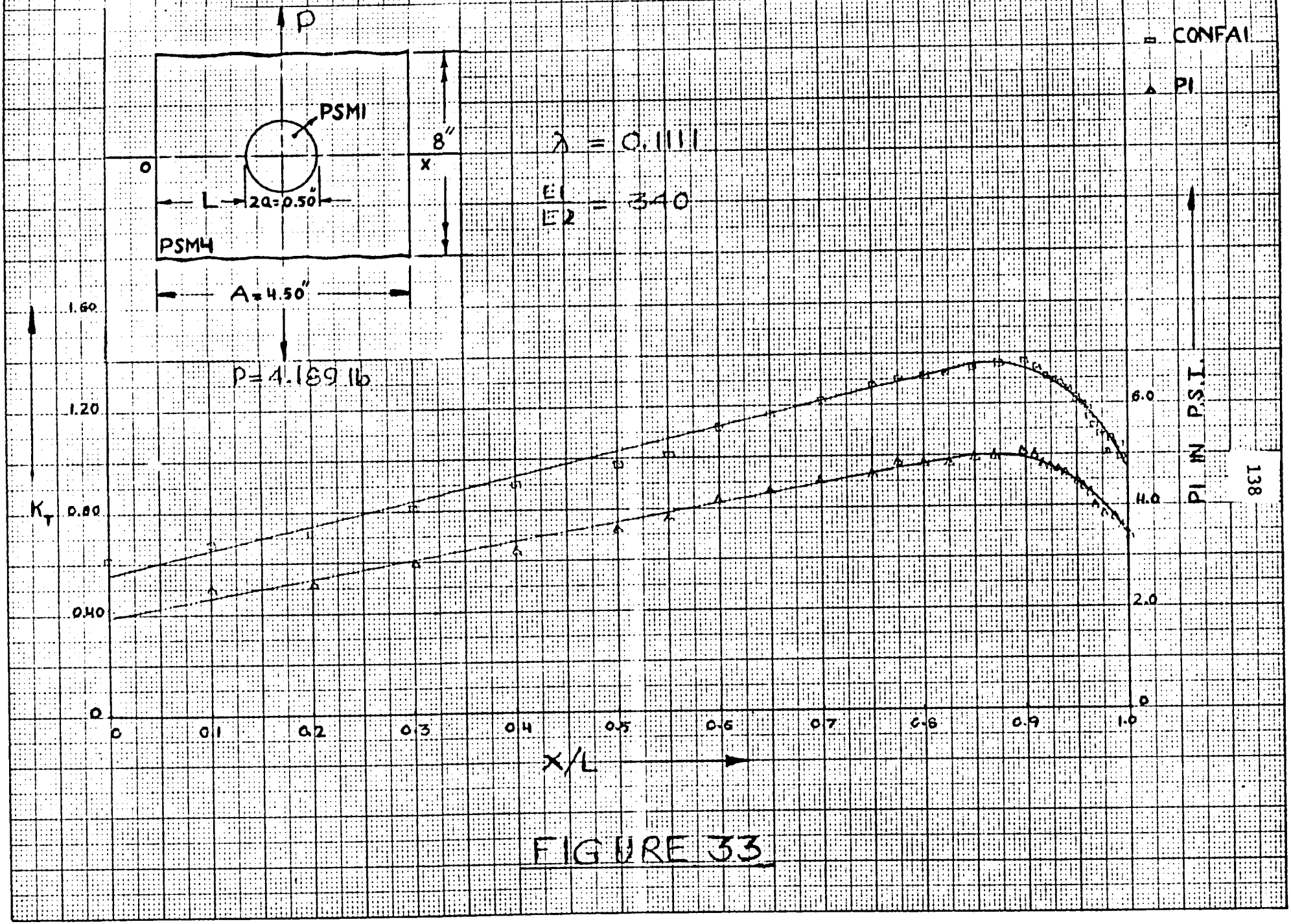
P
PSM1
8"
0
X
L
2a=0.50"
PSM4
A=4.50"
P=4.1691b
λ = 0.1111
E1/E2 = 3.40
CONFAI
PI
PI IN P.S.I.
K_T
1.60
1.20
0.80
0.40
0
6.0
4.0
2.0
0
0
0.1
0.2
0.3
0.4
0.5
0.6
0.7
0.8
0.9
1.0
X/L
138

FIGURE 33

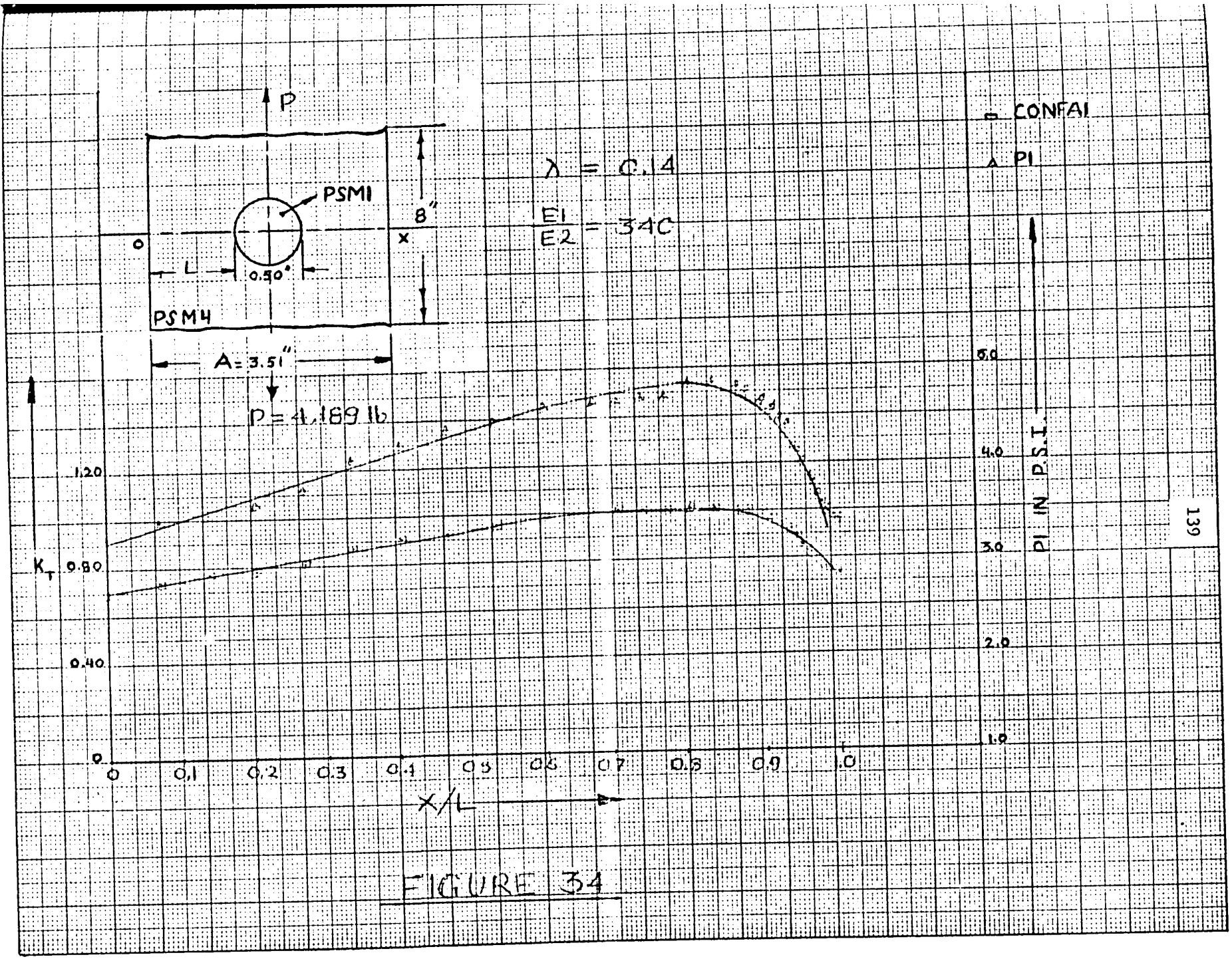
P
PSM1
8"
0
x
L
0.50"
PSM4
A = 3.51"
P = 4.169 lb
λ = 0.14
E1/E2 = 34C
CONFAI
PI
PI IN P.S.I.
5.0
4.0
3.0
2.0
1.0
K_T
1.20
0.80
0.40
0
0.1
0.2
0.3
0.4
0.5
0.6
0.7
0.8
0.9
1.0
X/L

FIGURE 34

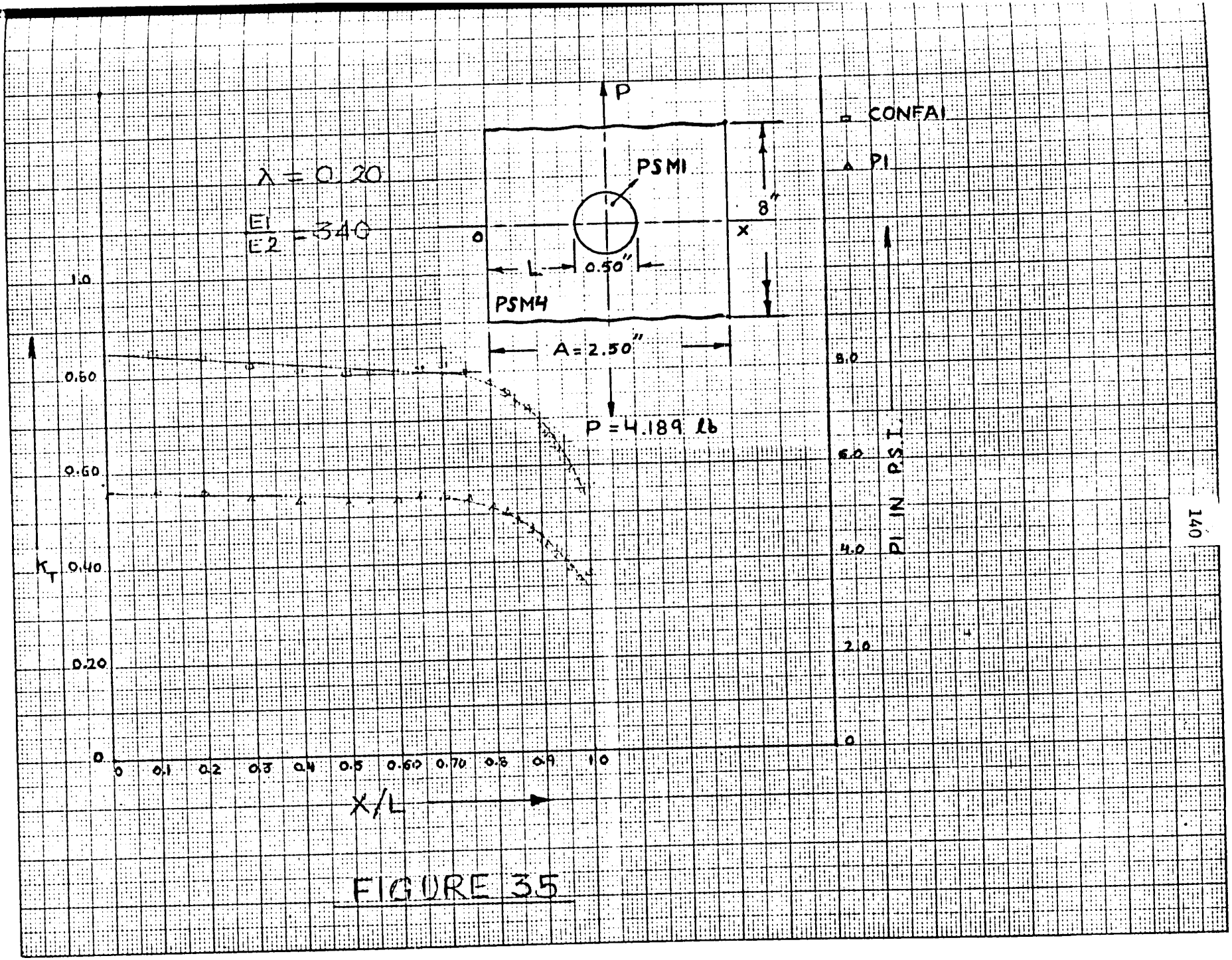
λ = 0.20
E1/E2 = 340
P
PSM1
PSM4
8"
x
0
L
0.50"
A = 2.50"
P = 4.189 lb
CONFAI
PI
PI IN PSI
1.0
0.60
0.60
0.40
0.20
0
K_T
0
0.1
0.2
0.3
0.4
0.5
0.60
0.70
0.8
0.9
1.0
X/L
8.0
6.0
4.0
2.0
0

FIGURE 35

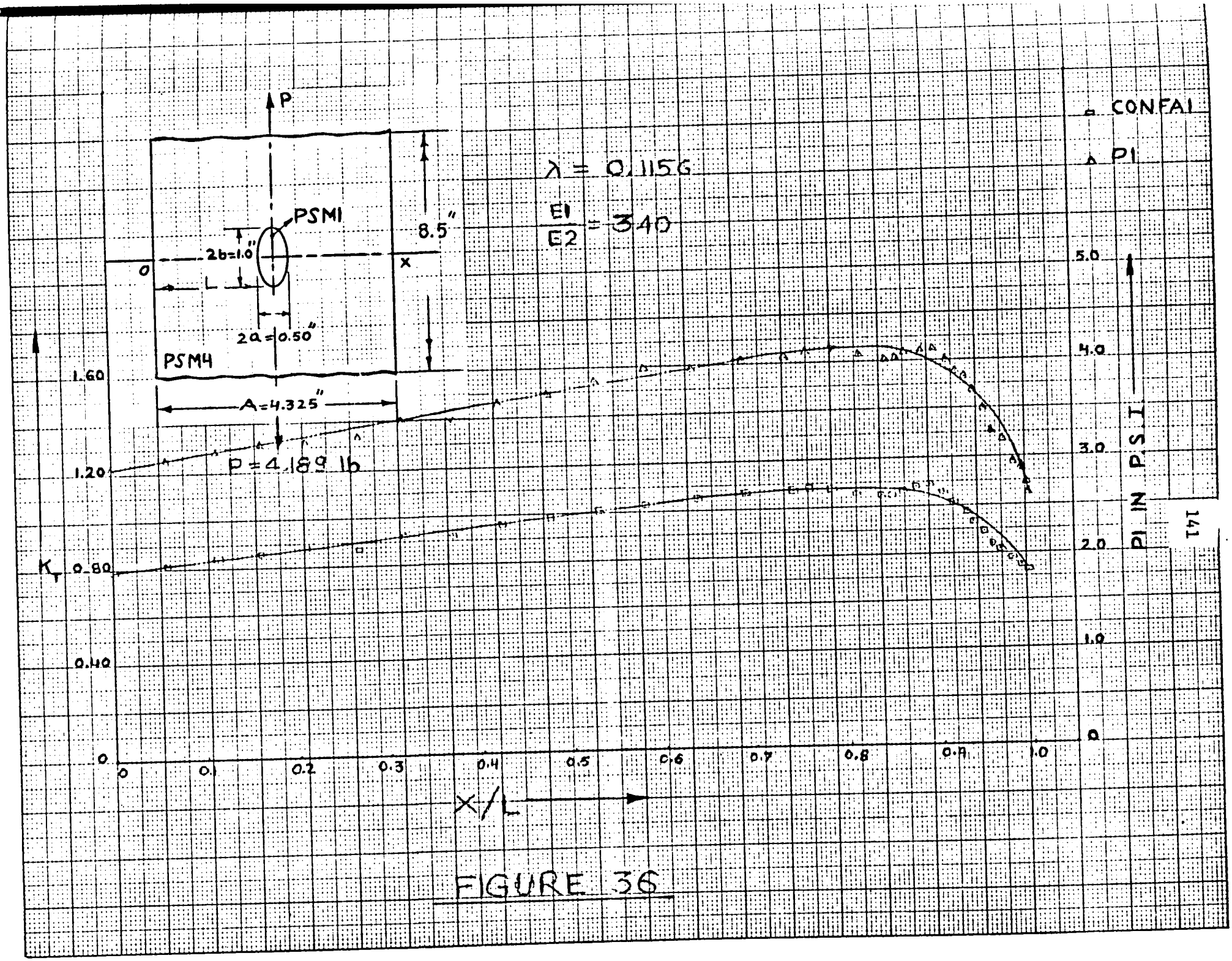
P
PSM1
8.5"
2b=1.0"
0
x
L
2a=0.50"
PSM4
A=4.325"
P=4.189 lb
λ = 0.1156
E1/E2 = 340
CONFAI
P1
PI IN P.S.I.
5.0
4.0
3.0
2.0
1.0
0
1.60
1.20
0.80
0.40
0
K_T
0
0.1
0.2
0.3
0.4
0.5
0.6
0.7
0.8
0.9
1.0
X/L
141

FIGURE 36

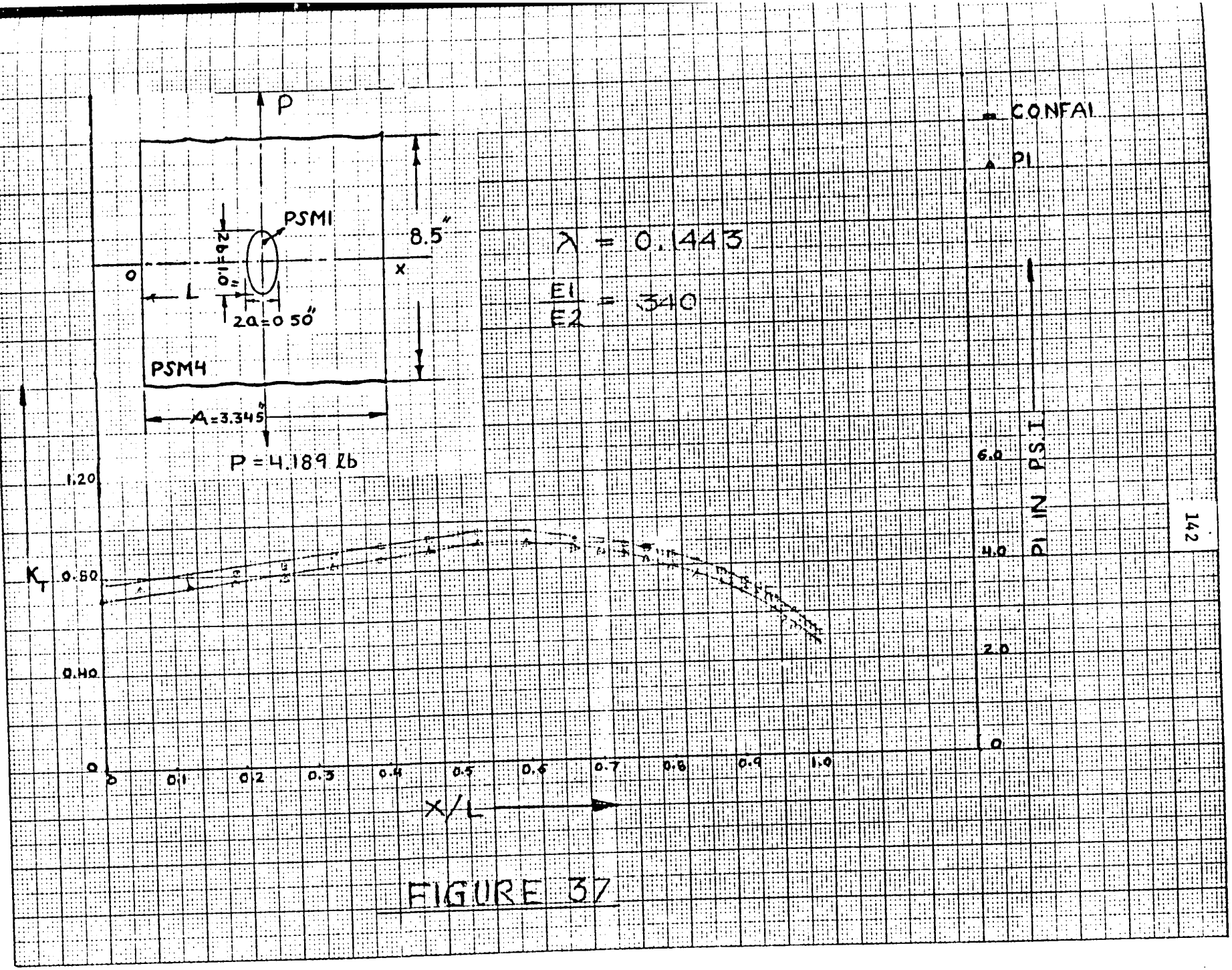
P
PSM1
8.5"
2b=0.10"
0
L
x
2a=0.50"
PSM4
A=3.345"
P = 4.189 lb
λ = 0.1443
E1/E2 = .340
CONFAI
P1
P1 IN PSI
6.0
4.0
2.0
0
1.20
0.80
0.40
0
K_T
0
0.1
0.2
0.3
0.4
0.5
0.6
0.7
0.8
0.9
1.0
X/L

FIGURE 37

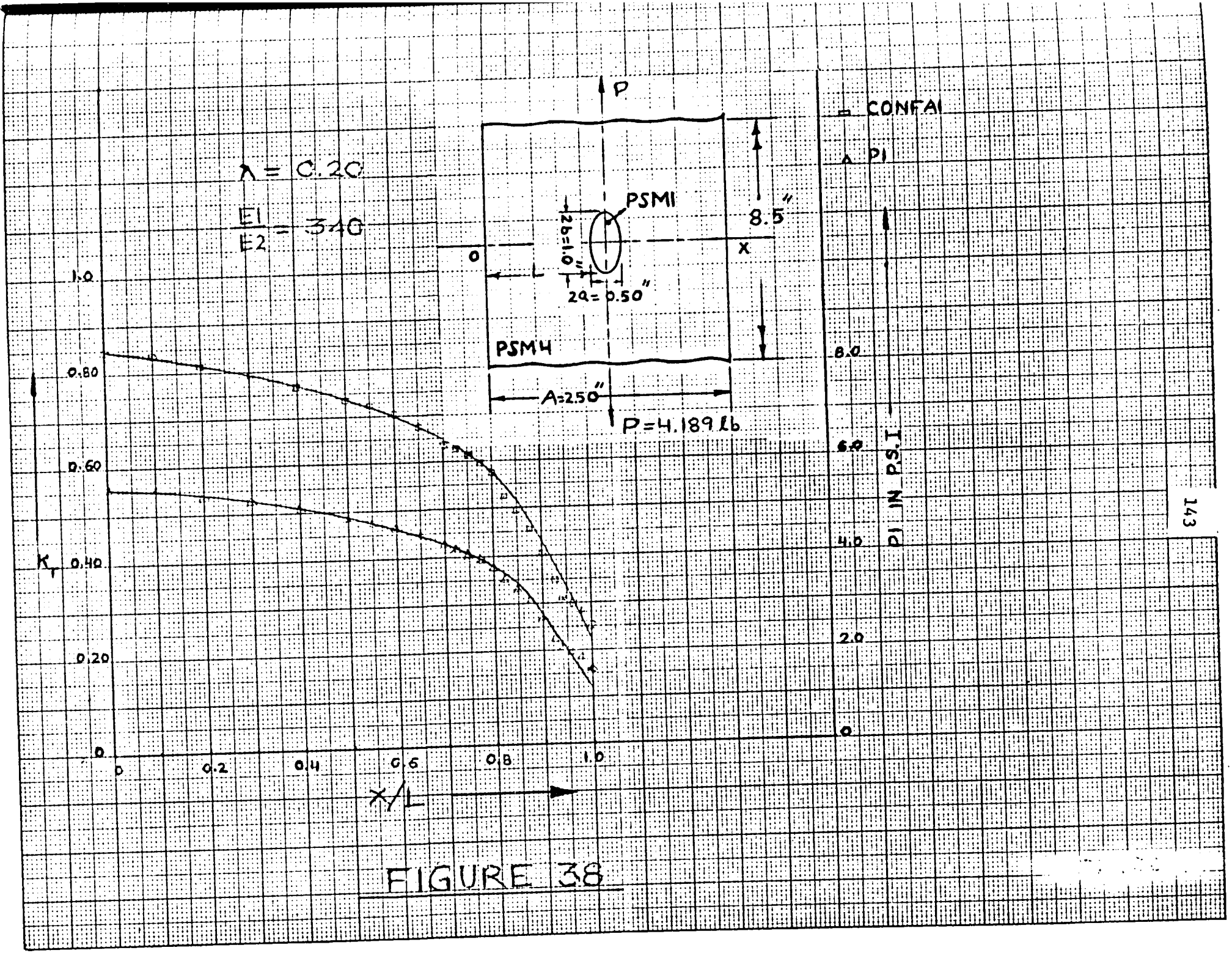
P
□ CONFAI
△ PI
λ = C.2C
EI/E2 = 3.1C
PSMI
8.5"
2a=1.0"
2a= 0.50"
0
X
PSM4
A=2.50"
P=4.189 lb
1.0
0.80
0.60
0.40
0.20
0
K_T
8.0
6.0
4.0
2.0
0
PI IN P.S.I
0
0.2
0.4
0.6
0.8
1.0
X/L

FIGURE 38

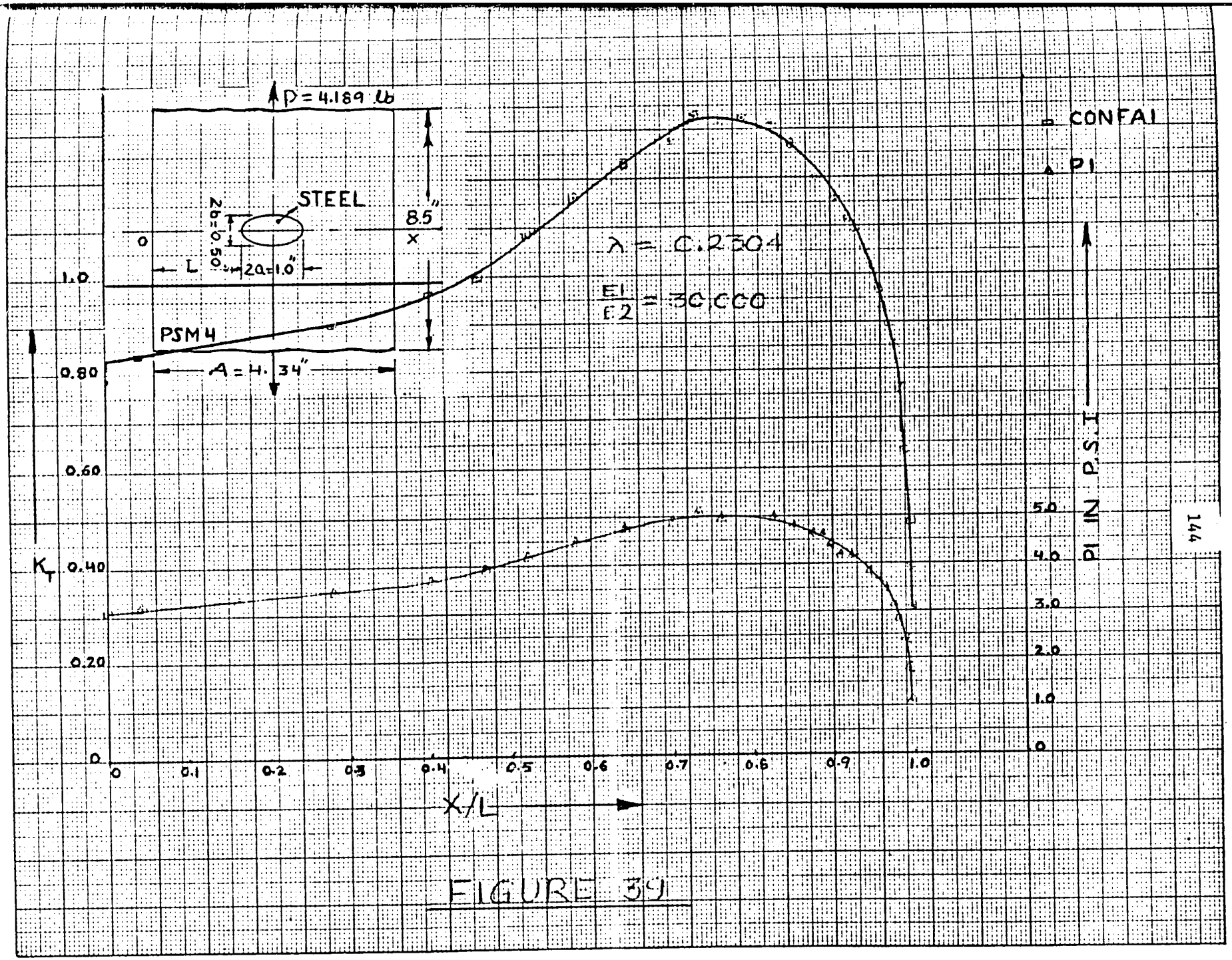
P = 4.189 lb
STEEL
2b=0.50"
2a=1.0"
L
0
x
8.5"
PSM4
A = 4.34"
λ = 0.2304
EI/E2 = 30,000
CONFAI
PI
PI IN P.S.I.
K_T
1.0
0.80
0.60
0.40
0.20
0
0.1
0.2
0.3
0.4
0.5
0.6
0.7
0.8
0.9
1.0
X/L
5.0
4.0
3.0
2.0
1.0
0

FIGURE 39

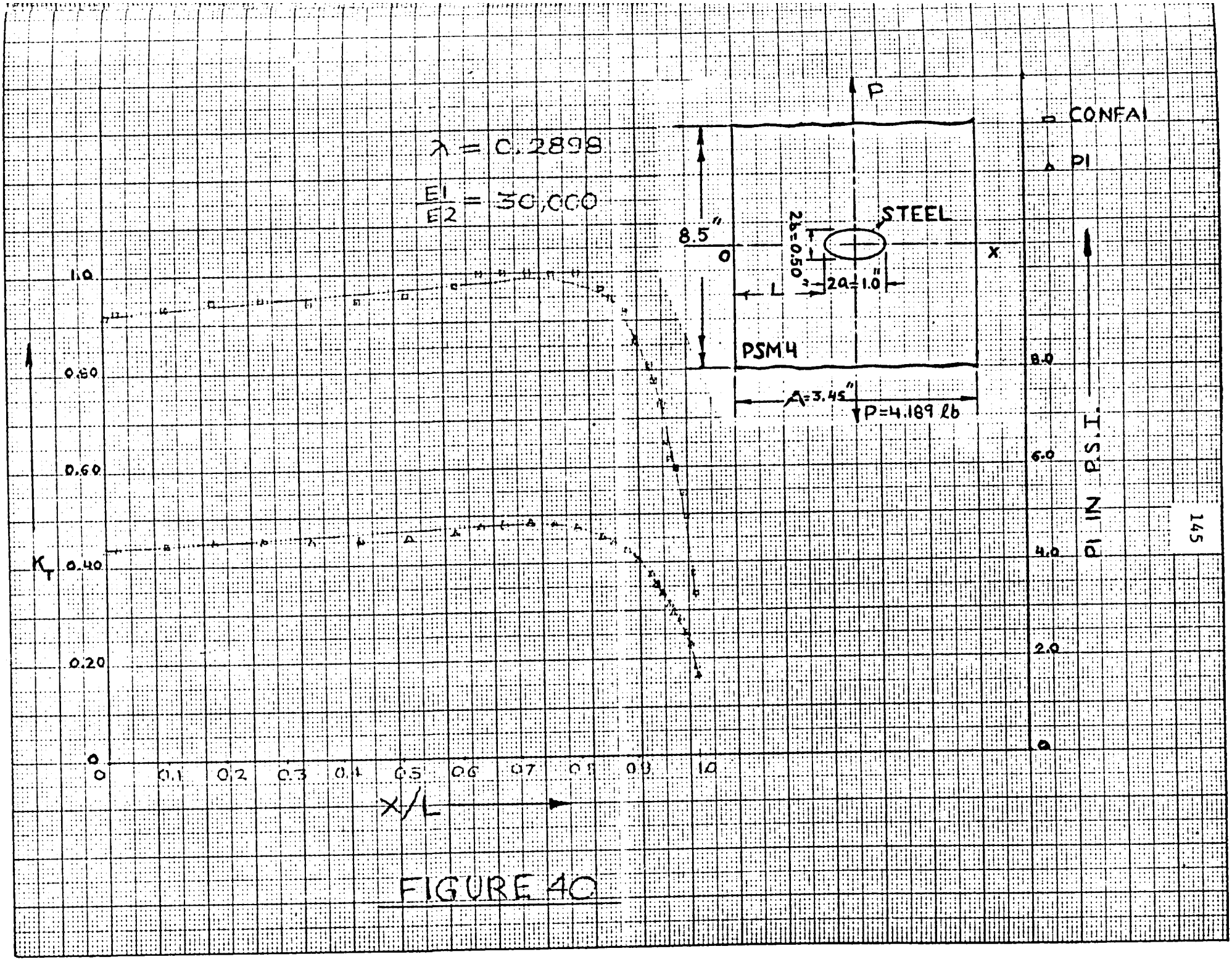
λ = 0.2898
E1/E2 = 30,000
P
8.5"
0
2b=0.50"
STEEL
x
L
2a=1.0"
PSM4
A=3.45"
P=4.189 lb
CONFAI
PI
PSI IN PI
8.0
6.0
4.0
2.0
0
1.0
0.80
0.60
0.40
0.20
0
K_T
0
0.1
0.2
0.3
0.4
0.5
0.6
0.7
0.8
1.0
X/L

FIGURE 40

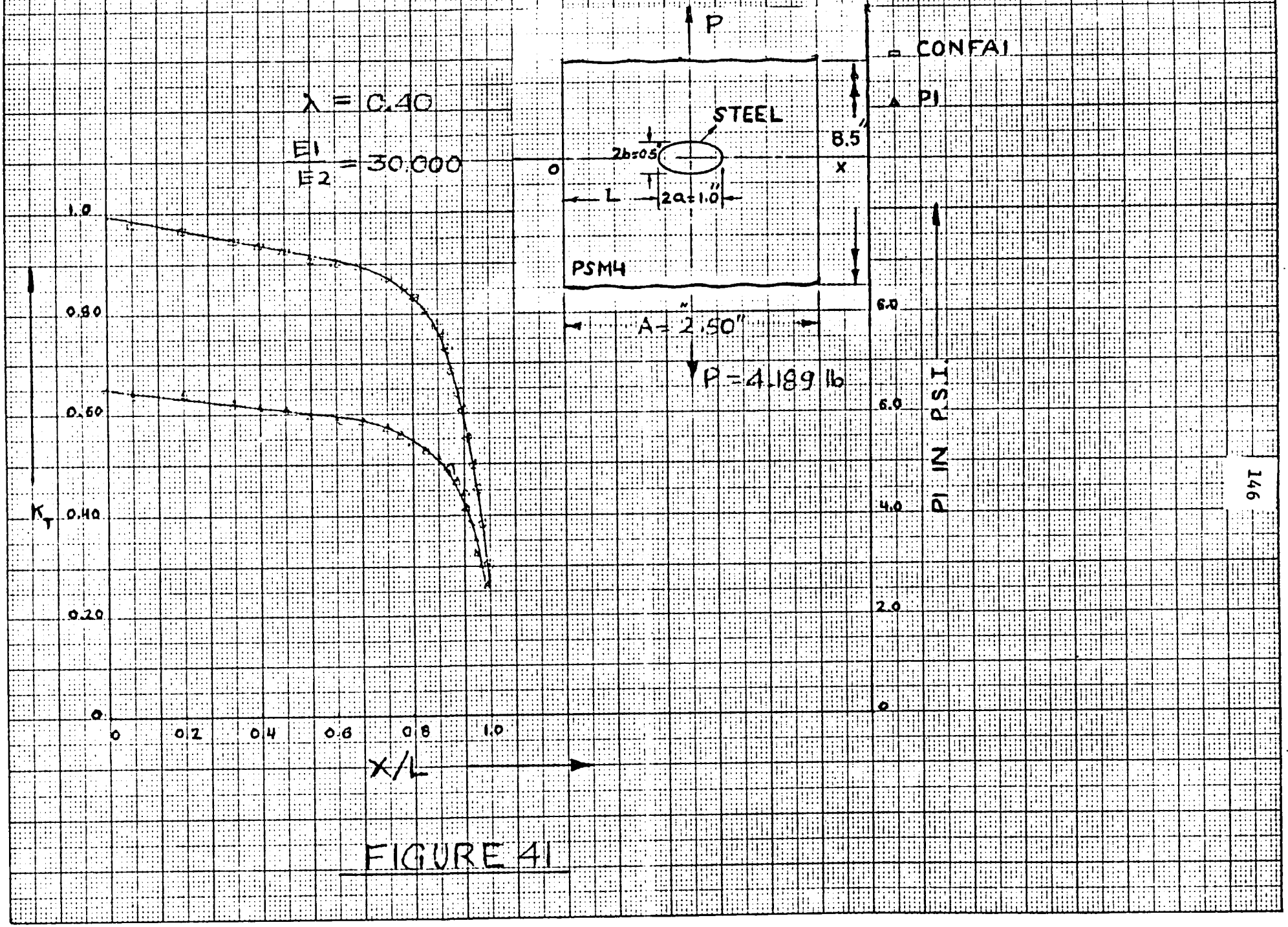
P
CONFAI
PI
STEEL
2b=0.5"
8.5"
0
X
L
2a=1.0"
PSM4
A=2.50"
P=4,189 lb
λ = 0.40
E1/E2 = 30,000
1.0
0.80
0.60
0.40
0.20
0
K_T
0
0.2
0.4
0.6
0.8
1.0
X/L
6.0
6.0
4.0
2.0
0
PI IN P.S.I.

FIGURE 41

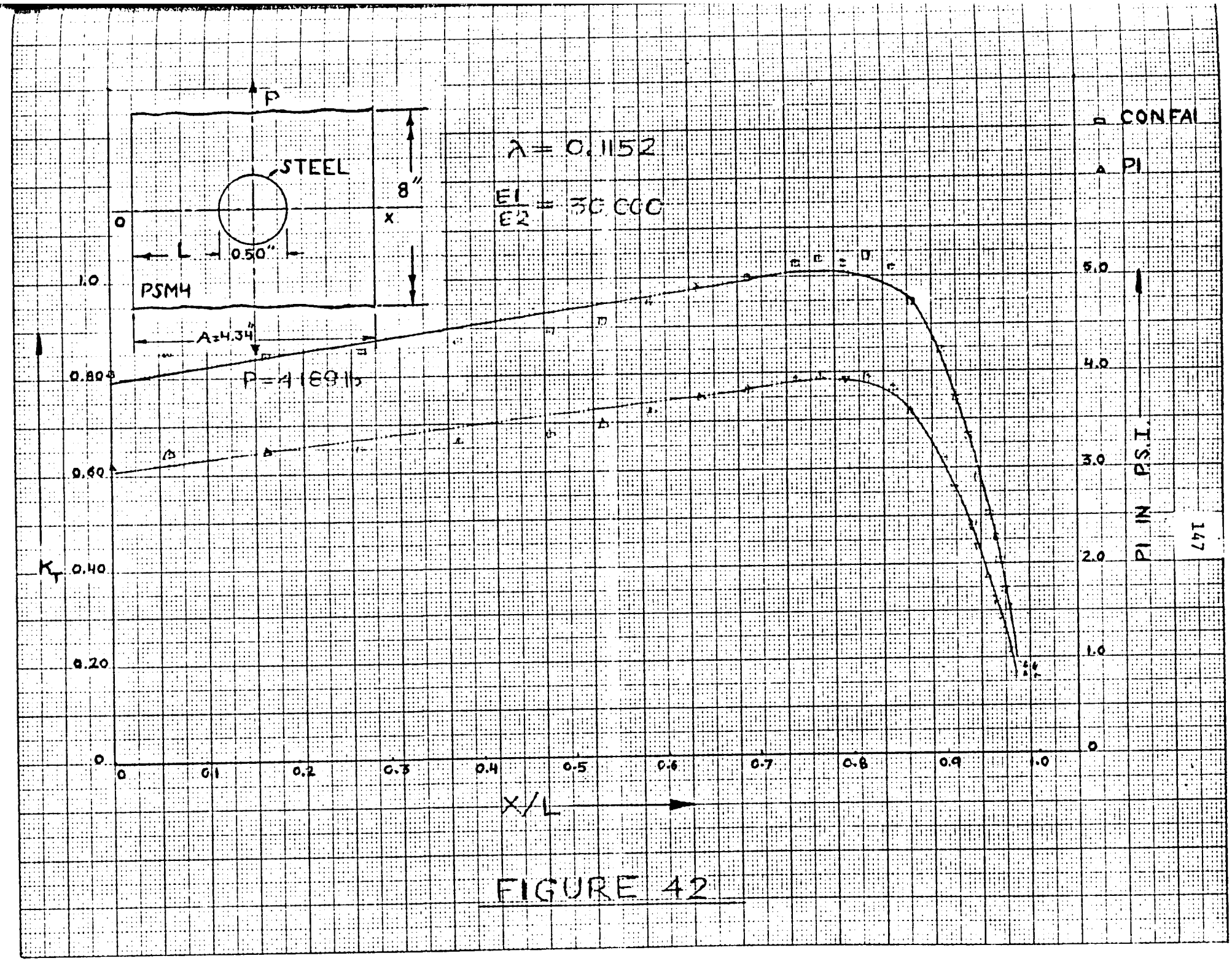
P
STEEL
8"
0
x
L
0.50"
PSM4
A=4.34"
λ = 0.1152
E1/E2 = 30 000
P = 4169 lb
1.0
0.80
0.60
0.40
0.20
0
K_T
0
0.1
0.2
0.3
0.4
0.5
0.6
0.7
0.8
0.9
1.0
X/L
CONFAL
PI
5.0
4.0
3.0
2.0
1.0
0
PI IN PSI'S
147

FIGURE 42

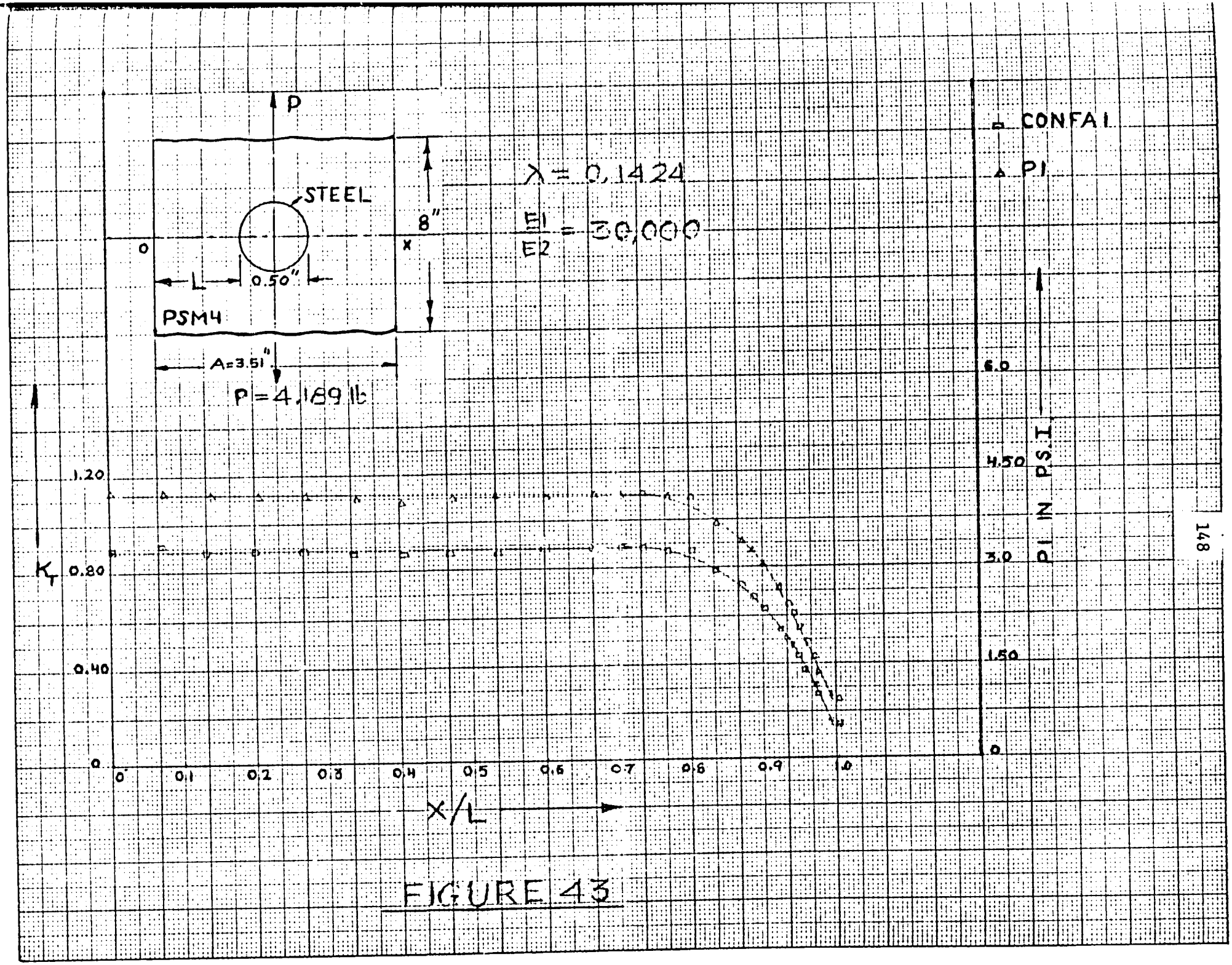
P
STEEL
8"
0
L
0.50"
PSM4
A=3.51"
P=4,189 lb
λ = 0.1424
E1/E2 = 30,000
CONFAI
P1
6.0
4.50
3.0
1.50
0
PI IN P.S.I.
1.20
0.80
0.40
0
K_T
0
0.1
0.2
0.3
0.4
0.5
0.6
0.7
0.8
0.9
1.0
X/L

FIGURE 43

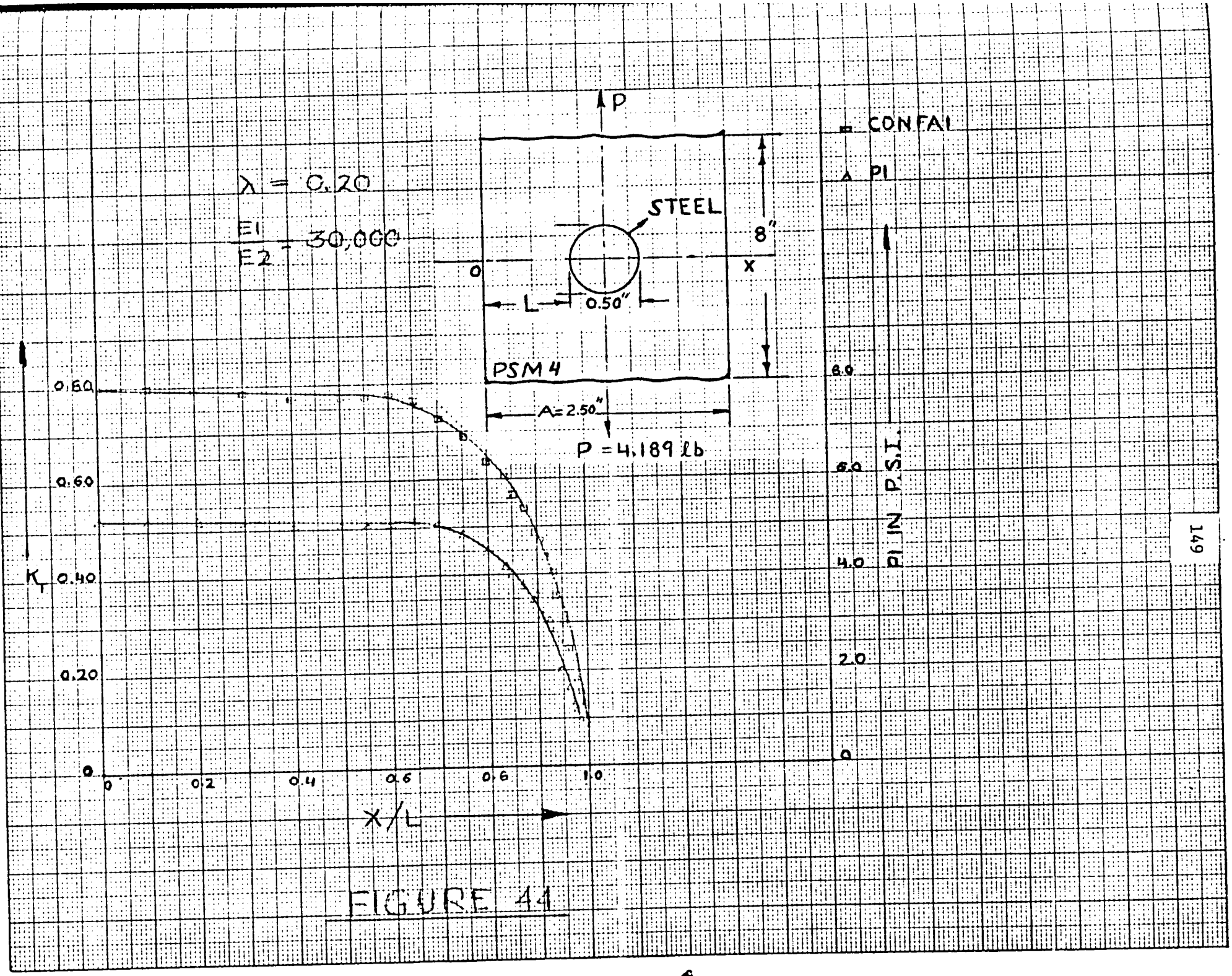
P
STEEL
8"
0
x
L
0.50"
PSM 4
A = 2.50"
P = 4,189 lb
λ = 0.20
E1/E2 = 30,000
0.80
0.60
0.40
0.20
0
K_T
0
0.2
0.4
0.6
0.8
1.0
X/L
CONFAI
PI
8.0
6.0
4.0
2.0
0
PI IN P.S.I.

FIGURE 44

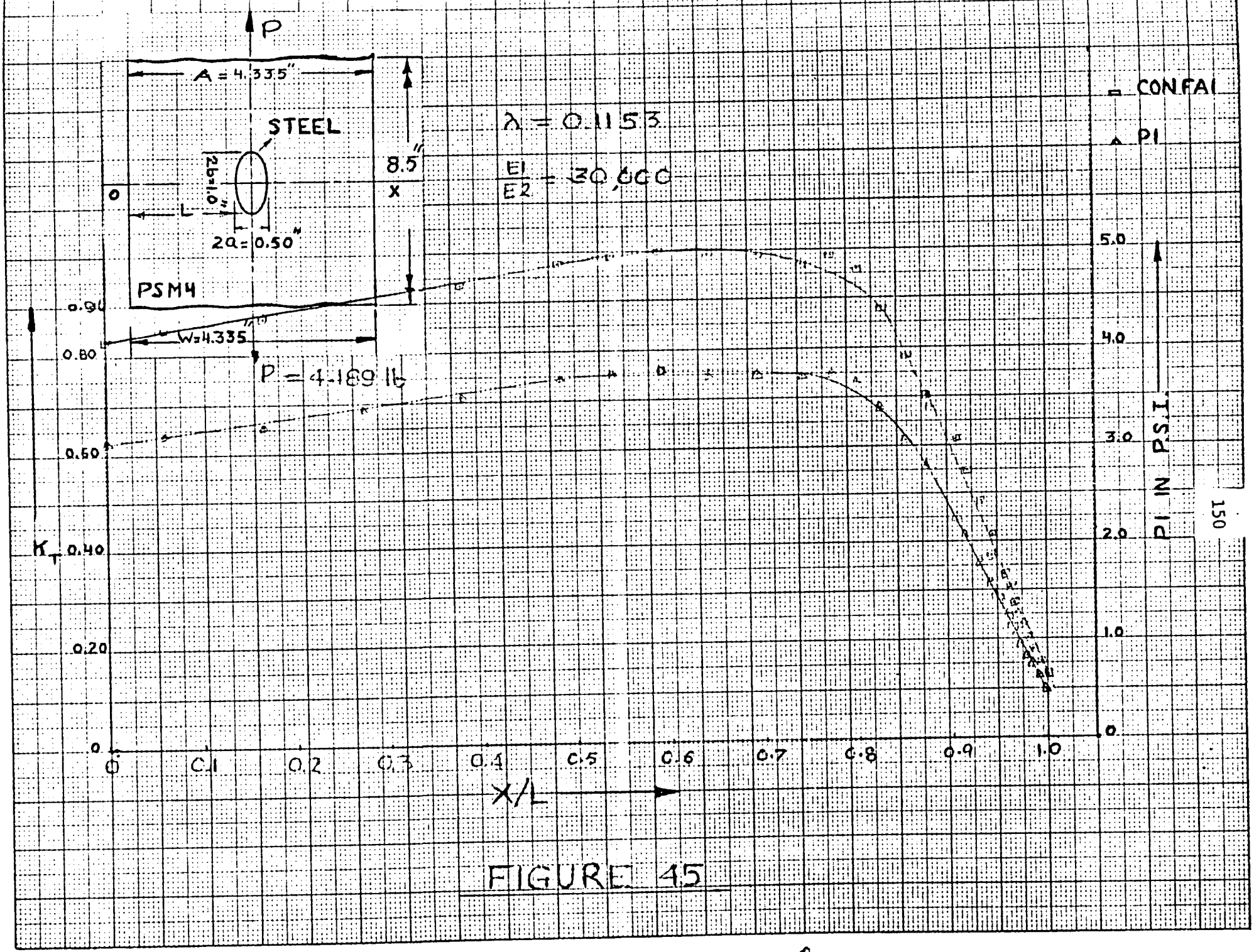
P
A = 4.335"
STEEL
2b=1.0"
2a = 0.50"
8.5"
x
0
L
PSM4
W=4.335"
P = 4.189 lb
λ = 0.1153
E1/E2 = 30,000
CONFAI
PI
PI IN PSI
150
5.0
4.0
3.0
2.0
1.0
0
0.90
0.80
0.50
0.40
0.20
K_T
0
0.1
0.2
0.3
0.4
0.5
0.6
0.7
0.8
0.9
1.0
X/L

FIGURE 45

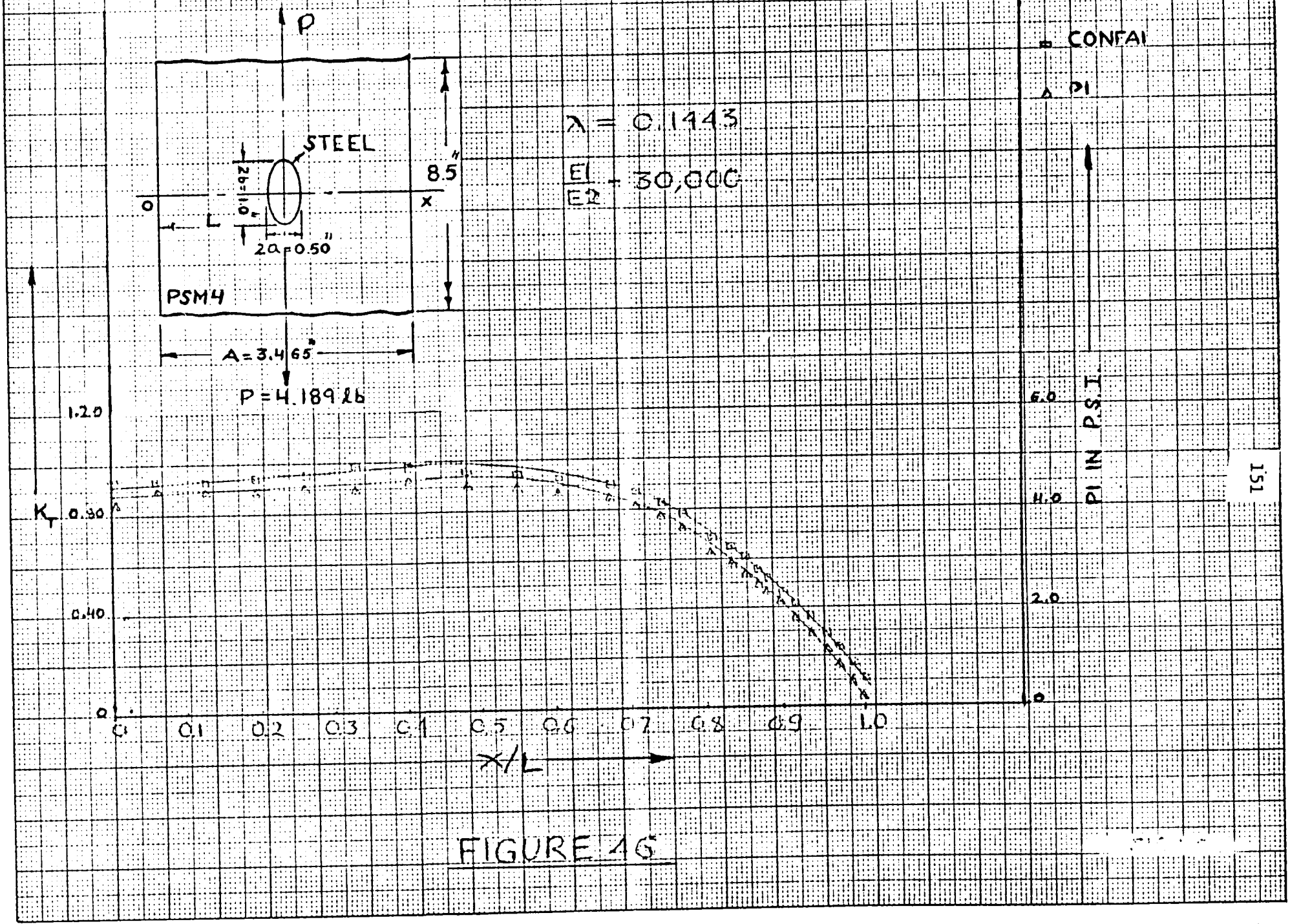
P
STEEL
2b=1.0"
2a=0.50"
8.5"
0
L
x
PSM4
A=3.465"
P=4.189 lb
λ = 0.1443
E1/E2 = 30,000
K_T
1.20
0.80
0.40
0
0
0.1
0.2
0.3
0.4
0.5
0.6
0.7
0.8
0.9
1.0
x/L
CONTAI
P1
6.0
4.0
2.0
0
PI IN P.S.I.
151

FIGURE 16

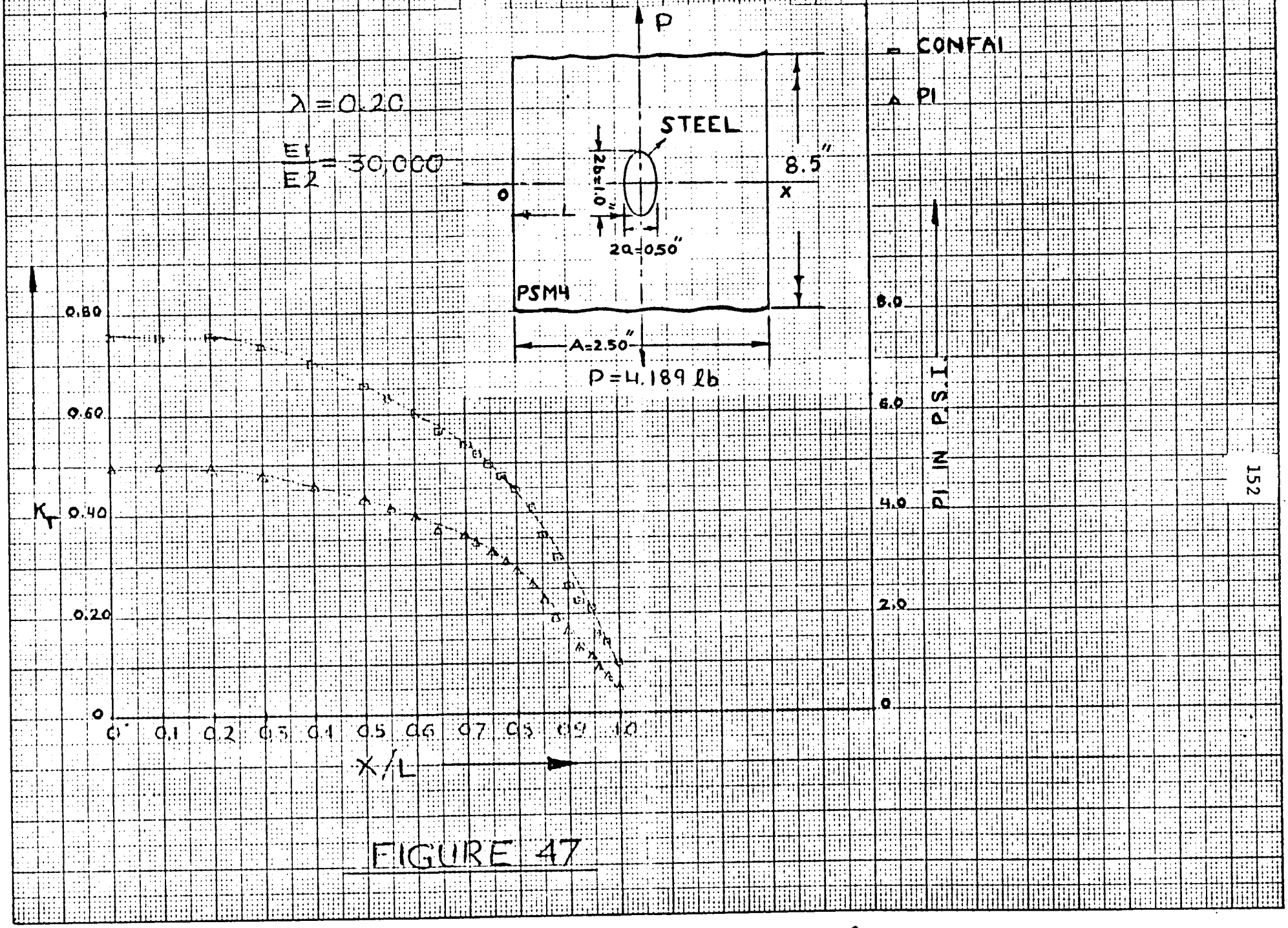
P
STEEL
2b=1.0"
2a=0.50"
8.5"
x
0
L
PSM4
A=2.50"
P=4.189 lb
λ=0.20
E1/E2=30,000
CONFAL
PI
PI IN P.S.I.
8.0
6.0
4.0
2.0
0
0.80
0.60
0.40
0.20
0
Kt
0 0.1 0.2 0.3 0.4 0.5 0.6 0.7 0.8 0.9 1.0
X/L

FIGURE 47

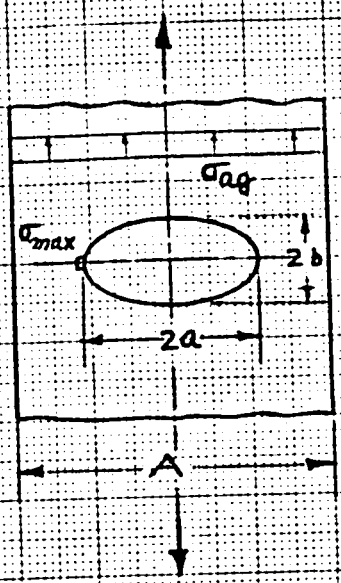

$$\mu = \frac{b}{a}$$

$$\lambda = \frac{2a}{A}$$

$$K_T = \frac{\sigma_{max}}{\sigma_{ag}}$$

$\mu = 0.50$

$\mu = 1$

$\mu = 2$

STRESS CONCENTRATION FACTORS K_T FOR POINTS UNDER MAXIMUM TENSION IN FINITE PLATE WITH ELLIPTICAL INSERT $\frac{E1}{E2} = \frac{1}{340}$

0.10 0.20 0.30 0.40 0.50

λ ⟶

FIG. 48

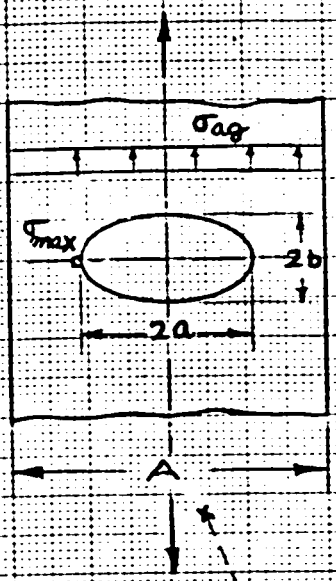

$$\mu = \frac{b}{a}$$

$$\lambda = \frac{2a}{A}$$

$$K_T = \frac{\sigma_{max}}{\sigma_{ag}}$$

$\mu = 0.50$

$\mu = 1$

$\mu = 2$

STRESS CONCENTRATION FACTORS K_T FOR POINTS UNDER MAXIMUM TENSION IN FINITE PLATE WITH AN ELLIPTICAL INSERT $\frac{E1}{E2} = 340$

0.10 0.20 0.30 0.40 0.50

λ ⟶

FIG. 49

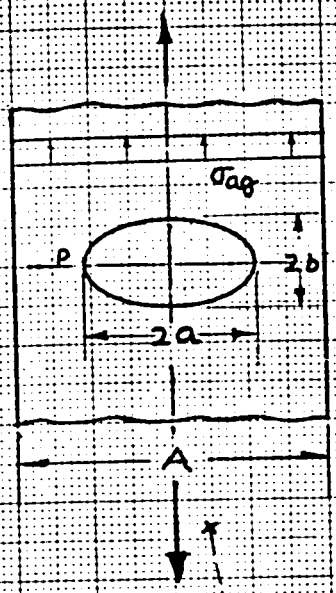

$$\mu = \frac{b}{a}$$

$$\lambda = \frac{2a}{A}$$

$$K_T' = \frac{\sigma_p}{\sigma_{ap}}$$

$\mu = 1$

$\mu = 2$

$\mu = 0.50$

STRESS CONCENTRATION FACTORS K_T' FOR POINTS 'P' UNDER MAXIMUM TENSION IN FINITE PLATE WITH AN ELLIPTICAL INSERT $\frac{E1}{E2} = 340$

0.10 0.20 0.30 0.40 0.50

λ ⟶

FIG. 50

STRESS CONCENTRATION FACTORS K_T FOR POINTS UNDER MAXIMUM TENSION IN FINITE PLATE WITH AN ELLIPTICAL INSERT $\frac{E_1}{E_2} = 30,000$

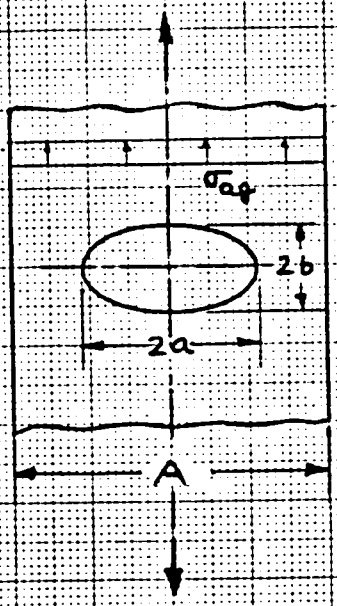

$\mu = \frac{b}{a}$

$\lambda = \frac{2a}{A}$

$K_T = \frac{\sigma_{max}}{\sigma_{av}}$

$\mu = 0.50$

$\mu = 2$

$\mu = 1$

0.10 0.20 0.30 0.40 0.50

λ ⟶

FIG 51

$$\mu = \frac{b}{a}$$

$$\lambda = \frac{2a}{A}$$

$$K_T' = \frac{\sigma_p}{\sigma_{ag}}$$

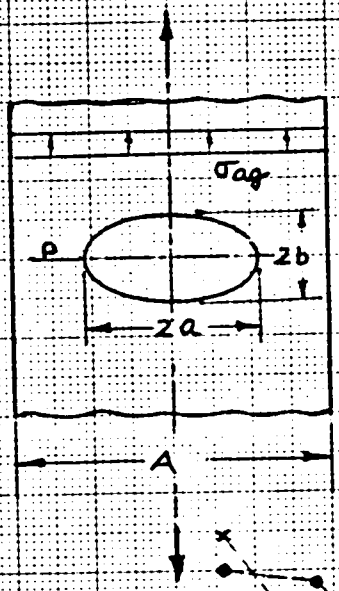

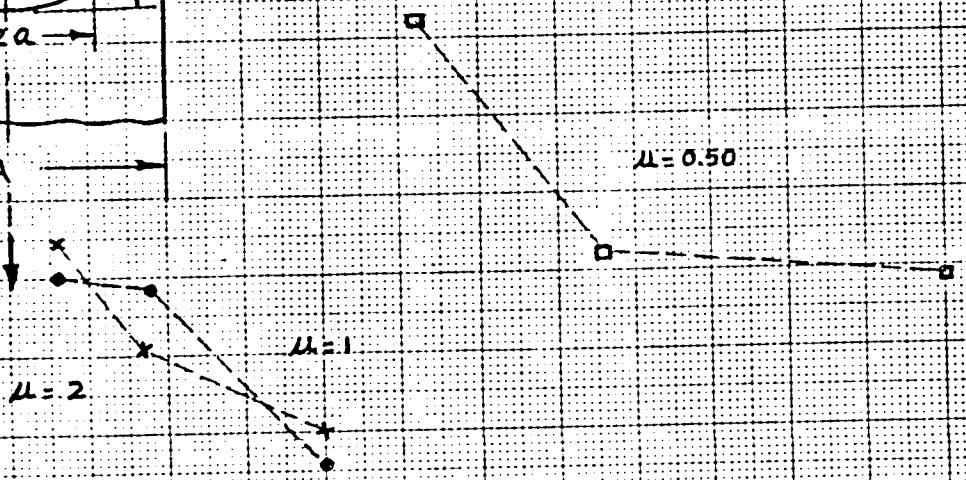

STRESS CONCENTRATION FACTORS K_T' FOR POINT 'P' UNDER MAXIMUM TENSION IN FINITE PLATE WITH AN ELLIPTICAL INSERT $\frac{E1}{E2} = 30,000$

0.10 0.20 0.30 0.40 0.50

λ ⟶

FIG. E2

5. REFERENCES

1. Bhargava, R.D. and Jaswon, M.A.," Two Dimensional Elastic Inclusion Problems," PROCEEDING CAMBRIDGE PHIL. SOCIETY, Vol. 57, 1961, pp 669-680.

2. Bhargava, R.D. and Kapoor, O.P.," Circular Inclusion in an Infinite Elastic Medium With a Circular Hole," PROCEEDING CAMBRIDGE PHIL. SOCIETY, Vol. 60,1964, pp675.

3. Daily, J.W. and Riley, W.F.," Experimental Stress Analysis," MCGRAW-HILL BOOK COMPANY, NEW YORK.

4. Donnell, L.H.," Stress Concentrations Due to Elliptical Discontinuities in Plates Under Edge Forces," VON KARMAN ANNIVERSARY VOLUME,CALIFORNIA INSTITUTE OF TECH.,PASADENA, 1941, pp 293.

5. Dundurs, J.M. and Hetenyi, M.," The Elastic Plane With a Circular Insert Loaded by a Radial Force," JOURNAL OF APPLIED MECHANICS, March 1961,pp 103.

6. Durelli, A.J., Parks, V.J. and Feng, H.C.," Stressess Around an Elliptical Hole in a Finite Plate Subjected to Axial Loading," JOURNAL OF APPLIED MECHANICS, March 1962, pp 192.

7. Faddeeva, V.N.," Computional Methods of Linear Algebra," DOVER PUBLICATIONS, INC., NEW YORK.

8. Fox,L. and Mayers, D.F," Computating Methods for Scientists and Engineers," CLARENDON PRESS, OXFORD.

9. Frocht, M.M.," Photoelasticity, Vols. 1 and 2," JOHN WILEY AND SONS, INC., NEW YORK.

10. Hamming, R.W.," Numerical Methods for Scientists and Engineers," MCGRAW-HILL BOOK COMPANY, INC., NEW YORK.

11. Hartranft, R.J. and Sih, G.C.," The Effect of Couple Stresses on the Stress Concentration of a Circular Inclusion," JOURNAL OF APPLIED MECHANICS, June 1965, pp 429.

12. Hetenyi, M.," Handbook of Experimental Stress Analysis," JOHN WILEY AND SONS, INC., NEW YORK.

13. Hughford," Advanced Mechanics of Materials," JOHN WILEY AND SONS, INC., NEW YORK.

14. IBM SYSTEM / 360 Scientific Subroutine Package, H20, 0205-3.

15. Murrill, P.W. and Smith, C.L.," Fortran IV Programming for Scientists and Engineers," INTERNATIONAL TEXTBOOK COMPANY, SCRANTON, PENNSYLVANIA.

16. Pathare, P.R.," A Computational Technique for the Efficient Handling of Large Matrices in the Analysis of Large Space Structures," THE INTERNATIONAL CONFERENCE ON SPACE STRUCTURES, BLACKWELL SCIENTIFIC PUBLICATIONS, OXFORD, Chapter 26.

17. Peterson, R.E.," Stress Concentration Design Factors," JOHN WILEY AND SONS, INC., NEW YORK.

18. Ralston, A. and Wilf, H.S.,"Mathematical Methods for Digidal Computers, Vols. II," JOHN WILEY AND SONS, INC., NEW YORK.

19. Thibodeau, W.E. and Wood, L.A.," Photoelastic Determination of Stresses Around Circular Inclusion," NATIONAL BUREAU OF STANDARD JOURNAL OF RESEARCH," Vol. 20, n 3, paper 1083, March 1938, pp 393.

20. Timoshenko, S. and Goodier, J.N.," Theory of Elasticity," MCGRAW-HILL BOOK COMPANY, INC., NEW YORK.